Titre: Title:	Electromechanical and Polarization Microscopy Evaluation of Cartilage Repair and Degeneration
Auteur: Author:	Adele Changoor
Date:	2011
Type:	Mémoire ou thèse / Dissertation or Thesis
Référence: Citation:	Changoor, A. (2011). Electromechanical and Polarization Microscopy Evaluation of Cartilage Repair and Degeneration [Thèse de doctorat, École Polytechnique de Montréal]. PolyPublie. https://publications.polymtl.ca/515/

UNIVERSITÉ DE MONTRÉAL

ELECTROMECHANICAL AND POLARIZATION MICROSCOPY EVALUATION OF CARTILAGE REPAIR AND DEGENERATION

ADELE CHANGOOR
INSTITUT DE GÉNIE BIOMÉDICAL
ÉCOLE POLYTECHNIQUE DE MONTRÉAL

THÈSE PRÉSENTÉE EN VUE DE L'OBTENTION
DU DIPLÔME DE PHILOSOPHIAE DOCTOR (Ph.D.)
(GÉNIE BIOMÉDICAL)
JANVIER 2011

UNIVERSITÉ DE MONTRÉAL

ÉCOLE POLYTECHNIQUE DE MONTRÉAL

Cette thèse intitulée:

ELECTROMECHANICAL AND POLARIZATION MICROSCOPY EVALUATION OF CARTILAGE REPAIR AND DEGENERATION

présentée par : CHANGOOR Adele
en vue de l'obtention du diplôme de : Philosophiae Doctor
a été dûment acceptée par le jury d'examen constitué de :

Mme HOEMANN Caroline, Ph.D., présidente
M. BUSCHMANN Michael, Ph.D., membre et directeur de recherche
Mme VILLEMURE Isabelle, Ph.D., membre
M. JURVELIN Jukka, Ph.D., membre

for Dad and Grandpa

ACKNOWLEDGEMENTS

I was privileged to work with many wonderful people during the course of my doctoral studies. I would especially like to thank my supervisor, Dr. Michael Buschmann, for his insightful guidance, scientific rigour, and for providing me with many opportunities to learn and grow during the course of my PhD.

Many thanks to the members of my thesis examining committee, Drs. Jukka Jurvelin, Caroline Hoemann, Isabelle Villemure and Gregory Patience, for their challenging questions and constructive suggestions.

My colleagues and friends at the Biomaterials and Cartilage Laboratory made my time in Montréal memorable. Collaborations with folks at Biomomentum, BioSyntech, and the Ontario Vet College brought new dimensions to my work and broadened my perspectives. Thanks for your expertise, encouragement and friendship. I enjoyed working with you all.

I am fortunate to have the love and support of my family, Mom, Christine & Cindy, and fiancé, Mike, who contributed in all the non-scientific ways to the successful completion of this thesis.

The funding for this research was provided by the Natural Sciences and Engineering Research Council of Canada (NSERC), BioSyntech Canada Inc., and the Canadian Arthritis Network (CAN).

RÉSUMÉ

L'arthrose est une condition physique prévalente pour laquelle aucun traitement permettant de modifier la maladie n'est disponible présentement. La recherche actuelle évalue des modèles pré-cliniques pour le développement et la vérification des approches thérapeutiques, ou de réparation, potentielles. Par la suite, des essais cliniques sont effectués sur des sujets humains sous conditions contrôlées pour évaluer l'efficacité des approches les plus prometteuses. Ces études représentent un effort considérable où le choix de méthodes sensibles et pertinentes pour l'évaluation du cartilage articulaire est très important pour leur succès.

Les études pré-cliniques sur l'arthrose impliquent l'utilisation de modèles de blessures d'impact, où une blessure mécanique initiale est créée sur la surface du cartilage, laquelle peut initier les voies de dégradation qui culminent éventuellement en arthrose. L'étude des premiers événements de cette trajectoire est importante car les phases immédiates et aiguës après la blessure sont caractérisées par une augmentation de la réponse cellulaire et des activités de dégradation, ce qui représente une période très propice où les interventions thérapeutiques pour atténuer la progression de la maladie peuvent être les plus efficaces. Dans de telles études, une méthode d'évaluation suffisamment sensible doit être utilisée pour détecter les changements se produisant dans la matrice extracellulaire du cartilage.

Dans les études cliniques, une évaluation directe de la qualité du tissu cartilagineux en réparation est réalisée histologiquement à l'aide de petites biopsies obtenues au cours d'une arthroscopie de réévaluation. Les systèmes actuels de notation des coupes histologiques évaluent un nombre de caractéristiques qui contribuent à la durabilité à long terme des tissus cartilagineux en réparation, mais omettent une catégorie spécifique qui permet l'évaluation structurée de l'organisation du collagène. Le réseau de fibrilles de collagène joue un rôle critique sur la capacité de chargement du cartilage et est donc possiblement indicateur de la durabilité de la réparation du cartilage à long terme. Concevoir un système de notation où différents niveaux

d'organisation du collagène pourraient être évalués selon une méthode sensible à l'orientation du collagène est nécessaire pour améliorer l'analyse de la qualité de la réparation du cartilage.

À ces fins, deux méthodologies d'évaluation du cartilage, les potentiels d'écoulement et la microscopie en lumière polarisée (PLM), ont été étudiées et les résultats ont été rapportés en quatre articles de revue. Les deux premiers concernent la sensibilité de la méthode des potentiels d'écoulement pour l'évaluation du cartilage et incluent aussi une étude sur les conséquences de l'entreposage au froid du cartilage sur ses propriétés. Les objectifs de ces articles étaient les suivants:

- Évaluer les effets de l'entreposage réfrigéré ou congelé du cartilage sur ses propriétés biomécaniques et électromécaniques.
- Évaluer la capacité de la méthode des potentiels d'écoulement à détecter les changements du cartilage immédiatement après une blessure d'impact localisée, et ce, pour des niveaux de contraintes distincts.

Les troisième et quatrième articles de revue décrivent le développement, les tests et la validation d'un système de notation par microscopie en lumière polarisée (PLM) pour évaluer l'organisation du collagène, et incluent des comparaisons détaillées utilisant la microscopie électronique à balayage (SEM). Les principaux objectifs de ces articles de revue étaient les suivants:

- Développer et tester un système de notation histologique qualitatif par PLM qui décrit les caractéristiques idéales d'organisation du collagène présent dans le cartilage articulaire de jeunes adultes.
- Comparer les caractéristiques structurelles du réseau de collagène dans des tissus cartilagineux normaux, dégradés et en réparation, et ce, en utilisant les méthodes PLM et SEM.

Les potentiels d'écoulement ont répondu aux changements du cartilage produits immédiatement après une blessure d'impact dans un modèle d'explants équins d'une manière dépendante de la dose reçue, c'est-à-dire que des réductions plus importantes des potentiels d'écoulement ont été observées avec l'augmentation de la contrainte maximale appliquée. Les

tests biomécaniques sur les disques cartilagineux prélevés ont démontré une tendance similaire dans les paramètres associés au réseau de collagène, mais ces essais ont été moins sensibles aux changements du cartilage que les potentiels d'écoulement. Cette étude est la première à démontrer la sensibilité des potentiels d'écoulement pour la détection des changements dans le cartilage suite à un impact mécanique. Ces résultats suggèrent que les potentiels d'écoulement sont une méthode appropriée pour surveiller les changements du cartilage dans les modèles de blessures d'impact, où la dégénération du cartilage débute par une lésion mécanique localisée qui éventuellement progresse jusqu'à l'arthrose. La sensibilité accrue de la méthode des potentiels d'écoulement comparativement aux essais biomécaniques, de même que leur nature non-destructive, permet d'envisager des études avec des mesures séquentielles résolues dans l'espace, où le cartilage pourrait être évalué au site de la blessure ainsi que dans les zones adjacentes au fil du temps.

Les effets de l'entreposage au froid du cartilage sur ses propriétés biomécaniques et électromécaniques ont été étudiés dans les explants bovins ostéochondraux. Ces études ont démontré que le cartilage pourrait être réfrigéré dans des chambres humides pour une période de 6 jours sans observer d'effets sur ses propriétés biomécaniques ou électromécaniques. Un seul cycle de gel-dégel à -20°C a produit un effet minimal sur les propriétés électromécaniques, sans changements biomécaniques évidents. Ces résultats apportent de nouvelles informations concernant cet aspect important pour les tests sur le cartilage.

Un nouveau système de notation en PLM a été développé et validé avec succès. Ce dernier fournit une évaluation qualitative des différents niveaux d'organisation du collagène dans des coupes histologiques de cartilage en réparation. Une excellente fiabilité inter-observateur a été observée quand le système de notation a été utilisé par des personnes formées à l'évaluation de biopsies de tissus cartilagineux normaux, dégradés et en réparation. Les études de validation utilisant le SEM ont confirmé que les orientations globales de collagène observées en PLM étaient la conséquence de la vraie orientation des fibres de collagène. Des comparaisons approfondies de la structure du collagène utilisant la PLM et le SEM ont permis d'identifier des différences dans les distributions de diamètres des fibres et dans les proportions des zones du

cartilage entre les tissus cartilagineux normaux, dégradés et en réparation. Ce travail a démontré que certaines stratégies de réparation du cartilage sont capables de produire une organisation stratifiée du collagène qui se rapproche de l'architecture du cartilage articulaire adulte. C'est la première étude qui fournit des preuves de cela à un niveau ultrastructural.

Les deux méthodes d'évaluation explorées au cours de cette thèse ont été jugées assez sensibles et appropriées pour l'évaluation du cartilage articulaire en dégénération et en réparation, et pourraient être facilement adaptées à d'autres domaines liés à la recherche sur le cartilage.

ABSTRACT

Osteoarthritis (OA) is a prevalent health condition for which no disease modifying strategies are presently available. Current research incorporates pre-clinical models for the development and testing of potential therapeutic or repair approaches, and subsequently, clinical trials are undertaken, where the most promising strategies are assessed in humans under controlled conditions. These are substantial endeavours requiring sensitive and appropriate evaluation methods for cartilage assessment to ensure their success.

Pre-clinical studies of OA include the use of impact injury models, where an initial mechanical insult to the cartilage surfaces can initiate degradative pathways that eventually culminate in OA. Studying early time points in this trajectory are desirable because the immediate and acute phases after injury are characterized by elevated cellular response and degradative activity, representing a window of opportunity where therapeutic intervention to mitigate disease progression may be the most effective. In such studies a sensitive method of cartilage assessment is required to monitor the changes expected to occur in the cartilage extracellular matrix.

In clinical trials, direct assessment of cartilage repair tissue quality is performed histologically using small biopsies obtained during a second-look arthroscopy. Current histological scoring systems evaluate a number of characteristics believed to contribute to the long term durability of repair tissues but lack a specific category where a structured evaluation of collagen organization is made. Collagen architecture plays a critical role in cartilage load bearing properties and is therefore likely indicative of the long term durability of cartilage repair tissues. Designing a score where different levels of collagen organization could be assessed using a method sensitive to collagen orientation is required to enhance the analysis of repair tissue quality.

To these ends, two cartilage evaluation methodologies, streaming potentials and polarized light microscopy (PLM), were investigated, and the findings reported in the form of four manuscripts. The first two concern the sensitivity of the streaming potential method for evaluating cartilage and include an assessment of the effect of cold storage on cartilage properties. The objectives of these articles were:

- To evaluate the effects of refrigerated or frozen storage on the biomechanical and electromechanical properties of cartilage.
- To assess the ability of the streaming potential method to detect cartilage changes immediately following localized impact injury at distinct peak stress levels.

The third and fourth articles describe the development, testing, and validation of a polarized light microscopy (PLM) score for evaluating collagen organization and include detailed comparisons using scanning electron microscopy (SEM). The main objectives of these articles were:

- To develop and test a qualitative histological score using PLM that captures the features of ideal collagen organization present in young adult hyaline articular cartilage.
- To compare structural features of the collagen network in normal, degraded and repair cartilage tissues using PLM and SEM methods.

Streaming potentials detected cartilage changes produced immediately after impact injury in an equine explant model in a dose-dependent manner, where greater reductions in streaming potentials occurred as peak stress increased. Biomechanical tests of isolated cartilage disks indicated a similar trend in parameters associated with the collagen network but these tests were less sensitive to cartilage changes than streaming potentials. This study is the first to demonstrate the sensitivity of streaming potentials to cartilage changes produced by blunt impact. These findings suggest that streaming potentials are an appropriate method for monitoring cartilage changes in impact injury models, where cartilage degeneration is initiated by a focal mechanical injury that eventually progresses to osteoarthritis. The heightened sensitivity compared with biomechanical testing and the non-destructive nature of the streaming potential method will allow

subsequent studies to consider spatially-resolved, sequential measurements where cartilage can be assessed at the site of injury as well as in adjacent areas over time.

The effects of cold storage on cartilage electromechanical and biomechanical properties were investigated in bovine osteochondral explants. These experiments demonstrated that cartilage could be refrigerated in humid chambers for a period of 6 days with no detectable detrimental effects to either biomechanical or electromechanical properties. A single freeze-thaw cycle at -20°C resulted in a nominal effect on electromechanical properties with no evident biomechanical changes. These findings contribute new information regarding this important aspect of cartilage testing.

A new polarized light microscopy score was successfully developed and validated that provides a qualitative evaluation of different levels of collagen organization in histological sections of human repair cartilage. Excellent inter-reader reliability was observed when the score was applied by trained individuals in the assessment of normal, degraded and repair cartilage biopsies. Validation studies using SEM confirmed that the global collagen orientations observed in PLM were a consequence of true collagen fibre direction. Further comparisons of collagen structure using both PLM and SEM identified differences in fibre diameter distributions and zone proportions among normal, degraded and repair cartilage tissues. This work demonstrated that certain cartilage repair strategies are capable of producing stratified collagen organization that approximates the architecture of mature hyaline articular cartilage and is the first to provide evidence of this on an ultrastructural level.

Both assessment methods explored during the course of this thesis were found to be sensitive and appropriate means of evaluating cartilage in degeneration and repair scenarios, and could be readily adapted to other areas of cartilage research.

CONDENSÉ EN FRANÇAIS

Introduction

Le cartilage articulaire couvre les extrémités des os dans les articulations synoviales, comme le genou, et est responsable d'assurer un mouvement sans friction et sans douleur. Le cartilage assure aussi la distribution des charges appliquées à l'os sous-chondral. Le cartilage a une matrice extracellulaire (ECM) complexe qui est principalement composée de grandes molécules de protéoglycanes hydratés emprisonnées dans un réseau de collagène fibrillaire très organisé. Le cartilage articulaire adulte est stratifié, avec des fibres de collagène orientées tangentiellement à la surface articulaire dans la zone superficielle (SZ), orientées de plus en plus aléatoirement dans la zone de transition (TZ) et alignées perpendiculairement à l'interface entre le cartilage et l'os dans la zone profonde (DZ) (Benninghoff, 1925; Bullough & Goodfellow, 1968; Hedlund, Mengarelli-Widholm, Reinholt, & Svensson, 1993; Hughes, Archer, & Gwynn, 2005; Kaab, Gwynn, & Notzli, 1998; Schenk, Eggli, & Hunziker, 1986; Xia, Moody, Alhadlaq, & Hu, 2003). Sous un chargement en compression, le liquide interstitiel associé à la matrice de protéoglycanes est sous pression, plaçant le réseau de collagène sous tension et permettant une rigidité dynamique et un support de charge élevés (Chen, Bae, Schinagl, & Sah, 2001; Li, Korhonen, Iivarinen, Jurvelin, & Herzog, 2008; Park, Krishnan, Nicoll, & Ateshian, 2003). Le réseau de collagène fournit l'architecture structurelle du cartilage, immobilise les protéoglycanes qui résistent à l'écoulement des fluides, et résiste ainsi à la compression et à l'expansion des tissus afin d'assurer un support de charges efficace.

La matrice extracellulaire du cartilage articulaire a une structure spécialisée et une fonctionnalité importante, mais sa capacité de régénération est faible. Elle est isolée des systèmes sanguin, nerveux et lymphatique, et son entretien est la responsabilité d'une population dispersée de chondrocytes, environ 1-10% en volume, qui sont nourris par le liquide synovial lors des activités physiologiques normales (O'Hara, Urban, & Maroudas, 1990). Ces conditions rendent le cartilage sensible aux maladies dégénératives.

Dans l'arthrose (OA), la capacité de réparation des chondrocytes est excédée par les processus de dégradation (Bora & Miller, 1987; Loeser, 2006; Mandelbaum & Waddell, 2005). L'intégrité du cartilage peut être compromise par des facteurs comme les traumatismes, les blessures, l'obésité, le vieillissement, ou l'inflammation, lesquels produisent des contraintes anormales ou causent des processus métaboliques irréguliers dans le cartilage, menant finalement à l'arthrose (Aigner, Rose, Martin, & Buckwalter, 2004; Mandelbaum & Waddell, 2005). L'OA qui se développe suite à une blessure articulaire est décrite comme l'arthrose post-traumatique (PTOA), et des études suggèrent que la PTOA se développe dans environ 50% des patients qui subissent une blessure articulaire traumatique (Lotz, 2010; Lotz & Kraus, 2010).

Dans les derniers stades de l'arthrose, la douleur et la perte des fonctions articulaires sont des manifestations courantes. La dégradation du cartilage y est substantielle et une intervention chirurgicale est souvent la seule option pour le soulagement des symptômes. Par contre, les événements survenant au début de l'arthrose, tels que les dommages aigus de l'ECM et l'apoptose des cellules, sont asymptomatiques. Au cours des stades immédiats et aigus suivant l'apparition d'une lésion articulaire, les processus dégénératifs et de remodelage du cartilage sont très actifs. Cette période est donc idéale pour l'administration d'agents thérapeutiques pouvant modérer la progression de la maladie, offrant ainsi un grand potentiel de prévention (Lotz, 2010; Mandelbaum & Waddell, 2005; Scott & Athanasiou, 2006). En PTOA, où l'événement traumatique initial est connu, il existe une opportunité unique pour intervenir dans le premier stade.

Des interventions préventives ou thérapeutiques, qui ciblent les premiers stades de l'arthrose lorsque la dégénérescence du cartilage est potentiellement réversible, doivent être développées (Lotz, 2010). L'évaluation de ces approches nécessite des modèles pré-cliniques et des méthodes d'évaluation du cartilage capables de détecter les changements dégénératifs subtils attendus au début de la progression de la maladie, qui peuvent se produire sans détérioration visible de la surface du cartilage. Les méthodes biomécaniques actuelles d'évaluation de propriétés fonctionnelles du cartilage pourraient ne pas avoir la sensibilité nécessaire pour distinguer les changements mineurs du cartilage (Kleemann, Krocker, Cedraro, Tuischer, &

Duda, 2005), et d'autres méthodes objectives d'évaluation de la qualité du cartilage devraient être explorées.

Les dommages au cartilage, où l'os sous-chondral demeure intact, induit l'apoptose des chondrocytes et suscite une réponse de réparation des chondrocytes ayant survécu. Cependant, cette réponse est souvent inadéquate et une lésion permanente du cartilage peut éventuellement se former, ce qui rend l'articulation vulnérable à la dégénérescence (Buckwalter & Brown, 2004; Hunziker, 2002). Plusieurs activités de recherche se concentrent sur le développement de techniques pour la réparation des lésions focales du cartilage (Brittberg et al., 1994; Saris et al., 2008; Crawford, Heveran, Cannon, Foo, & Potter, 2009; Hoemann et al., 2005; Kon et al., 2010; Shive et al., 2006; Mithoefer, McAdams, Williams, Kreuz, & Mandelbaum, 2009)

Dans les études cliniques, l'efficacité des procédures de réparation du cartilage peut être évaluée indirectement par l'examen clinique, par les résultats rapportés par le patient, et par l'imagerie par résonance magnétique, ainsi que directement par l'évaluation histologique des biopsies des tissus cartilagineux en réparation récupérées au cours d'une arthroscopie de réévaluation (*second look* en anglais). Des systèmes de notation histologique sont actuellement utilisés pour caractériser la qualité du tissu cartilagineux en réparation par l'évaluation de caractéristiques spécifiques qui semblent contribuer à la durabilité à long terme (Mainil-Varlet et al., 2003; Mainil-Varlet et al., 2010; Roberts et al., 2003). Toutefois, aucun de ces systèmes n'inclut de catégorie pour l'évaluation de l'organisation du réseau de collagène, lequel joue un rôle critique sur la capacité de chargement du cartilage. Puisque la structure du réseau de collagène est très importante, une méthode pour caractériser systématiquement l'organisation du réseau de collagène dans les tissus cartilagineux en réparation est justifiée et souhaitable.

Dans cette thèse, deux méthodes pour évaluer le cartilage, soit les potentiels d'écoulement et la microscopie en lumière polarisée (PLM), ont été étudiées pour répondre aux besoins spécifiques rencontrés dans la recherche sur le cartilage. Le premier besoin était de trouver une méthode d'évaluation sensible pour détecter les changements subtils survenant dans le cartilage aux cours des premiers stades de l'arthrose. La méthode des potentiels d'écoulement a été

reconnue comme un candidat prometteur car il a démontré une plus grande sensibilité aux modifications du cartilage, comparativement aux tests biomécaniques, dans les études où les explants de cartilage ont été dégradés par des cytokines ou des enzymes. Le deuxième besoin est survenu au cours des études de réparation du cartilage, les systèmes de notation histologique actuellement utilisés pour évaluer la qualité des tissus cartilagineux en réparation s'avérant inadéquats pour évaluer l'architecture de collagène. Le réseau stratifié de collagène dans le cartilage articulaire est important en raison du rôle critique qu'il joue dans le support des charges, ce qui pourrait par conséquent en faire le meilleur indicatif de la durabilité des tissus cartilagineux en réparation. La PLM, qui est sensible à l'orientation du collagène fibrillaire, a été identifiée comme une méthode prometteuse pour l'élaboration d'un système de notation histologique qui décrit les caractéristiques détaillées de l'organisation idéale du collagène adulte auxquelles l'organisation du collagène dans les tissus cartilagineux en réparation peut être comparée. En conséquence, ces deux méthodes, les potentiels d'écoulement et la microscopie en lumière polarisée, ont été étudiées afin de déterminer si elles pouvaient répondre efficacement aux besoins identifiés.

Méthodologies de la thèse

Potentiels d'écoulement

Le cartilage présente un comportement électromécanique en raison de la charge négative des groupements sulfate et carboxyle sur les protéoglycanes, lesquels baignent dans le liquide interstitiel qui porte une charge nette positive due à l'équilibre de Donnan (Frank & Grodzinsky, 1987; Maroudas, 1967b; Maroudas, Muir, & Wingham, 1969; Sun, Guo, Likhitpanichkul, Lai, & Mow, 2004). Pendant la compression, les cations de chlorure mobiles en excès sont déplacés par rapport aux protéoglycanes fixes, générant des potentiels d'écoulement. Les potentiels d'écoulement reflètent la structure et la composition du cartilage, et sont connus pour être sensibles à la dégradation induite par des enzymes ou des cytokines (Bonassar, Jeffries, Paguio, & Grodzinsky, 1995; Bonassar et al., 1997; Chen, Nguyen, & Sah, 1997; Frank, Grodzinsky, Koob, & Eyre, 1987; Garon, Legare, Guardo, Savard, & Buschmann, 2002; Legare et al., 2002)

Un dispositif arthroscopique basé sur la méthode des potentiels d'écoulement, l'Arthro-BST[1], est disponible. Il mesure les potentiels d'écoulement lors d'une indentation légère de la surface du cartilage et calcule un paramètre quantitatif, le potentiel d'écoulement intégré (SPI), qui reflète la composition, la structure, et les propriétés de support de charge du cartilage. Ce dispositif fournit une méthode d'évaluation du cartilage qui est objective, rapide, et qui n'endommage pas le cartilage de façon permanente (Garon, 2007).

Microscopie en lumière polarisée

Le réseau fibrillaire de collagène dans le cartilage articulaire a la propriété d'anisotropie et peut être évalué dans les coupes histologiques en utilisant la microscopie en lumière polarisée (PLM) linéaire. Cette méthode a été utilisée pour étudier de nombreux aspects du cartilage normale, du cartilage dégradé, et du tissue cartilagineux en réparation. La PLM est un bon candidat pour le développement d'un système de notation histologique pour l'évaluation des tissus cartilagineux en réparation, où différents niveaux d'organisation du collagène peuvent être systématiquement décrits.

La PLM linéaire peut être effectuée sur un microscope optique avec l'ajout de deux filtres, d'un polariseur et d'un analyseur (Modis, 1991). Le polariseur est placé après la source de lumière et assure que seule la lumière polarisée linéairement, c'est-à-dire la lumière dans un plan unique qui est perpendiculaire à la direction de propagation de la lumière, est transmise à l'échantillon. Les matériaux optiquement anisotropes changent la direction de la lumière polarisée, un effet appelé biréfringence. C'est le cas des tissus fibrillaires contenant du collagène, tels que le cartilage articulaire, et cela peut être observé dans les coupes histologiques. La structure fibrillaire divise la lumière polarisée incidente en deux rayons orthogonaux d'une manière qui dépend de la direction du collagène à chaque point dans la coupe. Le filtre analyseur, placé après l'échantillon et à un angle droit avec le polariseur, recombine ces rayons pour créer l'image observée. L'orientation de l'analyseur assure que seule la lumière dont la polarisation est altérée par le tissu est transmise. L'intensité du signal résultant indique donc les régions du tissu

1 Biomomentum Inc., Laval, Quebec, Canada

ayant la capacité de modifier la polarisation de la lumière, donc qui sont optiquement actives, ou en d'autres termes biréfringentes, anisotropes, ou orientées. Dans le cartilage articulaire normal, la PLM révèle deux régions biréfringentes qui représentent les très orientées SZ et DZ, séparées par une zone non biréfringente, non orientée, la TZ (Arokoski et al., 1996; Hughes, et al., 2005; Kaab, et al., 1998; Kiraly et al., 1997; Korhonen et al., 2002; Rieppo et al., 2003; Speer & Dahners, 1979).

Les résultats des études utilisant les deux méthodes décrites précédemment sont présentés comme quatre articles de revues. Les hypothèses, descriptions des résultats et conclusions de chaque article sont résumés dans chacune des quatre sections suivantes.

Article I : Les effets de l'entreposage réfrigéré ou congelé du cartilage sur ses propriétés biomécaniques et électromécaniques

Les tests électromécaniques et biomécaniques sur le cartilage articulaire in vitro fournissent des informations importantes sur la structure et la fonction de ce tissu. Les difficultés à obtenir des tissus cartilagineux frais et la longueur des expériences nécessitent souvent un protocole d'entreposage qui peut affecter négativement les propriétés fonctionnelles du cartilage. Les trois hypothèses, qui ont été testées dans cet article concernant les effets de l'entreposage au froid du cartilage sur ses propriétés biomécaniques et électromécaniques, sont:

Hypothèse 1: l'entreposage réfrigéré à 4°C pendant 6 jours provoquera des changements détectables des propriétés biomécaniques et électromécaniques du cartilage.

Hypothèse 2: l'entreposage réfrigéré à 4°C pendant 12 jours mènera à des changements plus substantiels des propriétés biomécaniques et électromécaniques du cartilage comparativement à ceux observés après six jours.

Hypothèse 3: l'entreposage congelé à -20°C, exposant le cartilage à un seul cycle de gel-dégel, réduira les propriétés biomécaniques et électromécaniques du cartilage.

Dans l'expérience, on utilise une articulation de genou d'un jeune bovin. Les effets d'entreposage à 4ºC, pendant 6 et 12 jours, ou pendant un seul cycle de gel-dégel à -20ºC ont été examinés. Les mesures électromécaniques sont effectuées avec l'Arthro-BST, et, par la suite, des disques de cartilage de 3 mm de diamètre ont été isolés pour les essais biomécaniques en compression non-confinée. Les propriétés du cartilage ont ainsi été évaluées, y compris le potentiel d'écoulement intégré (SPI), le module élastique des fibrilles (Ef), le module à l'équilibre (Em) et la perméabilité hydraulique (k). Les disques de cartilage ont également été examinés histologiquement.

La première hypothèse, concernant l'entreposage réfrigéré à 4°C pendant 6 jours, a été réfutée. Les propriétés électromécaniques et biomécaniques ont été maintenues et ces résultats ont été appuyés par la coloration Safranin-O/Fast Green, où les échantillons au jour 6 étaient similaires aux contrôles. La seconde hypothèse, concernant l'entreposage réfrigéré à 4°C pendant 12 jours, a été soutenue par nos résultats expérimentaux. Des changements statistiquement significatifs ont été observés pour le SPI, qui a diminué à 32,3±5,5% des valeurs contrôles ($p<0,001$), et pour les propriétés biomécaniques, où Ef a diminué à 31,3±41,3% des valeurs contrôles ($p=0,046$), Em à 6,4±8,5% des valeurs contrôles ($p<0,0001$), et une augmentation de k à 2676,7±2562,0% des valeurs contrôles ($p=0,004$). Ces résultats indiquent que le tissu cartilagineux a été affaibli, que sa rigidité était substantiellement inférieure à celle des échantillons au jour 6 ou des contrôles. La coloration Safranin-O/Fast Green a révélé une perte quasi-complète des protéoglycanes dans ces échantillons. La troisième hypothèse, soit qu'un seul cycle de gel-dégel entraînerait une forte diminution des propriétés du cartilage, n'a pas été soutenue. Une tendance vers une diminution statistiquement significative de la SPI a été observée, mais ce changement était de petite taille et les valeurs SPI étaient en moyenne 94,2 ± 6,2% des valeurs contrôles ($p=0,083$). Aucun changement statistiquement significatif n'a été détecté pour tous les paramètres biomécaniques et les sections histologiques n'ont pas démontré de modifications par rapport aux contrôles.

En résumé, ces résultats indiquent que le cartilage frais pourrait être entreposé dans une chambre humide à 4ºC pour un maximum de 6 jours sans effets néfastes sur les propriétés

électromécaniques et biomécaniques du cartilage. Un seul cycle de gel-dégel à -20°C a produit un effet minimal sur les propriétés électromécaniques du cartilage, sans changements biomécaniques évidents. Une comparaison avec la littérature a suggéré qu'une attention particulière devrait être accordée à la manière dont les échantillons sont décongelés après congélation, notamment en réduisant le temps de décongélation à des températures élevées.

Article II : Un dispositif arthroscopique basé sur les potentiels d'écoulement est sensible aux changements du cartilage immédiatement après l'impact dans un modèle équin d'impact d'arthrose

Les études pré-cliniques qui ciblent les premiers stades de l'arthrose sont nécessaires pour développer des interventions thérapeutiques qui peuvent atténuer la progression de la maladie. Dans ces stades premiers, la dégradation du cartilage n'est pas trop avancée et ces études pourraient bénéficier d'une méthode d'évaluation suffisamment sensible pour détecter les changements subtils se produisant dans la matrice extracellulaire du cartilage. Par conséquent, l'objectif de cet article était de déterminer si des mesures de potentiels d'écoulement par indentation manuelle peuvent détecter les modifications du cartilage qui suivent immédiatement l'impact mécanique, et de comparer leur sensibilité à des tests biomécaniques. Dans cette étude, on a testé les deux hypothèses suivantes:

Hypothèse 1: Les potentiels d'écoulement peuvent distinguer les changements dans le cartilage produits par des impacts de différents niveaux d'une manière dépendante de la dose reçue.

Hypothèse 2: Les potentiels d'écoulement sont plus sensibles aux changements dans le cartilage articulaire produits par une blessure d'impact comparativement aux tests biomécaniques.

Une paire de genoux équins a été utilisée dans cette étude et 36 positions indépendantes ont été identifiées sur chaque trochlée. Des blessures d'impact localisées ont été infligées à l'un des trois niveaux de contrainte sélectionnés avec un dispositif fait sur mesure. Les propriétés du cartilage ont été évaluées par des mesures de potentiels d'écoulement, avant et après l'impact,

avec le dispositif Arthro-BST, et par des tests de relaxation de contrainte en compression non-confinée sur des disques cartilagineux isolés. Comme pour l'article I, ces tests fournissent le potentiel d'écoulement intégré (SPI), le module élastique des fibrilles (Ef), le module à l'équilibre (Em) et la perméabilité hydraulique (k). Plusieurs coupes histologiques ont été colorées à la Safranin-O/Fast Green, et d'autres sont demeurées non colorées pour les observations en PLM.

Les trois niveaux de blessures d'impact localisées, soient faible, 17,3 ± 2,7 MPa (n = 15), moyen, 27,8 ± 8,5 MPa (n = 13), ou élevé, 48,7 ± 12,1 MPa (n = 16), ont été livrés avec un temps de montée d'environ 1 ms. Les impacts ont provoqué des changements du cartilage d'une manière dépendante de la dose reçue. Les impacts élevés et, à un degré moindre, les impacts moyen ont causé des dommages immédiats et mesurables au réseau de collagène. Ils ont été détectés comme une réduction de la SPI et Ef, couplée à une augmentation de la perméabilité (k), bien qu'il n'y ait pas suffisamment de temps pour qu'une perte substantielle des protéoglycanes se produise, tel que démontré par Em et les coupes colorées en Safranin-O.

La première hypothèse, soit que les potentiels d'écoulement peuvent distinguer les changements dans le cartilage produits par des impacts de différents niveaux, a été partiellement confirmée. Les valeurs SPI ont été réduites en fonction du niveau de contrainte de l'impact et ces observations ont été soutenues par des différences statistiquement significatives détectées suite aux impacts élevés ($p < 0,001$) et moyens ($p = 0,006$) par rapport aux contrôles.

La seconde hypothèse, soit que le SPI est plus sensible à ces changements que les tests biomécaniques, a été vérifiée. Ef, ce qui représente la rigidité du réseau de collagène, a été significativement réduit pour les échantillons à impact élevé seulement ($p<0,001$ trochlée latérale, $p=0,042$ trochlée médiale), dont la perméabilité a également augmenté ($p=0,003$ trochlée latérale, $p=0,007$ trochlée médiale). Bien que les propriétés électromécaniques et biomécaniques aient toutes deux diminué en fonction du niveau de contrainte de l'impact, l'ampleur de l'effet a été systématiquement supérieure pour le SPI comparativement aux paramètres biomécaniques, et ce, pour les trois niveaux d'impact. Cette sensibilité supérieure des mesures de SPI aux changements du cartilage a également été démontrée par des réductions statistiquement

significatives ($p<0.05$) en SPI après les impacts élevés et moyens, tandis que Ef et k ont détecté des lésions du cartilage de manière statistiquement significative après des impacts élevés seulement.

Les données ont montré des corrélations significatives, de façon modérée à forte ($p<0,05$, $n=68$) entre SPI et Ef ($r=0,857$), Em ($r=0,493$), log (k) ($r =-0,484$), et avec l'épaisseur du cartilage ($r=-0,804$). Enfin, les modifications histologiques dues à l'impact ont été limitées à la présence de dommages dans la zone superficielle, lesquels ont augmenté avec le niveau de contrainte de l'impact. Les observations en microscopie à lumière polarisée ont permis d'observer des petites fissures dans la surface articulaire qui n'étaient pas visibles dans les coupes colorées.

Les mesures avec les potentiels d'écoulement ont été plus sensibles aux changements du cartilage articulaire causés par les blessures d'impact localisées que les paramètres biomécaniques mesurés sur les échantillons isolés. Le dispositif Arthro-BST pourrait faire des mesures sans dommage permanent au cartilage. Les corrélations entre le SPI et les paramètres biomécaniques soutiennent encore davantage la relation entre les mesures électromécaniques, qui sont faites *in situ*, et les propriétés intrinsèques du cartilage.

Ce type de modèle d'impact, combiné avec les potentiels d'écoulement pour détecter les changements subtils du cartilage, pourrait fournir un système modèle approprié pour tester l'efficacité d'agents thérapeutiques pour atténuer la progression de l'arthrose dans les premiers stades de la maladie. Puisque la méthode des potentiels d'écoulement fonctionne sans endommager le cartilage de façon permanente, l'évaluation séquentielle du cartilage dans le temps est possible pour des modèles *in vivo* similaires, où la dégénérescence initiale est locale mais pourrait graduellement impliquer une plus grande surface articulaire.

Article III : Une méthode de microscopie en lumière polarisée pour une notation précise et fiable de l'organisation de collagène dans les tissus cartilagineux en réparation

Dans les études cliniques, l'efficacité des procédures de réparation du cartilage pourrait être évaluée directement par l'évaluation histologique de petites biopsies du tissu cartilagineux en réparation récupérées au cours d'une arthroscopie de réévaluation après une certaine période de suivi. Les systèmes actuels de notation des coupes histologiques sont utilisés pour caractériser la qualité du tissu cartilagineux en réparation (Mainil-Varlet, et al., 2003; Mainil-Varlet, et al., 2010; Roberts, et al., 2003). Toutefois, aucun des systèmes de notation disponibles ne comprend une catégorie distincte pour l'évaluation de l'organisation du réseau de collagène, laquelle est essentielle à la capacité de chargement du cartilage et à sa durabilité (Hughes, et al., 2005; Julkunen et al., 2009; Moger et al., 2009). Une méthode pour caractériser systématiquement l'organisation du réseau de collagène est justifiée, cette composante de la matrice extracellulaire du cartilage étant fonctionnellement importante. Pour cette raison, l'objectif de cet article était de développer et de tester un système de notation histologique qualitatif par PLM qui décrit les caractéristiques idéales d'organisation du collagène présent dans le cartilage articulaire de jeunes adultes. Les deux hypothèses suivantes on été testées:

Hypothèse 1: Le système de notation proposé par PLM peut caractériser systématiquement l'organisation du collagène dans les biopsies humaines de cartilage normal et dégradé, et aussi dans les tissus cartilagineux en réparation.

Hypothèse 2: Le système de notation proposé par PLM est hautement reproductible lorsqu'il est appliqué par plusieurs observateurs formés.

Le système de notation par PLM utilise une échelle ordinale de 0-5 pour évaluer l'ampleur de la ressemblance entre l'organisation du réseau de collagène et celle du cartilage articulaire de jeunes adultes (score de 5) ou d'un tissu totalement désorganisé (score de 0). La fiabilité inter-observateur a été évaluée en utilisant les coefficients de corrélation intraclasse (ICC) pour accord. Les ICCs ont été calculés à partir des scores de trois observateurs formés qui

ont évalué indépendamment des coupes histologiques à l'aveugle obtenues à partir de biopsies humaines de cartilages normaux (n=4), dégradés (n=2) et en réparation (n=22).

Le système de notation par PLM réussit à distinguer les cartilages normaux ou dégradés, et les tissus cartilagineux en réparation, ces derniers affichant une plus grande complexité dans la structure du collagène. Une excellente reproductibilité inter-observateur a été observée avec des ICC pour accord de 0,90 [de la ICC(2,1)] (limite inférieure de 95%, intervalle de confiance est 0,83) et 0,96 [de la ICC(2,3)] (limite inférieure de 95%, intervalle de confiance est 0,94), indiquant la fiabilité des résultats d'un seul observateur et la moyenne des scores des trois observateurs respectivement.

Ce système de notation par PLM offre un nouveau mode d'évaluation systématique de l'organisation de collagène dans les tissus cartilagineux en réparation. Le réseau de fibrilles de collagène joue un rôle critique sur la capacité de chargement du cartilage et sur la durabilité de la réparation du cartilage, mais il n'a pas suffisamment été évalué dans les tissus cartilagineux en réparation par les systèmes de notation histologique présentement disponibles. On propose que le nouveau système de notation par PLM soit utilisé avec les autres systèmes de notation actuels pour avoir une évaluation plus complète de la qualité des tissus cartilagineux en réparation.

Article IV: Les caractéristiques structurelles du réseau de collagène du cartilage normal, du cartilage dégradé et du tissu cartilagineux en réparation observés en lumière polarisée et en microscopie électronique à balayage

La structure du collagène a été caractérisée en utilisant des méthodes de PLM et de microscopie électronique à balayage (SEM) pour obtenir des données importantes sur cet aspect de la matrice extracellulaire qui est essentiel pour le fonctionnement biomécanique et la durabilité du cartilage. Le système de notation par PLM (Article III) et de nouvelles méthodes développées en SEM ont été utilisés pour comparer les caractéristiques structurelles du réseau de collagène dans le cartilage normal (n=6), dans le cartilage dégradé (n=6), et dans le tissu cartilagineux en réparation (n=22). Les deux hypothèses suivantes ont été testées:

Hypothèse 1: Les notations de l'organisation globale du collagène, évaluée séparément avec PLM et SEM, sont fortement corrélées.

Hypothèse 2: Les différences dans les caractéristiques structurelles du réseau de collagène, y compris les proportions des zones et les diamètres des fibres de collagène, sont spécifiques aux types de tissus, soit le cartilage normal, dégradé et en réparation.

L'organisation du collagène (CO) a été évaluée par le système de notation par PLM (Article III) et les proportions des zones ont été mesurées sur les images en PLM. Des images SEM à fort grossissement ont été capturées à partir d'emplacements assortis aux images PLM. Les orientations des fibres de collagène ont été évaluées par SEM et ont été comparées à celles observées par PLM. L'organisation du collagène a également été évaluée dans des images SEM individuelles et combinées pour produire un score SEM-CO pour l'organisation globale du collagène analogue au système de notation par PLM-CO. Les diamètres des fibres de collagène ont été mesurés par SEM en utilisant un logiciel calibré. Toutes les notes ont été réalisées indépendamment par trois observateurs formés.

Les notations PLM-CO et SEM-CO, pour évaluer l'organisation globale du collagène, ont été corrélées, $r=0,786$ ($p<0,00001$, $n=32$), après exclusion de deux cas atypiques. L'orientation des fibres observée par PLM a été validée par SEM, où la correspondance entre PLM et SEM s'est produite pour 91,6% des images. Un excellent accord entre les orientations du collagène, observées au PLM et au SEM, a confirmé que les caractéristiques de biréfringence sont une conséquence de l'orientation réelle des fibres de collagène. Les proportions des zones profonde (DZ), transitoire (TZ) et superficielle (SZ) du cartilage sont en moyenne 74,0±11,4%, 18,6±8,7%, et 7,3±1,5% dans le cartilage normal, et 45,6±11,0%, 47,2±10,4% et 9,5±4,3% dans le cartilage dégradé, respectivement. Les diamètres des fibres dans le cartilage normal augmentent avec la profondeur de la surface articulaire: 55,8±15,9nm (SZ), 87,5±17,9nm (TZ) et 108,2±21,4nm (DZ). Les diamètres des fibres ont été plus faibles dans les biopsies de tissus cartilagineux en réparation, soient 60,4±9,3nm (SZ), 63,2±12,8nm (TZ) et 67,2±16,8nm (DZ). Les cartilages

dégradés avaient de plus larges gammes de diamètres des fibres et des distributions bimodales, reflétant peut-être une nouvelle synthèse et un remodelage. Les biopsies de réparation ont révélé le potentiel de certaines procédures de réparation du cartilage à produire une organisation zonale du collagène ressemblant à la structure native du cartilage articulaire.

Ces études comparatives effectuées avec les méthodes PLM et SEM ont identifié des différences spécifiques dans la structure du réseau de collagène, y compris les diamètres des fibres et les proportions des zones, entre le cartilage normal et les cartilages dégradés ou les tissus cartilagineux de réparation. Ces données offrent une évaluation détaillée de la structure du réseau de collagène, qui pourrait être utile dans l'élaboration de stratégies de réparation du cartilage capable de recréer l'architecture fonctionnelle du collagène. Le système de notation par PLM pour évaluer l'organisation du collagène a été validé en utilisant les images SEM en montrant que l'organisation du collagène déduite à l'aide des caractéristiques de biréfringence en PLM reflète l'ultrastructure du collagène, qui était directement visible au SEM. Enfin, cette étude est la première à fournir des preuves ultrastructurales de fibres de collagène dans les tissus cartilagineux en réparation ressemblant à l'architecture stratifiée du cartilage articulaire adulte.

Conclusions

Les potentiels d'écoulement et la microscopie en lumière polarisée ont été des méthodes appropriées d'évaluation du cartilage capable de répondre aux exigences de deux besoins spécifiques identifiés dans les domaines de la dégénérescence du cartilage et de la réparation. Les potentiels d'écoulement sont une méthode prometteuse pour évaluer les changements subtils du cartilage attendus au cours des premiers stades de dégénérescence dans des modèles pré-cliniques de PTOA. En plus, les conséquences de l'entreposage réfrigéré et congelé sur les propriétés biomécaniques et électromécaniques du cartilage ont été élucidées, permettant de formuler des recommandations pertinentes pour les essais sur le cartilage. Un nouveau système de notation par PLM a été développé et validé, fournissant une méthode d'évaluation systématique de l'organisation du collagène dans les tissus cartilagineux en réparation, une caractéristique essentielle pour la fonction du cartilage et un indicateur probable de la durabilité du tissu réparé.

D'autres études sur la structure du réseau de collagène en PLM et SEM ont permis d'identifier un certain nombre de différences liées au type de tissus, y compris des variations dans la distribution des diamètres des fibres et dans les proportions des zones dans le cartilage dégradé et les tissus cartilagineux en réparation, par rapport au cartilage normal. Les potentiels d'écoulement et la microscopie en lumière polarisée ont été des méthodes d'évaluation appropriées pour le cartilage articulaire dans les scénarios de dégénérescence et de réparation.

Les études contenues dans cette thèse ont apporté plusieurs nouvelles conclusions pertinentes. Les articles I et II ont été les premiers à signaler la sensibilité de la méthode des potentiels d'écoulement aux changements du cartilage induits par une blessure d'impact ou des conditions d'entreposage à froid. La polyvalence de la méthode des potentiels d'écoulement a été démontrée et les corrélations avec les propriétés intrinsèques du cartilage ont été établies. L'article III a introduit un nouveau système de notation par PLM qui offre une méthode systématique pour évaluer les différents niveaux d'organisation du collagène dans les tissus cartilagineux en réparation. Enfin, l'article IV a apporté la première preuve ultrastructurale que les fibres de collagène dans les tissus cartilagineux en réparation peuvent s'approcher de la structure stratifiée du collagène du cartilage articulaire adulte.

TABLE OF CONTENTS

LIST OF TABLES

LIST OF FIGURES

LIST OF SYMBOLS AND ABBREVIATIONS

ACI	Autologous chondrocyte implantation
ASTM	American society for testing and materials
CO	Collagen organization
dGEMRIC	Delayed gadolinium-enhanced magnetic resonance imaging of cartilage
DZ	Deep zone
ECM	Extracellular matrix
E_1	Tensile Young's modulus of the transverse plane
E_3	Compressive Young's modulus in the axial direction
Em	Matrix modulus
Ef	Fibril modulus
GAG	Glycosaminoglycan
H_A	Aggregate modulus
IL-1α	Interleukin-1α
IL-1ß	Interleukin-1ß
ICC	Intraclass correlation coefficient
ICRS	International cartilage repair society
IRHD	International rubber hardness degree
k	Hydraulic permeability
KOOS	Knee injury and osteoarthritis outcome score
MHz	Megahertz
MMP	Matrix metalloproteinase
MPa	Megapascal
MRI	Magnetic resonance imaging
OA	Osteoarthritis
OCT	Optical coherence tomography
OL	Orientation label
PLM	Polarized light microscopy

PLM-CO	Collagen organization evaluated in PLM
PLM-OL	Predominant orientation observed in each ROI viewed in PLM
PS-OCT	Polarization sensitive optical coherence tomography
PTOA	Post-traumatic osteoarthritis
ROI	Region of interest
s	Second
SEM	Scanning electron microscopy
SEM-CO	Collagen organization evaluated in SEM
SEM-OL	Predominant orientation observed in each SEM image
SF-36	Short Form 36-item health survey
SPI	Streaming potential integral
SZ	Superficial zone
T	Tesla
TIMP	Tissue inhibitors of matrix metalloproteinase
T2	Transverse relaxation time
TZ	Transitional zone
US	Ultrasound
υ_m	Poisson's ratio
υ_{eff}	Effective Poisson's ratio
WOMAC	Western Ontario and McMaster Universities arthritis index

INTRODUCTION

Osteoarthritis (OA) is among the most prevalent chronic health conditions in Canada, affecting more than 10% of adults in the general population[2]. OA is described as a progressive and permanent deterioration of articular cartilage, and can negatively impact quality of life particularly at the later stages of the disease. Risk factors for OA include obesity, age, heredity and joint injury among others (Mandelbaum & Waddell, 2005), and present treatment strategies target symptom relief as no disease modifying agents are currently available (Lotz, 2010).

Current research efforts target many aspects of OA, ranging from improving the present understanding of normal cartilage development and mechanisms of degeneration to the development of cartilage repair strategies. Pre-clinical studies are integral to the development and testing of potential therapeutic or repair approaches and clinical trials are essential for assessing the efficacy of the most promising candidates in humans. These types of studies are substantial undertakings and having responsive evaluation methods for assessing cartilage changes are important to their success.

Preventative or therapeutic interventions that target the early stages of OA, when cartilage degeneration is still potentially reversible, need to be developed (Lotz, 2010). Testing these approaches requires pre-clinical models and cartilage assessment methods capable of monitoring the subtle degradative changes expected early on in the disease progression that can occur without visible cartilage surface disruption. Current biomechanical methods for evaluating cartilage functional properties may lack the required sensitivity to distinguish low-grade cartilage changes (Kleemann, et al., 2005) and other objective methods of evaluating cartilage quality should be explored.

In clinical studies, the efficacy of cartilage repair procedures can be gauged indirectly by clinical examination, patient reported outcomes, and magnetic resonance imaging (MRI), as well

---

2 Public Health Agency of Canada, 2010. « Life with Arthritis in Canada: A Personal and Public Health Challenge » ISBN: 978-1-100-15986-7.

as directly by histological assessment of repair tissue biopsies retrieved arthroscopically after a specified follow-up period. Histological scoring systems are used to characterize cartilage repair tissue quality by rating specific features that are expected to contribute to long-term durability (Mainil-Varlet, et al., 2003; Mainil-Varlet, et al., 2010; Roberts, et al., 2003). However, none of the available scoring systems include a separate category for evaluating collagen network organization, which is central to cartilage biomechanical properties and durability and whose specialized anisotropic structure is a hallmark of mature articular cartilage (Hughes, et al., 2005; Julkunen, et al., 2009; Moger, et al., 2009). A method for systematically characterizing organization of the functionally important collagen network in repair cartilage tissues is warranted.

In this thesis, the use of streaming potentials and polarized light microscopy were explored as promising methodologies for detecting early cartilage changes in a pre-clinical injury model of OA, and for assessing collagen structure in human cartilage repair tissue, respectively. Streaming potentials result from cartilage composition, structure and function, thus recommending the method for this particular application where subtle cartilage changes associated with early degeneration are expected to occur. The sensitivity of the streaming potential method to cartilage changes produced by mechanical impact was not known and needed to be evaluated. Polarized light microscopy is sensitive to collagen orientation, providing a suitable method for developing a structured assessment of collagen organization in human repair cartilage, where evaluation is limited to histological approaches. Until these studies were undertaken, no comprehensive histological score for evaluating collagen structure was available. This type of evaluation is warranted as collagen structure is heavily implicated in cartilage load bearing, and could act a surrogate for predicting the long-term durability of cartilage repair tissues.

Organization of the Thesis

The body of the thesis is structured into seven chapters, which are framed by the Introduction and Conclusions & Recommendations sections. Chapter 1 contains a review of the

literature, consisting of relevant information about articular cartilage in degeneration and repair, as well as current cartilage assessment methods, in order to provide context for the work described in the subsequent chapters. The thesis objectives and hypotheses are summarized in Chapter 2. They were subdivided into four sets that were addressed in each of four separate journal articles, which are contained in Chapters 3 to 6 respectively. A general discussion follows in Chapter 7, where interesting points related to the thesis as a whole are critically discussed. Finally, the Conclusions & Recommendations section summarizes the main conclusions of the thesis and describes recommendations for future work.

CHAPTER 1. REVIEW OF THE LITERATURE

1.1 Articular Cartilage

Articular cartilage covers the ends of bones in synovial joints, such as the knee, and macroscopically appears white and glassy in young, healthy joints. It is responsible for withstanding loading and transmitting applied forces to underlying subchondral bone and other joint tissues. The articular surfaces are bathed in synovial fluid, where the low coefficient of friction, approximately 0.013 (Charnley, 1960; Yao, Laurent, Johnson, R., & D., 2003), enables pain-free, near-frictionless motion.

1.1.1 Composition

These functions are possible because of the specialized composition and structure of articular cartilage. The extracellular matrix (ECM) is mainly composed of hydrated proteoglycan molecules trapped in a highly organized network of fibrillar collagens.

Proteoglycans are glycosaminoglycan (GAG) chains covalently linked to a protein core (Neame, 1993) (**Figure 1.1**). The GAGs, consisting of repeating disaccharides, have high charge density due to the presence of negatively charged carboxyl and sulphate groups. Proteoglycans bind to interstitial fluid, composed of water and electrolytes (Li, Buschmann, & Shirazi-Adl, 2003), and contain an excess of positive mobile ions due to Donnan equilibrium. The fibrillar collagen network primarily concerns collagen types II, VI and XI, where 90-95% is type II (Kish, Modis, & Hangody, 1999; Responte, Natoli, & Athanasiou, 2007). Collagen type II molecules are formed of triple helices of polypeptide chains, which assemble into heterofibrils with collagen types VI and XI that eventually collect into fibre bundles. As cartilage matures, collagen fibres increase in diameter, become crosslinked, and form a characteristic network structure. Cartilage is sparsely populated by chondrocytes, approximately 1-10% by volume, that regulate ECM development (Hunziker, Kapfinger, & Geiss, 2007; Responte, et al., 2007) and subsequently maintain cartilage in adulthood by preserving a balance between synthesis and degradation

(Mandelbaum & Waddell, 2005). Typically, adult human cartilage consists of 65-85% water, 12-24% collagen, 3-6% GAG and 16,000-90,000 chondrocytes per milligram of wet tissue (Hoemann, 2004).

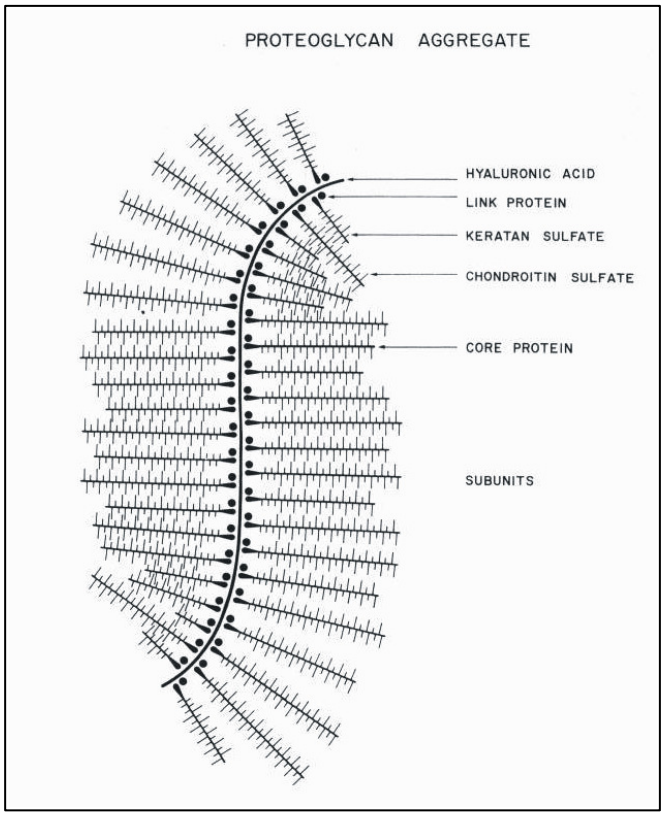

Figure 1.1: Schematic of a proteoglycan macromolecule. The glycosaminoglycans, keratin sulphate and chondroitin sulphate, are negatively charged. *Source:* originally created by Rosenberg (1975) and reprinted in Mow & Lai (1979).

1.1.2 Structure

Relative concentrations of collagen, proteoglycan and water vary with depth from the articular surface. The depth dependent organization of the ECM is described as three zones and one layer, namely the superficial zone (SZ), transitional zone (TZ), deep zone (DZ), and the calcified cartilage layer (**Figure 1.2**). The SZ, occupying approximately 5-10% of total non-calcified thickness in humans and animals (Kurkijarvi et al., 2008; Nissi et al., 2006), has the

lowest concentration of proteoglycans, as well as densely packed collagen fibres that lie tangentially with respect to the articular surface (Hunziker, Quinn, & Hauselmann, 2002). Chondrocytes align with the collagen fibres and thus appear flat and elongated (Poole, 1993). In the TZ, proteoglycan concentration increases, collagen fibres become thicker and more randomly oriented, and cells assume a rounded morphology (Hunziker, et al., 2002). The DZ is characterized by the thickest collagen fibres, which are oriented perpendicularly to the cartilage-bone interface, and the highest concentration of proteoglycans. Chondrocytes here are rounded and tend to form columns aligned with collagen (Hunziker, et al., 2002; Poole, 1993). A depth dependent water gradient, inversely related to proteoglycan distribution, is also present, with water content decreasing from a peak in the SZ to a minimum in the DZ (Aydelotte & Kuettner 1993). The structural properties described above apply generally to animal and human cartilages but can be influenced by age, activity, species, and topographical location on the joint surface.

Compared with the SZ, zonal proportions of the transitional and deep zones vary considerably with species, age and location on the joint surface (Poole, 1993). The DZ is typically the largest zone, averaging 63-75% in human knees (Kurkijarvi, et al., 2008; Nissi, et al., 2006), or 60-90% in animal species (Arokoski, et al., 1996; Hughes, et al., 2005; Hunziker, 1992; Hyttinen et al., 2001; Kaab, et al., 1998; Moger, et al., 2009; Nissi, et al., 2006; Panula et al., 1998; Rieppo, et al., 2003; Xia, et al., 2003; Yarker, Aspden, & Hukins, 1983). Consequently, the TZ generally occupies 20%-26% in humans and up to 30% in animal species. Aside from biological differences, discrepancies in zonal proportions can also reflect the assessment method selected. For example, some investigators determine zone boundaries based on chondrocyte morphology in stained histological sections (Buckwalter et al., 1988; Hunziker, 1992; Poole, 1993), while others use polarized light microscopy, where zones are delineated based on birefringence characteristics of collagen fibres (Kurkijarvi, et al., 2008; Nissi, et al., 2006).

Finally, the calcified cartilage layer provides an interface between cartilage and underlying subchondral bone (Poole, 1993). It commences at the tidemark or calcification front and ends at the cement line, which indicates the beginning of the cortical subchondral bone plate (Madry, van Dijk, & Mueller-Gerbl, 2010; Hwang, Ngo, & Saito, 1990). Large-diameter collagen

fibre bundles extend from the DZ into calcified cartilage, providing an anchor that contributes to cartilage functional properties and durability (Archer, Redman, Khan, Bishop, & Richardson, 2006).

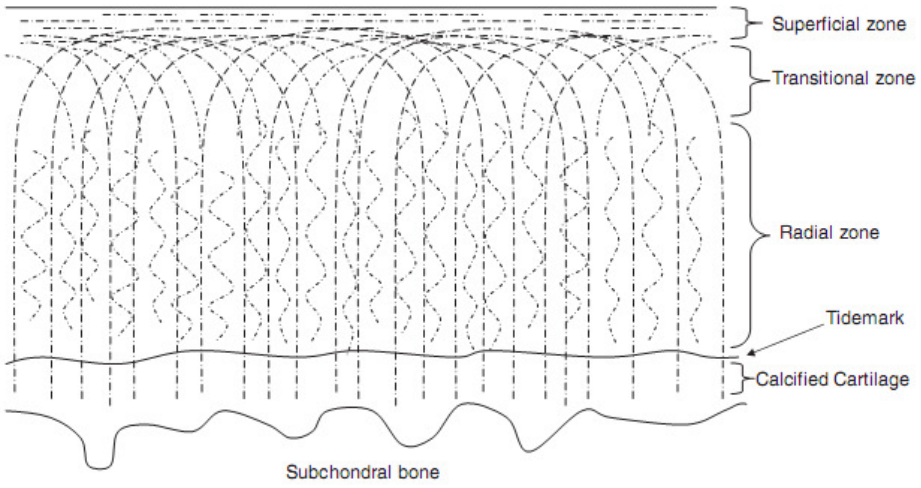

Figure 1.2: Schematic representation of collagen organization in the three zones of articular cartilage, the superficial zone (SZ), transitional zone (TZ) and deep or radial zone (DZ), as well as the calcified cartilage layer. *Source:* Ugryumova et al. (2005).

1.1.3 Development

The heterogeneous composition and organization of mature articular cartilage is a consequence of post-natal endochondral development, which reaches completion in early adulthood (Hunziker, 2009; Hunziker, et al., 2007).

In the early post-natal period, chondrocytes, differentiated from mesodermal stem cells, generate a cartilaginous tissue that operates as a scaffold for the development of joint tissues, including bone, meniscus, synovium and cartilage (Hunziker, 2009; Pacifici et al., 2006). This isotropic immature cartilage serves as both an articulating layer and a growth plate that contributes to the elongation and radial expansion of the epiphyseal bone (**Figure 1.3**). Throughout childhood the pool of chondroprogenitor cells, which are precursors to chondrocytes

and reside in the superficial zone, continue to proliferate and rapidly lay down immature cartilage that is resorbed and remodelled into epiphyseal bone. In this process all of the immature cartilage, except for the superficial zone, is remodelled into bone, meaning that the chondroprogenitor cells are continually laying down new immature cartilage (Hunziker, et al., 2007). During puberty, the role of these cells change; epiphyseal growth ceases and they differentiate into cells that can produce mature articular cartilage (Hunziker, et al., 2007). Understanding the natural mechanisms by which mature articular cartilage is formed is critical for optimizing repair strategies for articular cartilage (Hunziker, 2009).

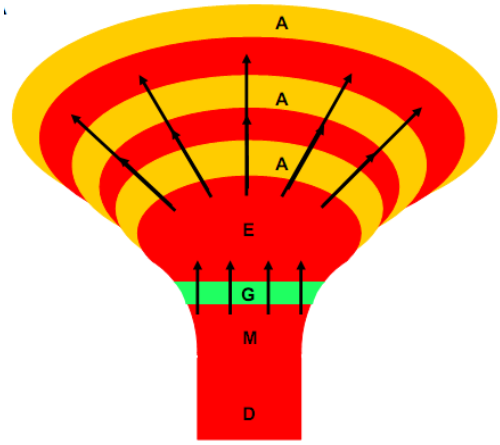

Figure 1.3: Schematic of post-natal endochondral development, where the articular cartilage layer (A) serves as a growth plate for expanding the epiphyseal bone in longitudinal, radial and lateral directions. The metaphysis (M) and diaphysis (D) are elongated by the true growth plate (G). *Source:* Hunziker et al. (2007).

1.1.4 Biomechanics

Cartilage function arises from its heterogeneous structure. Cartilage is described as a biphasic, fibre-reinforced, poroelastic material, in which the pores of the extracellular fibre-reinforced solid phase are infused with interstitial fluid (Li, et al., 2003; Soulhat, Buschmann, & Shirazi-Adl, 1999). Under compression, interstitial fluid associated with proteoglycan macromolecules is displaced as it flows out of the deformed solid matrix thereby pressurizing the

fluid and allowing for load-bearing (Ateshian, 2009; Chen, et al., 2001; Korhonen et al., 2003; Li, et al., 2003; Park, et al., 2003). The collagen network is placed in tension as it attempts to restrain the swollen proteoglycan matrix and resist tissue expansion (Cohen, Lai, & Mow, 1998; Soulhat, et al., 1999).

Cartilage is a viscoelastic material and its non-linear behaviour can be assessed by a variety of biomechanical testing methods, which use one of two standard loading protocols (Ateshian, 2009; Korhonen, 2003). In stress-relaxation, a step deformation is applied to which cartilage has an initial elastic response followed by a time dependent relaxation response that proceeds until equilibrium with the applied load is achieved. Creep behaviour is also observed in viscoelastic materials, where a constant load produces a time-dependent deformation response (**Figure 1.4**).

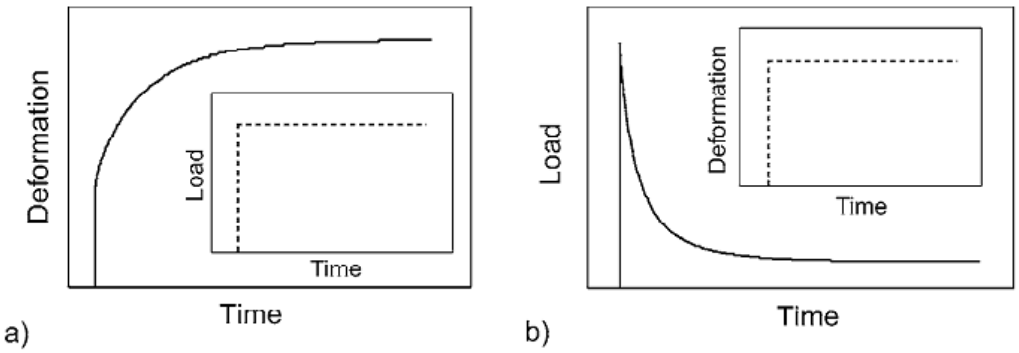

Figure 1.4: Schematic illustrating the two standard loading protocols used in cartilage biomechanical testing, (a) creep and (b) stress relaxation. *Source:* Korhonen (2003).

Common cartilage biomechanical testing geometries include indentation, confined and unconfined compression (**Figure 1.5**). In indentation testing, loading is applied through an indenter to test cartilage while it remains on the joint surface. Compression tests are carried out in either confined or unconfined geometries on full thickness cartilage disks extracted from the joint surface. In confined compression, the disk is placed in a chamber that ideally provides complete confinement of the lateral edges and the disk surface is in contact with a porous platen. In unconfined compression, the lateral edges of the cartilage disk remain free and the disk surfaces

are contact flat, non-porous platens. Unconfined compression and indentation may provide better representations of physiological loading compared to confined compression because interstitial fluid is permitted to flow laterally in these geometries.

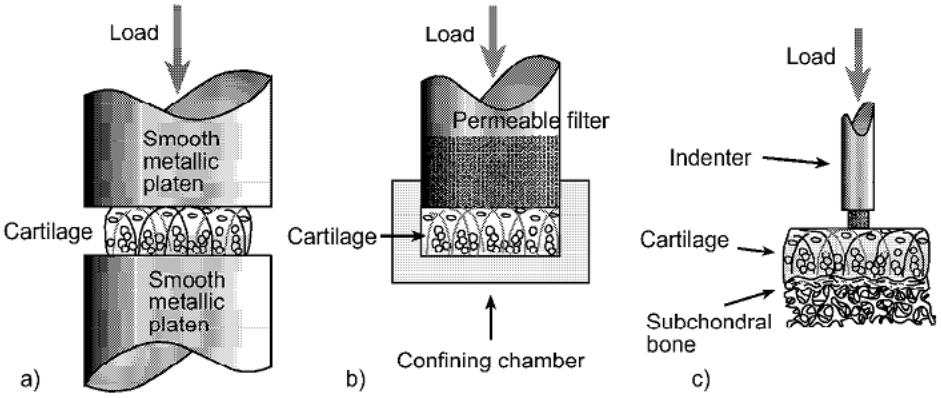

Figure 1.5: Common geometries for biomechanical testing of articular cartilage, including (a) unconfined compression, (b) confined compression, and (c) indentation. *Source:* Korhonen (2003).

Many mathematical models have been developed that describe the load bearing behaviour of cartilage and can be used to interpret results obtained during biomechanical testing and procure relevant cartilage material properties. These include the isotropic biphasic model (Mow, Kuei, Lai, & Armstrong, 1980), the transversely isotropic model (Cohen, Lai, Chorney, Dick, & Mow, 1992) and the fibril-network-reinforced biphasic model (Soulhat, et al., 1999) for which analytical solutions in confined and unconfined compression are possible. Analytical models of indentation tests are difficult to attain because of the complex boundary conditions related to this geometry (Lu, Miller, Chen, Guo, & Mow, 2007; Mow, Gibbs, Lai, Zhu, & Athanasiou, 1989).

Biphasic Model

The biphasic model of cartilage is based on poroelastic theory, where the constitutive equations describe an elastic solid containing pores filled with a fluid (Mow, et al., 1980). In this model, the elastic solid accounts for both collagen and proteoglycan components and is assumed

to be isotropic. The fluid phase is water containing electrolytes and is considered to be inviscid, meaning that is has no viscosity and is unable to support shear stresses. Model parameters include aggregate modulus, H_A, defined as the intrinsic elastic modulus of the solid matrix, and hydraulic permeability, k, describing the rate of fluid flow out of the tissue. k changes as the specimen is being compressed, and the value determined by the model fit is an averaged permeability for the duration of the mechanical test.

The biphasic model was used to fit experimental data collected in confined compression geometry under both creep and stress relaxation protocols (Mow, et al., 1980). In creep tests, the theoretical curve initially over predicted strain but coincided with the experimental data after 40 seconds (**Figure 1.6**). This initial overshoot occurred because the cartilage disk was incompletely confined in the testing chamber, violating a model assumption and consequently invalidating model predictions. Model assumptions at the lateral boundaries of the sample dictate complete confinement, that is, the solid and fluid components experience zero displacement at the lateral boundaries. It is not possible to satisfy this condition experimentally at the beginning of a test and the lack of confinement resulted in a substantial decrease in measured stress (Buschmann, Soulhat, Shirazi-Adl, Jurvelin, & Hunziker, 1998). As the test proceeded, the cartilage disk underwent an initial lateral expansion until complete contact with the testing chamber was achieved and model predictions became valid. In stress relaxation tests in confined compression, the theoretical curve reportedly differed minimally from the experimental data (Mow, et al., 1980), while in unconfined compression geometry peak stresses consistently exceeded those predicted by the model (Armstrong, Lai, & Mow, 1984).

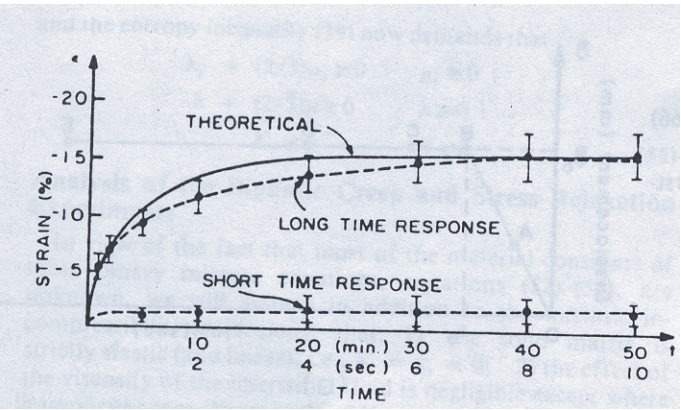

Figure 1.6: The biphasic model fit of experimental creep data initially over predicts strain due to incomplete confinement. *Source:* Mow et al. (1980).

The validity of model assumptions regarding specimen-platen interaction has also been investigated (Buschmann, et al., 1998). The biphasic model assumes that the porous platen displaces the solid cartilage component uniformly and the fluid component remains in contact with bath. However, histological studies have shown that cartilage interdigitates with the porous platen, which influences the stress profile generated in the cartilage sample, and can lead to incorrect estimates of model parameters (Buschmann, et al., 1998).

Transversely-isotropic Biphasic Model

The transversely-isotropic biphasic model introduces a transverse isotropic plane to the solid matrix of the biphasic model (Armstrong, et al., 1984; Cohen, et al., 1992). The transverse plane can account for the combination of tensile and compressive forces experienced by the solid matrix when it is loaded in unconfined geometry. The model parameters include E_1, which describes the tensile Young's modulus of the transverse plane, E_3, the compressive Young's modulus in the axial direction, and k, hydraulic permeability. Model assumptions include those described for the biphasic model as well as the following: the specimen-platen interface is frictionless, no shear stresses are experienced, fluid flow occurs in the radial direction only, uniform axial strain is applied, and solid deformation occurs in the radial direction independently of axial position. Finally, Poisson's ratio was set to 0, as in the biphasic model, because the

equilibrium load intensity was determined to be the same in either confined or unconfined compression (Cohen, et al., 1992).

The transversely-isotropic model was compared to the biphasic model using stress-relaxation data obtained from unconfined compression tests of bovine growth plate samples, where a compressive axial strain of 10% was applied in 131 s. The transversely-isotropic biphasic model produced a superior fit of the experimental data compared with the previous biphasic model (**Figure 1.7**). The time to relaxation was considerably faster and the peak stress estimated more accurately. For one sample, the values E_1 and E_3 were reported as 4.3 MPa and 0.64 MPa respectively, compared to a modulus of 1.08 MPa for the whole matrix generated by the biphasic model. Permeability values were in the same range for both models, $5x10^{-15}$ $m^4/N \cdot s$ for the transversely-isotropic biphasic model compared to $15.5x10^{-15}$ $m^4/N \cdot s$ for the biphasic model.

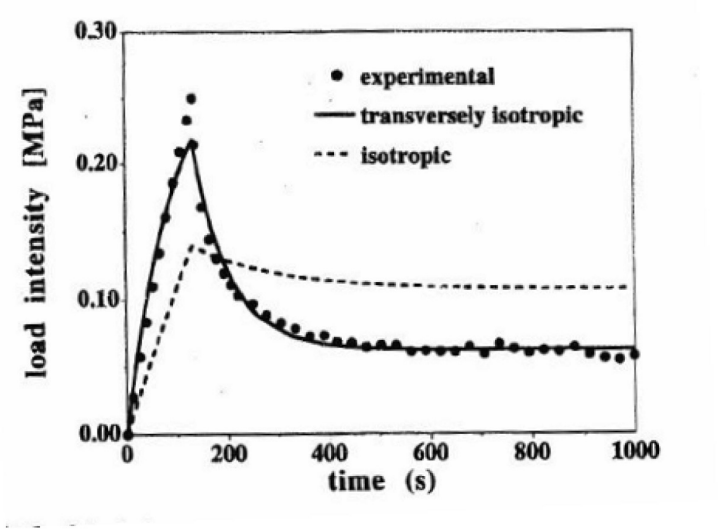

Figure 1.7: Example of experimental stress relaxation data fit with both the biphasic (isotropic) model and the transversely-isotropic biphasic model. Notable improvements due to the presence of the transverse plane include the decrease in relaxation time and the increase in peak stress estimation. Source: Cohen et al. (1998).

Fibril-network-reinforced Model

The fibril-network-reinforced model of cartilage builds on the isotropic biphasic model by adding nonlinear fibrils in all three directions (r, θ, z) of a cartilage disk, which represent the collagen component and only contribute in tension to provide lateral stiffness (**Figure 1.8**) (Soulhat, et al., 1999). The proteoglycan component is modeled as an isotropic, fluid filled, elastic porous solid. The model, derived using poroelastic theory, is completely defined by the parameters Em, υ_m, Ef, and k, where Em is the modulus of the drained matrix, Ef is the tensile fibril modulus, υ_m is Poisson's ratio, and k is hydraulic permeability. Several assumptions are made in this model, including that a homogenously distributed fibril network is used, although it is recognized that adult articular cartilage has depth dependent organization. In addition, a perfectly flat, non-porous compression platen is assumed, which allows no adhesions to occur between the platen and the specimen and consequently shear stresses are nil. The free lateral edges of the cartilage disk experience no stress, and the velocities of the fluid and solid phases indicate no circumferential velocity but the presence of both radial and axial velocities (Soulhat, et al., 1999).

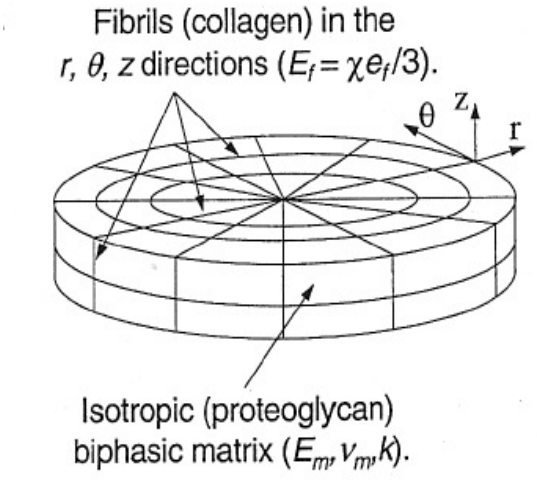

Figure 1.8: Schematic of a cartilage disk illustrating the axes and geometry used in the fibril-network-reinforced biphasic model of cartilage. *Source:* Soulhat et al. (1999).

The fibril-network-reinforced biphasic model is versatile and can fit experimental data obtained from stress-relaxation tests in confined or unconfined compression geometry. In unconfined compression, the fibril-network reinforced model provides better estimates of peak stress resulting from fibril stiffening (**Figure 1.9**) compared with the isotropic model (Mow, et al., 1980) and behaves similarly to the transversely- isotropic model (Cohen, et al., 1992). However, in confined compression, the fibril-network-reinforced biphasic model and the transversely- isotropic model do not predict the same behaviour because the fibril network does not operate in confined compression while the transverse plane stiffens, which overestimates stress. A limitation of the fibril-network-reinforced biphasic model is that it can only successfully capture the transient peak stress when effective Poisson's ratio, $\upsilon_{eff,}$ is between 0 and 0.05. This is lower than the average value of Poisson's ratio, 0.185±0.065, obtained by direct optical measurement of cartilage disks under axial load (Jurvelin, Buschmann, & Hunziker, 1997) but it is necessary for computing the model parameters using curve-fitting procedures.

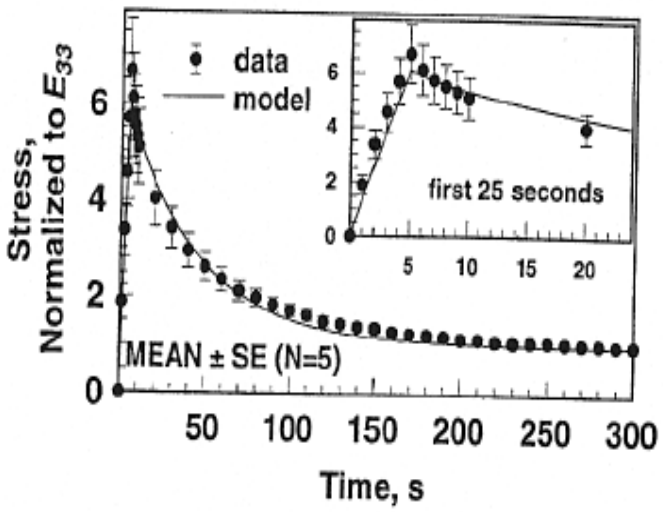

Figure 1.9: Fibril-network-reinforced model fit to experimentally collected stress relaxation data. The peak stress and relaxation time are successfully captured. *Source:* Soulhat et al. (1999).

The fibril-network-reinforced model has a distinct advantage over the other models described above, in that the parameters of the fibril-network-reinforced biphasic model are directly related to the two major extracellular matrix components of cartilage, providing an

analytical solution linked to cartilage structure. Korhonen et al. (2003) confirmed these relationships using enzymes to selectively degrade ECM components in cartilage explants. In proteoglycan depleted cartilage disks, achieved by incubating with chondroitinase ABC, Em was reduced by 64±28% and Ef by 11±9% compared to normal cartilage. These findings reflected the intended proteoglycan loss as well as maintenance of the collagen network, confirmed by Safranin-O staining and polarized light microscopy respectively (Rieppo, et al., 2003). Collagenase digested disks had dramatically reduced Ef, 69±5%, reflecting collagen network disruption, coupled with a 44±18% reduction in Em resulting from secondary proteoglycan loss, again supported by Safranin-O staining and polarized light microscopy analyses (Rieppo, et al., 2003). These findings illustrate the important role of the collagen network in trapping proteoglycan molecules, which were lost once the collagen network was compromised. Permeability, k, increased in both chondroitinase ABC and collagenase treated samples, although a greater increase in fluid flow occurred in cartilage disks digested with collagenase because they experienced both collagen network disruption and proteoglycan loss.

In summary, mature articular cartilage is a complex connective tissue with specialized composition and structure that forms during post-natal endochondral development. Articular cartilage enables load bearing by transmitting applied loads to underlying subchondral bone and facilitates motion by providing smooth gliding surfaces. The functional properties of cartilage can be evaluated during in vitro experiments in a variety of testing geometries where analytical models are used to determine cartilage material properties. Subsequent sections in this literature review will describe cartilage during degeneration and repair and summarize methods for cartilage assessment.

1.2 Cartilage Degeneration

The specialized and functionally important extracellular matrix of mature articular cartilage has limited intrinsic regenerative capacity. It is isolated from blood, nervous and lymphatic systems, and its maintenance is the responsibility of a sparse population of chondrocytes, approximately 1-10% by volume, that are nourished by synovial fluid during

normal physiological activity (O'Hara, et al., 1990). These conditions make cartilage susceptible to degenerative diseases.

1.2.1 Post-Traumatic Osteoarthritis

In osteoarthritis (OA), the repair capacity of the chondrocytes is overwhelmed by degradative processes (Bora & Miller, 1987; Loeser, 2006; Mandelbaum & Waddell, 2005). Cartilage can be compromised by factors including trauma, injury, obesity, aging, or inflammation, which produce abnormal stresses or cause irregular cartilage metabolic processes that eventually culminate in OA (Aigner, et al., 2004; Mandelbaum & Waddell, 2005) (**Figure 1.10**). OA that develops secondary to joint injury is described as post-traumatic osteoarthritis (PTOA), and studies suggest that PTOA develops in approximately 50% of patients that experience traumatic joint injury (Lotz, 2010; Lotz & Kraus, 2010).

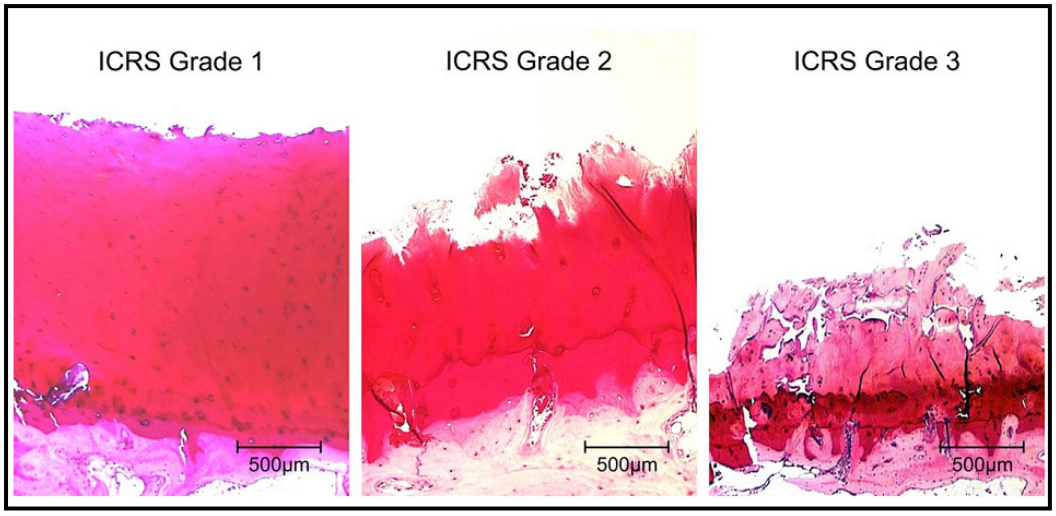

Figure 1.10: Safranin-o stained cartilage sections obtained from patients undergoing total knee arthroplasty. The extent of cartilage degeneration was assessed macroscopically using the ICRS grade where higher ICRS grades indicate more dramatic cartilage loss *Source:* Kleemann et al. (2005).

In the late stages of OA, pain and loss of joint function are common manifestations. Here, cartilage degradation is extensive and surgical intervention is likely the only option for symptom relief as disease modifying pharmaceutical treatments are not presently available. However, events occurring early in OA, such as acute ECM damage and cell apoptosis, are asymptomatic. During the immediate and acute stages after joint injury, cartilage degenerative and remodelling processes are elevated and this early time point represents an opportunity for administering therapeutic intervention to moderate disease progression that may have the greatest preventative potential (Lotz, 2010; Mandelbaum & Waddell, 2005; Scott & Athanasiou, 2006). In PTOA, where the initiating traumatic event is known, a unique window of opportunity for early intervention exists.

1.2.2 Cartilage Response to Joint Injury

Events that occur in cartilage following joint injury are related to the extent of mechanical damage and whether both cartilage and subchondral bone, or cartilage alone is implicated (Buckwalter & Brown, 2004; Mankin, 1982). Many of these events have been elucidated during experimental impact studies in cartilage explants or in vivo animal models, where impact injury is inflicted on articular surfaces, and the cellular response and changes to the ECM assessed (Bolam, Hurtig, Cruz, & McEwen, 2006; Borrelli, Zhu, Burns, Sandell, & Silva, 2004; Donohue, Buss, Oegema, & Thompson, 1983; Duda et al., 2001; Jeffrey, Gregory, & Aspden, 1995; Newberry, Mackenzie, & Haut, 1998; Quinn, Allen, Schalet, Perumbuli, & Hunziker, 2001; Repo & Finlay, 1977; Thompson, Oegema, Lewis, & Wallace, 1991; Torzilli, Grigiene, Borrelli, & Helfet, 1999; Weaver & Haut, 2005).

Cartilage response to impact includes loss of chondrocyte viability (Jeffrey, et al., 1995; Repo & Finlay, 1977) and upregulation of matrix-degrading enzymes by surviving cells. Chondrocytes are sensitive to mechanical injury, where even in the absence of visible cartilage surface damage chondrocyte viability decreased (Duda, et al., 2001). ECM degradation commences with mechanical damage to the collagen network eventually resulting in swelling and secondary loss of proteoglycans (Bolam, et al., 2006; Donohue, et al., 1983; Jeffrey, et al., 1995;

Thompson, et al., 1991; Thibault, Poole, & Buschmann, 2002). Initial damage is observed mainly as surface fissures, which compromise the SZ and undermine its ability to withstand shear forces and to contribute to cartilage load bearing and durability (Arokoski, et al., 1996; Korhonen, et al., 2002; Moger, et al., 2009), thereby putting the underlying cartilage at risk (Morel, Berutto, & Quinn, 2006). Results from biomechanical testing demonstrate that cartilage becomes mechanically weak due to the fragmented collagen network and proteoglycan depletion that are a consequence of impact injury (Newberry, et al., 1998; Weaver & Haut, 2005). Increased collagen fibre widths were observed several weeks after impact in scanning electron microscopy and possibly represent collagen fibre disorganization (Donohue, et al., 1983). Changes to the calcified cartilage layer, including vascular invasion and cellular cloning (Donohue, et al., 1983), as well as subchondral bone thickening below fissured cartilage (Isaac, Meyer, Kopke, & Haut, 2010; Newberry, et al., 1998) have also been reported in response to impact loading.

1.2.3 Models for Evaluating Therapeutic Strategies

Models for evaluating therapeutic strategies to prevent or slow the progression of OA should focus on the immediate and acute phases post-injury where cellular response and degradative activity are heightened (Lotz, 2010; Mandelbaum & Waddell, 2005; Scott & Athanasiou, 2006). Numerous models of PTOA have been reported in the literature, including those using cartilage explants or in vivo animal models. The strengths and weaknesses of these approaches are briefly summarized here and an equine model identified that could be appropriate for developing a model system of early PTOA.

The benefits of impact models using cartilage explants include that impact injury can be delivered at precise locations on the joint surface and the severity of impact controlled. In these types of studies, impacts are delivered using drop-tower devices, pendulums or free flight masses, which are capable of producing the high strain rates, with time to peak loads less than 30 ms, recommended for simulating impact injury (Aspden, Jeffrey, & Burgin, 2002; Scott & Athanasiou, 2006). Explant studies, where cartilage damage may range from mild to extensive, have demonstrated changes in the immediate and acute phases following impact such as

chondrocyte apopotosis, surface fissuring and depletion of ECM components (Duda, et al., 2001; Jeffrey, et al., 1995; Quinn, et al., 2001; Repo & Finlay, 1977; Thompson, et al., 1991; Torzilli, et al., 1999). Cartilage explants are less resilient to impact injury compared to cartilage in situ and are not suitable for studying the chronic effects of impact injury.

In vivo impact studies are often conducted in smaller animals like rabbits and dogs (Scott & Athanasiou, 2006) where impact injury can be inflicted either on closed joints (Isaac, et al., 2010) or directly on cartilage surfaces by introducing the impacting device into the joint space through a surgical incision (Borrelli, et al., 2004; Vrahas, Smith, Rosler, & Baratta, 1997; Zhang, Vrahas, Baratta, & Rosler, 1999). In general, control over the delivery of the mechanical insult is reduced in these in vivo models compared to explants, but they supply the appropriate physiological environment for assessing acute and chronic degenerative effects of impact in cartilage and other joint tissues.

Compared to smaller animals, equine models of OA are advantageous because the comparatively large stifle (knee) joint affords arthroscopic access to joint surfaces including the condyles and distal trochlea, and cartilage thickness approaches that measured in human knees (Frisbie, Cross, & McIlwraith, 2006). Bolam et al. (2006) reported irreversible cartilage degradation at 3 months, which continued to progress up to 6 months, following controlled localized impact of 60 MPa directly to the cartilage surface of the equine medial femoral condyle. At 3 months, cartilage degradative changes included proteoglycan depletion, cell apoptosis, and SZ fissuring. By 6 months, degradation was more extensive and overt fibrillation, exposed calcified cartilage, cartilage delamination and the appearance of OA lesions on the opposing joint surface were noted. Studying earlier time points in this model, where a trajectory towards OA has been established, could provide the desired model system of early PTOA where therapeutic strategies could be tested.

1.3 Cartilage Repair

Cartilage damage, where the subchondral bone remains intact, induces chondrocyte apoptosis and prompts a repair response from surviving chondrocytes. However, this response is often inadequate and a permanent cartilage lesion can eventually form that leaves the whole joint vulnerable to degeneration (Buckwalter & Brown, 2004; Hunziker, 2002). An area of considerable research activity centres on the development of techniques for repairing focal cartilage lesions, including cell therapies (Brittberg, et al., 1994; Saris, et al., 2008), in vitro generated tissue-engineered constructs (Crawford, et al., 2009; Kon, et al., 2010), scaffold-based solutions (Hoemann, et al., 2005; Shive, et al., 2006) and surgical techniques (Mithoefer, et al., 2009) that may lead to effective cartilage repair in humans. In some of these techniques, cartilage repair processes originate from the subchondral bone, in others from the implanted cells or tissue-engineered construct, and can involve additional interactions between these sources of repair and other joint tissues (Hunziker, 2002).

Microfracture, a common surgical technique, involves creating a number of small perforations in a debrided subchondral bone plate, causing bleeding into the defect. Mesenchymal cells from the bone marrow are thus encouraged to migrate to the stimulated site and fill the defect with a granulation tissue, which matures over 3-12 months and may eventually grow and remodel into fibrous tissue, fibrocartilage or hyaline-like cartilage (Buckwalter & Brown, 2004; Frisbie et al., 2003). Microfracture improves knee function in the first 24 months (Mithoefer, et al., 2009) and approximately 75% of treated patients have satisfactory clinical outcomes after 5 years (Knutsen et al., 2007). Microfracture combined with a polymer scaffold containing chitosan (Shive, et al., 2006) prolongs residency of the blood clot formed in the defect, which contains cells and other factors originating from bone marrow. The ensuing scaffold-guided repair tissue has shown improved hyaline character compared to microfracture alone in sheep (Hoemann, et al., 2005) and humans (Changoor et al., 2010; Hoemann et al., 2010; Methot et al., 2010; Stanish et al., 2010), after periods of 6 months and 1 year respectively.

In autologous chondrocyte implantation (ACI), the patient undergoes an initial surgery where a biopsy of cartilage is collected from a non-weight bearing site in the affected joint.

Chondrocytes obtained from the biopsy are amplified approximately 10-fold during cell culture and returned to the patient during a second surgery, where the cartilage lesion is debrided to the calcified cartilage layer and approximately 3 million passaged chondrocytes are injected below a periosteal flap (Brittberg, et al., 1994). While good clinical outcomes have been reported following ACI (Gillogly, Voight, & Blackburn, 1998), a recent prospective randomized clinical trial showed no advantage of ACI over microfracture, the conventional strategy for treating focal defects, five years post-surgery (Knutsen, et al., 2007).

Tissue engineered constructs are typically cell-seeded scaffolds cultured under conditions thought to encourage chondrocytes to synthesize an ECM. Many different types of constructs have been developed, including biphasic implants consisting of a porous calcium phosphate base with autologous cells cultured on top to create an articulating surface (Kandel et al., 2006), and stratified scaffolds formed from collagen type I and hydroxyapatite, where the upper portion of the scaffold was seeded with autologous chondrocytes (Kon, et al., 2010). Both of these constructs were designed to fill osteochondral defects and their performance tested in separate studies using sheep models (Kandel, et al., 2006; Kon, et al., 2010). A different tissue engineered construct, composed of autologous chondrocytes seeded on a bovine type I collagen matrix scaffold, was implanted in human knees during a prospective trial to evaluate safety (Crawford, et al., 2009). Patients experienced a reduction in pain and improved range of motion. Evaluation of repair tissue quality was limited to magnetic resonance imaging (MRI), which showed an improvement in cartilage organization, as stratified MRI T2 maps, in half of the patients at the end of the 24 month study (Crawford, et al., 2009).

In summary, a number of repair strategies are presently under development or clinically available for treating focal cartilage lesions. Studies report mixed repair tissue quality and clinical outcomes resulting from these approaches and a few have been tested in randomized controlled clinical trials. Producing an efficacious repair strategy that results in durable and functional repair cartilage requires investigators to understand the endochondral development processes from which native cartilage arises, and to assess repair tissue based on criteria for mature articular

cartilage, which includes the unique anisotropic structural organization of cells and ECM molecules (Hunziker, 2009).

1.4 Assessing Cartilage Quality

In humans, cartilage degeneration and the efficacy of strategies for cartilage repair can be assessed using a variety of outcome measures (**Table 1.1**). These may include patient reported outcomes, which consist of questionnaires evaluating pain, activity and quality of life, or clinical examination. MR imaging provides an indirect method for assessing the quality of repair tissue or extent of degeneration, where specialized protocols can provide some information about collagen structure and proteoglycan concentration. Direct histological assessment remains the most important outcome measure of repair tissue quality and in clinical trials it can be evaluated in biopsies, which are 2 mm diameter osteochondral cores collected from the centre of the repair site during a second-look arthroscopy procedure (Gudas et al., 2005; Mainil-Varlet, et al., 2003; Mainil-Varlet, et al., 2010; Roberts, et al., 2003; Saris, et al., 2008; Selmi et al., 2008).

Table 1.1: Methods currently employed for assessing cartilage quality clinically.

Assessment Method	Advantages	Disadvantages
Clinical Evaluation	• Patient self-evaluates general health, joint function and activity level using questionnaires • Clinical exam produces objective measures of joint function • Non-invasive, can be evaluated at multiple times during follow-up	• Clinical evaluation not necessarily related to cartilage tissue quality • These measures may not be able to predict long term success or durability of repair cartilage
MRI	• Specialized protocols for imaging specific biochemicals are available • Can provides three dimensional views of the whole joint • Non-invasive	• Limited spatial resolution • Complex data processing required • Challenge to standardize imaging protocols across centres • Cost
Blunt Probe for in situ Cartilage Assessment	• Non-destructive to cartilage • Assessment performed intra-operatively	• Invasive, requiring direct contact with the articular surface
Histological Evaluation of Cartilage Biopsies	• Direct visual assessment of cartilage quality • Biochemical constituents identified using histostaining and immunohistostaining methods • Histological scoring systems provide methods for systematic comparison • Collagen structure can be assessed in polarized light or scanning electron microscopy	• Possible detrimental effect at biopsy site • Overall cartilage quality inferred from histological assessments on a few sections from small biopsies, which may not be representative of the whole repair tissue.

1.4.1 Clinical Assessment

Clinical assessment is important for appreciating the extent of cartilage degeneration or as a measure of the success of cartilage repair procedures. It usually includes a combination of physical evaluation by a clinician and patient reported outcome measures.

Physical exams and clinical outcomes produce objective values that describe functional improvement. This could include measurements of range of motion, joint laxity, or the ability to perform certain tasks (Sernert et al., 1999; Wright, 2009).

Patient reported outcomes are assessed using questionnaires and provide important feedback about pain, function, activity levels, and quality of life (Roos & Lohmander, 2003; Ware & Sherbourne, 1992; Wright, 2009). These questionnaires may inquire about general health outcomes or be specific to a disease or articular joint. It is recommended that clinical research studies administer three questionnaires to the patient, one related to general health, one specific to the disease or injury experienced, and one related to activity level (Wright, 2009). The most commonly used general health survey is the validated medical outcomes study 36-item short form (SF-36), consisting of 36 questions related to physical function, emotion well-being and overall health status (Brazier et al., 1992; Ware & Sherbourne, 1992). For clinical studies involving cartilage injury in the knee, the Western Ontario and McMaster Universities arthritis index (WOMAC) or the knee injury and osteoarthritis outcome score (KOOS) are often used. The WOMAC consists of 24 questions covering pain, stiffness and physical function and is specific to the lower limbs, while the KOOS was developed as an extension of WOMAC and is specific to sports injury. The KOOS includes 42 questions covering pain, symptoms, daily living activities, sport and recreation function, and knee-related quality of life, and it is better suited to evaluating younger, more active patients (Roos & Lohmander, 2003). Activity level can be evaluated using either the Tegner or Marx activity level scales. The Tegner scale is used to assign an ordinal between 0 and 10 to describe a patient's activity level, where 0 indicates disability as a result of knee problems and 10 describes sports played at an elite level (Tegner & Lysholm, 1985). The Marx scale (Marx, Stump, Jones, Wickiewicz, & Warren, 2001) consists of four questions related to specific functions (running, cutting, decelerating and pivoting) and accounts for the frequency

at which these activities are performed. While the Tegner scale equates activity level with practicing specific sports, the Marx scale rates specific movements, and it is thought to be more generally applicable to different patient populations (Marx, et al., 2001; Wright, 2009). The above paragraph summarizes a handful of the most commonly used outcome measures administered to patients and represents a subset of the numerous scores available.

Both subjective patient reported outcomes and objective clinical measures are relevant when considering whether a particular cartilage repair procedure has produced a clinically important improvement for the patient. Clinical assessment can be performed prior to and following intervention, or at several times points during the follow up period, patient compliance permitting, providing sequential information over time. There is evidence that patient reported outcomes correspond to patient's expectations better than objective measures (Sernert, et al., 1999), though the role of questionnaires in determining the success or failure of any given procedure has been contentious (Heckman, 2006; Zarins, 2005). Clinical assessment is important because it accounts for patient satisfaction with the procedure, however good clinical outcome does not always correspond to good repair tissue quality, which may be more indicative of tissue durability over the long term (Henderson, Lavigne, Valenzuela, & Oakes, 2007; Knutsen, et al., 2007; Knutsen et al., 2004).

1.4.2 Magnetic Resonance Imaging (MRI)

Magnetic resonance imaging (MRI) can provide three-dimensional images of whole articular joints, which can be processed in order to quantify cartilage morphology using parameters like cartilage thickness, joint surface area and joint congruity, among others (Eckstein, Hudelmaier, & Putz, 2006). Specialized sequences have been developed for imaging cartilage composition, including delayed gadolinium enhanced MRI of cartilage (dGEMRIC) for estimating GAG content and transverse relaxation time (T2) for assessing collagen anisotropy. dGEMRIC requires an intravenous injection of gadolinium, a negatively-charged contrast agent that penetrates into cartilage over a period of approximately 60-90 minutes (Eckstein, et al., 2006; Trattnig, Domayer, Welsch, Mosher, & Eckstein, 2009) and distributes inversely with respect to

the GAG molecules. The resulting dGEMRIC images illustrate GAG distribution and content, and this method has been validated against biochemical analysis (Bashir, Gray, Hartke, & Burstein, 1999). T2 maps of cartilage, obtained without a contrast agent, reflect interstitial fluid content, collagen content and collagen organization (Kim, Ceckler, Hascall, Calabro, & Balaban, 1993; Kurkijarvi, et al., 2008; Mosher & Dardzinski, 2004; Nissi, et al., 2006). T2 transverse relaxation time is strongly influenced by proton mobility, specifically of the collagen-associated water molecules that are aligned with the long axis of collagen fibres and which have limited mobility within the tight cartilage ECM (Mlynarik, Szomolanyi, Toffanin, Vittur, & Trattnig, 2004; Mosher & Dardzinski, 2004). Because of these interactions between water and collagen, fibre orientation can be inferred from T2 images and corresponds with orientation observed by polarized light microscopy of histological sections (Kurkijarvi, et al., 2008; Nissi, et al., 2006).

Clinically, conventional MRI is used to observe the extent of cartilage degradation (e.g. lesion size) and other joint deficiencies, (e.g. ligament tears), as well as for pre-operative planning. Sequences for assessing cartilage composition are not routinely used at present, although T2 mapping could be readily incorporated into a standard clinical MRI session as contrast is not used and the scan time is estimated to be six minutes at 3 T (Trattnig, et al., 2009). dGEMRIC would be more challenging to implement because of the need to wait for contrast distribution, requiring a total appointment time of approximately two hours (Trattnig, et al., 2009). The non-invasive nature of MRI, coupled with the ability to observe specific ECM components, makes it a promising tool for clinical detection of cartilage degeneration and monitoring repair cartilage tissues (Mosher & Dardzinski, 2004; Trattnig, et al., 2009). However, while technological advances in MRI are ongoing, current clinical MRI scanners often lack the spatial resolution required to accurately capture the relatively thin cartilage layer and perform quantitative analyses. In addition, the variety of imaging sequences possible and the assortment of MRI systems in use make it difficult to standardize protocols across centres. Special attention to the confounding effects of some MRI artefacts is required to ensure that sensitivity and reproducibility of the scans are maintained in a clinical setting (Mosher & Dardzinski, 2004).

1.4.3 Histological Scoring of Biopsies

A number of histological scoring systems have been developed to evaluate biopsied repair cartilage (Rutgers, van Pelt, Dhert, Creemers, & Saris, 2010). Among these, the OsScore, ICRS I and ICRS II scoring systems are most widely used and provide semi-quantitative assessment of a number of tissue characteristics that are predicted to play a role in the long- term durability of repair cartilage. The OsScore (Roberts, et al., 2003) and ICRS I (Mainil-Varlet, et al., 2003) consist of seven and six categories respectively that are rated on ordinal scales. The OsScore categories (tissue morphology, matrix staining, surface architecture, chondrocyte clusters, mineral, blood vessels, and basal integration), are evaluated individually and summed to produce a single overall score. For the ICRS I scoring method (Mainil-Varlet, et al., 2003) readers compare with a panel of graded example images to rate six categories (surface smoothness, matrix hyaline/fibrous character, cell distribution, cell viability, subchondral bone, and abnormal cartilage mineralization) on scales of 0 to 3, which are not summed. A comparison between early versions of the OsScore and ICRS I, using repair tissue biopsies obtained 12 months post-ACI, demonstrated similar reproducibility and low coefficients of variance among three readers (Roberts, Darby, Menage, Evans, & Richardson, 2001).

The ICRS II system (Mainil-Varlet, et al., 2010; Rutgers, et al., 2010; Saris, et al., 2008) uses a visual analogue scale (VAS) to rate 14 categories with defined anchors at 0% and 100% positions. These categories include (1) tissue morphology, (2) matrix staining, (3) cell morphology, (4) chondrocyte clustering, (5) surface architecture, (6) basal integration, (7) formation of a tidemark, (8) subchondral bone formation, (9) inflammation, (10) abnormal calcification/debris, (11) vascularization, (12) surface/superficial assessment, (13) mid/deep zone assessment, and (14) overall assessment scale. These categories were selected to reflect the ICRS I categories and to include additional scores for negative features such as inflammation and vascularization.

While these scores described above rate a number of relevant tissue characteristics, none include a separate category that specifically evaluates collagen architecture, whose anisotropic structure is central to cartilage biomechanical properties and durability, and is an essential feature

of adult hyaline cartilage (Hughes, et al., 2005; Julkunen, et al., 2009; Moger, et al., 2009). The authors of the OsScore used polarized light to appreciate the collagen network when evaluating the tissue morphology category, where a score of 0 was assigned to fibrous tissue and a score of 3 to hyaline cartilage (Roberts, et al., 2003). Likewise, it is recommended that scoring the ICRS II category of tissue morphology involve viewing samples in polarized light, where VAS anchors are 'full thickness collagen fibres' at 0% and 'normal birefringence' at 100% (Mainil-Varlet, et al., 2010; Rutgers, et al., 2010). These categories acknowledge the importance of assessing collagen network structure and provide a first step towards accomplishing this goal, but neither captures the detailed features of collagen organization observed in mature articular cartilage.

1.4.4 Methods for Evaluating the Collagen Network

The fibrillar collagen network in articular cartilage is readily evaluated in histological sections using linear polarized light microscopy (PLM) and scanning electron microscopy (SEM). These methods have been used to study many aspects of normal, degraded and repair cartilage tissues and are good candidates for the development of a histological score for repair cartilage where different levels of collagen organization could be systematically described. Such a method could be used in conjunction with current histological scoring systems to provide a more complete assessment of cartilage repair tissue quality, as well as facilitate comparisons between different repair strategies.

PLM can be performed on a light microscope with the addition of two filters, a polarizer and analyzer (Modis, 1991). The polarizer is placed after the light source but before the specimen and ensures that only linearly polarized light, i.e. light in a single plane that is perpendicular to the direction of light propagation, is transmitted to the specimen. If the tissue through which the light passes is optically active (a property of anisotropic materials) then the direction of the polarized light changes; an effect called birefringence. Biological anisotropic specimens, such as fibrillar collagen, are birefringent, or double-refracting, and split the incident plane polarized light into two orthogonal rays, which have the same amplitudes but different speeds, reflecting the two indices of refraction. The split occurs when the incident polarized light interacts with

valence electrons of the fibrillar collagen structure, which occurs at each point in the tissue section. The extraordinary ray is in the same plane as the long axis of the collagen fibres, while the ordinary ray is referred to as 'direction independent'. The analyzer filter, placed after the specimen and at a right angle to the polarizer, recombines these two rays to produce the resulting image observed at the eyepiece. The orientation of the analyzer ensures that only light with a polarization that is altered by the tissue is passed. The intensity of the resulting signal therefore indicates regions of the tissue that are optically active, or in other terms, birefringent, anisotropic or oriented.

Birefringence is essentially the numerical difference between the extraordinary and ordinary rays when they are recombined at the analyzer. In unstained sections of cartilage, birefringence is almost entirely due to the orientation and organization of collagen fibres, as proteoglycans contribute only 6% of total birefringence (Kiraly, et al., 1997). In PLM, the highly organized collagen structure of hyaline cartilage appears as two birefringent regions, which are the SZ and DZ, separated by a non-birefringent TZ (Arokoski, et al., 1996; Hughes, et al., 2005; Kaab, et al., 1998; Kiraly, et al., 1997; Korhonen, et al., 2002; Rieppo, et al., 2003; Speer & Dahners, 1979). Regions of birefringent and non-birefringent tissue have also been observed in cartilage repair tissues, where PLM was considered when determining general tissue type (Mainil-Varlet, et al., 2003; Roberts, et al., 2003), describing specific features, such as collagen fibres anchoring to subchondral bone (Richardson, Caterson, Evans, Ashton, & Roberts, 1999; Roberts, et al., 2003; Roberts, Menage, Sandell, Evans, & Richardson, 2009), or for quantitative PLM measurements of repair cartilage anisotropy (Langsjo et al., 2010; Vasara et al., 2006).

While PLM provides a global view of collagen organization, the high resolution possible in SEM permits direct visualization of collagen fibres (Gardner, Salter, & Oates, 1997; Responte, et al., 2007; Zhou, Apkarian, Wang, & Joy, 2006). Briefly, in SEM, samples are coated with a conductive layer and subjected to an incident high-energy beam. Interactions between the electron beam and specimen surface ionize specimen atoms and produce secondary electrons, which are collected by a detector and processed, resulting in a digital SEM image (Zhou, et al., 2006). SEM has been previously used to study normal articular cartilage in parallel with PLM

(Hughes, et al., 2005; Kaab, et al., 1998; Speer & Dahners, 1979), providing information about collagen architecture in human and animal species. SEM studies of osteoarthritic cartilage illustrate the appearance of the collagen network at different stages of degeneration (particularly those changes occurring in the SZ), contribute to elucidating mechanisms of cartilage degradation, and provide cartilage fibre diameters in these tissues types (Clark & Simonian, 1997; Minns & Steven, 1977; Redler, 1974). SEM has also been used to describe features of the collagen network in repair tissues produced in tissue-engineered constructs (Riesle, Hollander, Langer, Freed, & Vunjak-Novakovic, 1998) or autologous chondrocyte implantation (Langsjo, et al., 2010), in animal models. No reports were found describing features of the collagen network observed using SEM in human cartilage repair tissues.

In summary, PLM and SEM are methods for evaluating collagen architecture in articular cartilage at different length scales. They could be used to develop a histological score that would provide an objective means of assessing collagen organization and contribute to a more incisive evaluation of cartilage repair tissue quality.

1.4.5 Methods for In Situ Cartilage Assessment

Cartilage tissue quality can be assessed in situ during arthroscopy procedures by using a blunt probe, a thin rod with a 90° hook and rounded blunt tip (**Figure 1.11**), that provides tactile feedback allowing the surgeon to qualitatively assess cartilage stiffness as well as explore other joint structures. This routine evaluation is non-destructive to cartilage and is considered the most important diagnostic performed during arthroscopic procedures (Spahn, Klinger, & Hofmann, 2009). There has been considerable interest in developing handheld devices that aim to acquire more detailed and objective information about cartilage quality intra-operatively, particularly as these technologies might be capable of detecting early degeneration before visible surface changes occur (Chu, Izzo, Irrgang, Ferretti, & Studer, 2007). These types of devices have been used to assess cartilage degeneration or repair cartilage tissues by measuring cartilage stiffness (Bae et al., 2003; Franz et al., 2001; Henderson, et al., 2007; Lyyra et al., 1999; Niederauer et al.,

2004), or imaging characteristics obtained by optical coherence tomography (Chu, et al., 2007; Chu et al., 2010) or ultrasound (Kaleva et al., 2011) methods.

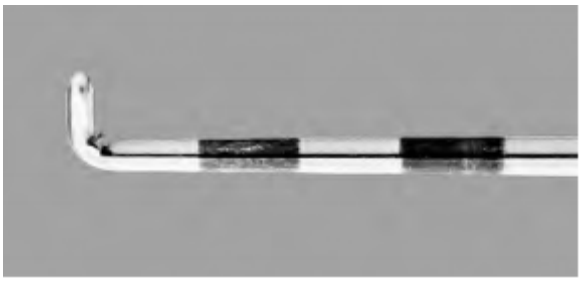

Figure 1.11: Blunt probe for palpating the articular surface during arthroscopic procedures *Source:* Smith & Nephew Endoscopy Division, Andover, Massachusetts.

Mechanical Stiffness

Handheld devices for mechanical evaluation of cartilage during arthroscopy are of interest because reduced cartilage compressive stiffness is recognized as an indicator of cartilage degeneration. Here, examples of two devices (or probes) for measuring cartilage indentation properties and their applications in laboratory and clinical settings are summarized.

An indentation probe, marketed as the Artscan[3], for measuring cartilage stiffness during arthroscopy was developed to provide objective assessments of cartilage softening (Lyyra, Jurvelin, Pitkanen, Vaatainen, & Kiviranta, 1995). The measurement rod of the device consists of a bending beam sheathed in a relatively rigid cover and both components are instrumented with strain gauges in separate Wheatstone bridge configurations. A plane-ended indenter, 300 μm in length and 1.3 mm in diameter, is attached to the end of the bending beam. The cover at the distal end of the measurement rod is inclined at 20° and serves as the reference plate during stiffness measurements. Measurements are made by aligning the reference plate to the cartilage surface

3 Artscan Oy, Helsinki, Finland. The Artscan is no longer commercially available.

and manually applying a constant 10 N force that presses the indenter into cartilage (**Figure 1.12**). Cartilage resistance to deformation produces measureable beam deflection that is then used to calculate instantaneous shear modulus (Lyyra, et al., 1995).

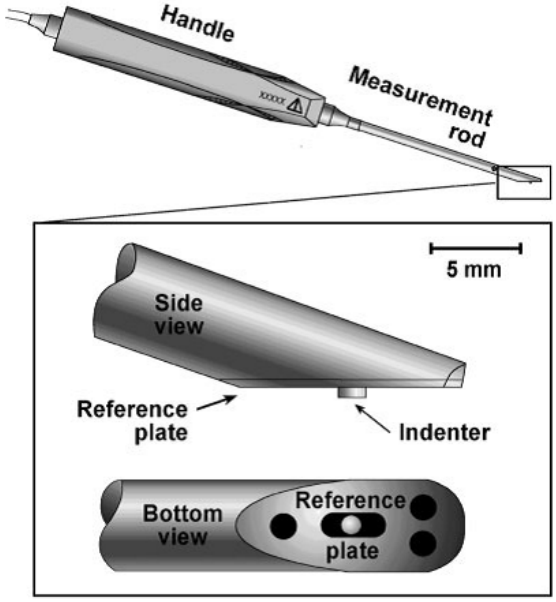

Figure 1.12: The Artscan device for in situ indentation measurements of cartilage. *Source:* Toyras et al. (2005).

A separate mechanical indentation device, marketed as the ACTAEON probe[4], uses a similar measurement principle (**Figure 1.13**). The handle of the probe connects to a disposable tip, consisting of a fixed outer shaft and an internal, movable drive shaft. The tip is positioned at the measurement site and a trigger released, which causes the on-board microprocessor to rapidly extend and retract the internal drive shaft to produce an indentation lasting approximately 100 ms with a maximum depth of 100 μm. Stiffness is measured by strain gauges and displayed on the handle in unitless International Rubber Hardness Degree (IRHD) values, ranging from 0 to 99. IRHD values are correlated to Young's modulus and the ACTAEON Probe is pre-calibrated using appropriate ASTM durometer standards (Bae, et al., 2003; Niederauer, et al., 2004).

4 OsteoBiologics, San Antonio, TX, USA. OsteoBiologics is now part of Smith and Nephew, Andover, MA, USA.

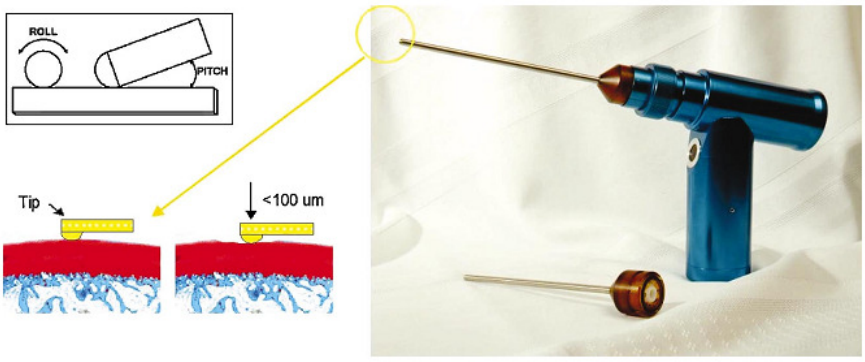

Figure 1.13: The ACTAEON Probe for in situ indentation measurements of cartilage. *Source:* Niederauer et al. (2004).

These mechanical probes have been used to measure cartilage stiffness in a number of in vitro experiments (examples include: Bae, et al., 2003; Franz, et al., 2001; Lyyra, et al., 1999; Niederauer, et al., 2004) as well as in clinical settings (Henderson, et al., 2007). Cartilage stiffness was compared to histological and biochemical assessments in bovine stifle joints degraded enzymatically (Lyyra, et al., 1999). Stiffness, measured with the Artscan probe, decreased with either diminished proteoglycan or collagen components, but larger decreases occurred in samples with reduced safranin-o staining, and normal SZ collagen organization, compared to samples with normal proteoglycan levels, but lacking SZ birefringence (Lyyra, et al., 1999). Similarly, stiffness measurements obtained with the ACTAEON probe changed with trypsin-induced proteoglycan depletion in cartilage explants from different species (Niederauer, et al., 2004). However, findings from a study using normal human knee cartilage (Franz, et al., 2001) suggested that instantaneous stiffness is mainly influenced by collagen network structure rather than proteoglycan content or total collagen content. This observation was supported by corresponding Mankin histological scores, which includes a category for structural integrity that correlated well with cartilage stiffness measurements (Franz, et al., 2001). A similar relationship between stiffness measurements made with the ACTAEON probe and a histological OA score in human cartilage was also observed (Bae, et al., 2003). These studies imply that instantaneous

stiffness may be more closely related to SZ structure and collagen organization, while the relationship with biochemical composition is less clear.

Clinically, the Artscan device was used to quantify stiffness of cartilage repair tissues produced by ACI and these stiffness values were compared to macroscopic grade, as well as tissue type determined histologically from biopsies (Henderson, et al., 2007). Repair cartilage stiffness was normalized to measurements made on adjacent cartilage and these values were a function of tissue quality, where hyaline cartilage had the highest normalized stiffness with sequentially lower ratios observed for hyaline-like, mixed hyaline-like/fibrocartilage, and fibrocartilage repair tissue types. Normalized stiffness corresponded to macroscopic grade, and while both parameters were statistically significantly reduced in fibrocartilage compared to hyaline cartilage, only macroscopic scores were significantly reduced in hyaline-like/fibrocartilage repairs compared to hyaline cartilage. However, stiffness measurements were able to identify that 50% of repairs with hyaline or hyaline-like tissue were stiffer than surrounding cartilage and this may represent an important feature contributing to repair tissue durability, since the resulting irregular load transmission could compromise the repair cartilage (Henderson, et al., 2007). These studies described above highlight the potential advantages of intra-operative objective measurements of cartilage for the diagnosis of cartilage degeneration and monitoring of repair tissue quality.

Optical Coherence Tomography (OCT)

Optical coherence tomography (OCT) images of cartilage are obtained by placing a super luminescent diode adjacent to the cartilage surface and capturing backscattered infrared light (Chu, et al., 2010; Li et al., 2005; Xie et al., 2008). This technology is capable of penetrating 1.5-2 mm into cartilage and produces cross-sectional images with resolutions comparable to low-power histology (**Figure 1.14**). OCT images exhibit a specific feature termed OCT form birefringence, described as “clearly distinguishable banding patterns” (Chu 2010), or otherwise described as phase retardation patterns (Xie, et al., 2008), in normal articular cartilage. Degraded cartilage is identified by a loss of the banding pattern observed in normal cartilage (Bear, Williams, Chu, Coyle, & Chu, 2010; Chu, et al., 2007; Li, et al., 2005). OCT form birefringence results from the angle of the OCT probe with respect to the cartilage surface and primarily

provides structural information about cartilage, including surface fibrillation and identifying tissue boundaries (Pan, Li, Xie, & Chu, 2003; Ugryumova, et al., 2005; Xie, Guo, Zhang, Chen, & Peavy, 2006a).

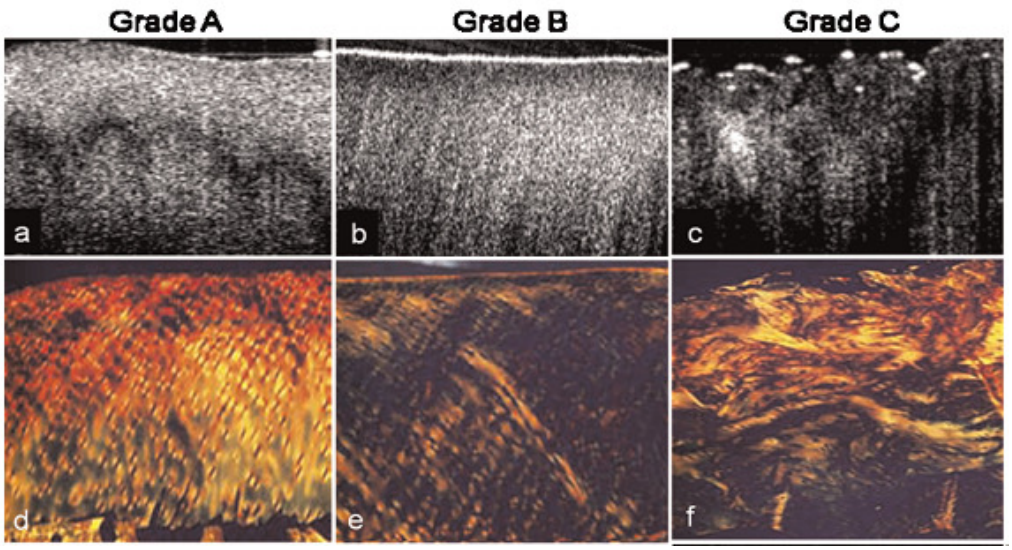

Figure 1.14: OCT images (a-c) and corresponding PLM images of picrosirius red-stained sections (d-f). Grading was based on OCT form birefringence characteristics, where Grade A (a,d) indicates an intact cartilage surface and normal OCT form birefringence characteristics, Grade B (b, e) denotes an intact surface but abnormal OCT form birefringence, and Grade C (c, f) means that an irregular cartilage surface is present. *Source:* Bear et al. (2010).

The OCT characteristics of normal and degraded cartilage have been compared to macroscopic scores obtained during conventional arthroscopic examination, polarized light microscopy and MRI T2 imaging with varying amounts of agreement (Bear, et al., 2010; Chu, et al., 2007; Chu, et al., 2010). Five out of seven patients with meniscal tears, diagnosed with normal cartilage by conventional arthroscopic scoring, had abnormal OCT images, suggesting that OCT could be more sensitive to early degenerative changes compared to the current clinical standard of assessment (Chu, et al., 2010). A comparison with PLM demonstrated that OCT images change as collagen organization decreases (**Figure 1.14**), but the OCT banding pattern does not appear to relate to zones of collagen organization or regions of birefringent and non-

birefringent cartilage that is readily observed in PLM (Bear, et al., 2010). The relationship between OCT and MRI T2 is less clear. T2 relaxation times measured in the SZ showed a correlation with OCT during in vitro experiments using osteochondral cores (Bear, et al., 2010), but a weaker relationship was reported for similar comparisons in a clinical setting (Chu, et al., 2010). These differences may be attributed to challenges with MRI and OCT image registration or to the different length scales employed by these methods, where T2 resolution is in millimetres compared with microns for OCT (Chu, et al., 2010).

A variation of OCT technology, polarization sensitive optical coherence tomography (PS-OCT), uses a polarized incident light source to produce phase retardation images reflecting collagen network organization (Ugryumova, Jacobs, Bonesi, & Matcher, 2009) but not proteoglycan content (Xie, et al., 2006a). PS-OCT has been used for imaging cartilage ex vivo (Liu et al., 2006; Ugryumova, et al., 2005; Ugryumova, et al., 2009; Xie, et al., 2006a; Xie, Guo, Zhang, Chen, & Peavy, 2006b) and could be adapted for clinical use, possibly in a similar format to the arthroscopic OCT probe that is currently approved for human use (Pan, et al., 2003)[5]. These studies demonstrate the potential for in situ imaging of cartilage to provide characteristics related to histology.

Ultrasound (US)

Ultrasound (US) backscatter, acquired with an US transducer placed in close proximity to the articular cartilage surface (**Figure 1.15**), results from the reflection of incident sound waves and their interaction with cartilage structure. These US signals can be used to visualize cartilage and the osteochondral interface, as well as for calculating quantitative parameters that are based on surface reflection and acoustic backscatter produced by the whole tissue. US is particularly sensitive to tissue boundaries because of differences in acoustic impedance occurring at these interfaces (Saarakkala et al., 2004), and corresponds to cartilage properties (Saarakkala, et al., 2004; Toyras et al., 2002; Viren et al., 2009).

---

5 Niris Imaging System, Imalux, Cleveland, OH, USA

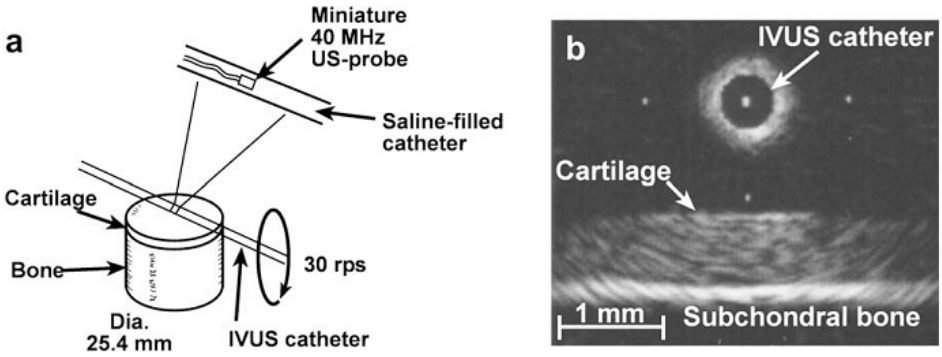

Figure 1.15: a) Schematic illustrating how US measurements of cartilage are made using a specialized miniature US probe (labelled IVUS catheter), and b) an example of an in situ US image of normal cartilage showing the typical appearance of the articular surface and osteochondral interface. *Source:* Viren et al. (2009).

In vitro studies have shown that quantitative US parameters are capable of identifying cartilage changes following enzymatic or mechanical degradation (Saarakkala, et al., 2004; Toyras, et al., 2002; Viren, et al., 2009). The US quantities that appear to be the best candidates for detecting early cartilage degradation are related to surface reflection and surface roughness. Enzymatic degradation induced in cartilage explants by collagenase, and followed by secondary proteoglycan loss, produced statistically significant decreases in surface reflection, while the cartilage surface remained smooth and intact (Viren, et al., 2009). In a separate study, cartilage explants were selectively depleted of either proteoglycan or collagen, producing a similar decrease in Young's modulus, but US surface reflection only decreased substantially due to collagenase treatment (Toyras, et al., 2002). This finding supports a relationship between integrity of the SZ collagen structure and US surface reflection that could be exploited clinically since collagen degradation is considered to be an irreversible degenerative change (Toyras, et al., 2002). US parameters, obtained simultaneously during indentation testing, had moderate to strong correlations with Young's modulus and dynamic modulus (Saarakkala, et al., 2004). In addition, increased sensitivity of US compared to indentation stiffness was demonstrated in cartilage explants where low-grade degradation was created mechanically by surface roughening (Viren et al., 2011). Cartilage thickness, visible in US images and related to US velocity,

compared closely with thickness obtained directly by a needle probe. Thickness differed by an average of 2 ± 99 μm between the two methods (Saarakkala, et al., 2004; Toyras, et al., 2002).

A miniature, high-frequency 40 MHz US probe, originally approved for clinical imaging of vascular walls, has been recently used to assess cartilage during a standard arthroscopic evaluation (Kaleva, et al., 2011). Quantitative US parameters were compared to ICRS macroscopic grade, assigned by the surgeon during arthroscopy, where higher grades indicate greater cartilage degradation. Quantitative parameters changed consistently with increasing ICRS grade, where surface reflection decreased and surface roughness increased. In addition, independent grading of US images, using a qualitative US score analogous to the ICRS grade, identified low-grade cartilage changes in cases where normal ICRS grades were assigned at arthroscopy (Kaleva, et al., 2011).

Taken together, these studies suggest that US could provide a quantitative method for identifying low grade cartilage changes, which correspond to tissue structure and histological appearance (Saarakkala, et al., 2004; Viren, et al., 2009), and that is more sensitive than standard arthroscopic evaluation. US transducers could be used alone to evaluate cartilage intra-operatively (Kaleva, et al., 2011; Viren, et al., 2009; Viren, et al., 2011), or possibly in conjunction with mechanical indentation measurements (Laasanen et al., 2002; Saarakkala, et al., 2004).

Streaming Potentials

Cartilage exhibits electromechanical behaviour resulting from an electrokinetic phenomenon, known as the streaming potential, which occurs when an electrolyte moves with respect to a fixed solid causing a change in electric potential. In cartilage, streaming potentials are generated during compression, when interstitial fluid carrying mobile positive ions is displaced relative to fixed proteoglycan molecules entrapped in the collagen network (Frank & Grodzinsky, 1987; Maroudas, 1968). An arthroscopic device based on the streaming potential method, the

Arthro-BST[6], is commercially available (**Figure 1.16**). It consists of a handheld arthroscopic probe with a sterile tip that contacts the articular cartilage surface, as well as associated electronics that collect and process the streaming potential signals. Streaming potentials are measured by an array of 37 microelectrodes on the spherical end of the sterile tip, which is used to lightly indent the cartilage surface. The streaming potentials are used to calculate a quantitative parameter, the streaming potential integral (SPI), determined by integrating the streaming potential signals over the spherical indenter at a pre-defined amplitude of compression that is reported in units of mV*mm^3. This device provides the means for objective, rapid, and non-destructive cartilage assessment in a variety of experimental and clinical settings (Garon, 2007).

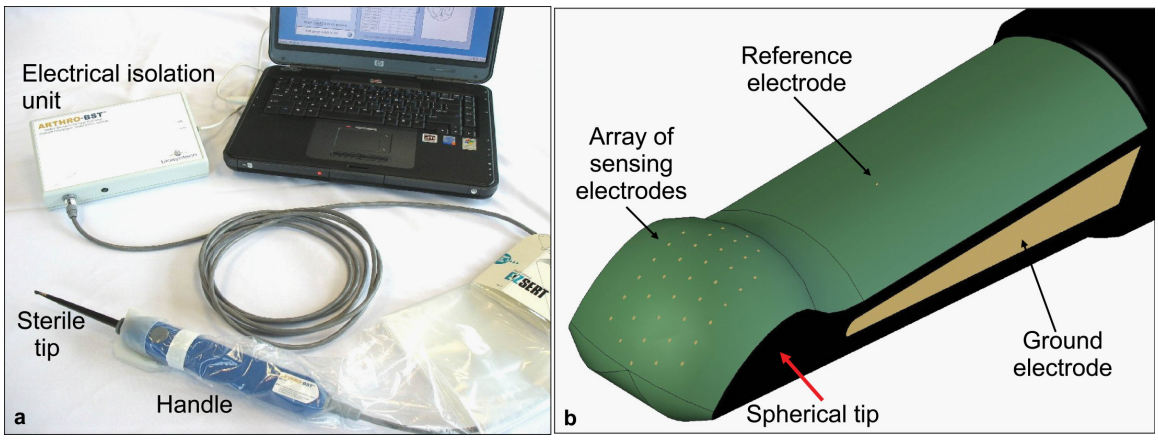

Figure 1.16: a) The Arthro-BST device for measuring cartilage streaming potentials, consisting of an arthroscopic handle, sterile tip and associated electronics. B) Streaming potentials are measured by an array of microelectrodes on the sterile tip, which is used to indent the articular surface. *Source:* Biomomentum Inc., Laval, Quebec, Canada.

The streaming potential is a sensitive measure of normal and degraded cartilage (Bonassar, et al., 1995; Bonassar, et al., 1997; Chen, et al., 1997; Frank, et al., 1987; Garon, et al., 2002; Legare, et al., 2002). In these studies, streaming potentials and biomechanical properties were measured simultaneously and obtained in either confined (Bonassar, et al., 1995;

6 Biomomentum Inc., Laval, Quebec, Canada

Bonassar, et al., 1997; Chen, et al., 1997; Frank, et al., 1987) or unconfined (Garon, et al., 2002; Legare, et al., 2002) compression under a variety of conditions. Notable findings from these investigations are summarized in the following paragraphs.

Streaming potentials successfully followed the kinetics of enzymatic digestion when chondroitinase ABC or trypsin were used to deplete proteoglycans in cartilage disks (Frank, et al., 1987). Additionally, these experiments demonstrated that while both streaming potentials and compressive stiffness decreased with time following enzyme addition, streaming potentials were more sensitive to changes occurring in cartilage. These authors suggest that cartilage containing partially cleaved proteoglycans may produce altered streaming potentials because these fragmented proteoglycans are more mobile than normal aggregates and during compression they become 'entrained in the fluid flow' and contribute less to the streaming potential. However, these partially fragmented proteoglycans can still provide compressive stiffness as long as they reside in the matrix (Frank, et al., 1987).

Bonassar et al. (1997) demonstrated the utility of streaming potentials for studying the inhibition of cartilage degradative processes where cartilage explants were cultured with agents known to induce degradation in combination with those that inhibit degradation. For example, ECM depletion was initiated by adding interleukin-1ß (IL-1ß), a cytokine that interacts with chondrocyte cell membrane receptors and results in an array of changes to cell metabolism including reduced synthesis of ECM components and upregulated production of matrix metalloproteinases (MMP). TIMPs (tissue inhibitors of metalloproteinases) were added to partially impede the effects of the IL-1 cascade specifically by inhibiting the degradative actions of the MMPs, which target collagen and lead to secondary proteoglycan loss. Changes in the physical properties of cartilage disks were assessed by streaming potentials and confined compression testing. A comparison between streaming potential and equilibrium modulus versus time in culture revealed the increased sensitivity of streaming potentials to the inhibitory action of TIMPs. For example, eight days after culture, the equilibrium modulus was equivalent to controls while the streaming potential was approximately 75% of controls. This was reflective of

the actual GAG content, which was reduced to approximately 45% of controls at this time point, as measured by biochemical assay.

Spatially resolved streaming potentials were measured in normal and degraded cartilage disks using a testing chamber modified to include a linear array of eight electrodes. Cartilage disks were positioned over the array so that streaming potentials could be measured at 300 μm intervals from the centre of the disk to the periphery during unconfined compression (Garon, et al., 2002; Legare, et al., 2002). Experimental data revealed streaming potential profiles with maximum potentials at the centre of the disk that decreased monotonically until reaching a minimum at the edge of the disk. These findings compared favourably with predictions from biphasic models, where electrokinetic coupling dictates that streaming potential profiles will correspond to fluid pressure profiles in which peak pressure occurs at the disk centre and decreases radially to a minimum at the disk periphery (Cohen, et al., 1998; Li, Soulhat, Buschmann, & Shirazi-Adl, 1999; Soulhat, et al., 1999).

Cartilage degradation was evaluated in this experimental system for measuring spatially resolved streaming potentials using explants cultured with the cytokine interleukin-1α (IL-1α) over 11 days. Streaming potential amplitudes decreased and changes in the radial streaming potential profiles were observed. The greatest decreases in streaming potential amplitude coincided temporally with the largest losses of GAG to the media. Over the 11 days of culture with IL-1α, radial profiles became increasingly flat, that is, the difference between the central streaming potential and that measured at the disk edge was greatly diminished. Sensitivity to degradation was detected following 1 day of culture, where streaming potential amplitude decreased only at the electrode located at the disk periphery, reflecting initial diffusion of IL-1α from the culture media into the disk. Biochemical assays revealed minute changes of ECM components at this time point coupled with minimal reductions in stiffness (Legare, et al., 2002).

In summary, these studies highlight the ability of the sensitive streaming potential method to assess cartilage function and quality. Features of spatially resolved streaming potential profiles support predictions of the biphasic model describing cartilage response to loading. In cartilage

degraded by enzymes or cytokines, streaming potentials corresponded to ECM changes, such as proteoglycan depletion and collagen II denaturation, as well as to decreased stiffness assessed in confined and unconfined compression.

CHAPTER 2. THESIS OBJECTIVES & HYPOTHESES

Two methodologies for evaluating cartilage, streaming potentials and polarized light microscopy, were explored in response to two specific needs encountered in cartilage research. The first was to find a sensitive assessment method for monitoring subtle cartilage changes occurring in early PTOA. The streaming potential method was recognized as a promising candidate because it demonstrated greater sensitivity to cartilage changes, compared to biomechanical testing, in explant studies where cartilage was modified by cytokines or enzymes. The second need arose from cartilage repair studies, where histological scoring systems presently used to assess repair cartilage quality in clinical trials were observed to inadequately evaluate collagen architecture. The stratified collagen network in articular cartilage is important because of the critical role it plays in load bearing, which may consequently render it the most indicative of the long term durability of repair cartilage. PLM, which is sensitive to fibrillar collagen orientation, was identified as a promising method for developing a histological score that captures the detailed features of ideal collagen organization observed in mature hyaline articular cartilage against which collagen organization in repair cartilage could be compared. Accordingly, these two methodologies, streaming potentials and polarized light microscopy, were investigated to determine whether they could successfully address the identified needs.

2.1 Sensitivity of Streaming Potentials

The suitability of streaming potentials for use in conjunction with the desired model of early PTOA (Section 1.2.3) was investigated using in vitro experiments on equine stifle (knee) joint surfaces. Streaming potential sensitivity was assessed in the immediate phase following impact injury to the articular surfaces. During the development of these experiments, the lengthy testing protocol raised questions about the effect that storing cartilage had on its functional properties. This important aspect of cartilage testing was explored in a separate study using bovine osteochondral explants. Consequently, the objectives and hypotheses of the first two articles are as follows:

2.1.1 Objective & Hypotheses for Article I

Objective: To evaluate the effects of refrigerated or frozen storage on the biomechanical and electromechanical properties of cartilage.

Hypothesis 1: Refrigerated storage at 4ºC for six days will cause detectable changes to cartilage biomechanical and electromechanical properties.

Hypothesis 2: Refrigerated storage at 4ºC for 12 days will lead to more substantial changes to cartilage biomechanical and electromechanical properties than those observed at six days.

Hypothesis 3: Frozen storage at -20ºC, exposing cartilage to a single freeze-thaw cycle, will result in diminished cartilage biomechanical and electromechanical properties.

2.1.2 Objective & Hypotheses for Article II

Objective: To assess the ability of the streaming potential method to detect cartilage changes immediately following localized impact injury at distinct peak stress levels.

Hypothesis 1: Streaming potentials can distinguish cartilage changes produced by impacts of different levels in a dose-dependent manner.

Hypothesis 2: Streaming potentials are more sensitive to changes in articular cartilage produced by impact injury than biomechanical tests.

2.2 Evaluation of Collagen Organization

The development and testing of a qualitative histological score for evaluating cartilage repair tissues was undertaken using PLM. Subsequently, experiments were performed comparing PLM to SEM, for validation purposes as well as to further explore structural characteristics of the

collagen network. These studies are described in the third and fourth papers with the following objectives and hypotheses:

2.2.1 Objective & Hypotheses for Article III

Objective: To develop and test a qualitative histological score using PLM that captures the features of ideal collagen organization present in young adult hyaline articular cartilage.

Hypothesis 1: The proposed PLM score can systematically characterize collagen organization in human biopsies of normal, degraded and repair cartilage tissues.

Hypothesis 2: The proposed PLM score is highly reproducible when applied by multiple trained readers.

2.2.2 Objective & Hypotheses for Article IV

Objective: To compare structural features of the collagen network in normal, degraded and repair cartilage tissues using PLM and SEM methods.

Hypothesis 1: Scores for overall collagen organization, assessed separately using PLM and SEM, are highly correlated.

Hypothesis 2: Differences in structural characteristics of the collagen network, including zonal proportions and collagen fibre diameters, are specific to normal, degraded and repair tissue types.

CHAPTER 3. ARTICLE I

Effects of refrigeration and freezing on the electromechanical and biomechanical properties of articular cartilage

A Changoor[1], L Fereydoonzad[1], A Yaroshinsky[2], MD Buschmann[1*]

Published in the Journal of Biomechanical Engineering in June 2010

Volume 132, Number 6, pp. 064502

[1]Institute of Biomedical Engineering, Department of Chemical Engineering,
École Polytechnique de Montréal, Montréal, Québec, Canada

[2]Biostatistics Consultant, San Francisco, CA, USA

[*]Corresponding author:
Institute of Biomedical Engineering, Department of Chemical Engineering
École Polytechnique of Montréal, P.O. Box 6079, Station Centre-Ville
Montreal, Québec, Canada, H3C 3A7
Tel.: 514-340-4711 ext. 4931
Fax: 514-340-2980
E-mail: michael.buschmann@polymtl.ca

Author's Contributions

Adele Changoor	Study conception and design, data acquisition, data analysis, statistical analysis, literature review, drafting and critical revision of the manuscript. Accepts responsibility for the integrity of the work as a whole. *The contributions of the first author were estimated at 85%.*
Liah Fereydoonzad	Data acquisition, critical revision of the manuscript
Alex Yaroshinsky	Statistical analysis, critical revision of the manuscript
Michael Buschmann	Study conception and design, drafting and critical revision of the manuscript. Accepts responsibility for the integrity of the work as a whole.

3.1 Abstract

Background: In vitro electromechanical and biomechanical testing of articular cartilage provides critical information about the structure and function of this tissue. Difficulties obtaining fresh tissue and lengthy experimental testing procedures often necessitate a storage protocol, which may adversely affect the functional properties of cartilage.

Method of Approach: The effects of storage at either 4ºC for periods of 6 and 12 days, or during a single freeze-thaw cycle at -20ºC were examined in young bovine cartilage. Non-destructive electromechanical measurements and unconfined compression testing on 3 mm diameter disks were used to assess cartilage properties, including the Streaming Potential Integral (SPI), Fibril Modulus (Ef), Matrix Modulus (Em) and Permeability (k). Cartilage disks were also examined histologically.

Results: Compared to controls, significant decreases in SPI (to 32.3 ± 5.5% of control values, $p<0.001$), Ef (to 31.3 ± 41.3% of control values, $p=0.046$), Em (to 6.4 ± 8.5% of control values, $p<0.0001$), and an increase in k (to 2676.7 ± 2562.0% of control values, $p=0.004$) were observed at day 12 of refrigeration at 4ºC, but no significant changes were detected at day 6. A trend towards detecting a decrease in SPI (to 94.2 ± 6.2% of control values, $p=0.083$) was identified following a single freeze-thaw cycle, but no detectable changes were observed for any biomechanical parameters. All numbers are mean ± 95% confidence interval.

Conclusions: These results indicate that fresh cartilage can be stored in a humid chamber at 4ºC for a maximum of 6 days with no detrimental effects to cartilage electromechanical and biomechanical properties, while one freeze-thaw cycle produces minimal deterioration of biomechanical and electromechanical properties. A comparison to literature suggested that particular attention should be paid to the manner in which specimens are thawed after freezing, specifically by minimizing thawing time at higher temperatures.

3.2 Introduction

The composition and highly specific organization of articular cartilage, composed of a hydrated proteoglycan matrix trapped in a primarily type II collagen network, allows this tissue to withstand and distribute applied mechanical loads. When cartilage is compressed, interstitial fluid attempts to flow out of the tissue through the dense proteoglycan matrix, thereby pressurizing the fluid and allowing for load bearing (Chen, et al., 2001; Korhonen, et al., 2003; Li, et al., 2008; Park, et al., 2003). The collagen fibres entrapping and retaining the proteoglycan matrix are placed under tension and restrain the tissue from expansion (Cohen, et al., 1998; Soulhat, et al., 1999). Biomechanical and electromechanical tests are used to assess cartilage functional properties and reflect its composition and structure (Bonassar, et al., 1995; Bonassar, et al., 1997; Garon, et al., 2002; Legare, et al., 2002; Temple-Wong et al., 2009). The limited availability of fresh animal or human articular cartilage and the lengthy testing procedures employed in some experimental protocols often require that cartilage is stored before or during an experiment. Understanding the effects of storage, which often include refrigeration or freezing, on biomechanical and electromechanical properties is critical to correctly designing testing protocols and interpreting their results.

Optimizing articular cartilage storage at 4ºC has been of interest for preserving allograft material (Allen et al., 2005; Ball et al., 2004; Williams et al., 2003). These studies have shown that chondrocyte viability can be maintained up to 14 days (Williams et al., 2005; Williams, et al., 2003), while GAG content and biomechanical properties, measured in indentation, confined compression, and tensile testing, remain unchanged up to 28 days (Ball, et al., 2004). Thomas et al. (1984) performed sequential indentation testing at multiple time points on the same joint surfaces and reported no changes after 4 days of 4ºC storage. In these studies, osteochondral plugs were typically stored in serum free culture medium that was sometimes supplemented with antibiotics or other additives (Allen, et al., 2005; Ball, et al., 2004; Thomas, Jimenez, Brighton, & Brown, 1984; Williams, et al., 2003). Charlebois et al. (2004) described a method of creating humid chambers that permitted chondrocytes to remain viable for up to 2 weeks at 4ºC. In summary, articular cartilage has been shown to retain certain biomechanical properties and

biochemical composition up to 28 days, and cell viability and density up to 14 days, during refrigerated storage.

Cartilage biomechanical properties, determined in indentation testing (Black, Shadle, Parsons, & Brighton, 1979; Kennedy, Tordonado, & Duma, 2007) and confined compression (Willett, Whiteside, Wild, Wyss, & Anastassiades, 2005) have been shown to degrade following freezing. However, several studies (Kempson, Spivey, Swanson, & Freeman, 1971; Kiefer et al., 1989; Swann, 1988) and anecdotal observations (Athanasiou, Rosenwasser, Buckwalter, Malinin, & Mow, 1991; Elmore, Sokoloff, Norris, & Carmeci, 1963) suggest that no changes in indentation properties occur due to freezing. Confined compression tests of osteochondral plugs, before and after storage at -20ºC immersed in PBS, resulted in statistically significant decreases in aggregate modulus (Willett, et al., 2005). Kennedy et al. (2007) reported that cartilage indentation stiffness decreased in whole bovine joints either frozen at -20ºC or flash-frozen to -80ºC. However, creep tests of individual condyles after freezing at 0ºC resulted in no change in instantaneous shear modulus but a statistically significant decrease in relaxed shear modulus and increase in creep rate, indicating that the ability to resist sustained loading was compromised (Black, et al., 1979; Parsons & Black, 1977). Similarly, indentation testing performed on osteochondral cores at physiological stress levels showed no effect due to freezing at -80ºC with or without DMSO as a protectant (Kiefer, et al., 1989), and whole human femoral heads tested prior to and following freezing at -20ºC did not result in changes in the response to indentation testing (Kempson, et al., 1971). In summary, several studies have reported substantial losses in biomechanical properties in articular cartilage subjected to a single freeze-thaw cycle, while others report the contrary; that the biomechanical properties of cartilage are not altered as a result of freezing.

Due to its composition and structure, articular cartilage exhibits electromechanical properties (Frank & Grodzinsky, 1987; Garon, et al., 2002; Maroudas, 1967b; Maroudas, et al., 1969; Sun, et al., 2004). Fixed negative charges on the sulphate and carboxylate groups of the proteoglycans entrapped in the collagen network are balanced by mobile positive ions in the interstitial fluid. When cartilage is compressed fluid flows out of the tissue displacing the mobile

positive ions relative to the fixed negative charges generating streaming potentials. Streaming potentials reflect cartilage composition and function and are sensitive to degradative changes (Bonassar, et al., 1995; Bonassar, et al., 1997; Chen, et al., 1997; Frank, et al., 1987; Garon, et al., 2002; Legare, et al., 2002). In general, degraded cartilage, which is typically proteoglycan depleted (Bora & Miller, 1987), yields lower streaming potentials compared to proteoglycan-rich normal articular cartilage (Chen, et al., 1997; Frank, et al., 1987; Garon, et al., 2002; Legare, et al., 2002; Sun, et al., 2004). To date, the effect of refrigerated or frozen storage on the electromechanical properties of articular cartilage has not been reported in the literature.

Current data summarized above indicates variable results with respect to the effect of freezing or refrigeration on the biomechanical properties of articular cartilage, and that the effects of storage on electromechanical properties are unknown. In the current study the effects of these commonly used storage temperatures on biomechanical and electromechanical properties of articular cartilage were examined. We included refrigeration at 4ºC in humid chambers for 6 days or 12 days, and freezing at -20ºC followed by thawing just prior to testing (1 freeze-thaw cycle). We hypothesized that, with respect to both electromechanical and biomechanical properties, 1. Storage at 4ºC for 6 days would cause detectable changes, 2. Storage at 4ºC for a period of 12 days would lead to more substantial changes than those observed by 6 days, and 3. A single freeze-thaw cycle would result in diminished properties.

3.3 Methods

3.3.1 Sample Preparation & Experimental Design

A young bovine stifle (knee) joint, approximately 6 months of age, was received fresh from a local butcher. The medial and lateral condyles were stored at 4ºC in humid chambers overnight. Humid chambers were created by placing the joint surface into an airtight container with saline-soaked kimwipes arranged so that they were not in direct contact with the articular surface (Charlebois, McKee, & Buschmann, 2004; Langelier & Buschmann, 2003).

Four regions on each condyle were identified using small diameter pins, placed such that there was sufficient joint surface around each pin to allow for non-destructive electromechanical measurements at eight sites and subsequent removal of four 3.5 mm diameter osteochondral cores at a subset of these sites for biomechanical testing and histology. On each condyle, two sites around each pin, labelled Control (n=8), were tested on day 1 prior to storage and two were labelled Storage, corresponding either to storage at 4ºC or -20ºC (n=8). The remaining four sites around each pin were used for sequential electromechanical testing, where electromechanical measurements could be made at all time points throughout the experiment (**Figure 3.1**).

In the refrigeration experiment, the medial femoral condyle was placed in a humid chamber at 4ºC during the intervals between days 1 & 6 and days 6 & 12. In the freezing experiment, the lateral femoral condyle was frozen at -20ºC for 7 days immediately following day 1 measurements. On day 7, it was thawed at room temperature in phosphate buffered saline (PBS) solution (Sigma-Aldrich, St-Louis, MO) for approximately 30 minutes prior to testing.

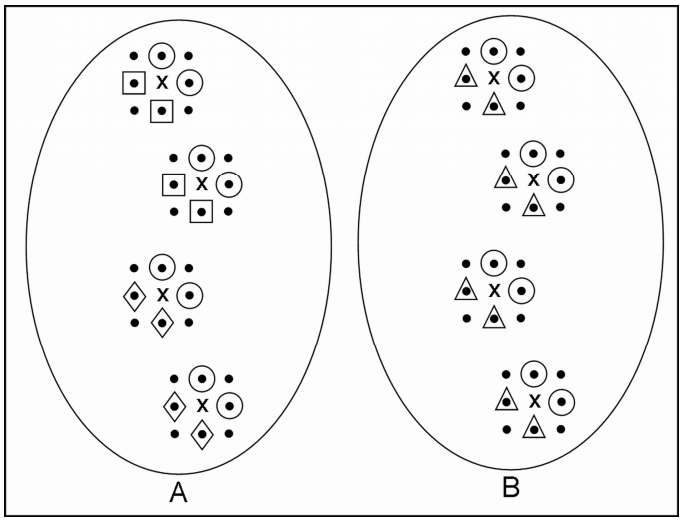

Figure 3.1: Schematic of the Experimental Design. (A) Medial femoral condyle used for the refrigeration experiment. (B) Lateral femoral condyle used for the freezing experiment. Four regions per condyle were marked with small diameter pins (x). Black dots (•) represent sites where electromechanical measurements were made (8 around each pin). Subsequently,

osteochondral cores were harvested from the medial femoral condyle on day 1 for Control sites (open circles, O), and for sites harvested after storage at 4ºC for 6 days (squares,□) and 12 days (diamonds,◇), and from the lateral femoral condyle at day 1 for Control sites (open circles, O) and at day 7 (triangles, Δ) for sites harvested after a single freeze-thaw cycle at -20ºC.

3.3.2 Electromechanical Measurements

The Arthro-BST^{TM}, an arthroscopic device for cartilage assessment (Biomomentum Inc., Laval, Québec, Canada), was used to non-destructively measure the electromechanical properties of cartilage during indentation. This hand-held tool records the streaming potential distribution generated during a light cartilage indentation, and calculates a quantitative parameter, the Streaming Potential Integral (SPI, mV*mm^3), at a standardized amplitude of compression of 150 µm. Electrical signals were measured by an array of 37 gold microelectrodes equally distributed on the hemispherical tip (radius of curvature =3.05 mm) of the Arthro-BST^{TM} device. A digital camera and software assisted users in identifying measurement positions and minimizing error due to positioning the Arthro-BST^{TM} device at each predefined location on the articular surface. Two users measured each site three times for a total of six electromechanical measurements per site. The joint surface was immersed in PBS solution for approximately 30 minutes prior to beginning measurements with the Arthro-BST^{TM}.

3.3.3 Unconfined Compression Testing

Osteochondral cores, isolated from the joint surface using a 3.5 mm diameter mosaicplasty punch (Smith & Nephew, Andover, MA), were stored in individual humid chambers at 4ºC for up to 24 hours. Each sample was tested in unconfined compression geometry using a Mach-1^{TM} Micromechanical Tester (Biomomentum Inc., Laval, Québec, Canada). Immediately prior to testing, the cartilage was separated from the underlying bone using a scalpel, re-punched with a 3 mm diameter biopsy punch and immersed in PBS for 15 min. Cartilage disk thickness was measured with an upright digital calliper (Mitutoyo, Kawasaki, Japan) and used to calculate the testing parameters, which consisted of five compression ramps of

2% strain applied at a rate of 0.4% strain per second. Between ramps, the cartilage was allowed to relax until the load decay was 0.01 g/min. The fibril-network-reinforced biphasic model was fit to the data to obtain fibril modulus (Ef), matrix modulus (Em) and permeability (k) (Fortin, Soulhat, Shirazi-Adl, Hunziker, & Buschmann, 2000; Li, et al., 1999; Soulhat, et al., 1999).

3.3.4 Histology

After biomechanical testing, cartilage disks were fixed in 5% Glutaraldehyde, 0.1M Sodium Cacodylate and embedded in paraffin. 5 μm sections were stained with Safranin-O/Fast Green.

3.3.5 Statistical Analysis

SPI measurements were analyzed separately for each experiment with respect to user, day and measurement repetition using a General Linear Model Repeated Measures ANOVA that permitted interactions between user and day, and user and measurement repetition. In the refrigeration portion of the study, a Tukey's post-hoc test was used to identify the specific day that produced significantly different SPI values since two storage times were considered in this experiment. Biomechanical properties obtained from unconfined compression testing and cartilage thickness were compared using t-tests. All statistical analyses were completed in Statistica v6.1 (StatSoft Inc., Tulsa, OK).

3.4 Results

3.4.1 Electromechanical Measurements

Electromechanical changes were detected in the refrigeration experiment, where a statistically significant decrease was found between days 1 & 12 ($p<0.001$, **Figure 3.2A**), representing an average decrease to 32.3 ± 5.5% (mean ± 95% confidence interval (CI)) of day 1 SPI values. No significant change occurred following 6 days of refrigerated storage and SPI

values were 101.2 ± 7.5% (mean ± 95% CI) of day 1 values (**Figure 3.2A**). In the freezing experiment, a trend towards a significant change was detected indicating a tendency for SPI to decrease following a single freeze-thaw cycle to an average of 94.2 ± 6.2% (mean ± 95% CI) of day 1 values, ($p=0.083$, **Figure 3.2B**). We do not consider this decrease to be biologically significant for in vitro experiments of cartilage electromechanical and biomechanical properties.

An effect of measurement repetition ($p=0.001$) was detected in the refrigeration group. A decrease in SPI with measurement repetition was detected at all time points, but was more pronounced at day 12, reflecting the reduced ability of degraded tissue to recover from indentation in the short time (on the order of several minutes) permitted between measurements. This can be appreciated as an increase in the average coefficient of variation from a maximum of 15% for day 1 and 6 SPI measurements compared to approximately 30% by day 12. The effect of measurement repetition was secondary and inconsequential compared to the very significant overall effect of storage time.

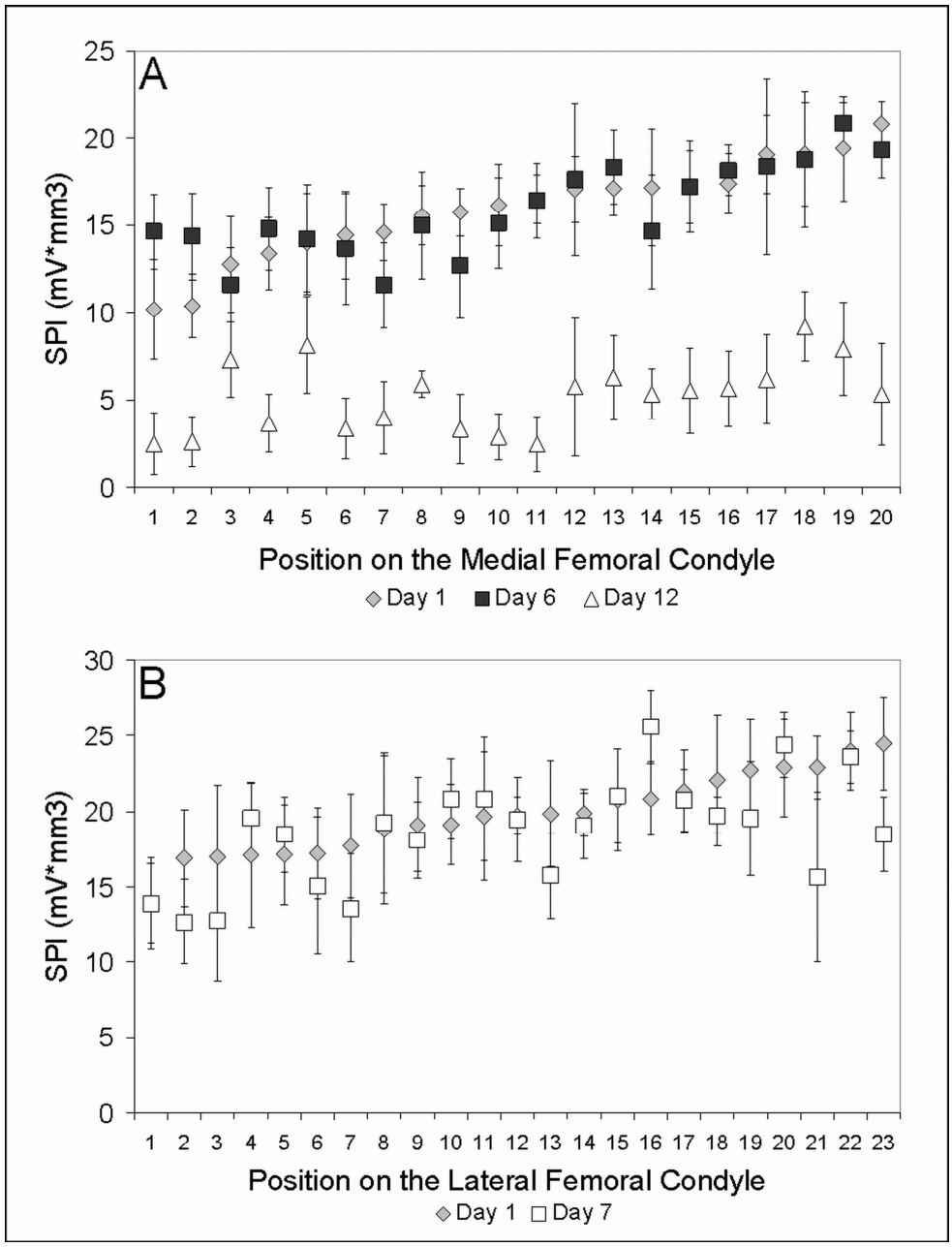

Figure 3.2: Sequential electromechanical measurements (mean ± standard deviation). A) Sites (n=20) on the medial femoral condyle where SPI was obtained prior to storage and at two time points during refrigeration at 4ºC. A statistically significant decrease ($p<0.001$) between days 1 and 12 was detected using a repeated measures ANOVA and Tukey's post hoc test. B) Sites (n=23) on the lateral femoral condyle where SPI was obtained before and after storage at -20C. Repeated measures ANOVA identified a tendency ($p=0.083$) for SPI to decrease following 7

days of frozen storage. Note that technical issues during osteochondral core extraction for biomechanical testing reduced the number of sites available for sequential electromechanical testing by one.

3.4.2 Biomechanical Parameters

Ef, Em and k, determined from the model fits of the fifth stress relaxation ramp for each sample, were compared. By day 12, Ef decreased to 31.3 ± 41.3% (mean ± 95% CI) and Em to 6.4 ± 8.5% (mean ± 95% CI) of day 1 values in a statistically significant manner with $p=0.046$ and $p<0.0001$ for Ef and Em respectively (**Figure 3.3**). There were no significant differences detected between days 1 & 6 in the refrigeration group or following freezing for these two parameters. Permeability (k) increased to 2676.7 ± 2562.0% (mean ± 95% CI) by day 12 of refrigerated storage compared to controls ($p=0.004$). However, there was no change in permeability after six days of refrigerated storage or as a result of freezing. Cartilage thickness was constant in all sample groups, ranging from approximately 1.5 to 2.5 mm.

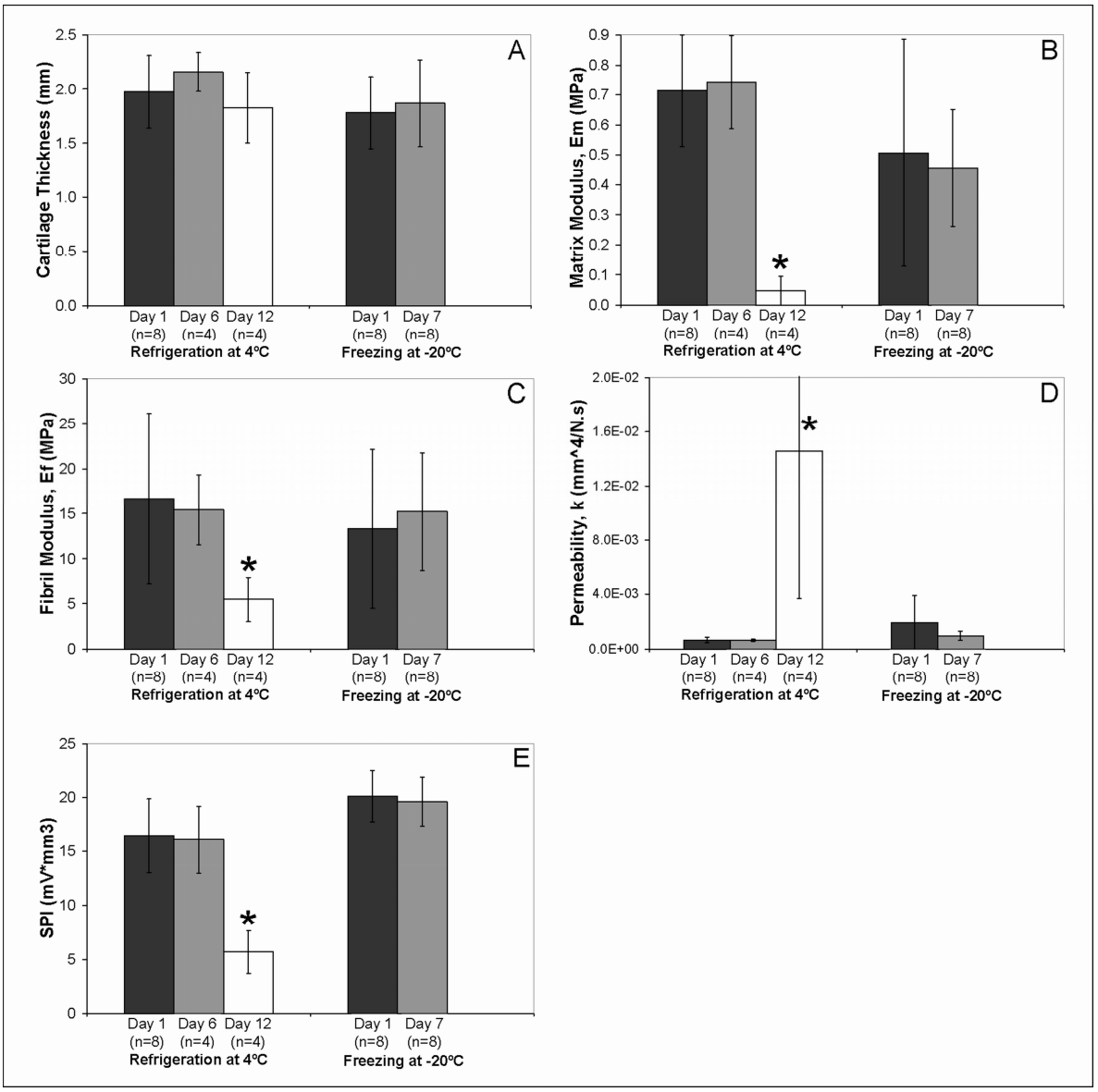

Figure 3.3: A) Cartilage thickness, B) Matrix modulus, C) Fibril modulus, D) Permeability, and E) SPI measurements at sites subsequently removed for biomechanical testing. All values are mean ± standard deviation. Stars (*) indicate statistically significant differences between day 12 and day 1 controls obtained using t-tests.

3.4.3 Histology

Safranin-O/Fast Green staining of cartilage disks in the refrigeration group show little to no change by day 6 but a significant loss of proteoglycan by day 12 (**Figure 3.4**). No evident pattern of histological changes was observed in cartilage disks frozen at -20ºC compared to controls. The high variability may reflect inconsistent levels of degradation due to uneven freezing across a relatively large joint surface. This is reflected histologically, where some samples displayed evidence of Safranin-O depletion and enlarged lacunae while others did not.

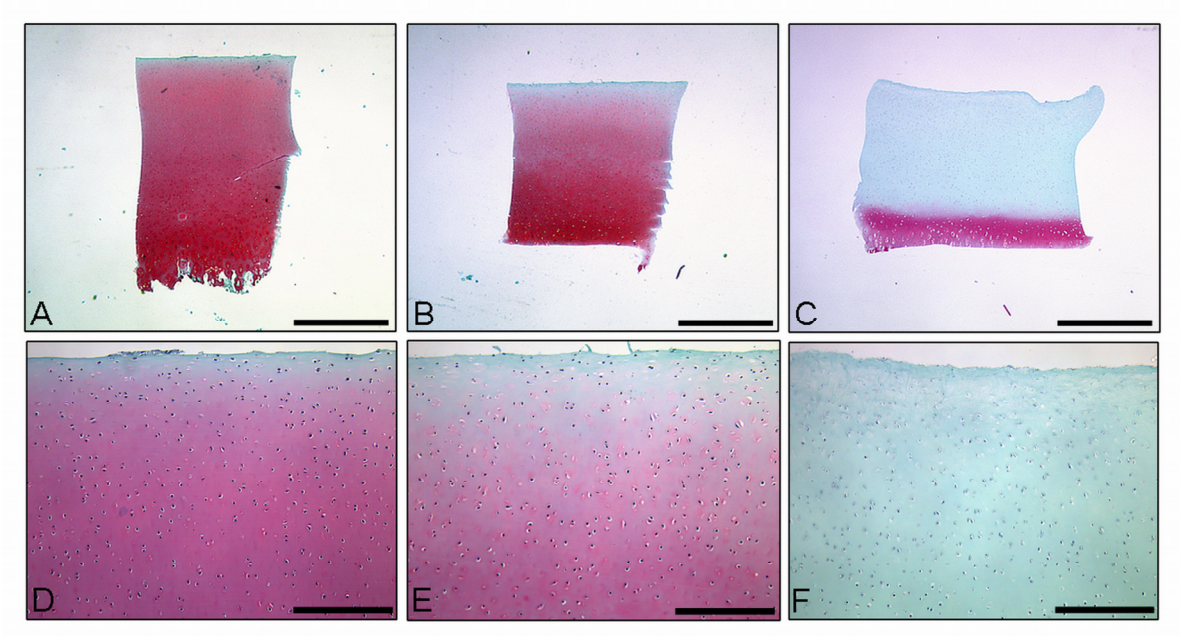

Figure 3.4: Representative Safranin-O/Fast Green stained sections from samples stored at 4ºC. A) & D) Day 1, B) & E) Day 6, C) & F) Day 12. In A, B & C the scale bar is 1 mm. In D, E, F the scale bar is 250 µm.

3.5 Discussion

Understanding the effects of frozen or refrigerated storage on articular cartilage is essential for proper protocol design and the interpretation of experimental findings where storage is often required. Our first hypothesis, that storing cartilage in humid chambers at 4ºC for 6 days

would result in detectable changes, was disproved. Electromechanical and biomechanical properties were maintained (**Figure 3.2A & Figure 3.3**) and these findings were supported by Safranin-O/Fast Green staining, where day 6 samples were similar to controls (**Figure 3.4**). Our second hypothesis was supported by our experimental results, as statistically significant changes in SPI and biomechanical properties were observed after 12 days of refrigerated storage, indicative of weakened cartilage tissue that was substantially less stiff than day 6 or day 1 controls (**Figure 3.2A & Figure 3.3**). Safranin-O/Fast Green staining revealed a near-complete loss of proteoglycan in these samples (**Figure 3.4C & F**). Our third hypothesis, that a single freeze-thaw cycle would result in severely diminished properties, was not supported. While a trend towards a statistically significant decrease in SPI was observed, these changes were small (5.8 ± 6.2% decrease compared to day 1), and no changes in biomechanical properties were detected (**Figure 3.2B & Figure 3.3**). No pattern of histological changes was detected in Safranin-O/Fast Green stained sections of frozen specimens.

3.5.1 Refrigeration up to 6 days in humid chambers maintains biomechanical and electromechanical properties of articular cartilage

In the refrigeration group, significant changes in electromechanical (**Figure 3.2A**), biomechanical (**Figure 3.3**) and histological (**Figure 3.4**) properties were observed at day 12 but no changes were detected at day 6. This preservation of properties for a duration of 6 days is less than other reports (Allen, et al., 2005; Ball, et al., 2004; Williams, et al., 2005; Williams, et al., 2003) and this difference can be attributed to several factors. The most influential factor is likely the various methods in which the samples were stored while at 4ºC. We selected a relatively simple storage method, the humid chamber (Charlebois, et al., 2004; Langelier & Buschmann, 2003), in contrast to the use of tissue culture media and conditions explored by investigators looking to preserve allograft tissue (Allen, et al., 2005; Ball, et al., 2004; Thomas, et al., 1984; Williams, et al., 2005; Williams, et al., 2003). Maintaining cartilage in tissue culture conditions improved chondrocyte viability (Ball, et al., 2004; Brighton et al., 1979), and appeared to allow recovery in Safranin-O staining by 28 days to baseline levels after a depleted superficial zone was observed at 14 days (Williams, et al., 2005). In addition, disparities between our findings and

those reported in the literature may result from the baseline to which comparison is made. For example, two studies (Ball, et al., 2004; Williams, et al., 2003) reported that cartilage compressive, tensile and indentation properties were maintained up to 28 days, however these conclusions were made by comparing samples stored for 7 versus 28 days, since pre-storage biomechanical testing was not performed.

Our findings indicate that gradual tissue degradation is occurring between days 6 and 12 of refrigeration in humid chambers, which may be due to gradual cell death resulting in the release of degradative enzymes (Fukui, Purple, & Sandell, 2001; Goldring & Goldring, 2004; Sandell & Aigner, 2001). This is earlier than the reported maximum of 2 weeks that cell viability was maintained in cartilage refrigerated in human chambers (Charlebois, et al., 2004), but comparable to the maintenance of metabolic activity for 5 days in osteochondral samples stored at 4ºC submerged in a nutrient solution (Schachar, Cucheran, McGann, Novak, & Frank, 1994). The underlying bone present in our samples may have provided a source of degradative factors as it was not irrigated nor immersed in culture media (Pennock et al., 2006). The substantial decrease in SPI observed at all sites on the joint surface at day 12 reflects a loss of proteoglycan, a relationship that is well documented (Bonassar, et al., 1995; Bonassar, et al., 1997; Chen, et al., 1997; Frank, et al., 1987; Legare, et al., 2002; Maroudas, 1967a; Treppo et al., 2000). Degradation is confirmed by changes to the parameters of the fibril-network-reinforced biphasic model, used to fit the stress relaxation ramps from unconfined compression testing, and which reflect the two major extracellular matrix constituents of cartilage (Korhonen, et al., 2003; Li, Shirazi-Adl, & Buschmann, 2003; Li, et al., 2003; Soulhat, et al., 1999). Specifically, Em is related to the stiffness of the drained proteoglycan matrix, and Ef, to the stiffness of the collagen fibre network (Korhonen, et al., 2003). The significant decreases in these two parameters indicate a weakening of the collagen network and loss of proteoglycan molecules, both of which are essential for load-bearing.

3.5.2 One freeze-thaw cycle exerts a nominal influence on electromechanical but no detectable changes to biomechanical properties of articular cartilage

A single freeze-thaw cycle caused a trend towards a significant but small decrease in cartilage electromechanical properties, but did not cause changes to biomechanical properties nor any pattern of histological changes. Taken together, it appears that one freeze-thaw cycle may lead to minor degradation to the extracellular matrix which can be detected by sensitive electromechanical measurements, but not by biomechanical or histological assessment methods.

Our biomechanical findings related to the effect of freezing agree with those of several studies (Elmore, et al., 1963; Kempson, et al., 1971; Kiefer, et al., 1989; Swann, 1988) but are contrary to the considerable reductions in material properties for indentation (Black, et al., 1979; Kennedy, et al., 2007) and confined compression properties (Willett, et al., 2005) reported by other investigators. A possible reason for these discrepancies in the literature may be due to differences in how investigators have treated their samples with respect to thawing and the time between thawing and mechanical testing. For example, Kennedy et al. (2007) froze whole joints with intact soft tissues and allowed them to thaw overnight at room temperature prior to testing, Willett et al. (2005) froze osteochondral dowels immersed in PBS at -20ºC and thawed them in a 37ºC water bath, and Black et al. (1979) froze samples to 0ºC for 5 minutes before thawing and incubating in media for 10 days at 37ºC. We speculate that it is possible that in these studies, where a substantial reduction in mechanical properties was detected, the considerable time spent at elevated temperatures provided a greater opportunity for degradative enzymes to operate (Harris & McCroskery, 1974; Li et al., 2004). In contrast, Kiefer et al. (1989), who reported that freezing caused no change in cartilage indentation properties, employed a shorter thawing procedure in which samples were submerged in phosphate buffered saline (PBS) for 15 minutes and then incubated in Ham's solution for 2 hours at 37ºC. In our study, the frozen joint surface was submerged in room temperature PBS for approximately 30 minutes before beginning electromechanical measurements. This is a comparatively short thawing procedure, which may have limited time for enzymatic degradation to occur, although this was not directly assessed. Based on these observations, we recommend that frozen cartilage be thawed rapidly and

subsequent mechanical tests conducted with minimal delay in order to limit degradative changes to the extracellular matrix.

3.5.3 Conclusions

Our findings indicate that joint surfaces can be stored in humid chambers at 4ºC up to 6 days without experiencing significant changes to cartilage electromechanical and biomechanical properties while storage for longer times can induce significant and biologically important degradation. A single freeze-thaw cycle produced small but detectable changes in electromechanical properties but not biomechanical properties. Streaming potentials provide a sensitive, non-destructive method for rapid cartilage assessment that is user independent. Future studies comparing different thawing protocols and the treatment of samples between thawing and mechanical testing could perhaps explain the discrepancies observed in the literature concerning the effect of freezing on cartilage biomechanical properties.

3.6 Acknowledgements

The authors gratefully acknowledge the technical assistance provided by Dr. Martin Garon and Dr. Eric Quenneville of Biomomentum Inc., Laval, Quebec, Canada, particularly with respect to the streaming potential measurements made with the Arthro-BST^{TM} device.

3.7 References

These are the references as they appear in the published version of the article and are in the style required by the Journal of Biomechanical Engineering. The references contained within the body of Chapter 3 correspond to the reference list at the end of the thesis.

[1] Korhonen, R. K., Laasanen, M. S., Toyras, J., Lappalainen, R., Helminen, H. J., and Jurvelin, J. S., 2003, "Fibril Reinforced Poroelastic Model Predicts Specifically Mechanical Behavior of

Normal, Proteoglycan Depleted and Collagen Degraded Articular Cartilage," J Biomech, 36(9), pp. 1373-1379.

[2] Park, S., Krishnan, R., Nicoll, S. B., and Ateshian, G. A., 2003, "Cartilage Interstitial Fluid Load Support in Unconfined Compression," J Biomech, 36(12), pp. 1785-1796.

[3] Li, L. P., Korhonen, R. K., Iivarinen, J., Jurvelin, J. S., and Herzog, W., 2008, "Fluid Pressure Driven Fibril Reinforcement in Creep and Relaxation Tests of Articular Cartilage," Med Eng Phys, 30(2), pp. 182-189.

[4] Chen, A. C., Bae, W. C., Schinagl, R. M., and Sah, R. L., 2001, "Depth- and Strain-Dependent Mechanical and Electromechanical Properties of Full-Thickness Bovine Articular Cartilage in Confined Compression," J Biomech, 34(1), pp. 1-12.

[5] Cohen, B., Lai, W. M., and Mow, V. C., 1998, "A Transversely Isotropic Biphasic Model for Unconfined Compression of Growth Plate and Chondroepiphysis," J Biomech Eng, 120(4), pp. 491-496.

[6] Soulhat, J., Buschmann, M. D., and Shirazi-Adl, A., 1999, "A Fibril-Network-Reinforced Biphasic Model of Cartilage in Unconfined Compression," J Biomech Eng, 121(3), pp. 340-347.

[7] Bonassar, L. J., Jeffries, K. A., Paguio, C. G., and Grodzinsky, A. J., 1995, "Cartilage Degradation and Associated Changes in Biochemical and Electromechanical Properties," Acta Orthop Scand Suppl, 266, pp. 38-44.

[8] Bonassar, L. J., Sandy, J. D., Lark, M. W., Plaas, A. H., Frank, E. H., and Grodzinsky, A. J., 1997, "Inhibition of Cartilage Degradation and Changes in Physical Properties Induced by Il-1beta and Retinoic Acid Using Matrix Metalloproteinase Inhibitors," Arch Biochem Biophys, 344(2), pp. 404-412.

[9] Garon, M., Legare, A., Guardo, R., Savard, P., and Buschmann, M. D., 2002, "Streaming Potentials Maps Are Spatially Resolved Indicators of Amplitude, Frequency and Ionic Strength Dependant Responses of Articular Cartilage to Load," J Biomech, 35(2), pp. 207-216.

[10] Legare, A., Garon, M., Guardo, R., Savard, P., Poole, A. R., and Buschmann, M. D., 2002, "Detection and Analysis of Cartilage Degeneration by Spatially Resolved Streaming Potentials," J Orthop Res, 20(4), pp. 819-826.

[11] Temple-Wong, M. M., Bae, W. C., Chen, M. Q., Bugbee, W. D., Amiel, D., Coutts, R. D., Lotz, M., and Sah, R. L., 2009, "Biomechanical, Structural, and Biochemical Indices of

Degenerative and Osteoarthritic Deterioration of Adult Human Articular Cartilage of the Femoral Condyle," Osteoarthritis Cartilage.

[12] Treppo, S., Koepp, H., Quan, E. C., Cole, A. A., Kuettner, K. E., and Grodzinsky, A. J., 2000, "Comparison of Biomechanical and Biochemical Properties of Cartilage from Human Knee and Ankle Pairs," J Orthop Res, 18(5), pp. 739-748.

[13] Allen, R. T., Robertson, C. M., Pennock, A. T., Bugbee, W. D., Harwood, F. L., Wong, V. W., Chen, A. C., Sah, R. L., and Amiel, D., 2005, "Analysis of Stored Osteochondral Allografts at the Time of Surgical Implantation," Am J Sports Med, 33(10), pp. 1479-1484.

[14] Ball, S. T., Amiel, D., Williams, S. K., Tontz, W., Chen, A. C., Sah, R. L., and Bugbee, W. D., 2004, "The Effects of Storage on Fresh Human Osteochondral Allografts," Clin Orthop Relat Res(418), pp. 246-252.

[15] Williams, S. K., Amiel, D., Ball, S. T., Allen, R. T., Wong, V. W., Chen, A. C., Sah, R. L., and Bugbee, W. D., 2003, "Prolonged Storage Effects on the Articular Cartilage of Fresh Human Osteochondral Allografts," J Bone Joint Surg Am, 85-A(11), pp. 2111-2120.

[16] Williams, J. M., Virdi, A. S., Pylawka, T. K., Edwards, R. B., 3rd, Markel, M. D., and Cole, B. J., 2005, "Prolonged-Fresh Preservation of Intact Whole Canine Femoral Condyles for the Potential Use as Osteochondral Allografts," J Orthop Res, 23(4), pp. 831-837.

[17] Thomas, V. J., Jimenez, S. A., Brighton, C. T., and Brown, N., 1984, "Sequential Changes in the Mechanical Properties of Viable Articular Cartilage Stored in Vitro," J Orthop Res, 2(1), pp. 55-60.

[18] Charlebois, M., McKee, M. D., and Buschmann, M. D., 2004, "Nonlinear Tensile Properties of Bovine Articular Cartilage and Their Variation with Age and Depth," J Biomech Eng, 126(2), pp. 129-137.

[19] Black, J., Shadle, C. A., Parsons, J. R., and Brighton, C. T., 1979, "Articular Cartilage Preservation and Storage. II. Mechanical Indentation Testing of Viable, Stored Articular Cartilage," Arthritis Rheum, 22(10), pp. 1102-1108.

[20] Kennedy, E. A., Tordonado, D. S., and Duma, S. M., 2007, "Effects of Freezing on the Mechanical Properties of Articular Cartilage," Biomed Sci Instrum, 43, pp. 342-347.

[21] Willett, T. L., Whiteside, R., Wild, P. M., Wyss, U. P., and Anastassiades, T., 2005, "Artefacts in the Mechanical Characterization of Porcine Articular Cartilage Due to Freezing," Proc Inst Mech Eng [H], 219(1), pp. 23-29.

[22] Kempson, G. E., Spivey, C. J., Swanson, S. A., and Freeman, M. A., 1971, "Patterns of Cartilage Stiffness on Normal and Degenerate Human Femoral Heads," J Biomech, 4(6), pp. 597-609.

[23] Kiefer, G. N., Sundby, K., McAllister, D., Shrive, N. G., Frank, C. B., Lam, T., and Schachar, N. S., 1989, "The Effect of Cryopreservation on the Biomechanical Behavior of Bovine Articular Cartilage," J Orthop Res, 7(4), pp. 494-501.

[24] Swann, A. C., 1988, "The Effect of Mechanical Stress on the Stiffness of Articular Cartilage and Its Role in the Aetiology of Osteoarthrosis," University of Leeds.

[25] Athanasiou, K. A., Rosenwasser, M. P., Buckwalter, J. A., Malinin, T. I., and Mow, V. C., 1991, "Interspecies Comparisons of in Situ Intrinsic Mechanical Properties of Distal Femoral Cartilage," J Orthop Res, 9(3), pp. 330-340.

[26] Elmore, S. M., Sokoloff, L., Norris, G., and Carmeci, P., 1963, "Nature Of "Imperfect" Elasticity of Articular Cartilage," Journal of Applied Physiology, 18(2), pp. 393-396.

[27] Parsons, J. R., and Black, J., 1977, "The Viscoelastic Shear Behavior of Normal Rabbit Articular Cartilage," J Biomech, 10(1), pp. 21-29.

[28] Frank, E. H., and Grodzinsky, A. J., 1987, "Cartilage Electromechanics--I. Electrokinetic Transduction and the Effects of Electrolyte Ph and Ionic Strength," J Biomech, 20(6), pp. 615-627.

[29] Maroudas, A., Muir, H., and Wingham, J., 1969, "The Correlation of Fixed Negative Charge with Glycosaminoglycan Content of Human Articular Cartilage," Biochim Biophys Acta, 177(3), pp. 492-500.

[30] Sun, D. D., Guo, X. E., Likhitpanichkul, M., Lai, W. M., and Mow, V. C., 2004, "The Influence of the Fixed Negative Charges on Mechanical and Electrical Behaviors of Articular Cartilage under Unconfined Compression," J Biomech Eng, 126(1), pp. 6-16.

[31] Maroudas, A., 1967, "Fixed Charge Density in Articular Cartilage," 7th International Conference on Medical and Biological Engineering, Stockholm, Sweden, p. 505.

[32] Chen, A. C., Nguyen, T. T., and Sah, R. L., 1997, "Streaming Potentials During the Confined Compression Creep Test of Normal and Proteoglycan-Depleted Cartilage," Ann Biomed Eng, 25(2), pp. 269-277.

[33] Frank, E. H., Grodzinsky, A. J., Koob, T. J., and Eyre, D. R., 1987, "Streaming Potentials: A Sensitive Index of Enzymatic Degradation in Articular Cartilage," J Orthop Res, 5(4), pp. 497-508.

[34] Bora, F. W., Jr., and Miller, G., 1987, "Joint Physiology, Cartilage Metabolism, and the Etiology of Osteoarthritis," Hand Clin, 3(3), pp. 325-336.

[35] Langelier, E., and Buschmann, M. D., 2003, "Increasing Strain and Strain Rate Strengthen Transient Stiffness but Weaken the Response to Subsequent Compression for Articular Cartilage in Unconfined Compression," J Biomech, 36(6), pp. 853-859.

[36] Fortin, M., Soulhat, J., Shirazi-Adl, A., Hunziker, E. B., and Buschmann, M. D., 2000, "Unconfined Compression of Articular Cartilage: Nonlinear Behavior and Comparison with a Fibril-Reinforced Biphasic Model," J Biomech Eng, 122(2), pp. 189-195.

[37] Li, L. P., Soulhat, J., Buschmann, M. D., and Shirazi-Adl, A., 1999, "Nonlinear Analysis of Cartilage in Unconfined Ramp Compression Using a Fibril Reinforced Poroelastic Model," Clin Biomech (Bristol, Avon), 14(9), pp. 673-682.

[38] Brighton, C. T., Shadle, C. A., Jimenez, S. A., Irwin, J. T., Lane, J. M., and Lipton, M., 1979, "Articular Cartilage Preservation and Storage. I. Application of Tissue Culture Techniques to the Storage of Viable Articular Cartilage," Arthritis Rheum, 22(10), pp. 1093-1101.

[39] Fukui, N., Purple, C. R., and Sandell, L. J., 2001, "Cell Biology of Osteoarthritis: The Chondrocyte's Response to Injury," Curr Rheumatol Rep, 3(6), pp. 496-505.

[40] Goldring, S. R., and Goldring, M. B., 2004, "The Role of Cytokines in Cartilage Matrix Degeneration in Osteoarthritis," Clin Orthop Relat Res(427 Suppl), pp. S27-36.

[41] Sandell, L. J., and Aigner, T., 2001, "Articular Cartilage and Changes in Arthritis. An Introduction: Cell Biology of Osteoarthritis," Arthritis Res, 3(2), pp. 107-113.

[42] Schachar, N. S., Cucheran, D. J., McGann, L. E., Novak, K. A., and Frank, C. B., 1994, "Metabolic Activity of Bovine Articular Cartilage During Refrigerated Storage," J Orthop Res, 12(1), pp. 15-20.

[43] Pennock, A. T., Robertson, C. M., Wagner, F., Harwood, F. L., Bugbee, W. D., and Amiel, D., 2006, "Does Subchondral Bone Affect the Fate of Osteochondral Allografts During Storage?," Am J Sports Med, 34(4), pp. 586-591.

[44] Li, L., Shirazi-Adl, A., and Buschmann, M. D., 2003, "Investigation of Mechanical Behavior of Articular Cartilage by Fibril Reinforced Poroelastic Models," Biorheology, 40(1-3), pp. 227-233.

[45] Li, L. P., Buschmann, M. D., and Shirazi-Adl, A., 2003, "Strain-Rate Dependent Stiffness of Articular Cartilage in Unconfined Compression," J Biomech Eng, 125(2), pp. 161-168.

[46] Harris, E. D., Jr., and McCroskery, P. A., 1974, "The Influence of Temperature and Fibril Stability on Degradation of Cartilage Collagen by Rheumatoid Synovial Collagenase," N Engl J Med, 290(1), pp. 1-6.

[47] Li, Z., Yasuda, Y., Li, W., Bogyo, M., Katz, N., Gordon, R. E., Fields, G. B., and Bromme, D., 2004, "Regulation of Collagenase Activities of Human Cathepsins by Glycosaminoglycans," J Biol Chem, 279(7), pp. 5470-5479.

CHAPTER 4. ARTICLE II

Streaming potential-based arthroscopic device is sensitive to cartilage changes immediately post-impact in an equine impact model of osteoarthritis

A Changoor[1], JP Coutu[1], M Garon[2], E Quenneville[2], MB Hurtig[3], MD Buschmann[1*]

Submitted to the Journal of Biomechanical Engineering in December 2010

[1]Institute of Biomedical Engineering, Department of Chemical Engineering
École Polytechnique de Montréal, Montréal, Québec, Canada

[2]Biomomentum Inc., Laval, Québec, Canada

[3]Comparative Orthopaedic Research Laboratory, Ontario Veterinary College, University of Guelph, Guelph, Ontario, Canada

[*]Corresponding author:
Institute of Biomedical Engineering, Department of Chemical Engineering
École Polytechnique of Montréal, P.O. Box 6079, Station Centre-Ville
Montreal, Québec, Canada, H3C 3A7
Tel.: 514-340-4711 ext. 4931
Fax: 514-340-2980
E-mail: michael.buschmann@polymtl.ca

Author's Contributions

Adele Changoor	Study conception and design, data acquisition, data analysis, statistical analysis, literature review, drafting and critical revision of the manuscript. Accepts responsibility for the integrity of the work as a whole. *The contributions of the first author were estimated at 85%.*
Jean-Philippe Coutu	Data acquisition, critical revision of the manuscript
Martin Garon	Statistical analysis, critical revision of the manuscript
Eric Quenneville	Critical revision of the manuscript
Mark Hurtig	Design of custom-built apparatus, acquisition of animal tissues, critical revision of the manuscript
Michael Buschmann	Study conception and design, drafting and critical revision of the manuscript. Accepts responsibility for the integrity of the work as a whole.

4.1 Abstract

Background: Models of post-traumatic osteoarthritis where early degenerative changes can be monitored are valuable for assessing potential therapeutic strategies. Current methods for evaluating cartilage mechanical properties may not capture the subtle cartilage changes expected at these earlier time points following injury. The objective of this study was to determine whether streaming potential measurements by manual indentation could detect cartilage changes immediately following mechanical impact and to compare their sensitivity to biomechanical tests.

Method of Approach: Impacts were delivered at one of three stress levels to specific positions on adult equine trochlea. Cartilage properties were assessed by streaming potential measurements, made pre- and post-impact using a commercially-available arthroscopic device, and by stress relaxation tests in unconfined compression geometry of isolated cartilage disks, providing the streaming potential integral (SPI), fibril modulus (Ef), matrix modulus (Em) and permeability (k). Histological sections were stained with Safranin-O and adjacent unstained sections examined in polarized light microscopy.

Results: Impacts were low, 17.3±2.7 MPa (n=15), medium, 27.8±8.5 MPa (n=13), or high, 48.7±12.1 MPa (n=16), and delivered using a custom-built spring-loaded device with a rise time of approximately 1 ms. SPI was significantly reduced after medium ($p=0.006$) and high ($p<0.001$) impacts. Ef, representing collagen network stiffness, was significantly reduced in high impact samples only ($p<0.001$ lateral trochlea, $p=0.042$ medial trochlea), where permeability also increased ($p=0.003$ lateral trochlea, $p=0.007$ medial trochlea). Significant ($p<0.05$, n=68) moderate to strong correlations between SPI and Ef ($r=0.857$), Em ($r=0.493$), $\log(k)$ ($r=-0.484$), and cartilage thickness ($r=-0.804$) were detected. Effect sizes were higher for SPI than Ef, Em and k, indicating greater sensitivity of electromechanical measurements to impact injury compared to purely biomechanical parameters. Histological changes due to impact were limited to the presence of superficial zone damage which increased with impact stress.

Conclusions: Non-destructive streaming potential measurements were more sensitive to impact-related articular cartilage changes than mechanical assessment of isolated samples. Correlations between electromechanical and biomechanical methods further support the relationship between non-destructive electromechanical measurements and intrinsic cartilage properties.

4.2 Introduction

Articular cartilage covers the ends of long bones in synovial joints, such as the knee, and is responsible for pain-free, virtually frictionless motion and distributing applied loads to underlying bone. It has a complex extracellular matrix (ECM) mainly composed of large, hydrated proteoglycan molecules trapped in a highly organized fibrillar collagen network. Under compression, interstitial fluid associated with the proteoglycan matrix is pressurized, placing the collagen network in tension, allowing for high dynamic stiffness and load-bearing (Chen, et al., 2001; Korhonen, et al., 2002; Li, et al., 2008; Park, et al., 2003). The collagen network provides the structural architecture of cartilage, immobilizes proteoglycan which resist fluid flow, and thereby resists tissue compression and expansion to provide effective load bearing.

Cartilage also exhibits electromechanical behaviour due to negatively-charged sulphate and carboxyl groups on proteoglycan which are bathed in extracellular fluid bearing a net positive charge due to Donnan equilibrium (Frank & Grodzinsky, 1987; Maroudas, 1967b; Maroudas, et al., 1969; Sun, et al., 2004). During compression, the excess positive mobile sodium ions are displaced relative to the fixed proteoglycan, generating streaming potentials. Streaming potentials reflect the structure and composition of cartilage and are known to be sensitive to enzymatic and cytokine induced degradation (Bonassar, et al., 1995; Bonassar, et al., 1997; Chen, et al., 1997; Frank, et al., 1987; Garon, et al., 2002; Legare, et al., 2002).

The stratified and functionally important ECM of articular cartilage forms during normal post-natal development processes and is maintained in adulthood by a sparse population of resident chondrocytes. Consequently, articular cartilage has limited intrinsic repair capacity. In osteoarthritis (OA), degradative processes overwhelm the ability of chondrocytes to maintain the ECM (Mandelbaum & Waddell, 2005). Arthritic cartilage is mechanically weak, due to the fragmented collagen network and proteoglycan depletion, and abnormally low streaming potentials are generated during compression. OA that develops following joint injury or trauma is described as post-traumatic osteoarthritis (PTOA), and studies suggest that 50% of these patients will develop OA 5-15 years after the initial mechanical insult (Lotz, 2010). Since the initiating

event in PTOA is known, a unique opportunity exists during the immediate and acute stages when degenerative and remodelling processes are elevated and where therapeutic intervention administered to moderate disease progression may have the greatest preventative potential (Lotz, 2010; Mandelbaum & Waddell, 2005; Scott & Athanasiou, 2006).

Evaluating potential therapeutic strategies require animal models of PTOA where early degenerative changes can be monitored. Impact models, where the location and severity of damage inflicted on the joint surface are controlled, are suited to this purpose (Scott & Athanasiou, 2006). Previous studies have delivered impacts using drop-tower devices, pendulums or free flight masses, which are capable of producing high strain rates (Scott & Athanasiou, 2006) with time to peak loads less than 30 ms (Aspden, et al., 2002). Explant impact studies have documented chondrocyte apoptosis and extracellular matrix fissuring and depletion as a result of impact loading (Jeffrey, et al., 1995; Quinn, et al., 2001; Repo & Finlay, 1977; Thompson, et al., 1991; Torzilli, et al., 1999).

In vivo studies are often performed in smaller animals like rabbits and dogs (Scott & Athanasiou, 2006) where impact is delivered to closed joints (Isaac, et al., 2010) or directly to the cartilage surface via a surgical incision (Borrelli, et al., 2004; Vrahas, et al., 1997; Zhang, et al., 1999). In vivo models generally have less control over the delivery of the mechanical insult, but provide the appropriate physiological environment for studying acute and chronic degenerative effects of impact, including upregulation of matrix-degrading enzymes, subchondral bone changes, and reduced biomechanical properties (Bolam, et al., 2006; Donohue, et al., 1983; Haut, Ide, & De Camp, 1995; Newberry, et al., 1998).

Equine models of OA are advantageous because the comparatively large stifle (knee) joint affords arthroscopic access to joint surfaces including the condyles and distal trochlea. Bolam et al. reported irreversible cartilage degradation at 3 months, which continued to progress up to 6 months, following localized impact of 60 MPa in equine medial femoral condyles. At 3 months, degradative changes included loss of sulphated glycosaminoglycans, superficial zone fissuring and mild synovitis. By 6 months, more overt fibrillation, cartilage delamination and lesions on

opposing joint surfaces were noted. Studying earlier time points in this model, where a trajectory towards OA has been established, could provide the desired model system of early PTOA where therapeutic strategies could be tested (Scott & Athanasiou, 2006). However, current methods for evaluating cartilage mechanical properties may be inadequate for measuring the subtle cartilage changes expected at these earlier time points. The sensitivity of the streaming potential method to degeneration (Bonassar, et al., 1995; Frank, et al., 1987; Legare, et al., 2002) makes it a promising candidate in this regard. A commercially available arthroscopic device, the Arthro-BST (Biomomentum Inc., Laval, Canada), non-destructively measures the electric potentials generated during cartilage compression and computes a quantitative parameter, the streaming potential integral (SPI), reflecting cartilage structure, composition and function.

In the present study, the ability of streaming potentials to detect cartilage changes following localized impacts at three distinct stress levels was assessed in vitro. We hypothesized that streaming potentials could distinguish between impact levels and that they were more sensitive than biomechanical tests.

4.3 Methods

4.3.1 Sample Preparation & Experimental Design

Both stifle (knee) joints from a 4 year old Standardbred horse with no pre-existing joint pathology were collected within 1 hour of sacrifice and stored at 4°C. The lengthy experimental protocol necessitated testing the right stifle 5 days after the left and it remained refrigerated with a closed joint capsule and intact surrounding musculature to limit degenerative changes.

36 arthroscopically accessible sites per trochlea were identified on the distal two-thirds of the joint surface (**Figure 4.1**). 12 sites were controls, and the remaining 24 sites assigned to one of three levels of impact. The placement of impact and control sites accommodated the normal variability in cartilage properties observed in this joint surface (Changoor et al., 2006) and seen during a pilot study.

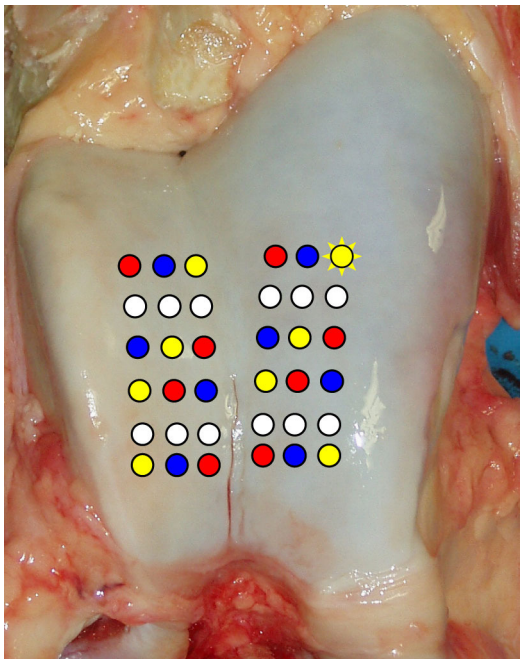

Figure 4.1: Schematic of a right equine trochlea with 36 positions identified as either non-impacted controls (white) or impact sites. Impact stress levels included 17 MPa (red), 28 MPa (blue), and 49 MPa (yellow). The star indicates the position that was considered an outlier from results of biomechanical tests. Not to scale.

4.3.2 Electromechanical Testing

The Arthro-BST, a hand-held arthroscopic device for cartilage assessment (Biomomentum Inc., Laval, Canada), was used to non-destructively measure electromechanical properties of articular cartilage during indentation. Streaming potentials were measured by an array of 37 gold microelectrodes equally distributed on the hemispherical tip (radius of curvature=3.05 mm) of the Arthro-BST device. Associated instrumentation and software captured the streaming potential distribution generated on the spherically shaped tip during a light cartilage indentation. A quantitative parameter, the streaming potential integral (SPI, $mV*mm^3$), was calculated at a standardized amplitude of compression of 150 µm determined by electrode-tissue contact signals analysed over time.

Two users measured each site three times for a total of six electromechanical measurements per site. This was done prior to impact and repeated following impact. A digital camera and LabVIEW software assisted users in identifying measurement sites and minimizing error due to repeated positioning of the Arthro-BST device at each predefined location. The joint surface was immersed in PBS solution for approximately 30 minutes prior to beginning electromechanical measurements.

4.3.3 Impact Delivery

Impacts, at one of three stress levels, were delivered using a custom-built impactor device, consisting of a spring-loaded shaft and sterilizable, 6.5 mm diameter plane-ended tip with rounded edges, designed for both in vitro and in vivo studies (Bolam, et al., 2006). Impacts were delivered manually by aligning the device so that the tip was perpendicular to the articular cartilage surface, then compressing the spring and releasing it to transfer the stored potential energy to the articular surface at rise times of approximately 1 ms. Spring compression was standardized by marking the shaft of the impactor at levels known to produce the desired impact stresses, which were established during a pilot study. The trochlea was secured mechanically and the cartilage surface covered with saline soaked kimwipes, when not being impacted, to prevent dehydration.

Impact stresses were derived from measurements made with a calibrated piezoelectric force transducer (Model 218C, PCB Piezotronics, Depew, NY, USA) placed in-line with the impactor tip and connected via a charge amplifier (Model 421A11, PCB Piezotronics, Depew, NY, USA) to a data acquisition card (Model USB6009, National Instruments) and LabVIEW software. The transducer signal was sampled at 48 kHz, and impact stress calculated by normalizing peak force to the cross-sectional area of the impactor tip, 32.7 mm^2.

Immediately following impacts, India ink (BD India Ink Reagent Droppers) was applied to the joint surface and electromechanical measurements repeated.

4.3.4 Unconfined Compression Testing

Osteochondral cores were isolated from all sites (n=72 for both trochlea) using a 3.5 mm diameter mosaic arthroplasty punch (Acufex, Smith & Nephew, Andover, MA) and stored in individual humid chambers at 4°C until biomechanical testing in unconfined compression geometry on one of two Mach-1 Micromechanical Testers (Biomomentum Inc., Laval, Canada).

Immediately prior to testing, cartilage was separated from the underlying bone, re-punched to 3 mm diameter, and equilibrated in PBS for 15 minutes. Cartilage disk thickness was measured, at 5 locations per disk, with an upright digital micrometer (Mitutoyo, Kawasaki, Japan), and used to calculate test parameters. An initial pre-compression was applied until the top of the cartilage disk was parallel with the bottom. Then, each disk was subjected to five stress relaxation ramps of 2% strain applied at a rate of 0.4% strain per second. Between ramps, relaxation was permitted until the load decay was 0.01 g/min. The fibril-network-reinforced biphasic model was fit to the data to obtain fibril modulus (Ef), matrix modulus (Em) and hydraulic permeability (k) (Fortin, et al., 2000; Li, et al., 1999; Soulhat, et al., 1999).

4.3.5 Histology

Following biomechanical testing, cartilage disks were fixed in a solution of 2.5% cetylpyridinium chloride (CPC), 4% paraformaldehyde, 0.1M sodium cacodylate, at 4°C. The inclusion of CPC prevents the loss of sulphated glycosaminoglycans to the fixation media, which can occur especially in impacted samples (Changoor, Quenneville, Garon, Hurtig, & Buschmann, 2009). Cartilage disks were fixed for a minimum of 1 week, paraffin embedded, and sectioned at 5 µm. Sections were stained with Safranin-O/fast green/iron hematoxylin and adjacent sections were mounted unstained for viewing in polarized light microscopy (PLM).

4.3.6 Statistical Analysis

Paired t-tests were used to compare pre- and post-impact SPI. Sensitivity testing was performed by running an equivalent non-parametric test, the Wilcoxon matched pairs test, for

comparison. A general linear model one-way ANOVA followed by Fisher's LSD post hoc tests were used to compare biomechanical parameters at impacted versus control sites. Effect size (the difference in means divided by pooled variance) was calculated between each impact group and controls in order to provide a sensitivity of each measurement parameter to impact. Correlations between SPI and biomechanical properties were also explored. Inter- and intra-user reliability of electromechanical measurements were obtained using intraclass correlation coefficients (ICC) for agreement, assessed simultaneously using a repeated measures design (Eliasziw, Young, Woodbury, & Fryday-Field, 1994). Statistical analyses were performed in Statistica v.9 (StatSoft Inc., Tulsa, OK) except ICCs, which were calculated using a custom-built LabVIEW function (LabVIEW v.8.6, National Instruments, Austin TX, USA) validated against results obtained with SPSS v.9 (SPSS Inc. Chicago, IL, USA).

4.4 Results

4.4.1 Impacts

Measured average impact stress delivered to the trochlear surfaces were either low, 17.3±2.7 MPa (n=15), medium, 27.8±8.5 MPa (n=13), or high, 48.7±12.1 MPa (n=16).

4.4.2 Electromechanical Measurements

SPI decreased as a function of impact stress on both the medial and lateral trochlear surfaces (**Figure 4.2**). When compared to pre-impact values, paired t-tests detected significantly reduced SPI following high ($p<0.001$, n=16) and medium ($p=0.006$, n=15) impacts, but not low impact ($p=0.544$, n=16). Considering the medial and lateral facets separately revealed that while high impacts significantly reduced SPI on both joint surfaces, medium impacts led to a significant reduction on the medial trochlea ($p=0.032$, n=7) and a trend towards a reduction on the lateral trochlea ($p=0.103$, n=8). Results obtained from an equivalent non-parametric test, the Wilcoxon matched pairs test, were concurrent with parametric testing and significantly ($p<0.05$) reduced SPI was detected in all cases described above, including medium impact on the lateral trochlear facet. These changes in SPI resulted in effect sizes (difference in pre- vs. post-impact

means ÷ pooled standard deviation) that increased as a function of impact stress and which were larger than effect sizes resulting from purely biomechanical tests (**Figure 4.3**).

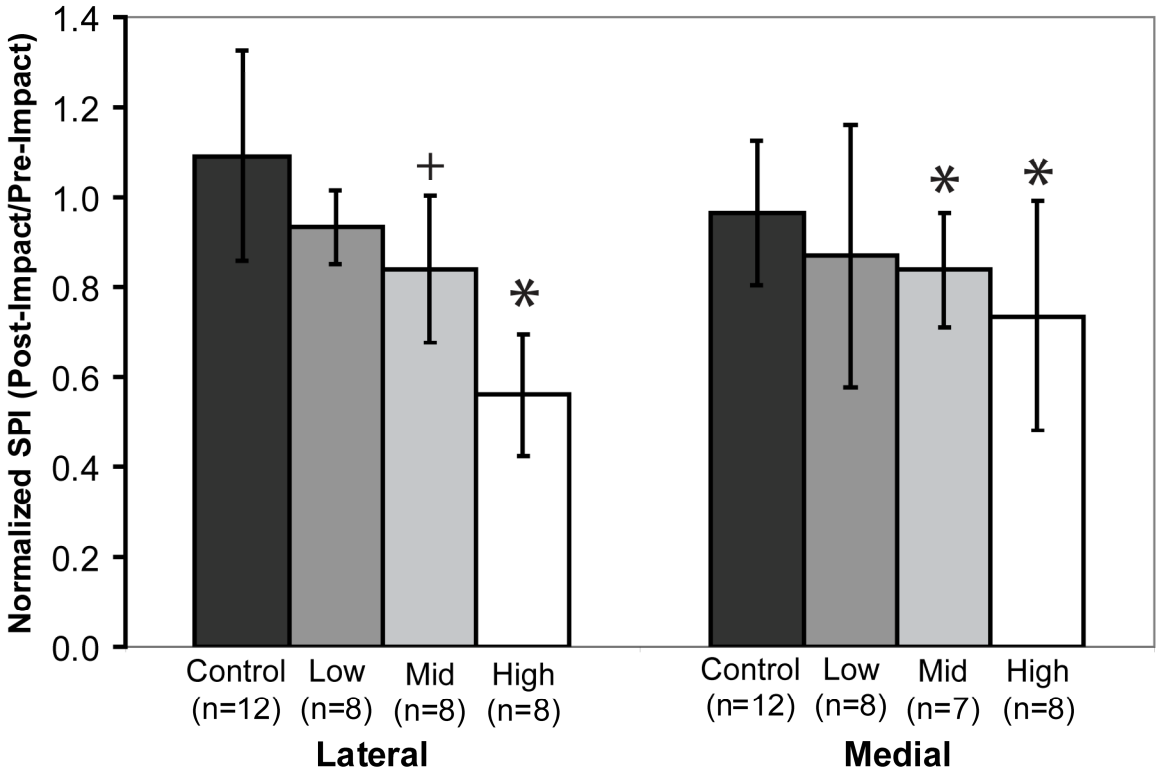

Figure 4.2: Normalized SPI values (mean ± standard deviation) for non-impacted controls (n=24), and sites receiving low (n=16), medium (n=15) and high (n=16) impacts. One site that received a medium impact was excluded because SPI measurements were inconsistent for both readers and had a high coefficient of variation approaching 30%. Results from paired t-tests comparing pre- and post-impact SPI are indicated with (*) for statistically significant differences ($p<0.05$) and (+) for statistical trends ($p<0.10$).

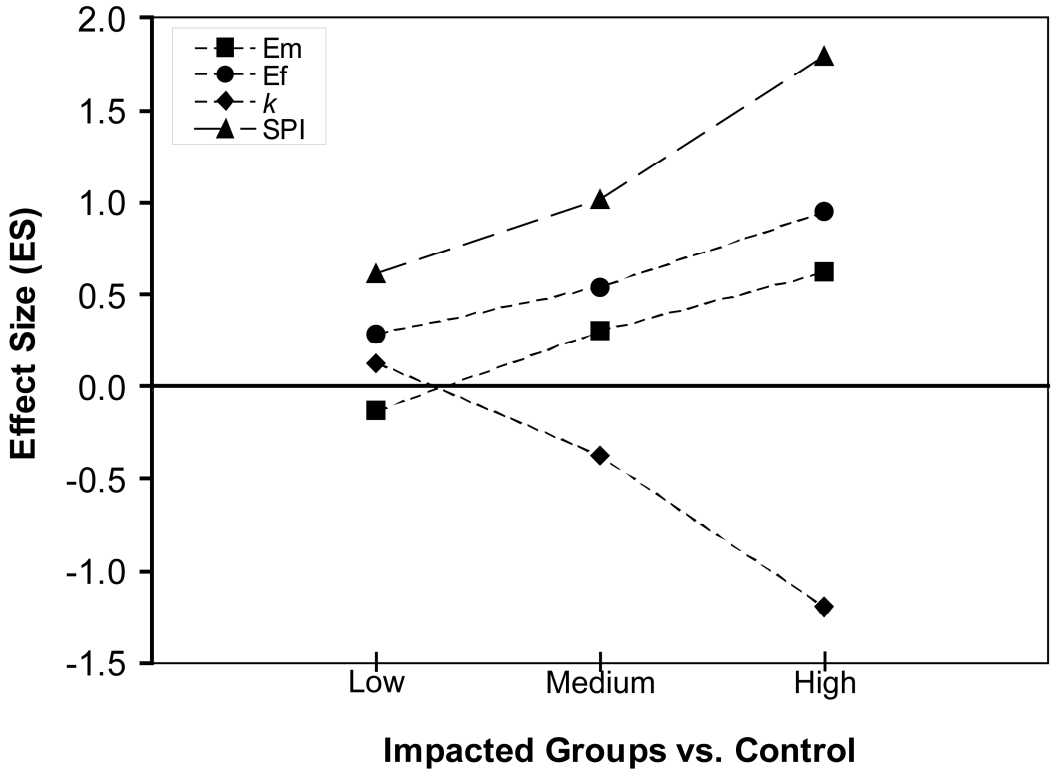

Figure 4.3: Effect sizes (difference in pre- vs. post-impact means ÷ by pooled variance) for each impacted group compared to non-impacted controls. Biomechanical and electromechanical parameters from medial and lateral trochlear surfaces were combined for a total of n=24 for non-impacted controls, n=15 for low impact, n=15 for medium impact, and n=14 for high impact. Higher effect sizes for SPI indicate greater sensitivity to cartilage changes than for purely biomechanical measurements.

Excellent intra- and inter-user agreement among SPI measurements were determined using ICCs and confirmed the user-independent nature of this streaming potential method (**Table 4.1**). ICCs are the ratio of variance in the sample population to that of the sample population plus measurement variance. Thus, ICCs close to 1 imply very low measurement variability relative to sample population variability. The inter-user ICC of 0.861 indicates excellent agreement between users' measurements, while intra-user (average) describes the reliability of using the average of a single user's three measurements. Individual intra-user ICCs, 0.898 and 0.917, describe the reliability of using a single measurement from User 1 or User 2 respectively. Due to the high

reliability and agreement among SPI measurements, average SPI was calculated from the six measurements (3 per user x 2 users) and used for all data analysis.

Table 4.1: Intraclass correlation coefficients and the lower boundary of the 95% confidence interval (CI) for intra- and inter-reader reliability of electromechanical measurements made with the Arthro-BST device. An ICC of 1.00 indicates perfect agreement.

Reliability	ICC (Agreement)	Lower 95% CI
Intra-reader (Reader 1)	0.898	0.869
Intra-reader (Reader 2)	0.917	0.914
Intra-reader (Average)	0.908	0.881
Inter-reader	0.861	0.831

4.4.3 Biomechanical Parameters

Impact produced dose-dependent changes in biomechanical parameters measured during unconfined compression testing, including diminished Ef and Em, and increased k (**Figure 4.4**). These observations were supported by statistical analysis where Ef, Em, and k, obtained from model fits of the fifth stress relaxation ramps, were compared by treatment. Compared to non-impacted controls, Ef, representing collagen network stiffness, was reduced by high impact ($p<0.001$ lateral, $p=0.042$ medial), with a parallel increase in permeability, k ($p=0.003$ lateral, $p=0.007$ medial). No statistically significant changes in Em, representing proteoglycan matrix stiffness, were detected. Additionally, statistically significant differences were detected between low or medium impact groups when compared to high impact, including higher Ef on the lateral trochlea ($p=0.042$ low impact, $p=0.035$ medium impact), and lower permeability on both lateral ($p=0.003$ low impact, $p=0.026$ medium impact) and medial ($p=0.027$ low impact, $p=0.036$ medium impact) joint surfaces. The articular cartilage was thinner ($p<0.001$) on the medial facet, 1.54±0.18 mm (n=36) compared to the lateral, 2.02±0.17 mm (n=36). Effect sizes for all biomechanical parameters increased with respect to impact level, with the largest changes associated with permeability, however all were lower than the effect sizes for SPI (**Figure 4.3**).

Four outliers were excluded from biomechanical data analysis. Two samples had large differences in thickness, approximately 30%, among the 5 thickness measurements made per sample, which caused them to appear stiffer. In this stress relaxation protocol, a pre-compression is applied to ensure that surfaces are parallel before the series of 5 ramps is applied. When a large difference in thickness occurs, the pre-compression is relatively large, placing the cartilage disk under significant load and compression in advance of the actual test. The other two outliers were at the same position on both trochlea (**Figure 4.1**). Cartilage characteristics here were inconsistent with the central trochlear region, exhibiting high SPI values, small thicknesses, and both were very resistant to impact damage, appearing normal at histology.

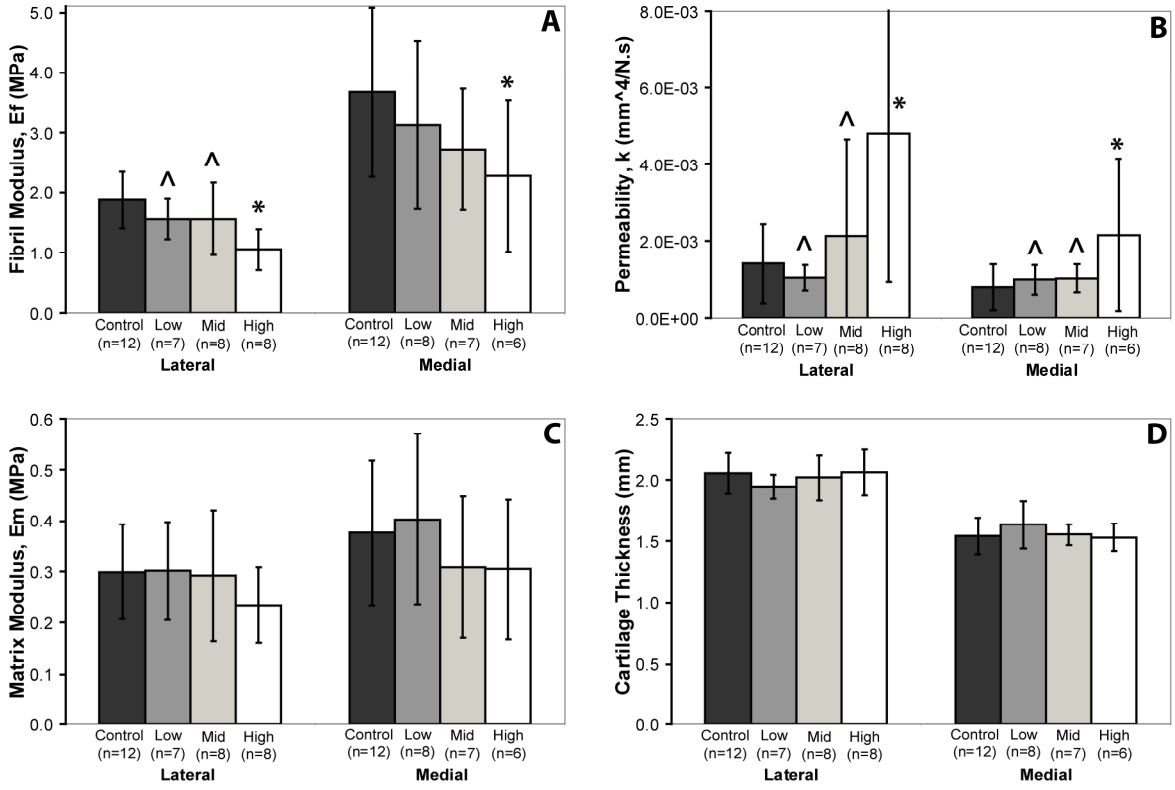

Figure 4.4: Biomechanical parameters obtained during unconfined compression testing including (A) Fibril modulus, (B) Permeability, (C) Matrix modulus, (D) Cartilage Thickness. (*) indicates statistically significant differences ($p<0.05$) between control and impacted cartilage. Statistical differences between low or medium impact compared to high impact are identified with (^).

4.4.4 SPI & Biomechanics Correlations

Linear regression analysis identified significant correlations between SPI and biomechanical parameters measured during unconfined compression testing (**Figure 4.5**). SPI was positively correlated with both Ef (r=0.857, p<0.0001, n=68) and Em (r=0.493, p<0.0001, n=68), and negatively correlated with cartilage thickness (r=-0.804, p<0.0001, n=68). A negative weak correlation with k (r=-0.343, p=0.004, n=68) was detected and this was improved to (r=-0.484, p<0.0001, n=68) when transformed to log(k).

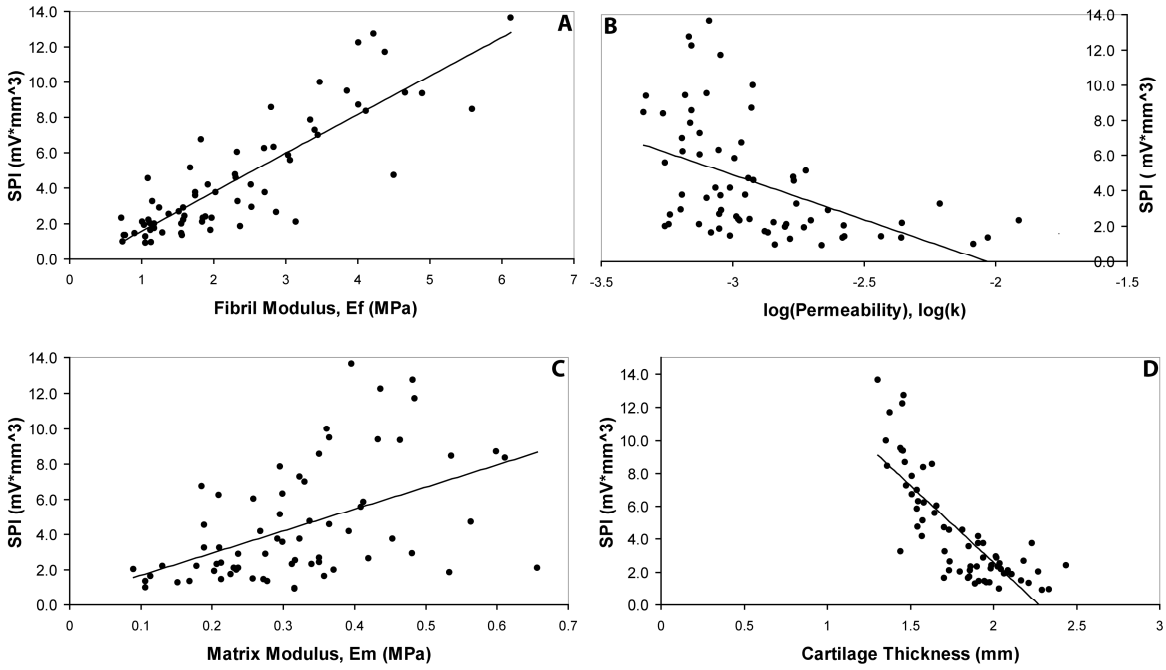

Figure 4.5: Scatterplots of SPI vs. biomechanical parameters obtained from unconfined compression testing. Correlations between SPI and (A) fibril modulus (r=0.857, p<0.0001, n=68), (B) permeability transformed to log(k) (r=-0.484, p<0.0001, n=68), (C) matrix modulus (r=0.493, p<0.0001, n=68), and (D) cartilage thickness (r=-0.804, p<0.0001, n=68).

4.4.5 Histology

India ink uptake allowed cartilage surface disruptions to be visualized immediately after impact (Meachim, 1972). Surface cracking and diffuse staining at high impact sites were

observed and contrasted with faint or no staining at low impact sites. Medium impact caused variable changes ranging from faint India ink staining to the appearance of minor cracking.

These macroscopic findings corresponded to light microscopy observations of the articular surface (**Figure 4.6** & **Figure 4.7**) where the majority of high impact sites had large surface tears extending into the transitional zone or upper deep zone. In some medium impact samples, surface roughening and small cracks, which rarely extended beyond the superficial zone, covered the cartilage surface, while in others the articular surface was relatively smooth with only limited evidence of impact. The surfaces of low impact disks exhibited minimal cracking and occasional superficial zone fissures. Control cartilage disks expectedly had smooth, intact articular surfaces, although some exhibited imperfections similar to the low impact group (**Figure 4.6**).

Polarized light microscopy (PLM) patterns were normal in all groups, with birefringent superficial and deep zones separated by a non-birefringent transitional zone (**Figure 4.6**). The majority of control cartilage disks had intense Safranin-O staining with some depletion at the articular surface (**Figure 4.7**). Impacted samples were more likely to exhibit weaker Safranin-o staining, both at the surface and the interterritorial matrix of the deep zone.

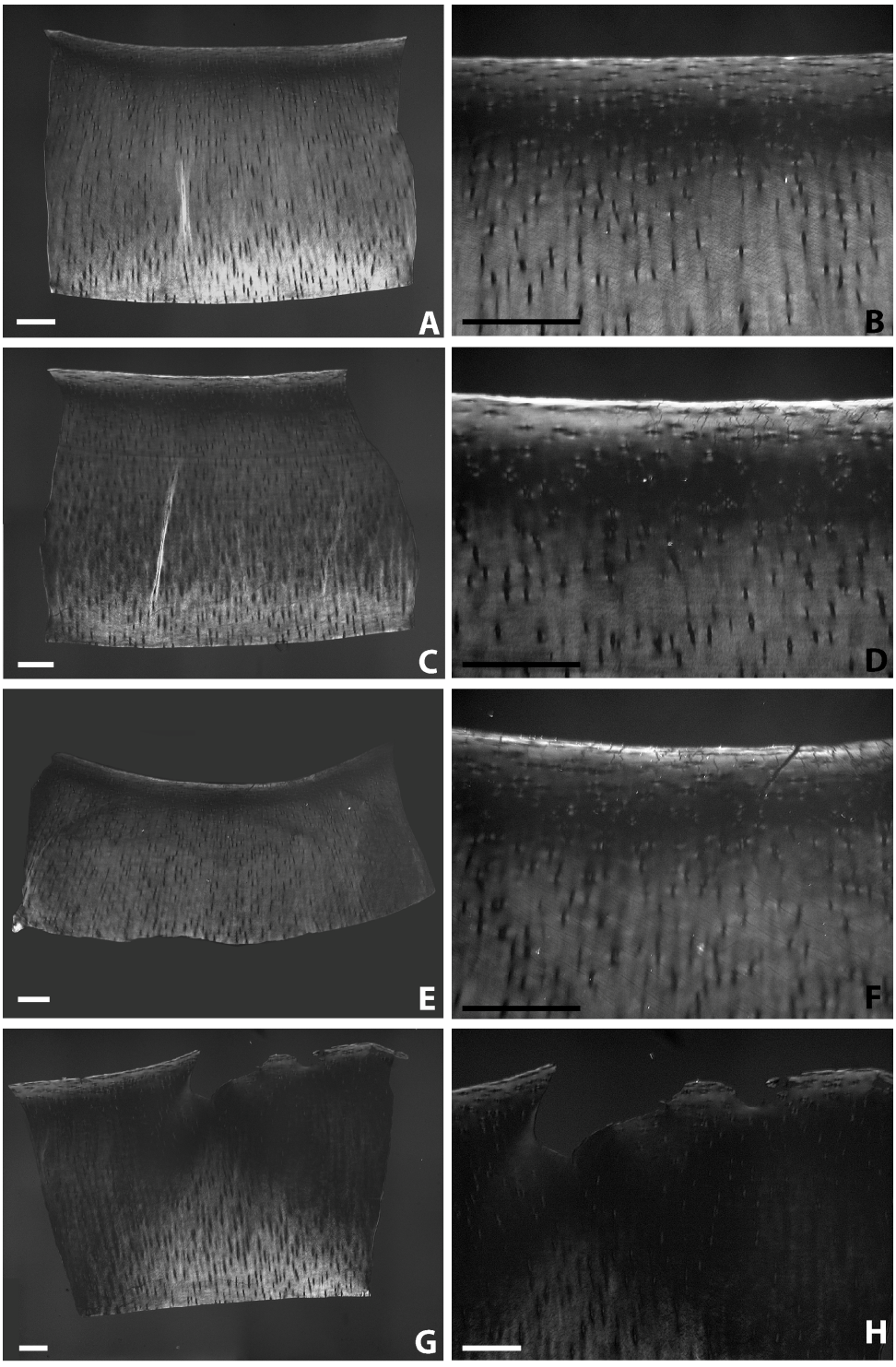

Figure 4.6: PLM images of full-thickness cartilage disks from (A) non-impacted control, and (B) low, (C) medium, and (D) high impact groups. Scale bars are 250 μm.

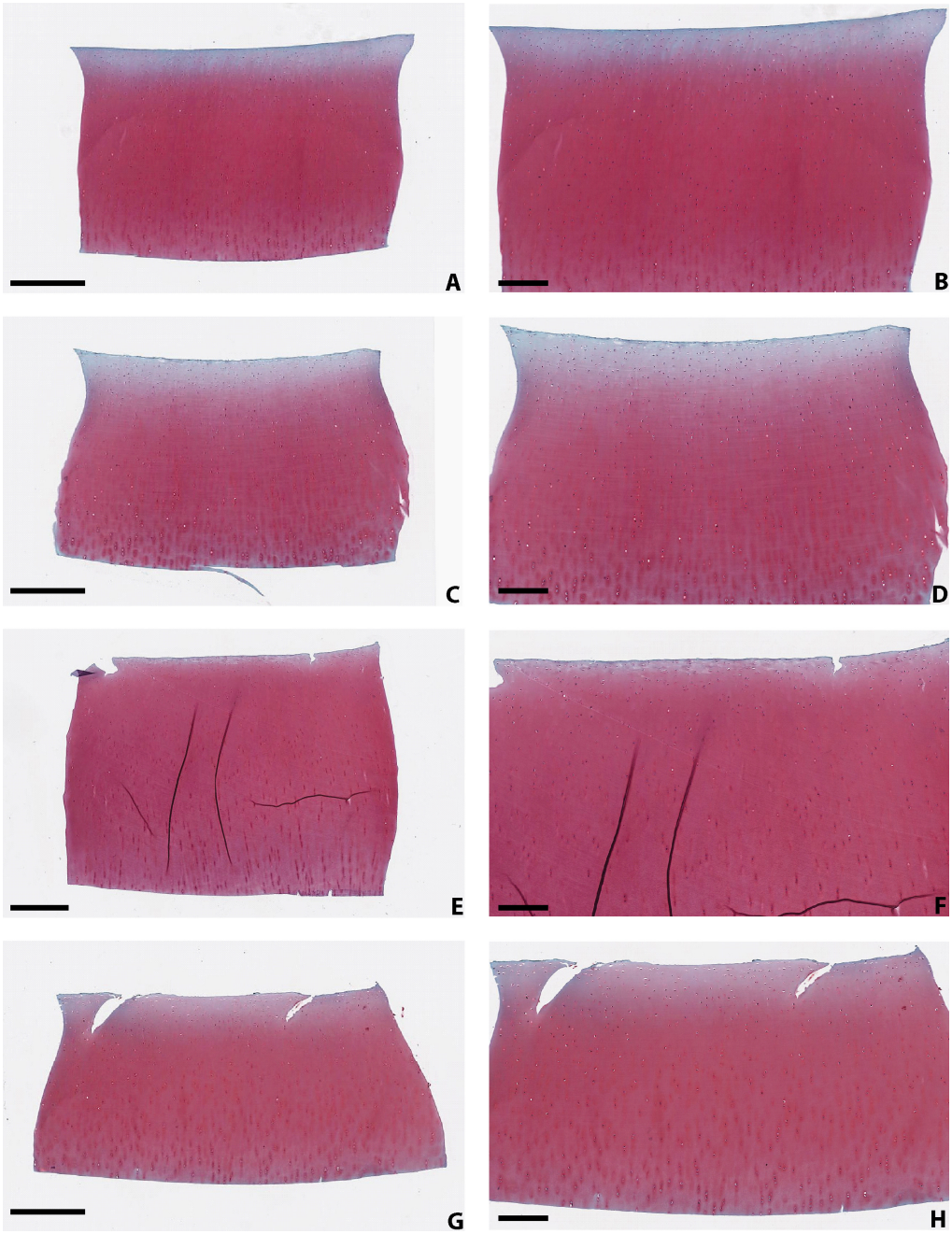

Figure 4.7: Safranin-O/Fast Green/Iron Hematoxylin stained images of full-thickness cartilage disks from (A&B) non-impacted control, and (C&D) low, (E&F) medium, and (G&H) high impact groups. Scale bars are 500 µm in (A, C, E, G) and 250 µm in (B, D, F, H).

4.5 Discussion

Dose-dependent cartilage changes occurred immediately in response to impact injury delivered to articular surfaces at either low (17.3±2.7 MPa), medium (27.8±8.5 MPa) or high (48.7±12.1 MPa) peak stress levels. High, and to a lesser extent medium, impacts caused immediate, measurable damage to the collagen network, detected as a reduction in SPI and Ef, coupled with an increase in k, but there was insufficient time for substantial proteoglycan loss to occur, reflected in an invariant Em (**Figure 4.4**) and intensely-stained Safranin-O sections (**Figure 4.7**). The first hypothesis, that streaming potentials could distinguish cartilage changes caused by impacts of different levels was partially supported. SPI values were reduced as a function of impact stress and these observations backed by statistically significant differences detected following high ($p<0.001$) and medium ($p=0.006$) impacts compared with controls. The second hypothesis, that SPI was more sensitive to these changes than biomechanical testing, was supported. While electromechanical and biomechanical properties were both reduced as a function of impact stress level, effect sizes for SPI were consistently higher than those for biomechanical parameters at all three impact levels (**Figure 4.3**). The superior sensitivity of SPI measurements to cartilage changes was also demonstrated by statistically significant reductions in SPI after both high and medium impacts, while Ef and k detected cartilage damage in a statistically significant manner only after high impact.

4.5.1 Increased sensitivity of SPI to impact compared to unconfined compression testing

Controlled impacts delivered to the articular surfaces resulted in varying degrees of cartilage damage (**Figure 4.6** & **Figure 4.7**). Compared with the surface fibrillation caused by high impact, sites that received medium impacts were roughened with superficial zone cracks observed only in occasional samples. This milder damage was reflected in both SPI and biomechanical properties, although SPI was more sensitive, as reflected in the larger effect sizes associated with this method and the statistically significant reduction in SPI, but not biomechanical properties, following medium impact.

Unconfined compression testing, where the lateral edges of the cartilage disk remain free while the top and bottom are in contact with flat, non-porous platens, is advantageous for assessing degradation. The resulting stress relaxation curves can be fit with the fibril-reinforced biphasic model (Li, et al., 2003; Soulhat, et al., 1999), where the model parameters specifically reflect the two major components of the ECM (Korhonen, et al., 2003). These investigators (Korhonen, et al., 2003) used enzymatic degradation to selectively diminish either collagen or proteoglycan in cartilage disks and demonstrated that Ef is related to the stiffness of the collagen fibre network and Em to the stiffness of the drained proteoglycan matrix. An increase in permeability was observed in both proteoglycan and collagen depleted cartilage, although a greater increase in fluid flow occurred when the collagen network was disrupted (Korhonen, et al., 2003). Drawbacks of this type of biomechanical testing include that cartilage disks must be isolated, that the accuracy of the test results are influenced by factors such as cartilage thickness variability, and finally the lengthy testing protocol requires cartilage disks to be stored, which limits the number of disks that can be tested before storage-related degradation adversely affects tissue properties (Changoor, Fereydoonzad, Yaroshinsky, & Buschmann, 2010).

Electromechanical measurements reflect cartilage material properties, which is illustrated by the statistically significant correlations identified between SPI and biomechanical parameters (**Figure 4.5**). Similar relationships have previously been observed in our laboratory (Garon, 2007).

Sensitivity of electromechanical measurements to damage caused by blunt impact at medium and high stress levels, averaging 28 and 49 MPa respectively, was demonstrated in this study (**Figure 4.2**). To the best of our knowledge, this is the first report describing the ability of streaming potentials to detect cartilage damage immediately following mechanical injury. Our findings agree with other reports showing that streaming potentials are an effective method for detecting degradative changes induced by cytokines or enzymatic modification (Bonassar, et al., 1995; Frank, et al., 1987; Legare, et al., 2002). Frank et al. (1987) measured streaming potentials and stiffness simultaneously in bovine cartilage explants where proteoglycans were enzymatically depleted with either chondroitinase-ABC or trypsin. Streaming potentials and

stiffness decreased with time following enzyme addition, although streaming potentials were more sensitive. Similarly, Légaré et al. (2002) cultured cartilage explants with interleukin-1α, a cytokine that suppresses proteoglycan and collagen synthesis by interacting with a chondrocyte membrane receptor. In this model, changes in streaming potential profiles were detected that corresponded to loss of proteoglycans to the culture media, collagen denaturation and an increase in tissue compliance.

The Arthro-BST (Biomomentum Inc., Laval, Canada) device employed in this study provided a rapid, non-destructive method for assessing streaming potentials where the calculation of the quantitative parameter (SPI) does not depend on the velocity of indentation or device orientation (Garon, 2007). The high intra- and inter-user ICCs obtained in the present study confirm the user-independent nature of the method (Changoor et al., 2007; Garon et al., 2007).

4.5.2 Comparison with early OA events

The three impact levels employed in this study corresponded to ranges described by previous investigators. The low stress level, averaging 17 MPa, was targeted because it is at the upper end of the physiological range reported for knee and hip joints, which can reach 18 MPa during daily activities (Hodge et al., 1989; Matthews, Sonstegard, & Henke, 1977), and is within the range, 15-20 MPa, suggested as a threshold for chondrocyte apoptosis (Torzilli, et al., 1999). Medium impact, averaging 28 MPa, falls within a range, 25-30 MPa, that has been shown to lead to degenerative changes in other animal models (Haut, 1989; Repo & Finlay, 1977; Scott & Athanasiou, 2006). Finally, the highest stress level, averaging 49 MPa, was selected because it is similar to the 60 MPa used previously in an equine model where osteoarthritic changes occurred (Bolam, et al., 2006). The three targeted stress levels were similar to those used by Borelli et al. (2004) where impacts were delivered using a weighted pendulum in an in vivo rabbit model.

Degradative changes observed at medium and high impacts, included increased India ink staining, fissuring, superficial zone damage, and diminished functional properties. These are similar to the ECM alterations described in the literature following impact, where initial

mechanical disruption of the collagen network results in swelling and secondary loss of proteoglycans (Bolam, et al., 2006; Buckwalter & Brown, 2004; Donohue, et al., 1983; Jeffrey, et al., 1995; Kurz et al., 2005; Lotz & Kraus, 2010; Patwari et al., 2001; Quinn, et al., 2001; Repo & Finlay, 1977; Thompson, et al., 1991). In the present study, average Em decreased at higher impact stress levels (**Figure 4.4**), although this reduction was not statistically significant. This finding was expected and results from the early time point after mechanical injury considered here. Biomechanical testing of cartilage disks occurred over several days following impact and disks were stored at 4°C in humid chambers immediately post- impact, where proteoglycan loss due to storage is minimal (Changoor, et al., 2010). Staining characteristics in histological sections were similar among groups, although impacted disks were more likely to display proteoglycan depletion at the surface and base of cartilage disks compared to controls.

Notably, our findings differed from Borrelli et al. (2004) who reported that rabbit cartilage tolerated peak stresses of 55 MPa with no surface disruptions. This could be due to a longer rise time, approximately 20 ms, compared to our study, where time to peak load was on the order of 1 ms. Higher strain rates cause increased cartilage damage compared to lower strain rates for the same peak stress (Anderson, Brown, Yang, & Radin, 1990; Quinn, et al., 2001). Additionally, those impacts were delivered in situ, where cartilage is more resilient to loading than in explants.

Although not assessed in this study, it is likely that in low and medium impacted samples where the cartilage surface remained intact, chondrocytes were damaged or underwent apoptosis (Buckwalter & Brown, 2004; Duda, et al., 2001; Morel, et al., 2006). Chondrocytes that survive respond to impact by releasing precursors to inflammatory cytokines (Chrisman, Ladenbauer-Bellis, Panjabi, & Goeltz, 1981), which may be sufficient to initiate degradative changes that eventually culminate in OA. This occurs at the impacted site and can spread to adjacent cartilage (Levin, Burton-Wurster, Chen, & Lust, 2001).

4.5.3 Conclusions

Immediate damage to articular cartilage was induced using a custom-built spring loaded impactor device at three stress levels, ranging from the upper end of physiological stress, 17.3±2.7 MPa, to levels previously shown to cause degradative cartilage changes, 27.8±8.5 MPa and 48.7±12.1 MPa. Streaming potentials were more sensitive to impact related damage than unconfined compression testing. Parameters from unconfined compression testing were significantly correlated to SPI, further establishing the relationship between non-destructive, electromechanical measurements and intrinsic cartilage properties. This type of impact model combined with streaming potentials to detect subtle cartilage changes could provide a model system suitable for testing the efficacy of therapeutic agents to mitigate disease progression in the early stages of PTOA. The non-destructive nature of the streaming potential method would make sequential assessment of cartilage over time possible for in vivo models where initial degeneration is focal but that could progress to gradually involve more of the articular surface.

4.6 Acknowledgements

The authors would like to acknowledge Viorica Lascau, for her expert preparation of the histological sections, as well as Michele Brydges and Michelle Beaudoin, for technical assistance provided at the Ontario Veterinary College. Funding provided by the Natural Sciences and Engineering Research Council of Canada (NSERC) and the Biomedical Science and Technology Research Group/Le Groupe de recherche en sciences et technologies biomédicales (GRSTB).

4.7 References

These are the references as they appear in the submitted version of the article and are in the style required by the Journal of Biomechanical Engineering. The references contained within the body of Chapter 4 correspond to the reference list at the end of the thesis.

[1] Chen, A. C., Bae, W. C., Schinagl, R. M., and Sah, R. L., 2001, "Depth- and Strain-Dependent Mechanical and Electromechanical Properties of Full-Thickness Bovine Articular Cartilage in Confined Compression," J Biomech, 34(1), pp. 1-12.

[2] Korhonen, R. K., Wong, M., Arokoski, J., Lindgren, R., Helminen, H. J., Hunziker, E. B., and Jurvelin, J. S., 2002, "Importance of the Superficial Tissue Layer for the Indentation Stiffness of Articular Cartilage," Med Eng Phys, 24(2), pp. 99-108.

[3] Li, L. P., Korhonen, R. K., Iivarinen, J., Jurvelin, J. S., and Herzog, W., 2008, "Fluid Pressure Driven Fibril Reinforcement in Creep and Relaxation Tests of Articular Cartilage," Med Eng Phys, 30(2), pp. 182-9.

[4] Park, S., Krishnan, R., Nicoll, S. B., and Ateshian, G. A., 2003, "Cartilage Interstitial Fluid Load Support in Unconfined Compression," J Biomech, 36(12), pp. 1785-96.

[5] Frank, E. H., and Grodzinsky, A. J., 1987, "Cartilage Electromechanics--I. Electrokinetic Transduction and the Effects of Electrolyte Ph and Ionic Strength," J Biomech, 20(6), pp. 615-27.

[6] Maroudas, A., 1967, "Fixed Charge Density in Articular Cartilage," eds., Stockholm, Sweeden, pp.

[7] Maroudas, A., Muir, H., and Wingham, J., 1969, "The Correlation of Fixed Negative Charge with Glycosaminoglycan Content of Human Articular Cartilage," Biochim Biophys Acta, 177(3), pp. 492-500.

[8] Sun, D. D., Guo, X. E., Likhitpanichkul, M., Lai, W. M., and Mow, V. C., 2004, "The Influence of the Fixed Negative Charges on Mechanical and Electrical Behaviors of Articular Cartilage under Unconfined Compression," J Biomech Eng, 126(1), pp. 6-16.

[9] Bonassar, L. J., Jeffries, K. A., Paguio, C. G., and Grodzinsky, A. J., 1995, "Cartilage Degradation and Associated Changes in Biochemical and Electromechanical Properties," Acta Orthop Scand Suppl, 266, pp. 38-44.

[10] Bonassar, L. J., Sandy, J. D., Lark, M. W., Plaas, A. H., Frank, E. H., and Grodzinsky, A. J., 1997, "Inhibition of Cartilage Degradation and Changes in Physical Properties Induced by Il-1beta and Retinoic Acid Using Matrix Metalloproteinase Inhibitors," Arch Biochem Biophys, 344(2), pp. 404-12.

[11] Chen, A. C., Nguyen, T. T., and Sah, R. L., 1997, "Streaming Potentials During the Confined Compression Creep Test of Normal and Proteoglycan-Depleted Cartilage," Ann Biomed Eng, 25(2), pp. 269-77.

[12] Frank, E. H., Grodzinsky, A. J., Koob, T. J., and Eyre, D. R., 1987, "Streaming Potentials: A Sensitive Index of Enzymatic Degradation in Articular Cartilage," J Orthop Res, 5(4), pp. 497-508.

[13] Garon, M., Legare, A., Guardo, R., Savard, P., and Buschmann, M. D., 2002, "Streaming Potentials Maps Are Spatially Resolved Indicators of Amplitude, Frequency and Ionic Strength Dependant Responses of Articular Cartilage to Load," J Biomech, 35(2), pp. 207-16.

[14] Legare, A., Garon, M., Guardo, R., Savard, P., Poole, A. R., and Buschmann, M. D., 2002, "Detection and Analysis of Cartilage Degeneration by Spatially Resolved Streaming Potentials," J Orthop Res, 20(4), pp. 819-26.

[15] Mandelbaum, B., and Waddell, D., 2005, "Etiology and Pathophysiology of Osteoarthritis," Orthopedics, 28(Suppl 2), pp. s207-14.

[16] Lotz, M. K., 2010, "New Developments in Osteoarthritis. Posttraumatic Osteoarthritis: Pathogenesis and Pharmacological Treatment Options," Arthritis Res Ther, 12(3), pp. 211.

[17] Scott, C. C., and Athanasiou, K. A., 2006, "Mechanical Impact and Articular Cartilage," Crit Rev Biomed Eng, 34(5), pp. 347-78.

[18] Aspden, R. M., Jeffrey, J. E., and Burgin, L. V., 2002, "Impact Loading of Articular Cartilage," Osteoarthritis Cartilage, 10(7), pp. 588-9.

[19] Jeffrey, J. E., Gregory, D. W., and Aspden, R. M., 1995, "Matrix Damage and Chondrocyte Viability Following a Single Impact Load on Articular Cartilage," Arch Biochem Biophys, 322(1), pp. 87-96.

[20] Quinn, T. M., Allen, R. G., Schalet, B. J., Perumbuli, P., and Hunziker, E. B., 2001, "Matrix and Cell Injury Due to Sub-Impact Loading of Adult Bovine Articular Cartilage Explants: Effects of Strain Rate and Peak Stress," J Orthop Res, 19(2), pp. 242-9.

[21] Repo, R. U., and Finlay, J. B., 1977, "Survival of Articular Cartilage after Controlled Impact," J Bone Joint Surg Am, 59(8), pp. 1068-76.

[22] Thompson, R. C., Jr., Oegema, T. R., Jr., Lewis, J. L., and Wallace, L., 1991, "Osteoarthrotic Changes after Acute Transarticular Load. An Animal Model," J Bone Joint Surg Am, 73(7), pp. 990-1001.

[23] Torzilli, P. A., Grigiene, R., Borrelli, J., Jr., and Helfet, D. L., 1999, "Effect of Impact Load on Articular Cartilage: Cell Metabolism and Viability, and Matrix Water Content," J Biomech Eng, 121(5), pp. 433-41.

[24] Isaac, D. I., Meyer, E. G., Kopke, K. S., and Haut, R. C., 2010, "Chronic Changes in the Rabbit Tibial Plateau Following Blunt Trauma to the Tibiofemoral Joint," J Biomech, 43(9), pp. 1682-8.

[25] Borrelli, J., Jr., Zhu, Y., Burns, M., Sandell, L., and Silva, M. J., 2004, "Cartilage Tolerates Single Impact Loads of as Much as Half the Joint Fracture Threshold," Clin Orthop Relat Res, 426), pp. 266-73.

[26] Vrahas, M. S., Smith, G. A., Rosler, D. M., and Baratta, R. V., 1997, "Method to Impact in Vivo Rabbit Femoral Cartilage with Blows of Quantifiable Stress," J Orthop Res, 15(2), pp. 314-7.

[27] Zhang, H., Vrahas, M. S., Baratta, R. V., and Rosler, D. M., 1999, "Damage to Rabbit Femoral Articular Cartilage Following Direct Impacts of Uniform Stresses: An in Vitro Study," Clin Biomech (Bristol, Avon), 14(8), pp. 543-8.

[28] Bolam, C. J., Hurtig, M. B., Cruz, A., and Mcewen, B. J., 2006, "Characterization of Experimentally Induced Post-Traumatic Osteoarthritis in the Medial Femorotibial Joint of Horses," Am J Vet Res, 67(3), pp. 433-47.

[29] Donohue, J. M., Buss, D., Oegema, T. R., Jr., and Thompson, R. C., Jr., 1983, "The Effects of Indirect Blunt Trauma on Adult Canine Articular Cartilage," J Bone Joint Surg Am, 65(7), pp. 948-57.

[30] Haut, R. C., Ide, T. M., and De Camp, C. E., 1995, "Mechanical Responses of the Rabbit Patello-Femoral Joint to Blunt Impact," J Biomech Eng, 117(4), pp. 402-8.

[31] Newberry, W. N., Mackenzie, C. D., and Haut, R. C., 1998, "Blunt Impact Causes Changes in Bone and Cartilage in a Regularly Exercised Animal Model," J Orthop Res, 16(3), pp. 348-54.

[32] Changoor, A., Hurtig, M. B., Runciman, R. J., Quesnel, A. J., Dickey, J. P., and Lowerison, M., 2006, "Mapping of Donor and Recipient Site Properties for Osteochondral Graft

Reconstruction of Subchondral Cystic Lesions in the Equine Stifle Joint," Equine Vet J, 38(4), pp. 330-6.

[33] Fortin, M., Soulhat, J., Shirazi-Adl, A., Hunziker, E. B., and Buschmann, M. D., 2000, "Unconfined Compression of Articular Cartilage: Nonlinear Behavior and Comparison with a Fibril-Reinforced Biphasic Model," J Biomech Eng, 122(2), pp. 189-95.

[34] Li, L. P., Soulhat, J., Buschmann, M. D., and Shirazi-Adl, A., 1999, "Nonlinear Analysis of Cartilage in Unconfined Ramp Compression Using a Fibril Reinforced Poroelastic Model," Clin Biomech (Bristol, Avon), 14(9), pp. 673-82.

[35] Soulhat, J., Buschmann, M. D., and Shirazi-Adl, A., 1999, "A Fibril-Network-Reinforced Biphasic Model of Cartilage in Unconfined Compression," J Biomech Eng, 121(3), pp. 340-7.

[36] Changoor, A., Quenneville, E., Garon, M., Hurtig, M. B., and Buschmann, M. D., 2009, "Streaming Potential-Based Arthroscopic Device Can Detect Changes Immediately Following Localized Impact in an Equine Impact Model of Osteoarthritis.," OARSI World Congress on Osteoarthritis, Montreal, Quebec, Canada, Osteo Cartil, 17 Supplement 1, pp. S53.

[37] Eliasziw, M., Young, S. L., Woodbury, M. G., and Fryday-Field, K., 1994, "Statistical Methodology for the Concurrent Assessment of Interrater and Intrarater Reliability: Using Goniometric Measurements as an Example," Phys Ther, 74(8), pp. 777-88.

[38] Meachim, G., 1972, "Light Microscopy of Indian Ink Preparations of Fibrillated Cartilage," Ann Rheum Dis, 31(6), pp. 457-64.

[39] Li, L. P., Buschmann, M. D., and Shirazi-Adl, A., 2003, "Strain-Rate Dependent Stiffness of Articular Cartilage in Unconfined Compression," J Biomech Eng, 125(2), pp. 161-8.

[40] Korhonen, R. K., Laasanen, M. S., Toyras, J., Lappalainen, R., Helminen, H. J., and Jurvelin, J. S., 2003, "Fibril Reinforced Poroelastic Model Predicts Specifically Mechanical Behavior of Normal, Proteoglycan Depleted and Collagen Degraded Articular Cartilage," J Biomech, 36(9), pp. 1373-9.

[41] Changoor, A., Fereydoonzad, L., Yaroshinsky, A., and Buschmann, M. D., 2010, "Effects of Refrigeration and Freezing on the Electromechanical and Biomechanical Properties of Articular Cartilage," J Biomech Eng, 132(6), pp. 064502.

[42] Garon, M., 2007, "Conception Et Validation D'une Sonde Arthroscopique Pour L'évaluation Des Propriétés Électromécaniques Fonctionelles Du Cartilage Articulaire," Ph.D. thesis, Ecole Polytechnique de Montreal, Montreal.

[43] Changoor, A., Quenneville, E., Garon, M., Cloutier, L., Hurtig, M., and Buschmann, M. D., 2007, "Streaming Potential-Based Arthroscopic Device Discerns Topographical Differences in Cartilage Covered and Uncovered by Meniscus in Ovine Stifle Joints.," Annual Meeting of the Orthopaedic Research Society, San Diego, California, USA, 32, pp. 631.

[44] Garon, M., Cloutier, L., Legare, A., Quenneville, E., Shive, M. S., and Buschmann, M. D., 2007, "Reliability and Correlation to Human Articular Cartilage Mechanical Properties of a Streaming Potential Based Arthroscopic Instrument.," T. o. t. t. A. M. o. t. O. R. Society, eds., San Diego, California, USA, 32, pp. 629.

[45] Hodge, W. A., Carlson, K. L., Fijan, R. S., Burgess, R. G., Riley, P. O., Harris, W. H., and Mann, R. W., 1989, "Contact Pressures from an Instrumented Hip Endoprosthesis," J Bone Joint Surg Am, 71(9), pp. 1378-86.

[46] Matthews, L. S., Sonstegard, D. A., and Henke, J. A., 1977, "Load Bearing Characteristics of the Patello-Femoral Joint," Acta Orthop Scand, 48(5), pp. 511-6.

[47] Haut, R. C., 1989, "Contact Pressures in the Patellofemoral Joint During Impact Loading on the Human Flexed Knee," J Orthop Res, 7(2), pp. 272-80.

[48] Buckwalter, J. A., and Brown, T. D., 2004, "Joint Injury, Repair, and Remodeling: Roles in Post-Traumatic Osteoarthritis," Clin Orthop Relat Res, 423), pp. 7-16.

[49] Kurz, B., Lemke, A. K., Fay, J., Pufe, T., Grodzinsky, A. J., and Schunke, M., 2005, "Pathomechanisms of Cartilage Destruction by Mechanical Injury," Ann Anat, 187(5-6), pp. 473-85.

[50] Patwari, P., Fay, J., Cook, M. N., Badger, A. M., Kerin, A. J., Lark, M. W., and Grodzinsky, A. J., 2001, "In Vitro Models for Investigation of the Effects of Acute Mechanical Injury on Cartilage," Clin Orthop Relat Res, 391 Suppl, pp. S61-71.

[51] Anderson, D. D., Brown, T. D., Yang, K. H., and Radin, E. L., 1990, "A Dynamic Finite Element Analysis of Impulsive Loading of the Extension-Splinted Rabbit Knee," J Biomech Eng, 112(2), pp. 119-28.

[52] Duda, G. N., Eilers, M., Loh, L., Hoffman, J. E., Kaab, M., and Schaser, K., 2001, "Chondrocyte Death Precedes Structural Damage in Blunt Impact Trauma," Clin Orthop Relat Res, 393), pp. 302-9.

[53] Morel, V., Berutto, C., and Quinn, T. M., 2006, "Effects of Damage in the Articular Surface on the Cartilage Response to Injurious Compression in Vitro," J Biomech, 39(5), pp. 924-30.

[54] Chrisman, O. D., Ladenbauer-Bellis, I. M., Panjabi, M., and Goeltz, S., 1981, "1981 Nicolas Andry Award. The Relationship of Mechanical Trauma and the Early Biochemical Reactions of Osteoarthritic Cartilage," Clin Orthop Relat Res, 161, pp. 275-84.

[55] Levin, A., Burton-Wurster, N., Chen, C. T., and Lust, G., 2001, "Intercellular Signaling as a Cause of Cell Death in Cyclically Impacted Cartilage Explants," Osteoarthritis Cartilage, 9(8), pp. 702-11.

CHAPTER 5. ARTICLE III

A polarized light microscopy method for accurate and reliable grading of collagen organization in cartilage repair

A Changoor[1], N Tran-Khanh[1], S Méthot[2], M Garon[3], MB Hurtig[4], MS Shive[2], MD Buschmann[1*]

Published in the journal Osteoarthritis and Cartilage in January 2011
Volume 19, Number 1, pp. 126-35

[1]Institute of Biomedical Engineering, Department of Chemical Engineering
École Polytechnique de Montréal, Montréal, Québec, Canada

[2]Piramal Healthcare (Canada), Laval, Québec, Canada

[3]Biomomentum Inc., Laval, Québec, Canada

[4]Comparative Orthopaedic Research Laboratory, Ontario Veterinary College, University of Guelph, Guelph, Ontario, Canada

[*]Corresponding author:
Institute of Biomedical Engineering, Department of Chemical Engineering
École Polytechnique of Montréal, P.O. Box 6079, Station Centre-Ville
Montreal, Québec, Canada, H3C 3A7
Tel.: 514-340-4711 ext. 4931, Fax: 514-340-2980
E-mail: michael.buschmann@polymtl.ca

Author's Contributions

Adele Changoor	Study conception and design, data acquisition, data analysis and interpretation, literature review, drafting and critical revision of the manuscript. Accepts responsibility for the integrity of the work as a whole. *The contributions of the first author were estimated at 85%.*
Nicolas Tran-Khanh	Data acquisition, interpretation of data, critical revision of the manuscript
Stephane Méthot	Data acquisition, interpretation of data, critical revision of the manuscript
Martin Garon	Statistical analysis, interpretation of data, critical revision of the manuscript
Mark Hurtig	Acquisition of animal tissues, interpretation of data, critical revision of the manuscript
Matthew Shive	Study conception and design, interpretation of data, critical revision of the manuscript
Michael Buschmann	Study conception and design, interpretation of data, drafting and critical revision of the manuscript. Accepts responsibility for the integrity of the work as a whole.

5.1 Abstract

Objectives: Collagen organization, a feature that is critical for cartilage load bearing and durability, is not adequately assessed in cartilage repair tissue by present histological scoring systems. Our objectives were to develop a new polarized light microscopy (PLM) score for collagen organization and to test its reliability.

Design: This PLM score uses an ordinal scale of 0-5 to rate the extent that collagen network organization resembles that of young adult hyaline articular cartilage (score of 5) versus a totally disorganized tissue (score of 0). Inter-reader reliability was assessed using Intraclass Correlation Coefficients (ICC) for Agreement, calculated from scores of three trained readers who independently evaluated blinded sections obtained from normal (n=4), degraded (n=2) and repair (n=22) human cartilage biopsies.

Results: The PLM score succeeded in distinguishing normal, degraded and repair cartilages, where the latter displayed greater complexity in collagen structure. Excellent inter-reader reproducibility was found with ICCs for Agreement of 0.90 [ICC(2,1)] (lower boundary of the 95% confidence interval is 0.83) and 0.96 [ICC(2,3)] (lower boundary of the 95% confidence interval is 0.94), indicating the reliability of a single reader's scores and the mean of all three readers' scores, respectively.

Conclusion: This PLM method offers a novel means for systematically evaluating collagen organization in repair cartilage. We propose that it be used to supplement current gold standard histological scoring systems for a more complete assessment of repair tissue quality.

5.2 Introduction

Collagen type II, one of two major extracellular matrix components of articular cartilage, forms a highly organized fibrillar network that plays a central role in cartilage biomechanical properties and durability. Hyaline articular cartilage is stratified, with collagen fibres in the superficial zone (SZ) oriented tangentially to the articular surface, becoming more randomly oriented in the transitional zone (TZ) and aligned perpendicularly to the cartilage-bone interface in the deep zone (DZ) (Benninghoff, 1925; Bullough & Goodfellow, 1968; Hedlund, et al., 1993; Hughes, et al., 2005; Kaab, et al., 1998; Schenk, et al., 1986; Xia, et al., 2003). The collagen network entraps and restrains large, hydrophilic proteoglycan molecules. During loading, the collagen network resists lateral expansion and interstitial fluid is forced out through the dense proteoglycan matrix, pressurizing the fluid and allowing for load bearing (Chen, et al., 2001; Korhonen, et al., 2003; Li, et al., 2008; Park, et al., 2003).

Considerable research activity centers on the repair of focal cartilage lesions using a range of cell therapies (Brittberg, et al., 1994; Saris, et al., 2008), in vitro generated tissue-engineered constructs (Crawford, et al., 2009; Kon, et al., 2010), scaffold-based solutions (Hoemann, et al., 2005; Shive, et al., 2006) and surgical techniques (Mithoefer, et al., 2009) that may lead to effective cartilage repair in humans. Cartilage repair processes originate from the subchondral bone, the implanted cells or tissue-engineered construct and further involve interactions between these two sources and other joint tissues (Hunziker, 2002). Microfracture, a surgical technique, produces small perforations in the debrided subchondral bone plate, recruiting mesenchymal cells from the marrow to fill the defect with a granulation tissue which matures over 3-12 months. In cell therapies, implanted chondrocytes or other cell types may adhere and proliferate to produce cartilage repair tissue. It is not presently known the extent to which either of these two sources of cartilage repair, or other approaches, can reconstitute the functionally important stratified structure of hyaline articular cartilage, which is a consequence of endochondral developmental processes (Hunziker, et al., 2007).

The quality of in vivo repaired cartilage in humans is often assessed histologically from 2 mm diameter osteochondral biopsies collected from the centre of the repair site (Gudas, et al., 2005; Mainil-Varlet, et al., 2003; Roberts, et al., 2003; Saris, et al., 2008; Selmi, et al., 2008). Presently, there are five published histological scoring systems for evaluating human repair cartilage (Rutgers, et al., 2010). The OsScore, ICRS I and ICRS II consist of various categories that are predicted to contribute to the long-term durability of repair cartilage (Rutgers, et al., 2010). The OsScore (Roberts, et al., 2003) and ICRS I (Mainil-Varlet, et al., 2003) methods are semi-quantitative, consisting of 7 and 6 categories respectively, and rated on ordinal scales. The OsScore categories are evaluated individually and summed to produce a single overall score (Roberts, et al., 2003). For the ICRS I, readers consult an image bank to rate 6 categories, whose scores are not summed (Mainil-Varlet, et al., 2003). The ICRS II (Mainil-Varlet, et al., 2010; Rutgers, et al., 2010; Saris, et al., 2008) uses visual analogue scales to rate 14 categories, with defined anchors at 0% and 100% positions, selected to reflect ICRS I categories and to include additional scores for negative features such as inflammation and vascularization.

None of these scores specifically evaluate collagen architecture, which is central to cartilage biomechanical properties and durability (Hughes, et al., 2005; Julkunen, et al., 2009; Moger, et al., 2009). The authors of the OsScore observed haematoxylin and eosin stained sections in polarized light to evaluate tissue morphology where fibrous tissue scored 0 and hyaline cartilage scored 3 (Roberts, et al., 2003). Similarly, ICRS II recommends viewing stained sections in polarized light when scoring tissue morphology with anchors of ‘full thickness collagen fibres’ at 0% and ‘normal cartilage birefringence’ at 100% (Mainil-Varlet, et al., 2010). These categories represent a first step towards assessing collagen network structure but neither captures the detailed features of collagen organization in adult articular cartilage. A systematic evaluation of the extent to which collagen organization in repair tissue approaches that of hyaline cartilage is warranted for this critical feature that may be the most indicative of long-term durability. To this end, we developed a qualitative polarized light microscopy (PLM) score to evaluate collagen organization in unstained histological sections. PLM is a powerful tool for studying the orientation of anisotropic materials, such as biological tissues containing fibrillar collagen (Kaab, et al., 1998; Williams, Uebelhart, Thonar, Kocsis, & Modis, 1996; Xia, et al.,

2003; Yarker, et al., 1983). In hyaline cartilage, linear PLM reveals the highly organized collagen of the SZ and DZ as two birefringent regions, separated by a non-birefringent region, the TZ (Arokoski, et al., 1996; Hughes, et al., 2005; Kaab, et al., 1998; Kiraly, et al., 1997; Korhonen, et al., 2002; Rieppo, et al., 2003; Speer & Dahners, 1979). In cartilage repair, regions of birefringent and non-birefringent tissue have been previously observed (Richardson, et al., 1999; Roberts, et al., 2003; Roberts, et al., 2009; Vasara, et al., 2006; White et al., 2006) although no systematic scoring scale describing the level of organization has been proposed.

Linear PLM can be performed on a light microscope with the addition of two filters, a polarizer and analyzer (Modis, 1991). The polarizer is placed after the light source and ensures only linearly polarized light, i.e. light in a single plane that is perpendicular to the direction of light propagation, is transmitted to the specimen. Optically anisotropic materials change the direction of polarized light, an effect called birefringence. This is true of fibrillar collagen-containing tissues, such as articular cartilage, and can be observed in histological sections. The fibrillar structure splits the incident polarized light into two orthogonal rays, in a way that depends on the direction of collagen at each point in the section. The analyzer filter, positioned after the specimen and at a right angle to the polarizer, recombines these rays to create the observed image. The orientation of the analyzer ensures that only light with a polarization that is altered by the tissue is transmitted. The intensity of the resulting signal therefore indicates regions of the tissue with a capacity to alter polarization and thus are optically active, or in other terms birefringent, anisotropic, or oriented.

PLM is ideal for evaluating cartilage collagen architecture because it is sensitive to collagen fibre orientation, yet simple enough to be generally applicable (Arokoski, et al., 1996; Hughes, et al., 2005; Hyttinen et al., 2009; Julkunen, et al., 2009; White, et al., 2006). Nonetheless, a systematic method needed to be developed and tested, which were the goals of the present study. We developed this PLM score to describe collagen organization on an ordinal scale ranging from total disorganization (score of 0) to the ideal collagen organization present in young adult hyaline articular cartilage (score of 5). We applied the PLM score to human biopsies of normal, degraded and repair cartilages to test these hypotheses: 1. Collagen organization in

human biopsies can be systematically characterized using the PLM score, and 2. The PLM score is highly reproducible when applied by multiple readers.

5.3 Materials & Methods

5.3.1 Tissue Sources & Processing

Human and equine cartilages were used to develop and test this PLM scoring method. Tissues were handled using procedures approved by the Ethics Committee at École Polytechnique de Montréal or that followed the guidelines of the Canadian Council on Animal Care.

The PLM score was developed using equine cartilage disks (n=4) harvested from a healthy 9 year old horse (Ontario Veterinary College, Guelph, ON, Canada), and osteochondral samples retrieved from five distinct sites in a single human knee that had undergone a marrow stimulation repair procedure, including tissue from the repair site on the medial femoral condyle (MFC) and from non-operated joint surfaces. Results relating to these samples have been partially reported in abstracts (Changoor, Nelea, Fereydoonzad, et al., 2009; Changoor, Nelea, Tran-Khanh, et al., 2009).

The PLM score was tested using human osteochondral biopsies, 2 mm in diameter, collected using 11G Jamshidi needles (Cardinal Health, ON, Canada) from tissue sources that were macroscopically normal, degraded or from sites that had undergone cartilage repair procedures. Normal cartilage samples were acquired from cadaveric knees (n=2, LifeLink Tissue Bank, Tampa, FL, USA), and large allografts (n=2, RTI Biologics Inc., Alachua, FL, USA), which were all previously frozen. Degraded cartilage samples (n=2) were obtained from tissue removed during a total hip arthroplasty, with one biopsy from the center of an OA lesion (Degraded 1) and the other from an adjacent, macroscopically normal region on the same joint surface (Degraded 2) (Research Institute of the McGill University Health Centre, Montréal, Québec Canada). Finally, cartilage repair samples (n=22) were retrieved during standardized

second-look arthroscopies approximately 13 months post-treatment with cartilage repair procedures based on bone marrow stimulation. These biopsies were retrieved during a randomized clinical trial, sponsored by BioSyntech Inc. (now part of Piramal Healthcare (Canada)) (Laval, Québec, Canada), where the ability of microfracture augmented with the cartilage repair device BST-CarGel® was compared to microfracture alone for repairing focal cartilage lesions. Biopsies were fixed in 10% neutral buffered formalin (NBF) at room temperature for a minimum of 24 hours up to 5 days. Decalcification was achieved by rocking samples placed in 0.5N HCl, 0.1%(v/v) glutaraldehyde for 30 hours at 4°C. Samples were post-fixed in 10% NBF overnight prior to paraffin embedding and sectioned at 5 μm.

Age-related changes were explored using separate human osteochondral sections from macroscopically normal MFCs (n=6) grouped based on age as either young (17 and 21 years), middle-aged (40 and 41 years) or old (56 and 58 years) (RTI Biologics Inc., Alachua, FL, USA). These samples were fixed in 10% NBF at 4°C for 32 days, decalcified in 0.5N HCl, 0.1%(v/v) glutaraldehyde for 13 days, paraffin embedded and sectioned at 5 μm. In a separate internal study, matrix changes were not observed in Safranin-O/Fast-Green stained sections of normal cartilage stored in fixative for up to 6 months (data not shown).

All sections were deparaffinized and rehydrated for mounting using a sequence of baths including toluene (Fisher Scientific Canada, Ottawa ON, Canada), a graded ethanol series (Commercial Alcohols, Boucherville, QC, Canada), and distilled water. They were mounted unstained in Permount (Fisher Scientific, Hampton, New Hampshire, USA), selected because its index of refraction, 1.55, is close to the range reported for fibrillar collagens, approximately 1.5 (Maurice, 1957; Vidal Bde & Vilarta, 1988; Yarker, et al., 1983). Ensuring similar refractive indices minimizes form birefringence, produced when a mismatch between the specimen and the media in which it is being observed is present, and which artificially increases optical activity (Kiraly, et al., 1997).

5.3.2 PLM Qualitative Score

The goal of the PLM score (**Table 5.1**, **Figure 5.1** & **Figure 5.2**) is to assess the extent to which a given sample demonstrates the collagen organization observed in young adult hyaline articular cartilage (score of 5) versus total disorganization (score of 0). It includes features that are important for successful cartilage repair and is applicable to repair tissues produced either by marrow stimulation or cell-based repair techniques. The key features of the PLM score, in order of importance, are: 1. DZ integration, 2. Presence of an SZ, 3. Multi-zone structure, and 4. Specific characteristics, such as appropriate zonal thicknesses, present in native hyaline cartilage.

A DZ is essential for basal integration of the repair tissue and this feature is given the highest priority in the PLM score. Perpendicularly-oriented collagen fibres provide an anchor between the repair tissue and the underlying subchondral bone, which is necessary to prevent tissue delamination (Archer, et al., 2006). The presence of a mainly vertically-oriented DZ, where the tissue above forms a second, non-oriented zone, yields a PLM score of 1 if it occupies less than 50% of the full thickness of non-calcified repair tissue, and a score of 2 if it is greater than 50% (**Figure 5.2a-c**). (Alternatively, in this latter case, the second zone above the DZ may be oriented in any direction except vertical). This distinction reflects the approximate DZ proportion observed in normal articular cartilage, which averages 62%-75% in the human knee when assessed by PLM (Kurkijarvi, et al., 2008; Nissi, et al., 2006) or 61%-92% in stained sections (Buckwalter, et al., 1988; Hunziker, 1992), and 60%-90% in animal species (Arokoski, et al., 1996; Hughes, et al., 2005; Hunziker, 1992; Hyttinen, et al., 2001; Kaab, et al., 1998; Moger, et al., 2009; Nissi, et al., 2006; Panula, et al., 1998; Rieppo, et al., 2003; Xia, et al., 2003; Yarker, et al., 1983). Zonal thicknesses vary with species, age and location on the joint surface. Fibres angled within ±30º from vertical are acceptable since they still provide an anchor for the repair tissue (Xia, et al., 2003) and it ensures that biopsies extracted at an angle are not penalized.

The SZ of hyaline cartilage plays important roles in load bearing and resisting degeneration (Arokoski, et al., 1996; Guilak, Ratcliffe, Lane, Rosenwasser, & Mow, 1994; Korhonen, et al., 2002; Moger, et al., 2009; Panula, et al., 1998), making its presence a desirable feature for repair cartilage tissues. In the PLM score, evidence of one additional zone of oriented

(non-vertical) tissue above the DZ, regardless of DZ thickness, receives a score of 2, whereas two or more additional zones, approximating the SZ and TZ, are assigned a score of 3 (**Figure 5.2c-d**). Smooth, horizontally-oriented SZs are rarely observed in repair cartilage produced by microfracture (Bi, Li, Doty, & Camacho, 2005) or cell-based therapies (Richardson, et al., 1999; Roberts, et al., 2003; Vasara, et al., 2006). To accommodate this variability, some flexibility is permitted in the PLM score concerning orientations in the zone(s) above the DZ. The zone approximating the SZ may have either horizontal or multiple orientations, meaning it could contain several pockets of oriented collagen that are not necessarily oriented in the same direction. The zone(s) approximating the TZ may be non-oriented or have any orientation that is neither parallel nor perpendicular to the articular surface, in order to render it distinct from the DZ and SZ.

In summary, repair tissues that receive a score of 3 out of 5 contain vertically-oriented deep zones and at least 2 additional zones approximating the transitional and superficial zones. Achieving a score of 3 therefore represents a high level of success for cartilage repair since this multi-zonal structure has seldom been seen in published PLM images of repair cartilages to date (Bi, et al., 2005; Mainil-Varlet, et al., 2010; Richardson, et al., 1999; Roberts, et al., 2003; Roberts, et al., 2009; Vasara, et al., 2006).

PLM scores above 3 are given when specific characteristics of native hyaline cartilage are present, including appropriate zonal thicknesses and fibre orientations. A score of 4 (**Figure 5.2e**) is assigned when the multi-zonal structure has the appropriate orientations for each of the 3 zones and approximate normal zonal proportions, where the DZ occupies roughly 50% of the full thickness of non-calcified tissue, with smaller TZ and SZ.

To receive a perfect PLM score of 5, the specimen must satisfy all previous requirements, and additionally zonal thicknesses should be laterally homogeneous and birefringence smooth in texture (**Figure 5.2f**). Our observations suggest that texture is associated with tissue type. Degraded tissues are often patchy and inconsistent while repair tissue can have a granular appearance, possibly due to the numerous small diameter fibres present (**Figure 5.3**). In contrast,

native cartilage has a smooth, uniform texture, where cell lacunae can be discerned (**Figure 5.3** & **Figure 5.4**). Normal human cartilage typically receives scores of 4-5, with 4 being the most common, as heterogeneity and lack of smooth birefringence can often be observed and appear to increase with age (**Figure 5.4**).

The detailed requirements for the PLM score (**Table 5.1**) were translated into a flowchart to facilitate scoring (**Figure 5.1**), which is performed by observing a mounted unstained section directly at a light microscope fitted with the appropriate filters for PLM. Direct observation is necessary because the reader must turn the section with respect to the fixed filters to observe the predominant direction of birefringent regions and confirm the lack of orientation in non-birefringent regions. Readers answer each successive question in the flowchart (**Figure 5.1**), in conjunction with consulting the word descriptions (**Table 5.1**) and example images (**Figure 5.2**), until a score is obtained. Additionally, these materials are provided for training individuals. **Figure 5.2** was created specifically for this purpose where each specimen is shown at multiple angles to illustrate the characteristics of the PLM score.

Table 5.1: The PLM Qualitative Score.

Score	Description
0	Evidence of fibre organization, seen as sparse bright patches throughout the specimen. These patches do not have parallel alignment at the surface of the specimen nor perpendicular alignment in the deep zone but are randomly oriented in the specimen.
1	Birefringent tissue of the expected orientation in the deep zone with fibres oriented mainly perpendicular (±30º) to the cartilage-bone interface and occupying less than approximately 50% of the thickness of the non-calcified tissue on average. Little additional evidence of birefringent tissue is apparent, other than randomly oriented patches. Birefringent tissue may have inconsistent thickness and intensity of birefringence across the lateral direction of the specimen. The specimen texture may be smooth, patchy or granular.
2	Identical to a Score of 1 except that the deep zone occupies **more** than approximately 50% of the thickness of the non-calcified tissue. Alternatively, a second region of birefringent tissue may be present above the deep zone that may have any orientation (parallel to the articular surface, obliquely oriented to the articular surface or multiple orientations) except for vertical. In this case, the deep zone may then occupy less than 50% of the thickness of the non-calcified tissue.
3	Zonal organization with birefringent tissue in the deep zone perpendicular to the cartilage-bone interface (±30º), and birefringent tissue at the articular surface that is either aligned parallel to the surface or that has multiple orientations. These two zones are separated by a third non-birefringent region that is appropriate to the species from which the specimen was taken; for example, in human articular cartilage it may be a thin, non-uniform region that is difficult to distinguish compared to the consistent dark band observed in equine articular cartilage. Alternatively, the two birefringent zones are separated by a birefringent region with orientation that is neither parallel nor perpendicular. Zonal thicknesses are heterogeneous across the lateral direction of the specimen. The specimen texture may be smooth, patchy or granular.
4	Identical to a Score of 3 except that the orientation in the superficial zone must be parallel to the surface, and that the transitional zone must be non-birefringent, indicating that it is non-oriented. In addition to these characteristics each zone should approximate the zonal proportions for the species from which the specimen was taken; for example, in human articular cartilage, the deep zone should be the largest, occupying greater than 50% of the total thickness of non-calcified tissue. The transitional and superficial zones are smaller, and the transitional zone may be larger than the superficial zone.
5	Distinct superficial and deep zones with uniform birefringence indicating parallel and perpendicularly oriented fibres respectively, separated by a transitional zone that is non-oriented. Zonal thicknesses are appropriate for the species, age and location from which the specimen was taken and are relatively homogeneous across the lateral direction of the specimen. Overall, the specimen birefringence has a uniform, smooth texture and is neither granular nor patchy.

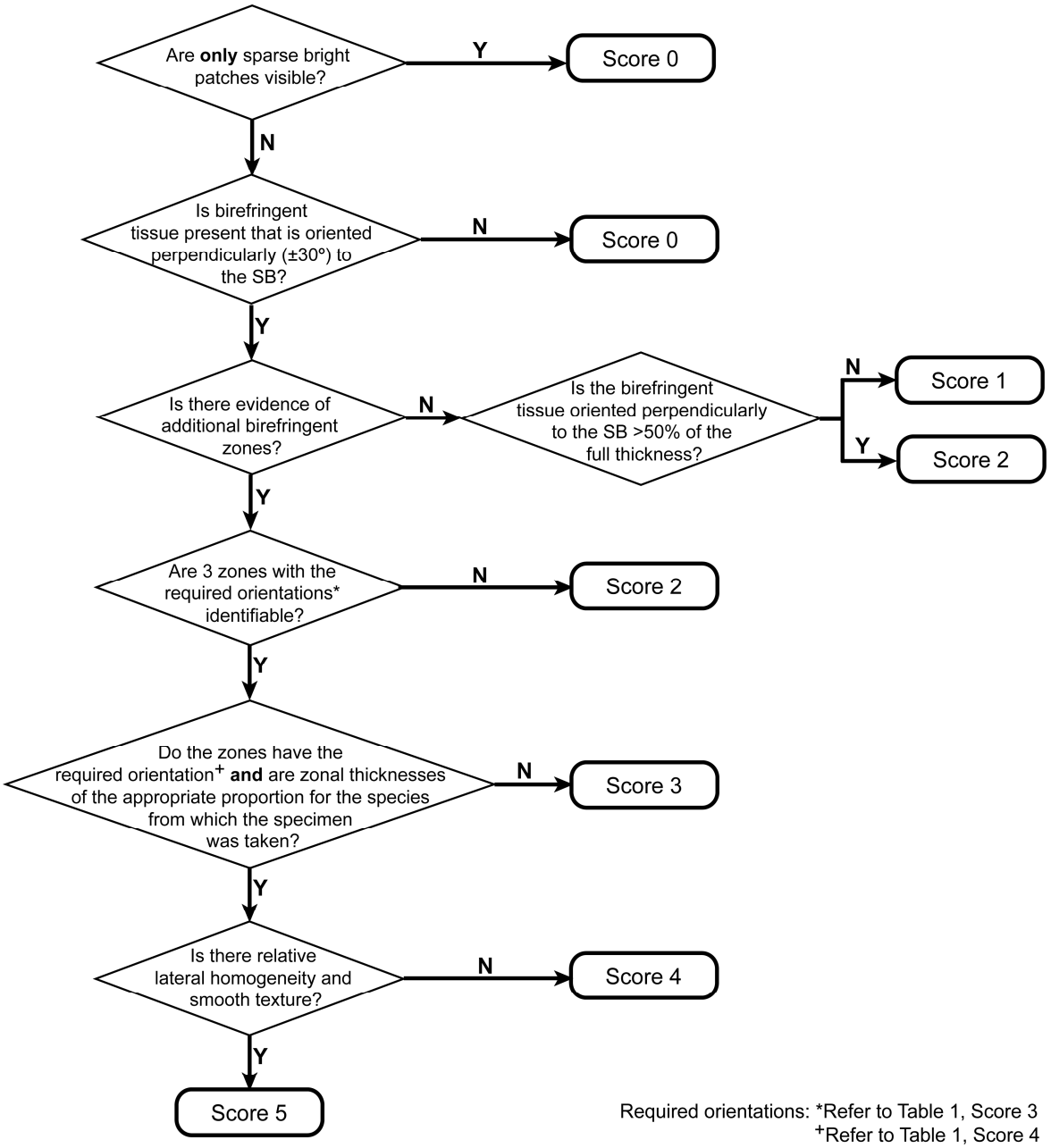

Figure 5.1: A flow chart of the PLM Qualitative Score where the descriptive statements (**Table 5.1**) have been translated into a series of Yes/No questions in order to assist readers when evaluating histological sections.

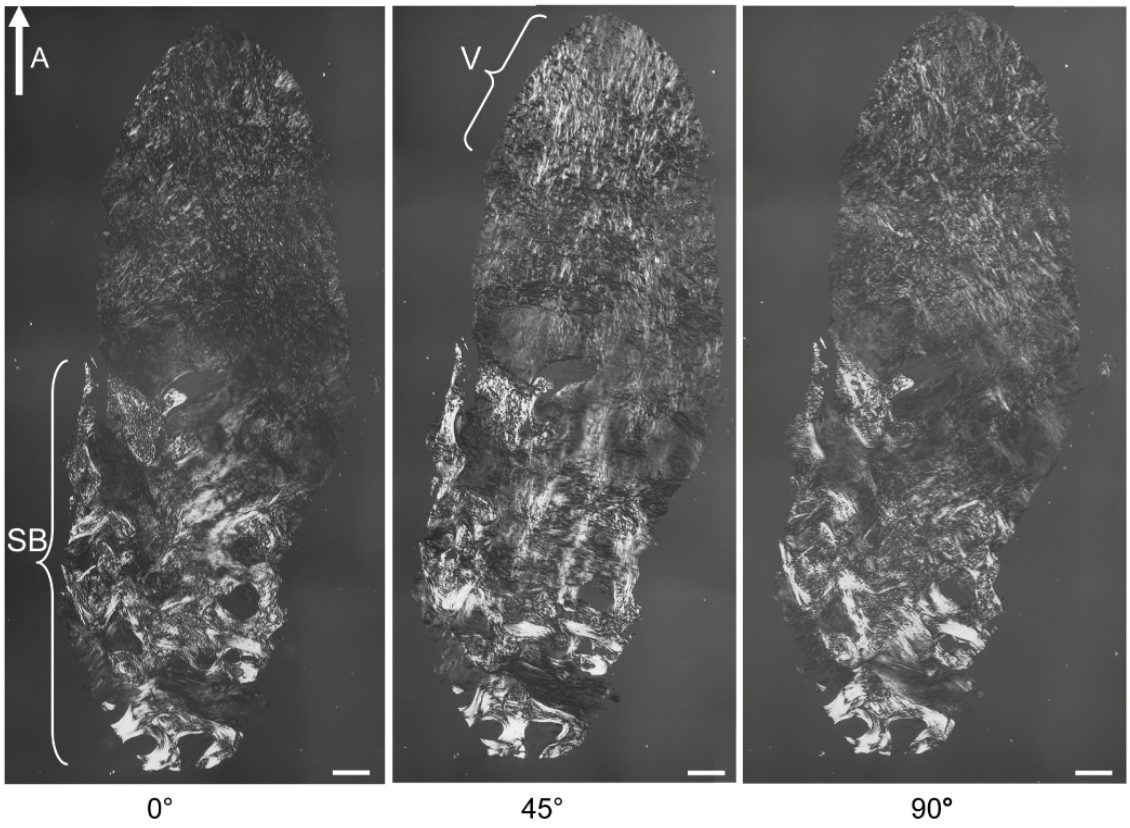

Figure 5.2a: Example of a human osteochondral biopsy that received a PLM Score of 0 out of 5 because it lacks a vertically-oriented deep zone. At all angles relative to the analyzer (A), the birefringent subchondral bone component (SB), occupying ~50% of the specimen thickness, is apparent, but there is no evidence of birefringent tissue adjacent to the subchondral bone. At 45° a region of vertically-oriented tissue (V) is observed at the tip of the non-calcified tissue that has a granular texture. Scale bars are 250 µm.

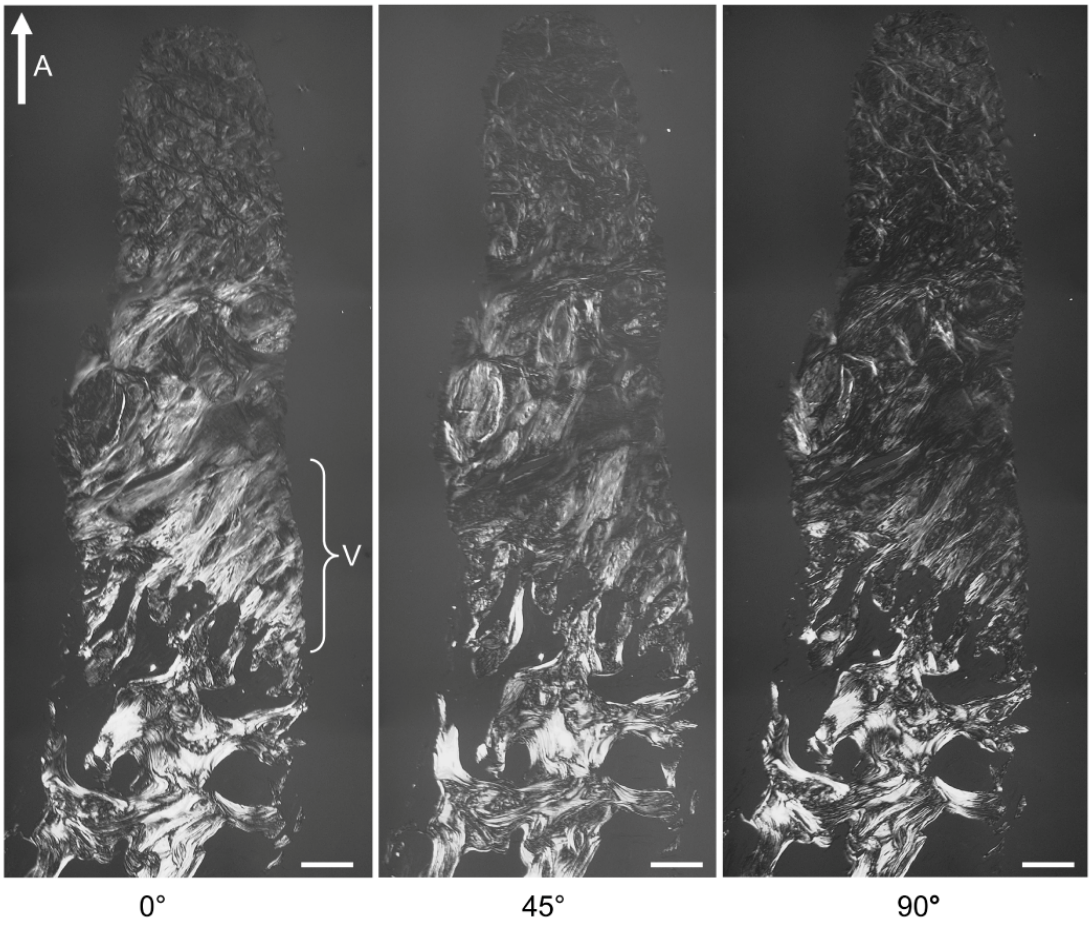

Figure 5.2b: Example of a human osteochondral biopsy that received a PLM Score of 1 out of 5. A vertically-oriented deep zone (V) is mainly visible at 0° because the bone-cartilage interface is angled. Rotating the specimen reveals that there is little additional evidence of collagen organization above the deep zone. Angles are relative to the analyzer filter (A). Scale bars are 250 µm.

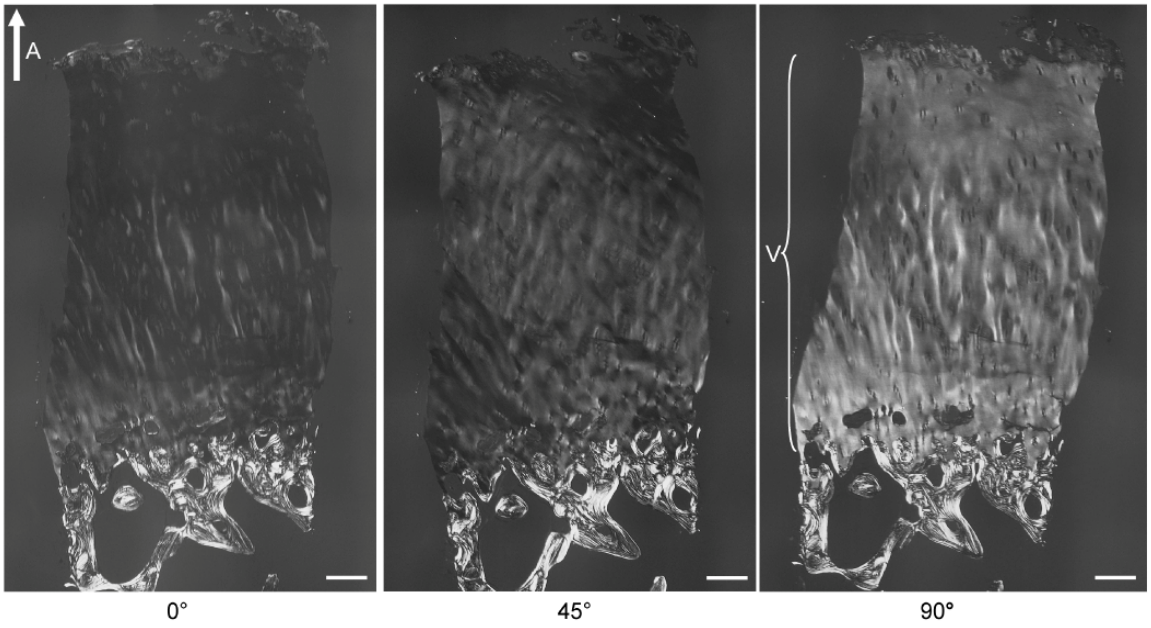

Figure 5.2c: Example of a human osteochondral biopsy that received a PLM Score of 2 out of 5. A mainly vertically-oriented deep zone (V) is present that occupies approximately 90% of the full thickness of non-calcified tissue. The texture of this specimen is described as patchy. Angles are relative to the analyzer filter (A). Scale bars are 250 µm

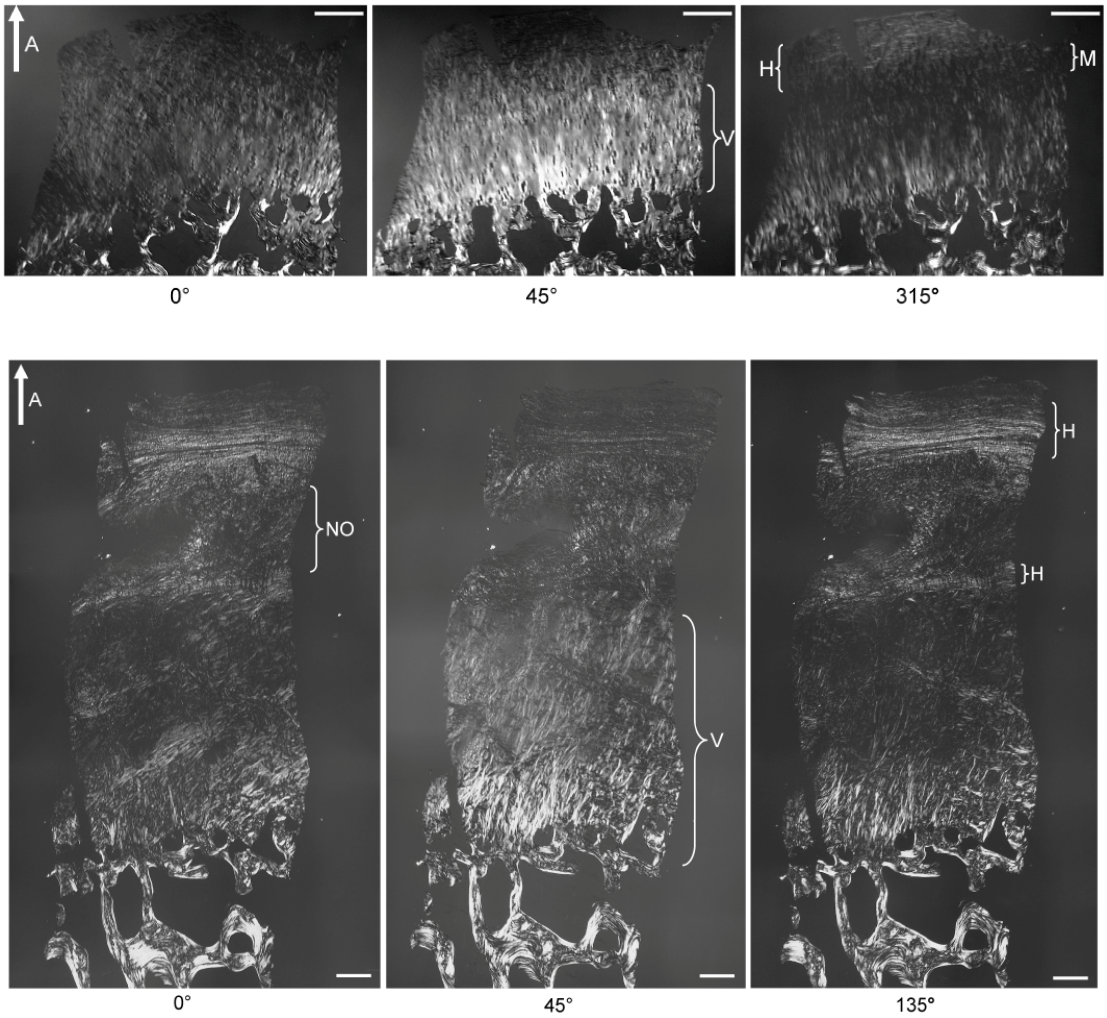

Figure 5.2d: Examples of human osteochondral biopsies that received PLM scores of 3 out of 5. Upper panel: A vertically-oriented deep zone (V) is present and accompanied by a horizontally-oriented superficial zone (H), as well as a region that approximates the transitional zone and has multiple orientations (M). Lower panel: A mainly vertically-oriented deep zone (V) is present along with several additional regions of oriented (H) and predominantly non-oriented tissue (NO). Both of these examples have granular textures. Angles are relative to the analyzer filter (A). All scale bars are 250 µm.

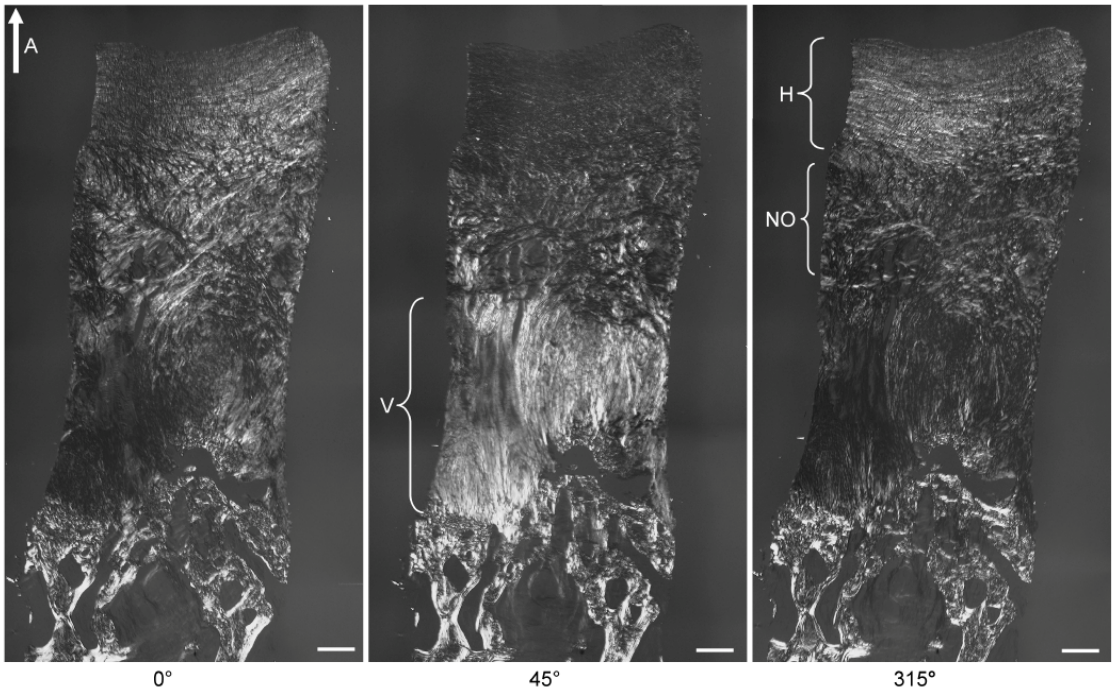

Figure 5.2e: Example of a human osteochondral biopsy that received a PLM Score of 4 out of 5. Three zones are present with appropriate orientations. The deep zone occupies ~50% of the total thickness of non-calcified tissue (V), while the superficial (H) and transitional (NO) zones are smaller. The texture of this sample is best described as granular. Angles are relative to the analyzer filter (A). Scale bars are 250 µm.

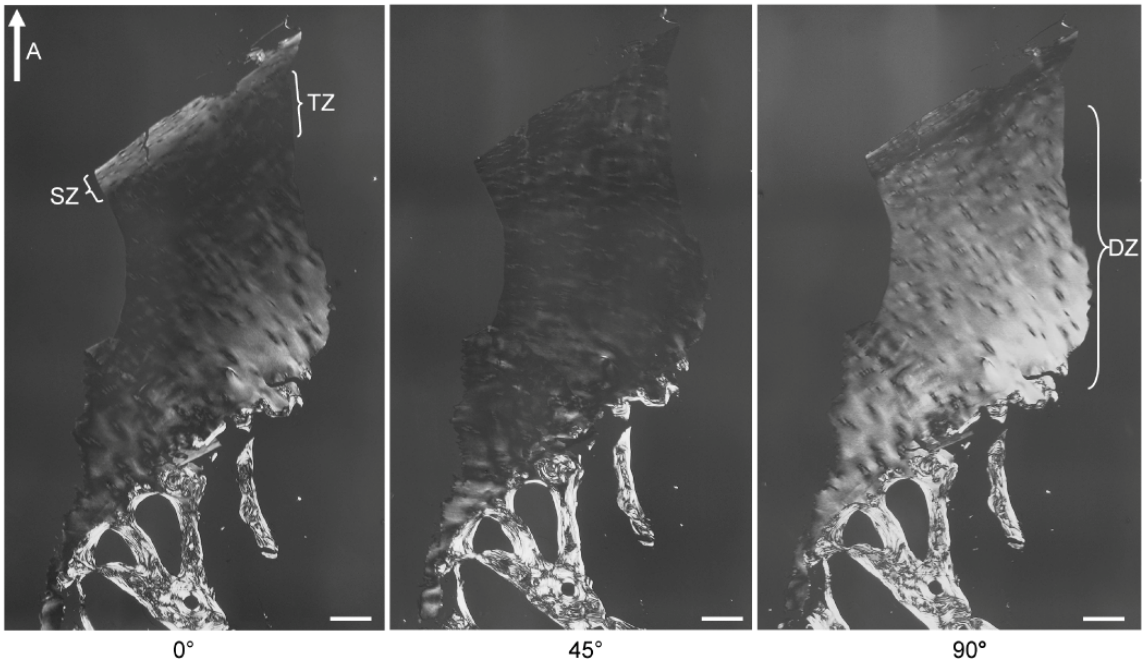

Figure 5.2f: Example of a human osteochondral biopsy that received a PLM Score of 5 out of 5. Three distinct zones (SZ, TZ, DZ) with uniform birefringence are present that are of the appropriate orientations and zonal proportions, and the specimen has a smooth texture. Note that the angled nature of this biopsy makes it difficult to capture uniform birefringence at a single angle. Angles are relative to the analyzer filter (A). Scale bars are 250 µm.

5.3.3 Evaluation of Inter-reader Reliability

Inter-reader reliability was evaluated using normal (n=4), degraded (n=2) and repair (n=22) biopsies. Sections were blinded and scored independently by three trained readers. Reader training involved demonstrating how to apply the PLM score using several human and equine examples with various levels of collagen organization. Inter-reader agreement was analyzed using two cases of the Intraclass Correlation Coefficient for Agreement (ICC) (McGraw & Wong, 1996a, 1996b; Shrout & Fleiss, 1979). The first case, denoted ICC(2,1), estimates the reliability of using any one reader's scores, while the second case, ICC(2,3), estimates the reliability of the mean score of all three readers. ICC calculations were performed using a custom-built LabVIEW function (LabVIEW v.8.6, National Instruments, Austin, TX, USA) validated against results obtained with SPSS v.9 (SPSS Inc., Chicago, IL, USA).

5.3.4 PLM Image Processing

PLM images, required for reporting purposes, were captured at the microscope (Zeiss Axiolab) using a CCD Camera (Hitachi HV-F22 Progressive Scan Colour 3-CCD). Subsequent image processing included extracting the green plane from the original RGB image, equalizing to improve contrast, and deconvoluting to sharpen edges (Northern Eclipse v7.0, Empix Imaging Inc., Mississauga, ON, Canada). Often several images, captured with a 5x objective lens, were required to cover specimens in sufficient detail. These images were merged using the MosaicJ plugin in ImageJ v.1.42q (National Institutes of Health, USA).

5.4 Results

5.4.1 Inter-reader Reliability of the PLM Score

Inter-reader reliability was assessed using 28 normal, degraded and repair biopsies (**Figure 5.3**, **Table 5.2**). The ICCs, ICC(2,1) and ICC(2,3), represent the ratio of variance in the sample population to that from the sample population plus reader-dependent variance. The values of ICC(2,1) and ICC(2,3), where a value of 1 signifies perfect agreement, were 0.90 (lower

boundary of the 95% confidence interval is 0.83) and 0.96 (lower boundary of the 95% confidence interval is 0.94), respectively. These values indicate excellent inter-reader reproducibility, where ICC(2,1) of 0.90 describes the expected reliability for any one reader, which increases to 0.96 (ICC(2,3)) when the mean scores of three readers are used.

High inter-reader agreement reflects the ability of the PLM score to be interpreted and applied effectively by different trained individuals. In all samples, scores among readers did not deviate by more than 1 ordinal. When samples were ranked from the highest to lowest score for each user, the general hierarchy was the same, with normal ranging from 3-5, degraded scoring 2, and repair ranging from 0-3, reflecting the variable collagen organization possible in repair tissues.

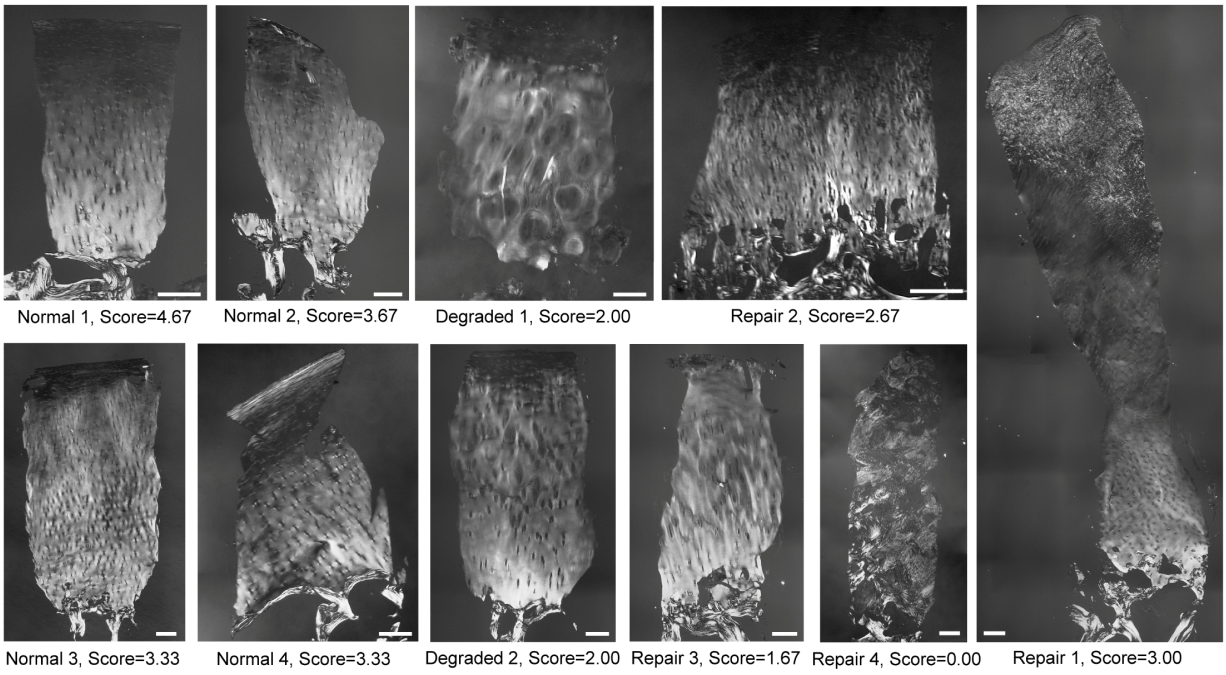

Figure 5.3: PLM images of human osteochondral biopsies used to determine inter-reader variability. The 4 repair samples shown here were selected from the group of 22 repair biopsies. The angle of each image with respect to the analyzer was selected to demonstrate maximum birefringence in the deep zone. As a result, other birefringent regions may be present but are not apparent here. Each image, except Repair 2, is a composite of several individual images captured at the microscope and merged using software. All scale bars are 250 µm.

Table 5.2: PLM scores by reader for the cohort of human osteochondral biopsies used to determine inter-reader variability, including normal (n=4), degraded (n=2) and a subset (n=4) from the total group of 22 repair biopsies.

Sample	Reader			Average
	1	2	3	
Normal 1	4	5	5	4.67
Normal 2	4	3	4	3.67
Normal 3	3	3	4	3.33
Normal 4	3	4	3	3.33
Repair 1	3	3	3	3.00
Repair 2	3	3	2	2.67
Degraded 1	2	2	2	2.00
Degraded 2	2	2	2	2.00
Repair 3	2	1	2	1.67
Repair 4	0	0	0	0.00

5.4.2 Age-related Hyaline Cartilage Appearance

Differences in birefringence were observed in normal cartilage from various age groups (**Figure 5.4**). The most apparent changes were detected in the SZ. In young adult cartilage, receiving PLM scores of 5, relatively uniform birefringence in the SZ was observed, while in older cartilage SZ thickness varied or partial tears/minor fibrillation were present that altered birefringence patterns, often resulting in PLM scores of 4. The preliminary findings on this small group (n=6) suggest age-dependent birefringent changes to which the PLM score is sensitive.

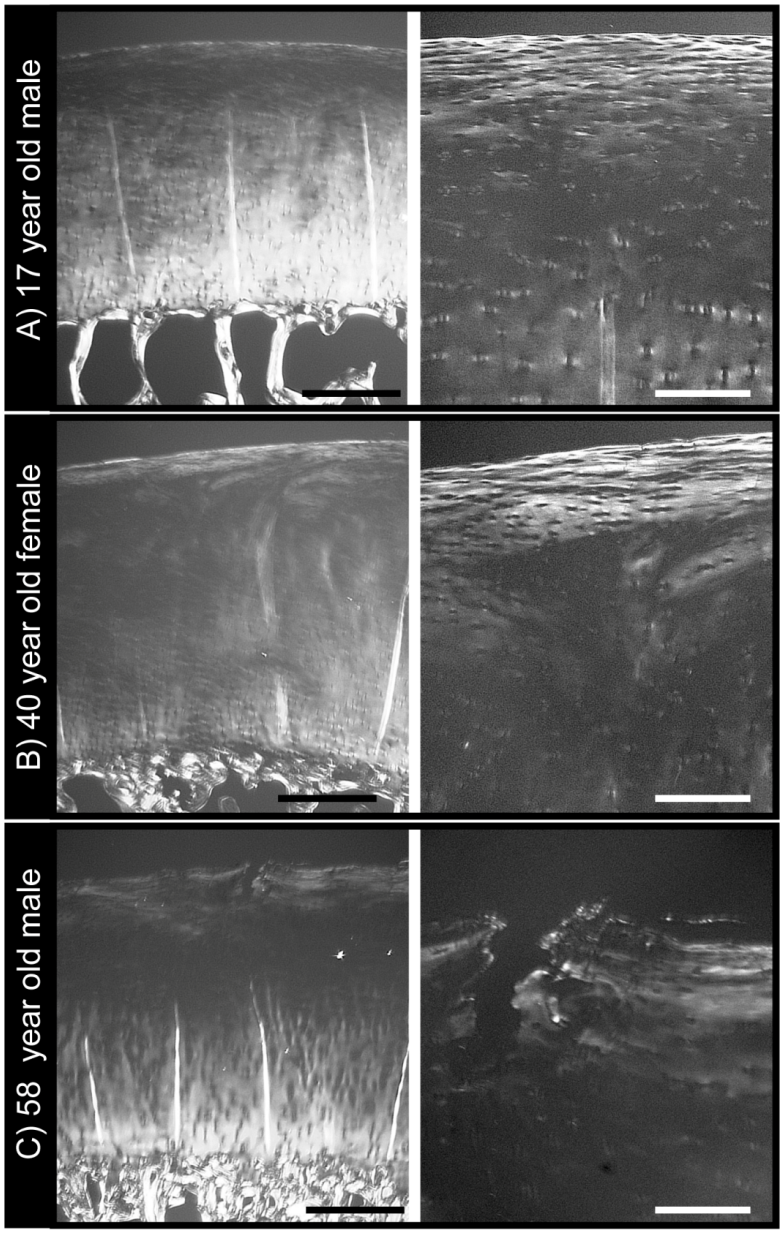

Figure 5.4: Representative PLM images of hyaline articular cartilage from the central medial femoral condyles of macroscopically normal cadaveric knees. Full thickness images (left column) where scale bars are 1 mm and their superficial zones (right column) where scale bars are 250µm. A) Section from a 17 year old male that received a PLM score of 5. B) Section from a 40 year old female that received a PLM score of 4. C) Section from a 58 year old male that received a PLM Score of 4.

5.5 Discussion

The PLM score provides a systematic method for assessing collagen architecture in repair cartilage, a feature that is insufficiently evaluated by present histological scores, and which is central to cartilage biomechanical properties and durability (Archer, et al., 2006; Julkunen, et al., 2009; Moger, et al., 2009). Both hypotheses were supported by our data. Systematic assessment of human biopsies was achieved, where the greater complexity in collagen structure observed in repair versus normal and degraded tissues was successfully captured by the PLM score (**Figure 5.3**, **Table 5.2**). High ICCs confirm that the PLM score can be applied reliably by individual readers [ICC(2,1)=0.90] or by using the mean scores of three readers [ICC(2,3)=0.96].

5.5.1 Comparison to previous PLM studies for native cartilage & repair tissues

PLM has been used extensively to study fibrillar collagen in articular cartilage, including describing its unique network structure (Benninghoff, 1925; Hughes, et al., 2005; Kaab, et al., 1998), documenting changes to collagen organization during development (Hyttinen, et al., 2009; Julkunen, et al., 2009; Rieppo et al., 2009) or aging (Gyarmati, Foldes, Kern, & Kiss, 1987; Hyttinen, et al., 2001). PLM has also been used to validate other collagen imaging modalities (Bear, et al., 2010; Bi, et al., 2005; White, et al., 2006), and for observing changes during loading (Arokoski, et al., 1996; Moger, et al., 2009; Panula, et al., 1998) or degradation (Vaatainen et al., 1998; Williams, et al., 1996).

Applying PLM as a tool to evaluate collagen organization in repair cartilage is becoming more prevalent with several studies using PLM to examine histological sections qualitatively (Bi, et al., 2005; Gooding et al., 2006; Knutsen, et al., 2004; Richardson, et al., 1999; Roberts, et al., 2003; Roberts, et al., 2009) and quantitatively (Langsjo, et al., 2010; Rieppo et al., 2008; Vasara, et al., 2006).

These authors identify several advantages of PLM for analyzing repair cartilage, including its ability to distinguish hyaline cartilage from fibrocartilage in samples that demonstrate hyaline-

like characteristics in light microscopy (Mainil-Varlet, et al., 2003; Roberts, et al., 2009), and PLM offers a means to observe collagen organization, which is not possible with traditional histological staining methods (Rieppo, et al., 2008). PLM has been used qualitatively to observe overall collagen architecture in order to describe a general tissue type (fibrocartilage, hyaline etc.) (Mainil-Varlet, et al., 2003; Roberts, et al., 2003), or to highlight specific characteristics such as collagen anchoring to subchondral bone (Richardson, et al., 1999; Roberts, et al., 2003; Roberts, et al., 2009). These are examples where the PLM score, which offers a more systematic assessment of different levels of collagen organization, could be employed to facilitate comparisons between repair tissues.

Overall collagen fibre anisotropy differences in repair cartilage produced by autologous chondrocyte transplantation compared to controls were detected using quantitative PLM, though specific zonal structure was not described (Langsjo, et al., 2010). Vasara et al. (2006) reported that similar measurements were extremely variable, limiting their value and leading the authors to conclude that the repair collagen structure had no resemblance to hyaline cartilage. However, in the two representative images reported, areas of birefringent tissue are present, indicating some level of organization even though they lack complete hyaline-like organization. The high variability associated with these types of quantitative PLM methods, when applied to repair cartilage, may indicate that perhaps a more generally applicable score, such as the PLM score, would be better suited to assessing collagen organization in these tissues.

These previous studies highlight the need for a qualitative PLM score that is inherently more flexible than quantitative methods, but that provides a systematic and reproducible method for evaluating collagen fibre organization in repair cartilage.

5.5.2 Distinguishing the PLM score vs. other approaches

Collagen architecture is critical to cartilage function and durability, and therefore likely a strong predictor of the long-term success of repair cartilages. The OsScore (Roberts, et al., 2003; Roberts, et al., 2009), ICRS I (Mainil-Varlet, et al., 2003; Moriya et al., 2007) and ICRS II

(Mainil-Varlet, et al., 2010; Saris, et al., 2008), rate a variety of tissue characteristics and all recommend using PLM as a component in gauging a general tissue type but do not describe nor allocate a separate category where different levels of collagen organization can be classified. This PLM score specifically analyses collagen architecture, gauging the extent that the collagen network resembles that of young adult hyaline cartilage, which may be more appropriate for analyzing repair cartilages given the variability possible for these tissues. As patient reported outcomes relating to the repair samples described could not be accessed for comparison, the suitability of the PLM score for assessing cartilage was instead evaluated against ICRS I & II. Moderate ($0.7<r<0.8$) and high ($r>0.8$) correlations between the PLM score and 3 ICRS I (matrix, cell distribution, subchondral bone) and 7 ICRS II (tissue morphology, matrix staining, cell morphology, surface architecture, superficial assessment, mid-deep assessment, overall assessment) categories were detected (Changoor, Nelea, Tran-Khanh, et al., 2009; Méthot et al., 2009). These relationships are logical because these categories rate features associated with collagen organization (Mainil-Varlet, et al., 2003; Mainil-Varlet, et al., 2010). This PLM score can be used alongside other gold standard histological scoring systems to generate a more complete picture of repair tissue quality and assist in comparing tissues produced by different repair strategies.

5.5.3 Technical aspects affecting birefringence

PLM exploits the optical properties of fibrillar collagens, allowing collagen orientation to be inferred from the presence of birefringent/non-birefringent regions (Speer & Dahners, 1979; Yarker, et al., 1983). Birefringence occurs from changes to the direction of polarization of light passing through a histological section due to the direction of collagen at each point in the section. This effect is further influenced by factors such as collagen content, the sectioning plane, optical properties of the mounting media, staining, and specimen thickness (Kiraly, et al., 1997; Modis, 1991; Ortmann, 1975).

As the PLM score is qualitative, it is adaptable to histological sections with different characteristics, for example, thicknesses other than 5 μm, or stained sections where collagen is

not obscured. We recommend standardizing sample preparation to minimize the influence of these types of factors. In the present study, we used 5 µm thick unstained sections mounted in a medium with a similar refractive index to collagen, approximately 1.5, in order to minimize artificial form birefringence. Proteoglycans were not removed as they contribute only 6% of total birefringence (Kiraly, et al., 1997). Indeed, in these conditions, the main source of birefringence was the orientation of collagen fibres. More specifically, birefringence reflects the course of the large primary collagen fibres. There are many smaller, secondary fibres randomly oriented throughout the full thickness of cartilage (Julkunen, 2008; Speer & Dahners, 1979) that may contribute to overall birefringence.

A factor that we could not control was the sectioning plane. Typically for PLM, sectioning is done with respect to surface split line direction (Bullough & Goodfellow, 1968; Kiraly, et al., 1997; Speer & Dahners, 1979). Split lines are artificially created on the articular surface by piercing with a rounded needle, causing collagen fibres to split along lines of tensile stress and indicating SZ orientation (Benninghoff, 1925; Bottcher, Zeissler, Maierl, Grevel, & Oechtering, 2009; Bullough & Goodfellow, 1968; Meachim, Denham, Emery, & Wilkinson, 1974). Sections parallel to the split lines demonstrate different birefringence patterns compared to those cut perpendicularly (Bullough & Goodfellow, 1968; Kiraly, et al., 1997; Speer & Dahners, 1979). This difference is most apparent in the SZ where perpendicular sections, in which SZ fibres are transected, appear non-birefringent. However, human biopsies are small osteochondral cores extracted under conditions which are not amenable to monitoring the anatomical direction of the biopsy. Nonetheless, we did not encounter samples where oriented zones appeared non-birefringent during scanning electron microscopy (SEM) validation studies, where systematically sampled SEM images verified global collagen orientations observed in PLM. A strong correlation ($r \geq 0.80$) was detected between PLM and an analogous SEM score (Changoor, Nelea, Tran-Khanh, et al., 2009; Nelea et al., 2009).

5.5.4 Conclusions

This PLM score is a valuable new histological score offering a systematic, global assessment of collagen organization, a critical feature for successful repair cartilage function and durability. The authors recommend that it be used in addition to current histological scoring systems to enhance the assessment of cartilage repair tissue quality.

5.6 Acknowledgements

The authors would like to acknowledge Gaby Touma, Viorica Lascau, Genevieve Picard and Dr. Anik Chevrier for their contributions to this work. Funding was provided by the Natural Sciences and Engineering Research Council of Canada (NSERC), the Canadian Institutes of Health Research and BioSyntech Canada Inc.

5.7 References

These are the references as they appear in the published version of the article and are in the style required by the journal Osteoarthritis and Cartilage. The references contained within the body of Chapter 5 correspond to the reference list at the end of the thesis.

1. Benninghoff A. Form und bau der gelenkknorpel in ihren beziehungen zur funktion. Zeitschrift fur Zellforschung 1925;2:783-862.

2. Bullough P, Goodfellow J. The significance of the fine structure of articular cartilage. J Bone Joint Surg Br 1968;50(4):852-7.

3. Hedlund H, Mengarelli-Widholm S, Reinholt FP, Svensson O. Stereologic studies on collagen in bovine articular cartilage. APMIS 1993;101(2):133-40.

4. Hughes LC, Archer CW, ap Gwynn I. The ultrastructure of mouse articular cartilage: Collagen orientation and implications for tissue functionality. A polarised light and scanning electron microscope study and review. Eur Cell Mater 2005;9:68-84.

5. Kaab MJ, Gwynn IA, Notzli HP. Collagen fibre arrangement in the tibial plateau articular cartilage of man and other mammalian species. J Anat 1998;193 (Pt 1):23-34.

6. Schenk RK, Eggli PS, Hunziker EB. Articular cartilage morphology. In: Articular cartilage biochemistry, Kuettner K, Schleyerbach R, Hascall VC, Eds. New York: Raven Press 1986:3-22.

7. Xia Y, Moody JB, Alhadlaq H, Hu J. Imaging the physical and morphological properties of a multi-zone young articular cartilage at microscopic resolution. J Magn Reson Imaging 2003;17(3):365-74.

8. Chen AC, Bae WC, Schinagl RM, Sah RL. Depth- and strain-dependent mechanical and electromechanical properties of full-thickness bovine articular cartilage in confined compression. J Biomech 2001;34(1):1-12.

9. Korhonen RK, Laasanen MS, Toyras J, Lappalainen R, Helminen HJ, Jurvelin JS. Fibril reinforced poroelastic model predicts specifically mechanical behavior of normal, proteoglycan depleted and collagen degraded articular cartilage. J Biomech 2003;36(9):1373-9.

10. Li LP, Korhonen RK, Iivarinen J, Jurvelin JS, Herzog W. Fluid pressure driven fibril reinforcement in creep and relaxation tests of articular cartilage. Med Eng Phys 2008;30(2):182-9.

11. Park S, Krishnan R, Nicoll SB, Ateshian GA. Cartilage interstitial fluid load support in unconfined compression. J Biomech 2003;36(12):1785-96.

12. Brittberg M, Lindahl A, Nilsson A, Ohlsson C, Isaksson O, Peterson L. Treatment of deep cartilage defects in the knee with autologous chondrocyte transplantation. N Engl J Med 1994;331(14):889-95.

13. Saris DB, Vanlauwe J, Victor J, Haspl M, Bohnsack M, Fortems Y, et al. Characterized chondrocyte implantation results in better structural repair when treating symptomatic cartilage defects of the knee in a randomized controlled trial versus microfracture. Am J Sports Med 2008;36(2):235-46.

14. Crawford DC, Heveran CM, Cannon WD, Jr., Foo LF, Potter HG. An autologous cartilage tissue implant neocart for treatment of grade iii chondral injury to the distal femur: Prospective clinical safety trial at 2 years. Am J Sports Med 2009;37(7):1334-43.

15. Kon E, Delcogliano M, Filardo G, Fini M, Giavaresi G, Francioli S, et al. Orderly osteochondral regeneration in a sheep model using a novel nano-composite multilayered biomaterial. J Orthop Res 2010;28(1):116-24.

16. Hoemann CD, Hurtig M, Rossomacha E, Sun J, Chevrier A, Shive MS, et al. Chitosan-glycerol phosphate/blood implants improve hyaline cartilage repair in ovine microfracture defects. J Bone Joint Surg Am 2005;87(12):2671-86.

17. Shive MS, Hoemann CD, Restrepo A, Hurtig MB, Duval N, Ranger P, et al. BST-CarGel: In situ chondroinduction for cartilage repair. Operative Techniques in Orthopaedics 2006;16:271-8.

18. Mithoefer K, McAdams T, Williams RJ, Kreuz PC, Mandelbaum BR. Clinical efficacy of the microfracture technique for articular cartilage repair in the knee: An evidence-based systematic analysis. Am J Sports Med 2009;37(10):2053-63.

19. Hunziker EB. Articular cartilage repair: Basic science and clinical progress. A review of the current status and prospects. Osteoarthritis Cartilage 2002;10(6):432-63.

20. Hunziker EB, Kapfinger E, Geiss J. The structural architecture of adult mammalian articular cartilage evolves by a synchronized process of tissue resorption and neoformation during postnatal development. Osteoarthritis Cartilage 2007;15(4):403-13.

21. Gudas R, Kalesinskas RJ, Kimtys V, Stankevicius E, Toliusis V, Bernotavicius G, et al. A prospective randomized clinical study of mosaic osteochondral autologous transplantation versus microfracture for the treatment of osteochondral defects in the knee joint in young athletes. Arthroscopy 2005;21(9):1066-75.

22. Mainil-Varlet P, Aigner T, Brittberg M, Bullough P, Hollander A, Hunziker E, et al. Histological assessment of cartilage repair: A report by the histology endpoint committee of the international cartilage repair society (ICRS). J Bone Joint Surg Am 2003;85-A Suppl 2:45-57.

23. Roberts S, McCall IW, Darby AJ, Menage J, Evans H, Harrison PE, et al. Autologous chondrocyte implantation for cartilage repair: Monitoring its success by magnetic resonance imaging and histology. Arthritis Res Ther 2003;5(1):R60-73.

24. Selmi TA, Verdonk P, Chambat P, Dubrana F, Potel JF, Barnouin L, et al. Autologous chondrocyte implantation in a novel alginate-agarose hydrogel: Outcome at two years. J Bone Joint Surg Br 2008;90(5):597-604.

25. Rutgers M, van Pelt MJ, Dhert WJ, Creemers LB, Saris DB. Evaluation of histological scoring systems for tissue-engineered, repaired and osteoarthritic cartilage. Osteoarthritis Cartilage 2010;18(1):12-23.

26. Mainil-Varlet P, Van Damme B, Nesic D, Knutsen G, Kandel R, Roberts S. A new histology scoring system for the assessment of the quality of human cartilage repair: ICRS II. Am J Sports Med 2010.

27. Julkunen P, Harjula T, Iivarinen J, Marjanen J, Seppanen K, Narhi T, et al. Biomechanical, biochemical and structural correlations in immature and mature rabbit articular cartilage. Osteoarthritis Cartilage 2009;17(12):1628-38.

28. Moger CJ, Arkill KP, Barrett R, Bleuet P, Ellis RE, Green EM, et al. Cartilage collagen matrix reorientation and displacement in response to surface loading. J Biomech Eng 2009;131(3):031008.

29. Williams JM, Uebelhart D, Thonar EJ, Kocsis K, Modis L. Alteration and recovery of the spatial orientation of the collagen network of articular cartilage in adolescent rabbits following intra-articular chymopapain injection. Connect Tissue Res 1996;34(2):105-17.

30. Yarker YE, Aspden RM, Hukins DW. Birefringence of articular cartilage and the distribution on collagen fibril orientations. Connect Tissue Res 1983;11(2-3):207-13.

31. Arokoski JP, Hyttinen MM, Lapvetelainen T, Takacs P, Kosztaczky B, Modis L, et al. Decreased birefringence of the superficial zone collagen network in the canine knee (stifle) articular cartilage after long distance running training, detected by quantitative polarised light microscopy. Ann Rheum Dis 1996;55(4):253-64.

32. Kiraly K, Hyttinen MM, Lapvetelainen T, Elo M, Kiviranta I, Dobai J, et al. Specimen preparation and quantification of collagen birefringence in unstained sections of articular cartilage using image analysis and polarizing light microscopy. Histochem J 1997;29(4):317-27.

33. Korhonen RK, Wong M, Arokoski J, Lindgren R, Helminen HJ, Hunziker EB, et al. Importance of the superficial tissue layer for the indentation stiffness of articular cartilage. Med Eng Phys 2002;24(2):99-108.

34. Rieppo J, Toyras J, Nieminen MT, Kovanen V, Hyttinen MM, Korhonen RK, et al. Structure-function relationships in enzymatically modified articular cartilage. Cells Tissues Organs 2003;175(3):121-32.

35. Speer DP, Dahners L. The collagenous architecture of articular cartilage. Correlation of scanning electron microscopy and polarized light microscopy observations. Clin Orthop Relat Res 1979(139):267-75.

36. Richardson JB, Caterson B, Evans EH, Ashton BA, Roberts S. Repair of human articular cartilage after implantation of autologous chondrocytes. J Bone Joint Surg Br 1999;81(6):1064-8.

37. Roberts S, Menage J, Sandell LJ, Evans EH, Richardson JB. Immunohistochemical study of collagen types I and II and procollagen IIa in human cartilage repair tissue following autologous chondrocyte implantation. Knee 2009;16(5):398-404.

38. Vasara AI, Hyttinen MM, Pulliainen O, Lammi MJ, Jurvelin JS, Peterson L, et al. Immature porcine knee cartilage lesions show good healing with or without autologous chondrocyte transplantation. Osteoarthritis Cartilage 2006;14(10):1066-74.

39. White LM, Sussman MS, Hurtig M, Probyn L, Tomlinson G, Kandel R. Cartilage T2 assessment: Differentiation of normal hyaline cartilage and reparative tissue after arthroscopic cartilage repair in equine subjects. Radiology 2006;241(2):407-14.

40. Modis L. Physical backgrounds of polarization microscopy. In: Organization of the extracellular matrix: A polarization microscopic approach, Modis L, Ed. Boca Raton: CRC Press 1991:9-30.

41. Hyttinen MM, Holopainen J, van Weeren PR, Firth EC, Helminen HJ, Brama PA. Changes in collagen fibril network organization and proteoglycan distribution in equine articular cartilage during maturation and growth. J Anat 2009;215(5):584-91.

42. Changoor A, Nelea M, Fereydoonzad L, Rossomacha E, Shive MS, Buschmann MD. Assessment of collagen orientation in repair cartilage by polarized light and scanning

electon microscopies (abstract). Paper presented at: Transactions of the 55th Annual Meeting of the Orthopaedic Research Society 2009; Las Vegas, Nevada.

43. Changoor A, Nelea M, Tran-Khanh N, Méthot S, Fereydoonzad L, Rossomacha E, et al. Analysis of hyaline structure in human osteochondral biopsies by polarization light microscopy (abstract). Paper presented at: Transactions of the International Cartilage Repair Society 2009; Miami, Florida.

44. Maurice DM. The structure and transparency of the cornea. J Physiol 1957;136(2):263-86.

45. Vidal Bde C, Vilarta R. Articular cartilage: Collagen II-proteoglycans interactions. Availability of reactive groups. Variation in birefringence and differences as compared to collagen I. Acta Histochem 1988;83(2):189-205.

46. Archer CW, Redman S, Khan I, Bishop J, Richardson K. Enhancing tissue integration in cartilage repair procedures. J Anat 2006;209(4):481-93.

47. Kurkijarvi JE, Nissi MJ, Rieppo J, Toyras J, Kiviranta I, Nieminen MT, et al. The zonal architecture of human articular cartilage described by T2 relaxation time in the presence of Gd-DTPA2. Magn Reson Imaging 2008;26(5):602-7.

48. Nissi MJ, Rieppo J, Toyras J, Laasanen MS, Kiviranta I, Jurvelin JS, et al. T(2) relaxation time mapping reveals age- and species-related diversity of collagen network architecture in articular cartilage. Osteoarthritis Cartilage 2006;14(12):1265-71.

49. Buckwalter J, Hunziker E, Rosenberg L, Coutts R, Adams M, Eyre D. Articular cartilage: Composition and structure. In: Injury and repair of the musculoskeletal soft tissues, Woo SL-Y, Buckwalter J, Eds. Park Ridge: American Academy of Orthopaedic Surgeons 1988:405-25.

50. Hunziker E. Articular cartilage structure in humans and experimental animals. In: Articular cartilage and osteoarthritis: Workshop conference hoechst werk kalle-albert, Kuettner KE, Schleyerbach R, Peyron JG, Hascall VC, Eds. New York: Raven Press 1992:183-99.

51. Hyttinen MM, Arokoski JP, Parkkinen JJ, Lammi MJ, Lapvetelainen T, Mauranen K, et al. Age matters: Collagen birefringence of superficial articular cartilage is increased in

young guinea-pigs but decreased in older animals after identical physiological type of joint loading. Osteoarthritis Cartilage 2001;9(8):694-701.

52. Panula HE, Hyttinen MM, Arokoski JP, Langsjo TK, Pelttari A, Kiviranta I, et al. Articular cartilage superficial zone collagen birefringence reduced and cartilage thickness increased before surface fibrillation in experimental osteoarthritis. Ann Rheum Dis 1998;57(4):237-45.

53. Guilak F, Ratcliffe A, Lane N, Rosenwasser MP, Mow VC. Mechanical and biochemical changes in the superficial zone of articular cartilage in canine experimental osteoarthritis. J Orthop Res 1994;12(4):474-84.

54. Bi X, Li G, Doty SB, Camacho NP. A novel method for determination of collagen orientation in cartilage by fourier transform infrared imaging spectroscopy (FT-IRIS). Osteoarthritis Cartilage 2005;13(12):1050-8.

55. McGraw KO, Wong SP. Forming inferences about some intraclass correlations coefficients (vol 1, pg 30, 1996). Psychol Methods 1996;1(4):390.

56. McGraw KO, Wong SP. Forming inferences about some intraclass correlation coefficients. Psychol Methods 1996;1(1):30-46.

57. Shrout PE, Fleiss JL. Intraclass correlations: Uses in assessing rater reliability. Psychol Bull 1979;86(2):420-8.

58. Rieppo J, Hyttinen MM, Halmesmaki E, Ruotsalainen H, Vasara A, Kiviranta I, et al. Changes in spatial collagen content and collagen network architecture in porcine articular cartilage during growth and maturation. Osteoarthritis Cartilage 2009;17(4):448-55.

59. Gyarmati J, Foldes I, Kern M, Kiss I. Morphological studies on the articular cartilage of old rats. Acta Morphol Hung 1987;35(3-4):111-24.

60. Bear DM, Williams A, Chu CT, Coyle CH, Chu CR. Optical coherence tomography grading correlates with MRI T2 mapping and extracellular matrix content. J Orthop Res 2010;28(4):546-52.

61. Vaatainen U, Kiviranta I, Jaroma H, Arokosi J, Tammi M, Kovanen V. Collagen crosslinks in chondromalacia of the patella. Int J Sports Med 1998;19(2):144-8.

62. Gooding CR, Bartlett W, Bentley G, Skinner JA, Carrington R, Flanagan A. A prospective, randomised study comparing two techniques of autologous chondrocyte

implantation for osteochondral defects in the knee: Periosteum covered versus type I/III collagen covered. Knee 2006;13(3):203-10.

63. Knutsen G, Engebretsen L, Ludvigsen TC, Drogset JO, Grontvedt T, Solheim E, et al. Autologous chondrocyte implantation compared with microfracture in the knee. A randomized trial. J Bone Joint Surg Am 2004;86-A(3):455-64.

64. Langsjo TK, Vasara AI, Hyttinen MM, Lammi MJ, Kaukinen A, Helminen HJ, et al. Quantitative analysis of collagen network structure and fibril dimensions in cartilage repair with autologous chondrocyte transplantation. Cells Tissues Organs 2010;192(6):351-60.

65. Rieppo J, Hallikainen J, Jurvelin JS, Kiviranta I, Helminen HJ, Hyttinen MM. Practical considerations in the use of polarized light microscopy in the analysis of the collagen network in articular cartilage. Microsc Res Tech 2008;71(4):279-87.

66. Moriya T, Wada Y, Watanabe A, Sasho T, Nakagawa K, Mainil-Varlet P, et al. Evaluation of reparative cartilage after autologous chondrocyte implantation for osteochondritis dissecans: Histology, biochemistry, and MR imaging. J Orthop Sci 2007;12(3):265-73.

67. Méthot S, Hoemann C, Rossomacha E, Garon M, Shive MS, Tremblay J, et al. ICRS I and ICRS II scoring of human osteochondral biopsies: Reader variability and sensitivity to staining method (abstract). Paper presented at: Transactions of the International Cartilage Repair Society 2009; Miami, Florida.

68. Ortmann R. Use of polarized light for quantitative determination of the adjustment of the tangential fibres in articular cartilage. Anat Embryol (Berl) 1975;148(2):109-20.

69. Julkunen P. Relationships between structure, composition and function of articular cartilage [Doctoral Dissertation]. Kuopio: Faculty of Natural and Environmental Sciences, University of Kuopio; 2008.

70. Bottcher P, Zeissler M, Maierl J, Grevel V, Oechtering G. Mapping of split-line pattern and cartilage thickness of selected donor and recipient sites for autologous osteochondral transplantation in the canine stifle joint. Vet Surg 2009;38(6):696-704.

71. Meachim G, Denham D, Emery IH, Wilkinson PH. Collagen alignments and artificial splits at the surface of human articular cartilage. J Anat 1974;118(Pt 1):101-18.

72. Nelea M, Changoor A, Méthot S, Garon M, Shive MS, Tremblay J, et al. Collagen ultrastructure in human osteochondral biopsies (abstract). Paper presented at: Transactions of the International Cartilage Repair Society 2009; Miami, Florida.

CHAPTER 6. ARTICLE IV

Structural characteristics of the collagen network in human normal, degraded and repair articular cartilages observed in polarized light and scanning electron microscopies

A Changoor[1], M Nelea[1], S Méthot[2], N Tran-Khanh[1], A Chevrier[1], A Restrepo[2], MS Shive[2], MD Buschmann[1*]

Submitted to the journal Osteoarthritis and Cartilage in January 2011

[1]Institute of Biomedical Engineering, Department of Chemical Engineering
École Polytechnique de Montréal, Montréal, Québec, Canada

[2]Piramal Healthcare (Canada), Laval, Québec, Canada

[*]Corresponding author
Institute of Biomedical Engineering, Department of Chemical Engineering
École Polytechnique of Montréal, P.O. Box 6079, Station Centre-Ville
Montreal, Québec, Canada, H3C 3A7
Tel.: 514-340-4711 ext. 4931
Fax: 514-340-2980
E-mail: michael.buschmann@polymtl.ca

Author's Contributions

Adele Changoor	Study conception and design, data acquisition, data analysis and interpretation, statistical analysis, literature review, drafting and critical revision of the manuscript. Accepts responsibility for the integrity of the work as a whole. *The contributions of the first author were estimated at 85%.*
Monica Nelea	Study conception and design, data acquisition, interpretation of data, critical revision of the manuscript
Stephane Méthot	Data acquisition, interpretation of data, critical revision of the manuscript
Nicolas Tran-Khanh	Data acquisition, interpretation of data, critical revision of the manuscript
Anik Chevrier	Data acquisition, interpretation of data, critical revision of the manuscript
Alberto Restrepo	Clinical trial design and management, retrieval of repair cartilage biopsies, interpretation of data, critical revision of the manuscript
Matthew Shive	Clinical trial design and management, retrieval of repair cartilage biopsies, interpretation of data, critical revision of the manuscript
Michael Buschmann	Study conception and design, interpretation of data, drafting and critical revision of the manuscript. Accepts responsibility for the integrity of the work as a whole.

6.1 Abstract

Objective: This study characterizes collagen organization in human normal (n=6), degraded (n=6) and repair (n=22) cartilages, using polarized light (PLM) and scanning electron (SEM) microscopies.

Design: Collagen organization (CO) was assessed using a newly-developed PLM-CO score, and zonal proportions measured. SEM images were captured from locations matched to PLM. Fibre orientations were assessed in SEM and compared to those observed in PLM. CO was also assessed in individual SEM images and combined to generate an SEM-CO score for overall collagen organization analogous to PLM-CO. Fibre diameters were measured in SEM.

Results: PLM-CO and SEM-CO scores were correlated, $r=0.786$ ($p<0.00001$, $n=32$), after excluding two outliers. Orientation observed in PLM was validated by SEM since PLM/SEM correspondence occurred in 91.6% of samples. Proportions of the deep (DZ), transitional (TZ) and superficial (SZ) zones averaged 74.0±11.4%, 18.6±8.7%, and 7.3±1.5% in normal, and 45.6±11.0%, 47.2±10.4% and 9.5±4.3% in degraded cartilage, respectively. Fibre diameters in normal cartilage increased with depth from the articular surface, 55.8±15.9nm (SZ), 87.5±17.9nm (TZ) and 108.2±21.4nm (DZ). Fibre diameters were smaller in repair biopsies, 60.4±9.3nm (SZ), 63.2±12.8nm (TZ) and 67.2±16.8nm (DZ). Degraded cartilage had wider fibre diameter ranges and bimodal distributions, possibly reflecting new collagen synthesis and remodelling. Repair tissues revealed the potential of some cartilage repair procedures to produce zonal collagen organization resembling native articular cartilage structure.

Conclusion: This detailed assessment of collagen architecture could benefit the development of cartilage repair strategies intended to recreate functional collagen architecture.

6.2 Introduction

The biomechanical properties and durability of articular cartilage depend primarily on the highly organized, fibrillar collagen type II network (Archer, et al., 2006; Korhonen, et al., 2002; Kovach & Athanasiou, 1997). In mature cartilage, it consists of three zones where collagen fibres are oriented tangentially to the articular surface in the superficial zone (SZ), have no predominant orientation in the transitional zone (TZ) and become aligned perpendicularly to, and finally anchored in, the underlying subchondral bone in the deep zone (DZ) (Benninghoff, 1925; Hedlund, et al., 1993; Hwang, et al., 1990; Schenk, et al., 1986; Wang et al., 2009). This stratified architecture results from post-natal endochondral development processes (Bland & Ashhurst, 1996; Hunziker, et al., 2007; Julkunen, et al., 2009; van Turnhout et al., 2010). However, once this mature structure is achieved, the turnover rate of collagen becomes extremely low (Bank, Bayliss, Lafeber, Maroudas, & Tekoppele, 1998; Eyre, 2002), contributing to the limited intrinsic repair capacity of normal adult articular cartilage.

Numerous strategies for repairing focal cartilage defects are being explored, including tissue engineered constructs (Crawford, et al., 2009; Kon, et al., 2010), cell therapies (Brittberg, et al., 1994; Saris, et al., 2008), scaffold-based solutions (Hoemann, et al., 2005; Shive, et al., 2006) and surgical techniques (Gudas, et al., 2005; Mithoefer, et al., 2009). These approaches engage extrinsic repair processes originating from the subchondral bone, implanted cells or tissue-engineered constructs, which may additionally interact with other joint tissues. These repair strategies aim to generate a lasting durable and functional repair cartilage tissue. Consequently, recreating a stratified collagen network similar to that of native hyaline articular cartilage is paramount (Hunziker, 2009; Responte, et al., 2007).

Collagen organization and other structural features of the collagen network, including collagen fibre diameters, have been directly compared between normal and osteoarthritic cartilages (Clark & Simonian, 1997; Minns & Steven, 1977; Redler, 1974). However, relatively few reports provide analyses of the collagen network in repair cartilage tissues (Bi, et al., 2005; Gooding, et al., 2006; Richardson, et al., 1999; Vasara, et al., 2006) or tissue engineered constructs (Elder & Athanasiou, 2008; Kelly, Ng, Wang, Ateshian, & Hung, 2006; Riesle, et al.,

1998). More recently, quantitative analyses of stereological features, collagen fibre anisotropy and diameters in repair cartilage produced by autologous chondrocyte transplantation in a pig model were reported (Langsjo, et al., 2010). A qualitative PLM-CO score, for rating overall collagen organization in unstained histological sections of human repair cartilage was also recently developed (Changoor et al., 2011). Collagen network architecture was further explored in the present study, where the aim was to directly compare features of the network in normal, degraded and repair cartilage tissues. Linear polarized light microscopy (PLM) was used to acquire a global appreciation of collagen organization by using the newly developed PLM-CO score (Changoor, et al., 2011), while scanning electron microscopy (SEM) permitted evaluation of collagen ultrastructure.

PLM exploits the optical properties of anisotropic materials such as biological tissues containing fibrillar collagens. In linear PLM, a polarizer filter, inserted after the light source, limits light transmitted to the specimen to a single plane of polarization that is perpendicular to the direction of light propagation. The direction of light polarization can be altered by the orientation of collagen fibres at each point in the section, an effect called birefringence (Modis, 1991). The analyzer filter, placed after the specimen, ensures that only light with polarization modified by the specimen is passed to the eyepiece. Thus, the intensity of the resulting signal illuminates regions in the specimen capable of altering polarization, which are therefore optically active, or, in equivalent terms, oriented, anisotropic and birefringent. In normal, hyaline articular cartilage, PLM reveals two birefringent regions, representing the highly oriented SZ and DZ, separated by a non-birefringent, non-oriented TZ (Arokoski, et al., 1996; Hughes, et al., 2005; Kaab, et al., 1998; Kiraly, et al., 1997; Korhonen, et al., 2002; Rieppo, et al., 2003; Speer & Dahners, 1979).

PLM is a versatile tool for observing global collagen organization but it does not allow direct visualization of collagen fibres; rather, orientation is inferred from the optical characteristics of the sample (Kiraly, et al., 1997; Modis, 1991; Ortmann, 1975; Speer & Dahners, 1979). Conversely, the high resolution possible with SEM results in direct visualization of individual collagen fibres (Kiraly, et al., 1997; Modis, 1991; Ortmann, 1975; Speer &

Dahners, 1979). In the present study, PLM & SEM methods were used to systematically grade collagen organization in matched regions in normal, degraded and repair articular cartilages. We hypothesized that characterization of collagen organization obtained by these two methods would be highly correlated, and that differences exist in quantitative measures of zonal proportions and in collagen fibre diameters among these tissue types.

6.3 Methods

6.3.1 Tissue Sources & Processing

Human knee and hip osteochondral biopsies (n=34) were handled using procedures approved by the Ethics Committee at École Polytechnique de Montréal.

Human osteochondral biopsies, 2 mm in diameter, were collected using 11G Jamshidi needles (Cardinal Health, ON, Canada) from tissue sources that were macroscopically normal, degraded or from sites that had undergone cartilage repair procedures. Normal articular cartilage biopsies were acquired from cadaveric knees (n=2, LifeLink Tissue Bank, Tampa, FL, USA), and large allografts (n=2, RTI Biologics Inc., Alachua, FL, USA). Degraded articular cartilage biopsies (n=2) were obtained from tissue removed during a total hip arthroplasty (Research Institute of the McGill University Health Centre, Montreal, Quebec, Canada). Finally, cartilage repair biopsies (n=22) were retrieved during standardized, second-look arthroscopies, 13 months post-treatment during a randomized clinical trial, (initially sponsored by BioSyntech Canada Inc., now Piramal Healthcare (Canada), Montreal, Quebec, Canada), where the ability of microfracture augmented with the cartilage repair device BST-CarGel® was compared to microfracture alone for repairing focal cartilage lesions. Microfracture involves piercing a debrided subchondral bone plate, thus encouraging bone marrow cells to migrate to the stimulated site to form a granulation tissue that may grow and remodel into fibrous tissue, fibrocartilage or hyaline-like cartilage. Biopsies were fixed in 10% neutral buffered formalin (NBF) at room temperature for a minimum of 24 hours and up to 5 days. Decalcification was achieved by rocking samples placed in 0.5N HCl, 0.1%(v/v) glutaraldehyde for 30 hours at 4°C. Specimens were post-fixed in 10% NBF

overnight prior to paraffin embedding and sectioned at 5 µm. An additional normal (n=1) sample was obtained from the medial femoral condyle (MFC) of a 24 year old male (RTI Biologics Inc., Alachua, FL, USA). It was fixed in 10% NBF at 4°C for 32 days, decalcified in 0.5N HCl, 0.1%(v/v) glutaraldehyde for 13 days, paraffin embedded and sectioned at 5 µm. The 29 biopsies described above were included in an earlier publication describing the PLM-CO score for evaluating collagen organization (Changoor, et al., 2011).

Five additional biopsies, classified as either normal (n=1) or degraded (n=4), were added to this group. The normal biopsy was collected from the centre of a femoral head following femoral neck fracture where cartilage appeared macroscopically normal. The degraded biopsies, similar to those described above, were collected during hip arthroplasties from femoral heads where 3 were collected from the centre of osteoarthritic lesions and one was from a region adjacent to a lesion site (Research Institute of the McGill University Health Centre, Montreal, Quebec, Canada). These specimens were fixed in 10% NBF for a minimum of 30 days, decalcified in 10% EDTA/0.1% (v/v) paraffin for 17.5 hours at 37°C, embedded in paraffin and sectioned at 5 µm.

In total, 34 osteochondral biopsies, including normal (n=6), degraded (n=6), and repair (n=22) cartilages, were investigated using the PLM & SEM techniques for evaluating collagen structure described below. These designations were confirmed using adjacent safranin-O/fast green/iron hematoxylin stained sections (**Figure 6.1**).

Sections were deparaffinized and rehydrated. Sections for PLM analysis were mounted unstained in Permount (Fisher Scientific, Hampton, New Hampshire, USA). Adjacent sections for SEM analyses were post-fixed in a 2% glutaraldehyde/0.1M sodium cacodylate solution for 10 minutes and then rinsed and stored in distilled water for a minimum of 10 minutes prior to being transferred to an adhesive carbon tab mounted on an aluminum sample stub (Cedarlane Laboratories Ltd., Burlington, ON, Canada). A thin, uniform layer of gold was applied to the section using an Agar Manual Sputter Coater (Marivac Inc., Montréal, QC, Canada) and SEM images were obtained in conventional high-vacuum mode on a Quanta FEG 200 ESEM (FEI Company, Hillsboro, Oregon) with images captured at 20 kV and a working distance of 5 mm.

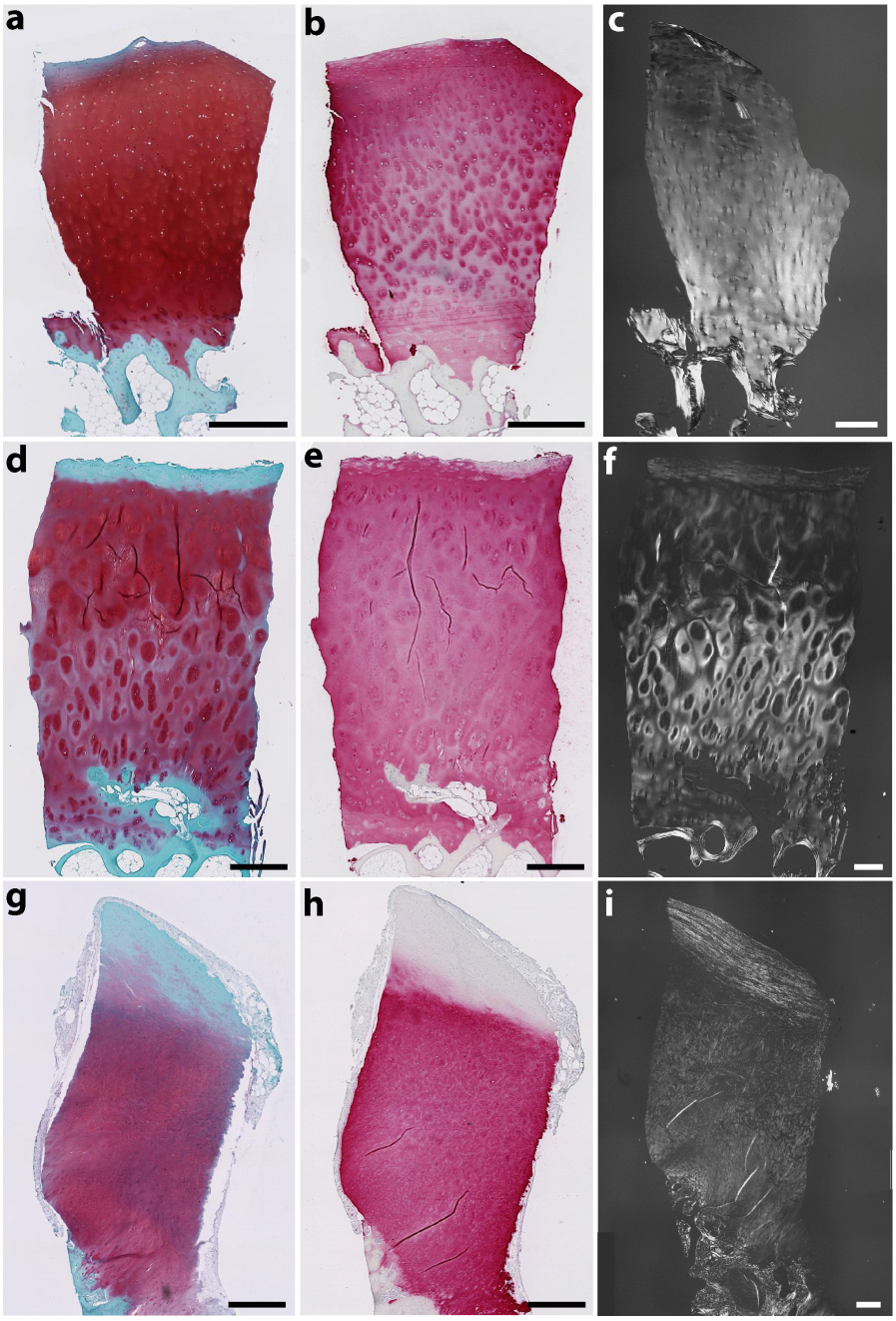

Figure 6.1: Histological images for (a-c) normal (PLM score=3.33, SEM CO score=4.70) and (d-f) degraded (PLM score=3.33, SEM CO score=2.93) samples. An example of high quality repair cartilage (g-h) that received a PLM-CO score of 3.00 and SEM-CO score of 4.72. Images are from consecutive sections with Safranin-O/Fast Green (a, d, g), collagen type II (b, e, h) or polarized light (c, f, i).

6.3.2 PLM Analyses

Collagen organization was evaluated using the PLM-CO score (**Table 6.1**), consisting of a 0-5 ordinal scale that rates the extent that collagen organization resembles the zonal structure observed in young adult hyaline articular cartilage (score of 5) versus a completely disorganized collagen architecture (score of 0) (Changoor, et al., 2011). Scoring was performed independently by three trained readers at a polarization light microscope, whose scores were averaged. PLM-CO scores for a subset of these samples, [normal (n=4), degraded (n=2) and repair (n=4)] were previously reported (Changoor, et al., 2011).

PLM collagen orientation was labelled (PLM-OL) in each region of interest (ROI) as either vertical, horizontal, oblique, multiple, or non-oriented (**Table 6.1** & **Table 6.2**, **Figure 6.2**). ROIs were defined as either a single zone (superficial, transitional, deep), or an area of birefringent or non-birefringent tissue. PLM-OL was identified by viewing the section at the microscope and turning it with respect to the fixed crossed polarizers. Orientation was referenced to the subchondral bone-cartilage interface.

Thicknesses and areas of each ROI and total non-calcified tissue were measured on digital PLM images using a customized Bioquant template (Bioquant Osteo II for Windows XP v8.0, 40.20 MSR, Nashville Tennessee, USA). PLM images were captured with a CCD Camera (Hitachi HV-F22 Progressive Scan Colour 3-CCD) mounted on the microscope. Image processing included extracting the green plane from the original RGB image, equalizing to improve contrast, and deconvoluting to sharpen edges (Northern Eclipse v7.0, Empix Imaging Inc., Mississauga, ON, Canada).

Table 6.1: Summary of outcomes obtained with PLM and SEM methods. ROIs are defined as either a single zone (superficial, transitional, deep), or an area of birefringent or non-birefringent tissue.

Score	Description	Measurement	Scale
PLM-CO	Qualitative assessment of overall collagen organization using a published PLM score (Changoor 2011)	View unstained 5µm sections at the microscope in linear polarized light	Ordinal : 0-5 Average calculated from scores of 3 readers. Complete scoring criteria describe in (Changoor 2011).
PLM-OL	Predominant orientation in each ROI identified	View unstained 5µm sections at the microscope in linear polarized light	1 of 5 orientation labels (Table 6, **Figure 6.2**).
SEM-CO	Observed orientation compared to that expected based on the zone where the image was taken	High-magnification SEM images are scored individually	Ordinal : 0-2 (**Table 6.3**)
Cumulative SEM-CO	SEM–CO scores averaged for each zone, then the averages summed over 3 zones	Mathematically	Continuous score: 0-6
SEM-OL	Predominant orientation observed in each SEM image	High-magnification SEM images are labelled individually.	1 of 5 orientation labels (**Figure 6.4**)
PLM-OL/ SEM-OL Correspondence	Correspondence between orientations observed in PLM and SEM	For each ROI, PLM-OL is compared to the panel of SEM images labelled with SEM-OL	Ordinal : 0-2 2=SEM/PLM agreement 1=partial agreement 0=no agreement
Zone proportions	Measurements of zone thickness and total thickness of non-calcified tissue	PLM images measured using software (Bioquant Osteo II)	Zonal percentages as a proportion of total non-calcified thickness
Fibre diameters	Measurements of fibre diameters	An average of 12±3 fibres measured in each high-magnification SEM image using software (XT-Docu)	Histograms of fibre diameters by zone

Table 6.2: Labels used to describe collagen orientation observed in PLM (PLM-OL). Orientations are described with respect to the subchondral bone interface and are illustrated in **Figure 6.2**. The orientation of each ROI was assessed by each of three readers who viewed mounted unstained sections at the linear polarized light microscope.

Orientation	Definition
Vertical	Predominant fibre orientation is perpendicular to the subchondral bone interface within ±30°.
Horizontal	Predominant fibre orientation is parallel to the subchondral bone interface within ±30°.
Oblique	Oriented tissue that is angled greater than ±30° from the vertical or horizontal axes.
Multiple	Orientation that is mixed, with either several orientations present, or oriented and non-oriented tissue present in the same ROI.
Non-oriented	Fibres that are predominantly non-birefringent.

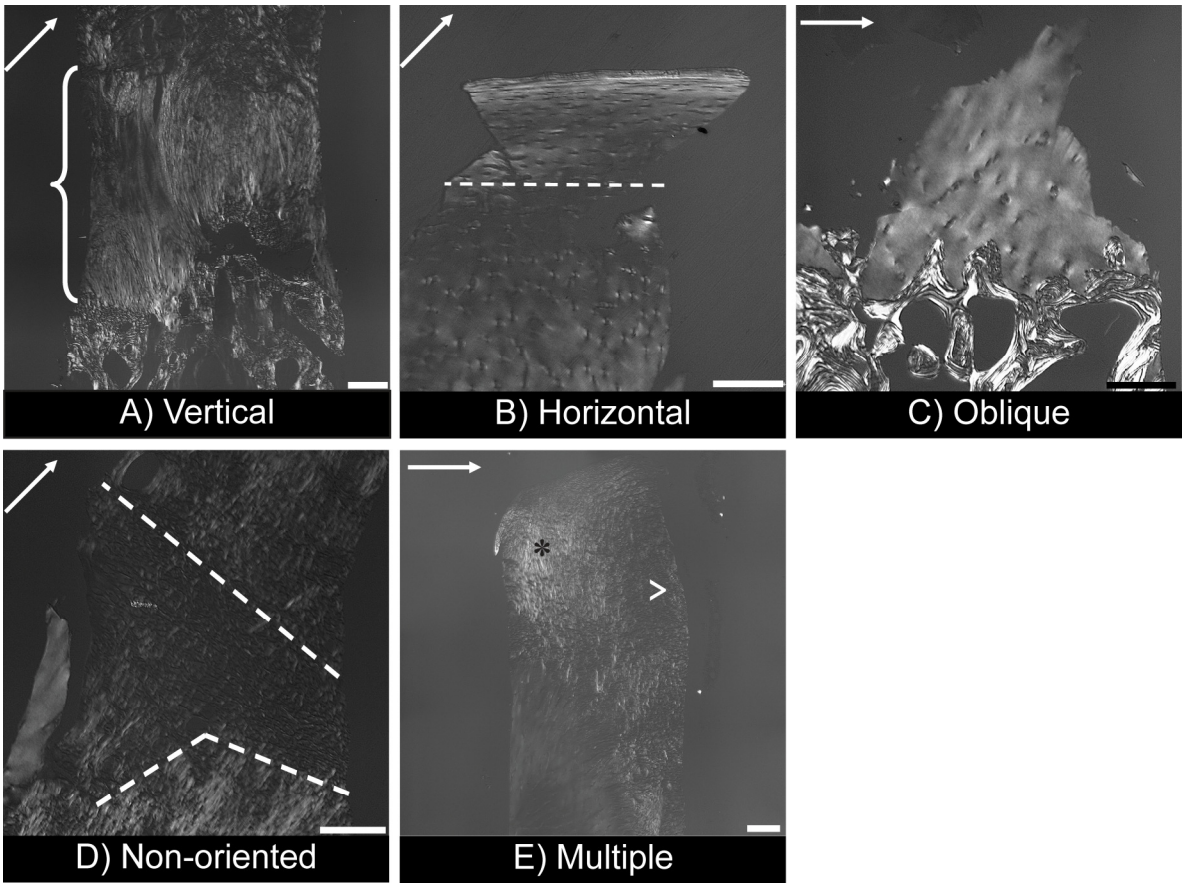

Figure 6.2: Reference PLM images illustrating collagen fibre orientations used to assign collagen orientation labels (PLM-OL). Arrows indicate the direction of the section with respect to the analyzer filter, where sections in A, B & D were at 45° and sections in C & E were at 90°. (A) Vertically oriented tissue, identified by the bracket, is perpendicular to the subchondral bone visible at the bottom of the image. (B) Horizontally oriented tissue is present above the dotted line. (C) Oblique cartilage emanating from subchondral bone. It becomes birefringent only at 90° indicating that fibres are at approximately 45° to the subchondral bone interface. (D) Non-oriented tissue is illustrated in the region bounded by dotted lines. Birefringent tissue can be observed at the bottom of the image. (E) An example of a region with multiple orientations, where the (*) indicates birefringent, predominantly vertically oriented tissue and the (>) indicates non-oriented tissue. Scale bars are 250 µm.

6.3.3 SEM Analyses

Low magnification (80x) SEM images were annotated with ROIs observed in PLM and sites for high magnification imaging were identified (**Figure 6.3**). These sites were placed at regular intervals over the ROI to ensure systematic sampling of collagen orientation. High magnification images (80,000x), averaging 16±6 images per sample, were captured at each pre-defined site and used to determine collagen orientation (SEM-OL), an overall collagen organization (Cumulative SEM-CO) score, and to measure fibre diameters (**Table 6.1**). These outcome measures were developed and tested during separate unpublished validation studies, which were approved by an independent quality assurance unit.

SEM collagen orientation labels (SEM-OL) describe the predominant orientation in each image (**Figure 6.4**). To assess whether the collection of SEM images captured for each ROI reflected the global orientation observed in PLM, the SEM-OL labels were compared to PLM-OL. A correspondence score, from 0 to 2 was assigned, where a score of 2 signified that SEM confirmed the orientation identified by PLM, 0 signified that it did not, and a score of 1 was intermediate. A correspondence score of 2 was assigned when SEM-OL matched PLM-OL in more than two-thirds of SEM images, a score of 1 if this criteria was satisfied by one-third to two-thirds of images, and a score of 0 when less than one-third of SEM images agreed with PLM. For example, in a panel of 9 SEM images, a score of 2 applied when at least 7 SEM images matched PLM, a score of 1 when 4-6 images reflected PLM, and a score of 0 if less than 3 agreed with PLM.

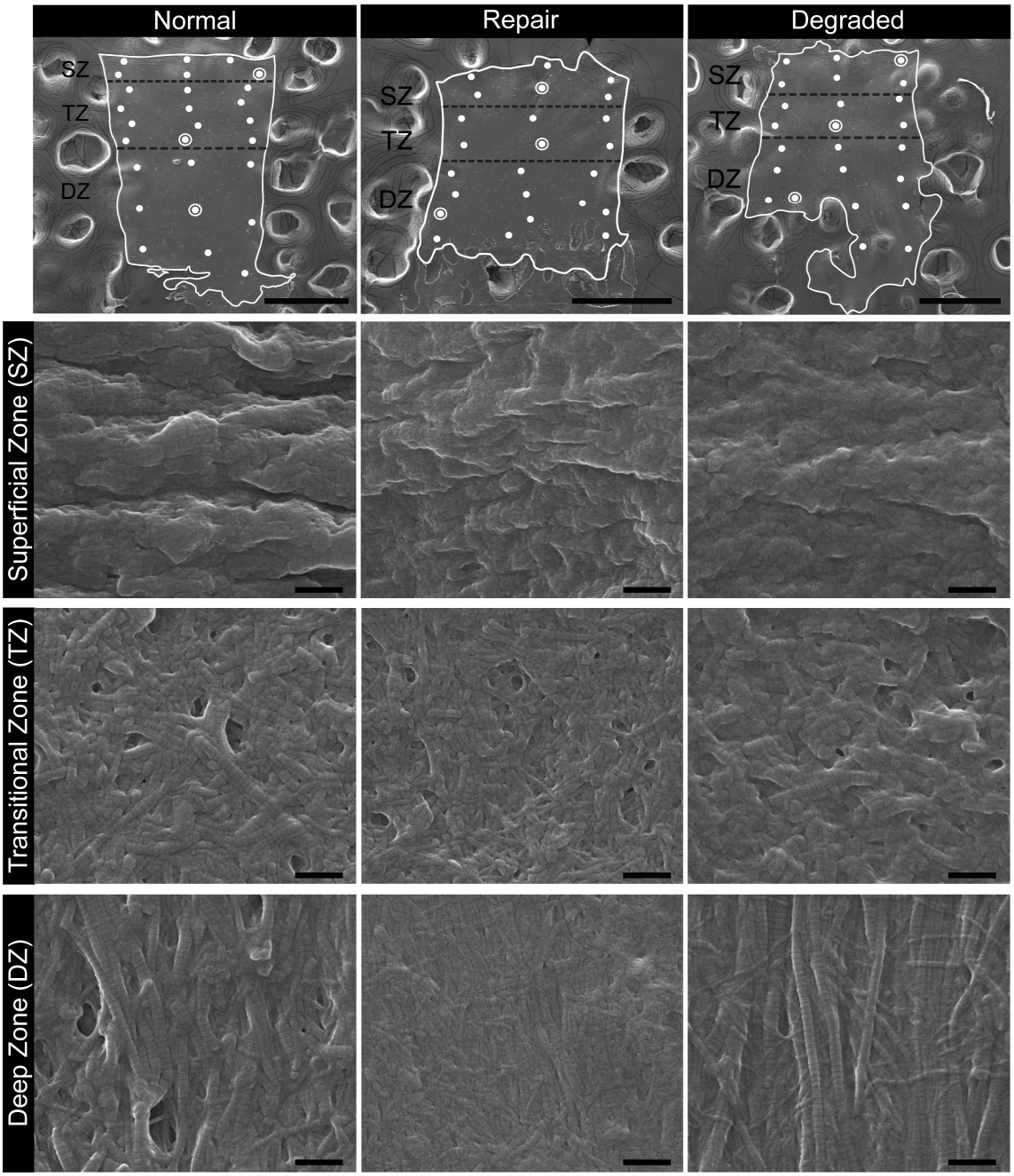

Figure 6.3: Examples of SEM images for normal, repair and degraded cartilages from the superficial, transitional and deep zones. The top row contains the low magnification SEM images (scale bars are 500 µm) with the non-calcified tissue outlined in white and surrounded by carbon substrate. Zones are identified (SZ, TZ, DZ), as well as the sites where high magnification images were captured (•). Subsequent rows contain one high magnification image per zone per cartilage

type and the location from which each image was captured is identified by (⊙) on the corresponding low magnification image. Scale bars are 500 nm for all high magnification images.

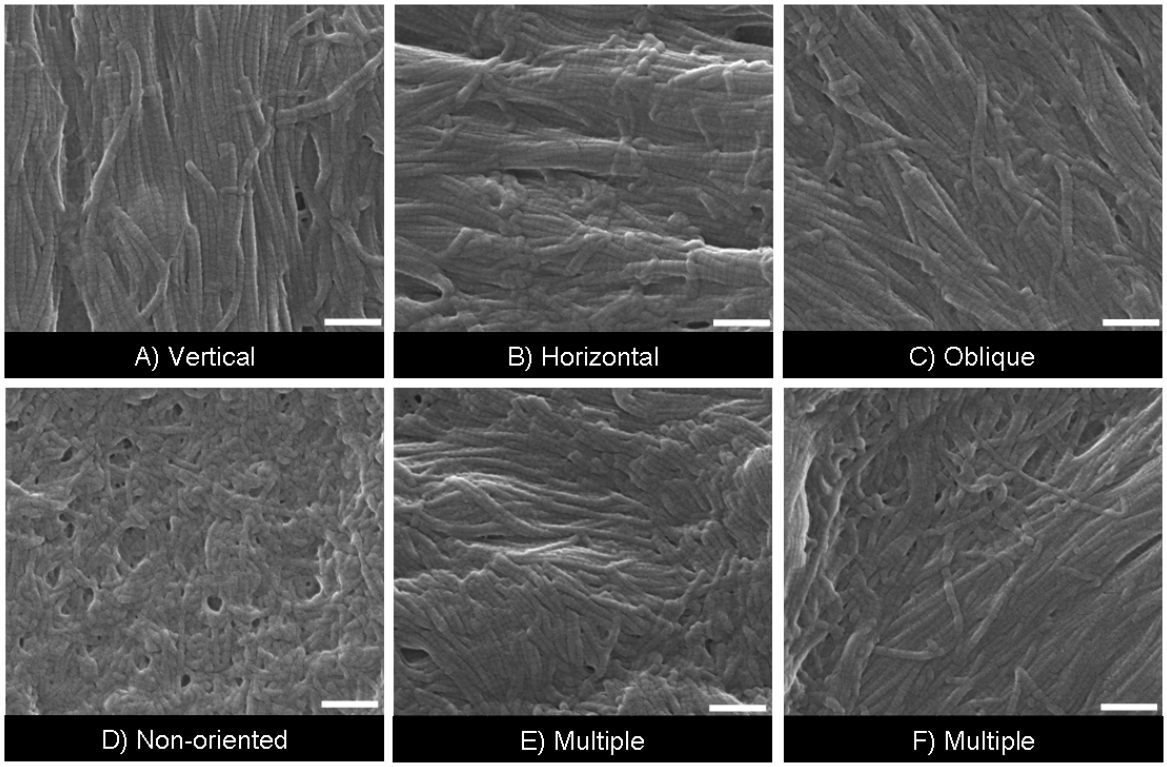

Figure 6.4: Reference SEM images illustrating the collagen fibre orientations used to assign collagen orientation labels (SEM-OL). The orientation labels Vertical (A), Horizontal (B), and Oblique (C), with reference to the horizontal cartilage-bone interface, were assigned if the majority of fibres were predominantly in one of these directions. Non-oriented was used to label images where no predominant orientation existed (D). Multiple indicated that either tissue of several different orientations were present (E) or that oriented and non-oriented tissue were present in the same images (F). Scale bars are 500 nm.

The SEM collagen organization (Cumulative SEM-CO) score was used to gauge the extent that overall collagen organization in a given sample resembled that of hyaline cartilage; an assessment analogous to the PLM-CO score (Changoor, et al., 2011). First, each ROI identified in PLM (**Figure 6.3**), was assigned to either SZ, TZ or DZ based mainly on its location within the sample. For example, an ROI adjacent to subchondral bone was assigned to the DZ, while an ROI at the articulating surface was assigned to the SZ. The orientation in each SEM image was then scored (SEM-CO) based on the orientation expected for that particular zone on an ordinal scale of 0-2 (**Table 6.3**). Appropriate orientation scored a 2 while inappropriate orientation scored a 0, with 1 being intermediate. Scoring was performed independently by three trained readers, and then averaged for each zone, and finally averaged scores were summed to produce a single Cumulative SEM-CO score per sample. Reader training involved a demonstration of how to assign orientations and SEM-CO scores by comparing against a bank of example images.

Table 6.3: The SEM collagen organization (SEM-CO) score for individual images. SEM-CO scores assess whether the orientation observed in an individual SEM image reflects the orientation expected for the zone from which it originated. The SEM-CO were averaged per zone and added to produce a Cumulative SEM-CO score reflecting overall collagen organization.

SEM-CO score	Superficial Zone	Transitional Zone	Deep Zone
2	Horizontal (±30°) orientation or smooth lamellar structure (**Figure 6.3**)	Non-oriented, or multiple orientations present.	Vertical (±30°) orientation
1	Partially horizontal with other orientations present	Oriented tissue that is neither horizontal nor vertical.	Partially vertical with other orientations present
0	Disorganized, vertical or multiple orientations	Vertical or horizontal orientation	Disorganized, horizontal or multiple orientations

Collagen fibre diameters were measured using XT Docu v.3.2 (Soft Imaging System GmbH, FEI Company, Hillsboro, OR). Calibration was performed from 10x to 200,000x magnifications with NIST-traceable MRS-4 patterns (Geller Microanalytical Laboratory, Boston,

MA). An average of 12±3 fibres were measured per image with an average of 16±6 images collected per sample.

6.3.4 Statistical Analysis

Coefficients of determination (R^2) and correlation coefficients (r) between the PLM-CO and SEM-CO scores were calculated. Outliers, defined as residuals greater than 2 standard deviations, were removed depending on Cook's distances, which evaluate the influence of individual data points on the regression model, and upon close examination of the data (Chatterjee & Hadi, 2006). Sensitivity testing was performed by running an equivalent non-parametric test, the Spearman rank order correlation, for comparison. Zonal distributions of fibre diameter measurements were examined using histograms. Analyses were performed in Statistica v.9 (StatSoft Inc., Tulsa, OK).

6.4 Results

6.4.1 SEM confirms collagen orientation observed in PLM

SEM-OL verified that global fibre orientations observed in PLM reflected collagen ultrastructure. SEM-OL/PLM-OL correspondence was confirmed in 91.6% of ROIs (76 of 83 ROIs) assessed from 28 biopsies, which received scores of 1 or 2. The remaining 8.4% (7 ROIs) received scores of 0, reflecting disagreement between PLM and SEM, and consisted mainly of regions described in PLM as having multiple orientations. The restricted field of view of the high-magnification SEM images, where one 80,000x image covers a 3.42 x 2.96 μm^2 area, did not always capture global orientation in regions where mixtures of oriented and non-oriented tissue were present.

6.4.2 PLM-CO and SEM-CO scores are moderately correlated

The Cumulative SEM-CO score was linearly correlated to the average PLM-CO score, r=0.681 (p=0.00001, R^2=0.463, n=34), and two outliers were identified with residuals greater

than two standard deviations and large Cook's distances compared to the other data points, indicating a greater than average influence on the regression model. Exclusion of these outliers improved the correlation to r=0.786 ($p<0.00001$, $R^2=0.618$, n=32) (**Figure 6.5**). Both outliers were repair cartilage with irregular tissue characteristics. The first (**Figure 6.5**, outlier A) was unusual because mixed mesenchymal tissue encroached on one side of the biopsy and occupied greater than 50% of the sample width, such that while a vertically oriented DZ was present it was small and deemed inadequate for anchoring the repair tissue to subchondral bone, resulting in a PLM-CO score of 0.33. The elevated SEM-CO score arose from the inclusion of additional zones present near the top of the sample, which are not considered in the PLM-CO score when a sufficient DZ is lacking. The second outlier (**Figure 6.5**, outlier B) was fragmented with part of the repair cartilage tissue completely separated. It received a PLM-CO score of 2.00 because the DZ occupied the full thickness of the portion of tissue attached to subchondral bone. The SEM-CO score was comparatively low due to orientation deviating from vertical, which may be attributed to the fragmented nature of this sample. After outlier removal, a moderate correlation was detected, demonstrating an internal consistency between the PLM-CO and SEM-CO methods for evaluating collagen organization.

Results obtained from an equivalent non-parametric test, the Spearman rank order correlation, were concurrent with parametric testing. Significant ($p<0.05$) correlations between PLM-CO and Cumulative SEM-CO were detected, where r=0.527 (n=34) and r=0.617 (n=32), when outliers were removed.

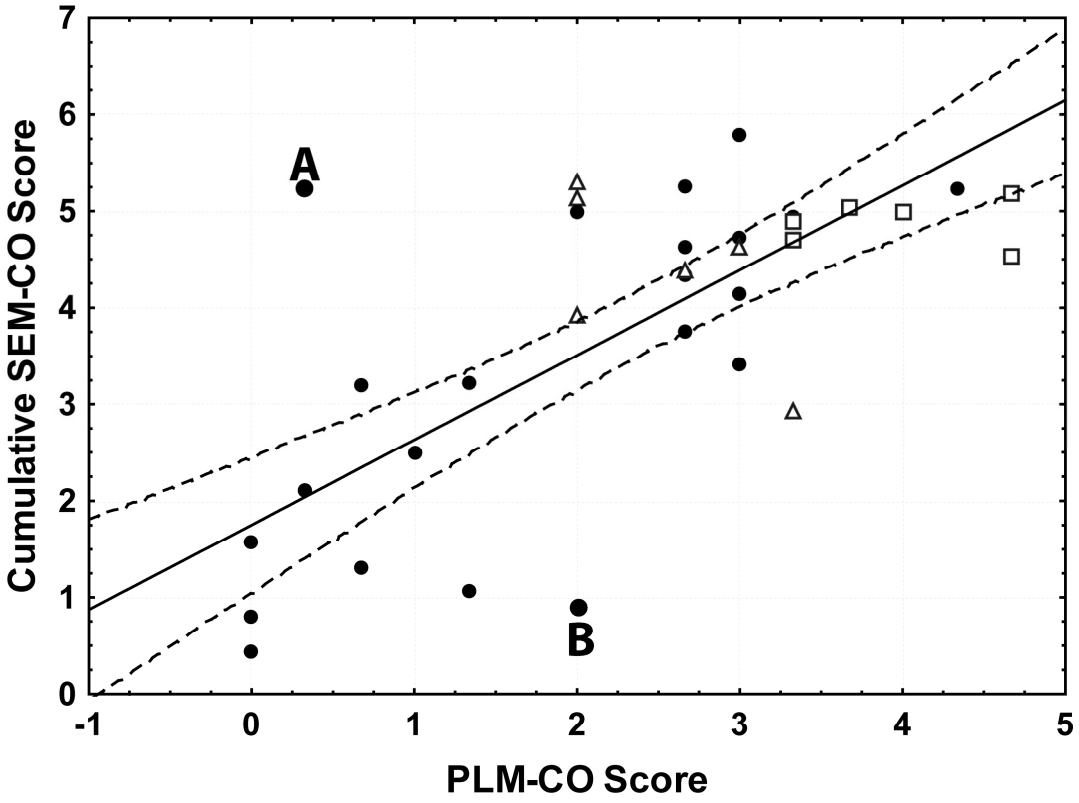

Figure 6.5: Scatterplot of the Cumulative SEM-CO score vs. PLM-CO score with linear regression and 95% confidence intervals for the dataset with two outliers removed (n=32). Outliers are superimposed on the scatterplot and identified as A & B. Data points are normal cartilage (□), degraded cartilage (△), or repair (•).

6.4.3 Zonal proportions

Normal cartilage biopsies (n=6), consisting of 5 from central MFCs and 1 from the central region of a femoral head, had zonal proportions ranging from 58-87% (74.0±11.4%, average ± standard deviation) in the DZ, 8-31% (18.6±8.7%) in the TZ, and 5-10% (7.3±1.5%) in the SZ.

Zonal proportions were altered in degraded cartilage where the DZ, TZ, and SZ occupied 33-59% (45.6±11.0%, n=4), 36-59% (47.2±10.4%, n=4), and 5-17% (9.5±4.3%, n=6), respectively. Three degraded biopsies originated from osteoarthritic lesions in the hip and 3 from MFCs. In 2 of 6 samples, no distinction could be made between the transitional and deep zones

(Bi, et al., 2005) and thus they were measured together. Both had predominantly vertical orientation in PLM, although non–uniform, with darkened areas indicating pericellular degradation (**Figure 6.1**).

The variable organization of the repair cartilage tissues prevented representative zonal proportions from being calculated for this group as a whole.

6.4.4 Collagen fibre diameters

Histograms of collagen fibre diameters illustrate characteristics related to tissue type (**Figure 6.6**, **Table 6.4**). In normal cartilage, a pattern of increasing diameters with depth from the articular surface was observed. Fibres in repair cartilage were smaller in diameter on average with narrower ranges in the TZ and DZ. Diameters in degraded cartilage exhibited a wider range compared to either normal or repair. Evidence of a bimodal distribution was present in 3 of 6 degraded samples, where the smaller population of fibres may result from remodelling processes. Fibre diameters could not always be measured in the SZ due to inadequate spatial resolution at 80,000× and the fragility of these thin sections to electron beam exposure at higher resolutions.

Table 6.4: Summary of fibre diameter measurements for 6 normal, 6 degraded, and 22 repair biopsies. Numbers are reported as average (AVG), standard deviation (SD), minimum (MIN), maximum (MAX), and total number of fibres (n) measured per zone.

	Superficial Zone (nm)				Transitional Zone (nm)				Deep Zone (nm)			
	AVG ± SD	MIN	MAX	n	AVG ± SD	MIN	MAX	n	AVG ± SD	MIN	MAX	n
Normal	55.8 ± 15.9	38.6	94.4	11	87.5 ± 17.9	42.9	145.6	400	108.2 ± 21.4	44.0	170.8	577
Degraded	--	--	--	--	83.9 ± 21.4	31.3	149.1	471	96.7 ± 26.3	28.2	204.6	548
Repair	60.4 ± 9.3	35.1	105.7	696	63.2 ± 12.8	22.1	117.1	1774	67.2 ± 16.8	23.1	131.5	1843

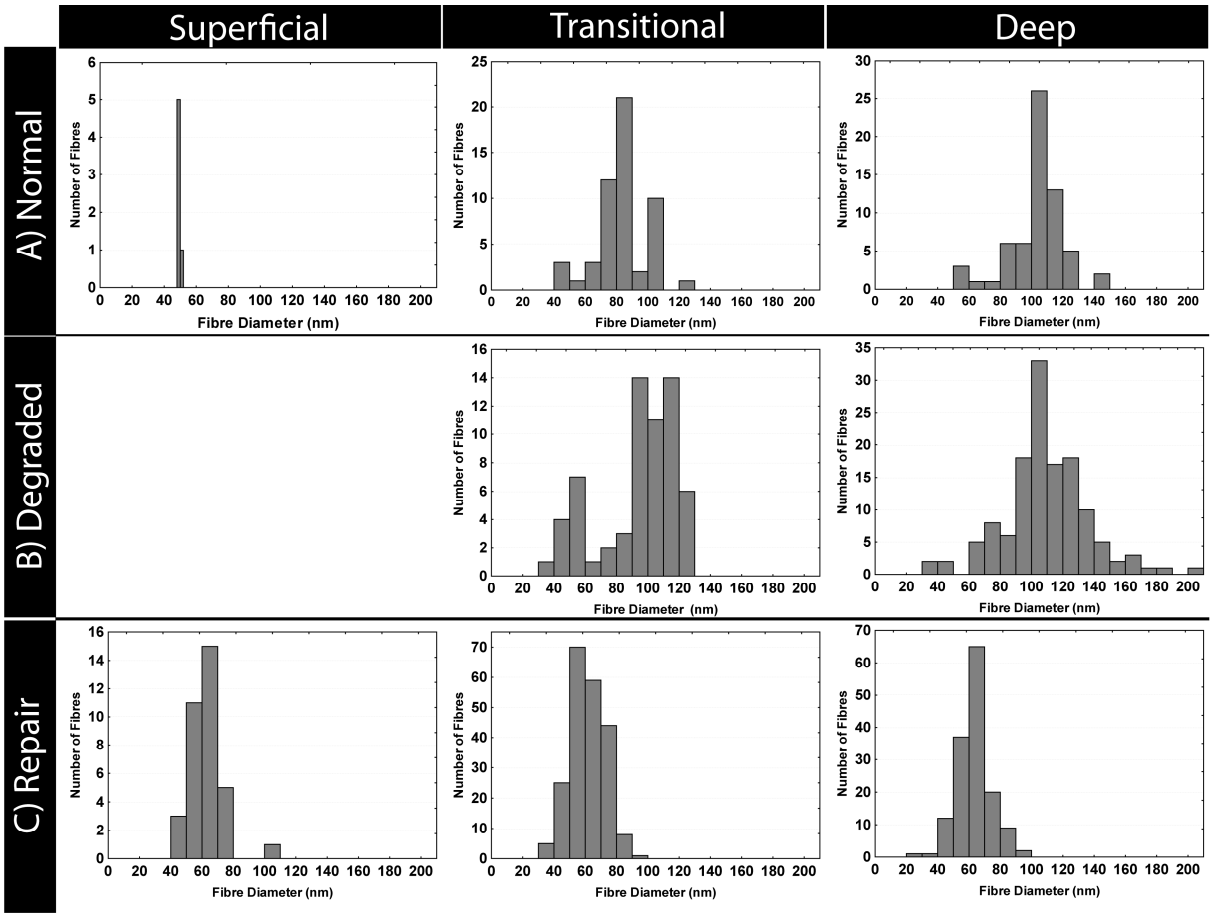

Figure 6.6: Representative histograms of collagen fibre diameters from normal (a-c), degraded (d-e) and repair (f-h) cartilage tissues. (a, f) are from superficial zones, (b, d, g) from transitional zones, and (c,e,h) from deep zones.

6.5 Discussion

In this study, PLM and SEM methods were used to characterize structural features of the collagen network in normal, degraded and repair cartilages. Both hypotheses, that PLM and SEM methods for assessing overall collagen network organization would be highly correlated, and that tissue types exhibit different zonal proportions and fibril diameter profiles, were supported by the data.

6.5.1 Validation of the PLM-CO score using SEM

The qualitative PLM-CO and SEM-CO scores evaluate overall collagen organization at different length scales. These analogous scores were correlated (r=0.786) (**Figure 6.5**). Minor discrepancies between the two methods were mainly associated with the highly localized nature of the SEM images. In principle, either method is appropriate for assessing collagen organization, however, while SEM is a powerful tool for observing ultrastructural details in biological samples at a submicrometric level, it requires specialized equipment and sample preparation methods, and is labour intensive. In contrast, PLM can be performed on routine unstained histological sections, and can be examined promptly on a light microscope equipped with polarization filters.

PLM relies on inferences about orientation based on the optical properties of fibrillar collagen and does not directly identify collagen fibres. We found a high correspondence between PLM-OL and SEM-OL methods (91.6%) establishing that the global orientations observed in PLM reflected the actual orientation of collagen fibres as described previously (Hughes, et al., 2005; Kaab, et al., 1998; Speer & Dahners, 1979). Thus, the PLM score could reasonably be incorporated into routine histological assessment of repair cartilages to provide an assessment of collagen organization, a critical feature that is likely indicative of long term durability and cartilage biomechanical properties, without adding significantly to study costs.

6.5.2 Features of Normal Articular Cartilage

Normal articular cartilage received PLM-CO scores from 3-5 (maximum 5) accompanied by cumulative SEM-CO scores greater than 4 (maximum 6) (**Figure 6.5**). PLM observations revealed a smooth texture with visible cell lacunae (Changoor, et al., 2011) (**Figure 6.1**) and SEM images reflected expected zonal orientations (**Figure 6.3**).

Proportions of total thickness averaged 74%, 19% and 7% for the DZ, TZ and SZ respectively. These values were similar to the approximate percentages of 63% (DZ), 26% (TZ) and 9% (SZ) reported by Kurkijarvi et al. (2008), and coincide with the ranges of 75.4±11.4% (DZ), 19.5±10.1% (TZ), and 5.2±2.2% (SZ) reported by Nissi et al. (2006).

Similarly, the pattern of fibre diameters increasing with depth from the articular surface (**Figure 6.6**) is consistent with previous reports in human (Hwang et al., 1992; Redler, 1974; Weiss, Rosenberg, & Helfet, 1968) and animal cartilages (Arokoski, et al., 1996; Clarke, 1971; Hedlund, et al., 1993; Langsjo, et al., 2010). Absolute diameters of collagen are more difficult to compare because they vary with anatomical location and the measurement technique used. For example, variability between studies using SEM may be associated with the thickness of the required conductive surface coating. Redler (1974) reported a 30 nm coating compared to the 1.3 nm gold layer estimated in this study.

6.5.3 Features of Degraded Articular Cartilage

PLM-CO scores were generally between 2 and 3 in degraded cartilage and all samples had a patchy texture, observed as a loss of birefringence pericellularly, and decreased Safranin-O staining in the interterritorial matrix (**Figure 6.1**). In 5 of 6 degraded biopsies, SEM-CO scores were higher than what might be expected based on the regression line (**Figure 6.5**). Zonal proportions were altered compared to normal, often with the DZ reduced and the TZ increased in size. However, the SZ proportion was similar to normal, approximately 9.5%, and mild to extensive surface roughening was present in some samples.

These features observed for degraded cartilage can be attributed to extracellular matrix alterations associated with early osteoarthritis, where enzymatic degradation mediated by chondrocytes leads to a disordered, non-birefringent, fibrillar collagen architecture in the pericellular matrix (Dodge & Poole, 1989; Hollander et al., 1995; Poole, 1997; Silver, Bradica, & Tria, 2001). Decreased crosslinking or interconnectedness in the interterritorial matrix reduces proteoglycan retention, resulting in decreased Safranin-O staining, although fibrils generally remain radially oriented (**Figure 6.3**; Chen & Broom, 1998). Proteoglycan depletion, commonly detected in softened and degraded cartilage, may have enhanced the appearance of collagen fibres in SEM, resulting in higher SEM-CO scores (**Figure 6.3** & **Figure 6.5**).

The bimodal distribution of collagen fibril diameters (**Figure 6.6**) and the larger range of diameters present in degraded cartilage compared to normal have not been previously reported, although the general ultrastructure of osteoarthritic cartilage has been described (Clark & Simonian, 1997; Hwang, et al., 1992; Redler, 1974; Weiss, et al., 1968). The novel observation of a population of smaller fibres suggests that remodelling processes are occurring. While the turnover rate in healthy adult cartilage is extremely low (Bank, et al., 1998; Eyre, 2002), chondrocytes in injured cartilage can increase synthesis of extracellular matrix components (Eyre, 2002; Lippiello, Hall, & Mankin, 1977; Nelson et al., 1998). Biomodal distributions of fibre diameters were not always observed likely due to a range of degradative changes.

6.5.4 Features of Repair Cartilage

Repair cartilage demonstrated considerably more variability and complexity with respect to collagen organization (**Figure 6.5**). Several biopsies received PLM-CO scores greater than 3, indicating the ability of certain cartilage repair procedures to produce repair tissue with multi-zonal collagen architecture at one year post-treatment. However, the variable organization observed prevented average zonal proportions for the repair cartilage group from being calculated. This study provides the first ultrastructural evidence of collagen fibres in repair cartilage approximating the stratified organization observed in native articular cartilage.

Our study is the first to report collagen fibre diameters from human repair cartilage. The range of fibre diameters, approximately 25-130 nm, contained a greater number of smaller fibres compared to normal cartilage (**Figure 6.6**). However, evidence of the pattern of larger fibres in the DZ that diminish near the articular surface was detected in 5 out of 11 multi-zonal repair specimens where measurements in 3 zones were obtained. Collagen fibre diameters in repair cartilage produced by autologous chondrocyte transplantation in an immature pig model ranged from 20-80 nm 1 year post-op, with occasional fibres greater than 100 nm (Langsjo, et al., 2010). A similar range was reported in tissue produced in a chondrocyte-polymer construct cultured with calf chondrocytes after 6 weeks under optimized bioreactor conditions (Riesle, et al., 1998). In both of these previous studies, measurements were made throughout the cartilage depth and were

comparable to controls, which were both immature animal models (Langsjo, et al., 2010; Riesle, et al., 1998). Thus, our study is the first to indicate that some cartilage repair procedures may reproduce zone dependent collagen fibre diameters.

The importance of recreating collagen structure in repair cartilage has been acknowledged in recent reviews (Hunziker, 2009; Responte, et al., 2007) primarily because it is recognized to be a critical factor for biomechanical function and durability of articular cartilage. Understanding the natural biological processes that lead to the characteristic anisotropy of mature cartilage is important for achieving this goal (Hunziker, 2009; Hunziker, et al., 2007) as is the ability to evaluate collagen organization in a way that allows comparisons between repair strategies. To date, studies describing collagen organization in cartilage repair, including autologous chondrocyte implantation or microfracture approaches in humans or animals, have employed qualitative PLM to describe general tissue morphology, or to illustrate collagen anchoring repair tissue to subchondral bone, but do not describe detailed characteristics of collagen organization (Bi, et al., 2005; Gooding, et al., 2006; Knutsen, et al., 2004; Richardson, et al., 1999; Roberts, et al., 2001; Roberts, et al., 2003; Roberts, et al., 2009). The recently developed qualitative PLM-CO score (Changoor, et al., 2011), which was validated in the present study, provides a means of systematically assessing collagen organization in repair tissues and could facilitate comparisons between different repair strategies.

6.5.5 Conclusions

Collagen structure was characterized using both PLM and SEM providing important data about this critical cartilage feature that is essential for successful biomechanical function and durability. We found that normal articular cartilage had multi-zonal organization with appropriate proportions, averaging 74%, 19% and 7% in the DZ, TZ & SZ respectively, and fibre diameters averaging 108.2±21.4 nm in the DZ and decreasing to 87.5±17.9 nm and 55.8±15.9 nm in the TZ and SZ respectively. Degraded articular cartilage had altered zonal proportions, approximately 46%, 47% and 10% (DZ, TZ, SZ), loss of pericellular birefringence, and evidence of bimodal fibre diameter distributions indicating remodelling. Repair cartilage biopsies revealed some

cartilage repair procedures are capable of producing stratified collagen architecture that approximates normal articular cartilage, although fibre diameters are thinner than normal at 1-year post-treatment. The PLM-CO score was also validated using systematically-sampled SEM images and offers a simple method for assessing collagen organization that reflects genuine collagen ultrastructure. The PLM-CO score can assist investigators in their efforts towards recreating the specialized collagen network structure of articular cartilage, which is an important endpoint for cartilage repair procedures.

6.6 Acknowledgements

The authors thank Dr. W.D. Stanish (Orthopaedic Surgery Department, Dalhousie University, Halifax, Canada), principal investigator of the multi-centre randomized clinical trial from which repair biopsies were obtained, as well as all of the participating surgeons, Drs. P. MacDonald (Pan Am Clinic, Winnipeg, Canada), N. Mohtadi (Orthopedics, University of Calgary Sports Medicine Center, Calgary, Canada), P. Marks (Sunnybrook Health Sciences Centre, Toronto, Canada), M. Malo (Hôpital du Sacré-Coeur de Montréal, Montreal, Canada), R. McCormack (New West Sports Medicine, Vancouver, Canada), J. Desnoyers (Orthopedic Surgery, Hôpital Charles LeMoyne, Greenfield Park, Canada), S. Pelet (Centre Hospitalier Affilié Universitaire de Québec (CHAUQ), Quebec City, Canada), G. Lopez (FREMAP Centro de Prevención y Rehabilitación, Madrid, Spain), J. Vaquero (Hospital General Universitario Gregorio Marañón, Madrid, Spain), F. Maculé (Hospital Clinic i Provincial de Barcelona, Barcelona, Spain).

Funding provided by the Natural Sciences and Engineering Research Council of Canada (NSERC), BioSyntech Canada Inc., and the Biomedical Science and Technology Research Group/Le Groupe de recherche en sciences et technologies biomédicales (GRSTB).

6.7 References

These are the references as they appear in the submitted version of the article and are in the style required by the journal Osteoarthritis and Cartilage. The references contained within the body of Chapter 6 correspond to the reference list at the end of the thesis.

1. Archer CW, Redman S, Khan I, Bishop J, Richardson K. Enhancing tissue integration in cartilage repair procedures. J Anat 2006;209(4):481-93.

2. Korhonen RK, Wong M, Arokoski J, Lindgren R, Helminen HJ, Hunziker EB, et al. Importance of the superficial tissue layer for the indentation stiffness of articular cartilage. Med Eng Phys 2002;24(2):99-108.

3. Kovach IS, Athanasiou KA. Small-angle HeNe laser light scatter and the compressive modulus of articular cartilage. J Orthop Res 1997;15(3):437-41.

4. Benninghoff A. Form und bau der gelenkknorpel in ihren beziehungen zur funktion. Zeitschrift fur Zellforschung 1925;2:783-862.

5. Hedlund H, Mengarelli-Widholm S, Reinholt FP, Svensson O. Stereologic studies on collagen in bovine articular cartilage. APMIS 1993;101(2):133-40.

6. Hwang WS, Ngo K, Saito K. Silver staining of collagen fibrils in cartilage. Histochem J 1990;22(9):487-90.

7. Schenk RK, Eggli PS, Hunziker EB. Articular cartilage morphology. In: Articular cartilage biochemistry, Kuettner K, Schleyerbach R, Hascall VC, Eds. New York: Raven Press 1986:3-22.

8. Wang F, Ying Z, Duan X, Tan H, Yang B, Guo L, et al. Histomorphometric analysis of adult articular calcified cartilage zone. J Struct Biol 2009;168(3):359-65.

9. Bland YS, Ashhurst DE. Development and ageing of the articular cartilage of the rabbit knee joint: Distribution of the fibrillar collagens. Anat Embryol (Berl) 1996;194(6):607-19.

10. Hunziker EB, Kapfinger E, Geiss J. The structural architecture of adult mammalian articular cartilage evolves by a synchronized process of tissue resorption and neoformation during postnatal development. Osteoarthritis Cartilage 2007;15(4):403-13.

11. Julkunen P, Harjula T, Iivarinen J, Marjanen J, Seppanen K, Narhi T, et al. Biomechanical, biochemical and structural correlations in immature and mature rabbit articular cartilage. Osteoarthritis Cartilage 2009;17(12):1628-38.

12. van Turnhout MC, Schipper H, Engel B, Buist W, Kranenbarg S, van Leeuwen JL. Postnatal development of collagen structure in ovine articular cartilage. BMC Dev Biol 2010;10:62.

13. Bank RA, Bayliss MT, Lafeber FP, Maroudas A, Tekoppele JM. Ageing and zonal variation in post-translational modification of collagen in normal human articular cartilage. The age-related increase in non-enzymatic glycation affects biomechanical properties of cartilage. Biochem J 1998;330 (Pt 1):345-51.

14. Eyre D. Collagen of articular cartilage. Arthritis Res 2002;4(1):30-5.

15. Crawford DC, Heveran CM, Cannon WD, Jr., Foo LF, Potter HG. An autologous cartilage tissue implant neocart for treatment of grade III chondral injury to the distal femur: Prospective clinical safety trial at 2 years. Am J Sports Med 2009;37(7):1334-43.

16. Kon E, Delcogliano M, Filardo G, Fini M, Giavaresi G, Francioli S, et al. Orderly osteochondral regeneration in a sheep model using a novel nano-composite multilayered biomaterial. J Orthop Res 2010;28(1):116-24.

17. Brittberg M, Lindahl A, Nilsson A, Ohlsson C, Isaksson O, Peterson L. Treatment of deep cartilage defects in the knee with autologous chondrocyte transplantation. N Engl J Med 1994;331(14):889-95.

18. Saris DB, Vanlauwe J, Victor J, Haspl M, Bohnsack M, Fortems Y, et al. Characterized chondrocyte implantation results in better structural repair when treating symptomatic cartilage defects of the knee in a randomized controlled trial versus microfracture. Am J Sports Med 2008;36(2):235-46.

19. Hoemann C, Hurtig M, Rossomacha E, Sun J, Chevrier A, Shive MS, et al. Chitosan-glycerol phosphate/blood implants improve hyaline cartilage repair in ovine microfracture defects. J Bone Joint Surg Am 2005;87(12):2671-86.

20. Shive MS, Hoemann CD, Restrepo A, Hurtig MB, Duval N, Ranger P, et al. BST-CarGel: In situ chondroinduction for cartilage repair. Operative Techniques in Orthopaedics 2006;16:271-8.

21. Gudas R, Kalesinskas RJ, Kimtys V, Stankevicius E, Toliusis V, Bernotavicius G, et al. A prospective randomized clinical study of mosaic osteochondral autologous transplantation versus microfracture for the treatment of osteochondral defects in the knee joint in young athletes. Arthroscopy 2005;21(9):1066-75.

22. Mithoefer K, McAdams T, Williams RJ, Kreuz PC, Mandelbaum BR. Clinical efficacy of the microfracture technique for articular cartilage repair in the knee: An evidence-based systematic analysis. Am J Sports Med 2009;37(10):2053-63.

23. Hunziker EB. The elusive path to cartilage regeneration. Adv Mater 2009;21(32-33):3419-24.

24. Responte DJ, Natoli RM, Athanasiou KA. Collagens of articular cartilage: Structure, function, and importance in tissue engineering. Crit Rev Biomed Eng 2007;35(5):363-411.

25. Clark JM, Simonian PT. Scanning electron microscopy of "fibrillated" and "malacic" human articular cartilage: Technical considerations. Microsc Res Tech 1997;37(4):299-313.

26. Minns RJ, Steven FS. The collagen fibril organization in human articular cartilage. J Anat 1977;123(Pt 2):437-57.

27. Redler I. A scanning electron microscopic study of human normal and osteoarthritic articular cartilage. Clin Orthop Relat Res 1974(103):262-8.

28. Bi X, Li G, Doty SB, Camacho NP. A novel method for determination of collagen orientation in cartilage by fourier transform infrared imaging spectroscopy (FT-IRIS). Osteoarthritis Cartilage 2005;13(12):1050-8.

29. Gooding CR, Bartlett W, Bentley G, Skinner JA, Carrington R, Flanagan A. A prospective, randomised study comparing two techniques of autologous chondrocyte implantation for osteochondral defects in the knee: Periosteum covered versus type I/III collagen covered. Knee 2006;13(3):203-10.

30. Richardson JB, Caterson B, Evans EH, Ashton BA, Roberts S. Repair of human articular cartilage after implantation of autologous chondrocytes. J Bone Joint Surg Br 1999;81(6):1064-8.

31. Vasara AI, Hyttinen MM, Pulliainen O, Lammi MJ, Jurvelin JS, Peterson L, et al. Immature porcine knee cartilage lesions show good healing with or without autologous chondrocyte transplantation. Osteoarthritis Cartilage 2006;14(10):1066-74.

32. Elder BD, Athanasiou KA. Effects of confinement on the mechanical properties of self-assembled articular cartilage constructs in the direction orthogonal to the confinement surface. J Orthop Res 2008;26(2):238-46.

33. Kelly TA, Ng KW, Wang CC, Ateshian GA, Hung CT. Spatial and temporal development of chondrocyte-seeded agarose constructs in free-swelling and dynamically loaded cultures. J Biomech 2006;39(8):1489-97.

34. Riesle J, Hollander AP, Langer R, Freed LE, Vunjak-Novakovic G. Collagen in tissue-engineered cartilage: Types, structure, and crosslinks. J Cell Biochem 1998;71(3):313-27.

35. Langsjo TK, Vasara AI, Hyttinen MM, Lammi MJ, Kaukinen A, Helminen HJ, et al. Quantitative analysis of collagen network structure and fibril dimensions in cartilage repair with autologous chondrocyte transplantation. Cells Tissues Organs 2010;192(6):351-60.

36. Changoor A, Tran-Khanh N, Methot S, Garon M, Hurtig MB, Shive MS, et al. A polarized light microscopy method for accurate and reliable grading of collagen organization in cartilage repair. Osteoarthritis Cartilage 2010;19(1):126-35.

37. Modis L. Physical backgrounds of polarization microscopy. In: Organization of the extracellular matrix: A polarization microscopic approach, Modis L, Ed. Boca Raton: CRC Press 1991:9-30.

38. Arokoski JP, Hyttinen MM, Lapvetelainen T, Takacs P, Kosztaczky B, Modis L, et al. Decreased birefringence of the superficial zone collagen network in the canine knee (stifle) articular cartilage after long distance running training, detected by quantitative polarised light microscopy. Ann Rheum Dis 1996;55(4):253-64.

39. Hughes LC, Archer CW, ap Gwynn I. The ultrastructure of mouse articular cartilage: Collagen orientation and implications for tissue functionality. A polarised light and scanning electron microscope study and review. Eur Cell Mater 2005;9:68-84.

40. Kaab MJ, Gwynn IA, Notzli HP. Collagen fibre arrangement in the tibial plateau articular cartilage of man and other mammalian species. J Anat 1998;193 (Pt 1):23-34.

41. Kiraly K, Hyttinen MM, Lapvetelainen T, Elo M, Kiviranta I, Dobai J, et al. Specimen preparation and quantification of collagen birefringence in unstained sections of articular cartilage using image analysis and polarizing light microscopy. Histochem J 1997;29(4):317-27.

42. Rieppo J, Toyras J, Nieminen MT, Kovanen V, Hyttinen MM, Korhonen RK, et al. Structure-function relationships in enzymatically modified articular cartilage. Cells Tissues Organs 2003;175(3):121-32.

43. Speer DP, Dahners L. The collagenous architecture of articular cartilage. Correlation of scanning electron microscopy and polarized light microscopy observations. Clin Orthop Relat Res 1979(139):267-75.

44. Ortmann R. Use of polarized light for quantitative determination of the adjustment of the tangential fibres in articular cartilage. Anat Embryol (Berl) 1975;148(2):109-20.

45. Gardner DL, Salter DM, Oates K. Advances in the microscopy of osteoarthritis. Microsc Res Tech 1997;37(4):245-70.

46. Zhou W, Apkarian RP, Wang ZL, Joy D. Fundamentals of scanning electron microscopy. In: Scanning microscopy for nanotechnology: Techniques and applications, Zhou W, Wang ZL, Eds. New York: Springer 2006:1-40.

47. Chatterjee S, Hadi AS. Simple linear regression. In: Regression analysis by example. Fourth Edition ed. Hoboken, New Jersey: John Wiley & Sons, Inc. 2006:21-52.

48. Kurkijarvi JE, Nissi MJ, Rieppo J, Toyras J, Kiviranta I, Nieminen MT, et al. The zonal architecture of human articular cartilage described by t2 relaxation time in the presence of Gd-DTPA2. Magn Reson Imaging 2008;26(5):602-7.

49. Nissi MJ, Rieppo J, Toyras J, Laasanen MS, Kiviranta I, Jurvelin JS, et al. T(2) relaxation time mapping reveals age- and species-related diversity of collagen network architecture in articular cartilage. Osteoarthritis Cartilage 2006;14(12):1265-71.

50. Hwang WS, Li B, Jin LH, Ngo K, Schachar NS, Hughes GN. Collagen fibril structure of normal, aging, and osteoarthritic cartilage. J Pathol 1992;167(4):425-33.

51. Weiss C, Rosenberg L, Helfet AJ. An ultrastructural study of normal young adult human articular cartilage. J Bone Joint Surg Am 1968;50(4):663-74.

52. Clarke IC. Articular cartilage: A review and scanning electron microscope study. 1. The interterritorial fibrillar architecture. J Bone Joint Surg Br 1971;53(4):732-50.

53. Dodge GR, Poole AR. Immunohistochemical detection and immunochemical analysis of type ii collagen degradation in human normal, rheumatoid, and osteoarthritic articular cartilages and in explants of bovine articular cartilage cultured with interleukin 1. J Clin Invest 1989;83(2):647-61.

54. Hollander AP, Pidoux I, Reiner A, Rorabeck C, Bourne R, Poole AR. Damage to type II collagen in aging and osteoarthritis starts at the articular surface, originates around chondrocytes, and extends into the cartilage with progressive degeneration. J Clin Invest 1995;96(6):2859-69.

55. Poole CA. Articular cartilage chondrons: Form, function and failure. J Anat 1997;191 (Pt 1):1-13.

56. Silver FH, Bradica G, Tria A. Relationship among biomechanical, biochemical, and cellular changes associated with osteoarthritis. Crit Rev Biomed Eng 2001;29(4):373-91.

57. Chen MH, Broom N. On the ultrastructure of softened cartilage: A possible model for structural transformation. J Anat 1998;192 (Pt 3):329-41.

58. Eyre DR, Weis MA, Wu JJ. Advances in collagen cross-link analysis. Methods 2008;45(1):65-74.

59. Lippiello L, Hall D, Mankin HJ. Collagen synthesis in normal and osteoarthritic human cartilage. J Clin Invest 1977;59(4):593-600.

60. Nelson F, Dahlberg L, Laverty S, Reiner A, Pidoux I, Ionescu M, et al. Evidence for altered synthesis of type ii collagen in patients with osteoarthritis. J Clin Invest 1998;102(12):2115-25.

61. Knutsen G, Engebretsen L, Ludvigsen TC, Drogset JO, Grontvedt T, Solheim E, et al. Autologous chondrocyte implantation compared with microfracture in the knee. A randomized trial. J Bone Joint Surg Am 2004;86-A(3):455-64.

62. Roberts S, Darby AJ, Menage J, Evans EH, Richardson JB. A histological assessment of aci-treated patients as an outcome of cartilage repair (abstract). Int J Exp Path 2001;82:A18-9.

63. Roberts S, McCall IW, Darby AJ, Menage J, Evans H, Harrison PE, et al. Autologous chondrocyte implantation for cartilage repair: Monitoring its success by magnetic resonance imaging and histology. Arthritis Res Ther 2003;5(1):R60-73.

64. Roberts S, Menage J, Sandell LJ, Evans EH, Richardson JB. Immunohistochemical study of collagen types I and II and procollagen IIa in human cartilage repair tissue following autologous chondrocyte implantation. Knee 2009;16(5):398-404.

CHAPTER 7. GENERAL DISCUSSION

The studies described in the preceding four chapters addressed the main research objectives of the thesis, which focused on testing two methodologies for cartilage evaluation, streaming potentials and polarized light microscopy. These methods were identified as promising candidates for filling cartilage assessment needs in ongoing research in the areas of cartilage degeneration and repair. Here, several points related to the thesis as a whole are discussed, including how the streaming potential and polarized light microscopy methods compare to other available technologies and their application in a clinical context, laboratory and clinical situations where the Arthro-BST device could be employed, as well as aspects of the experimental approach employed in Articles I & II.

7.1 Accessibility of Streaming Potentials and Polarized Light Microscopy in a Clinical Context

Current methods for evaluating cartilage quality may include clinical exams, patient reported outcomes and non-invasive MR imaging, and possibly direct probing of the articular surface during arthroscopy, where cartilage biopsies for histological analyses may be retrieved if indicated (**Table 1.1**). The results described in the preceding four chapters, support the use of streaming potentials and polarized light microscopy for providing new, relevant measures of cartilage quality that can enhance the repertoire of cartilage assessment methods currently available.

7.1.1 Streaming Potentials Compared to Other Technologies

Clinically, the streaming potential method can be employed during arthroscopy by using the handheld Arthro-BST device[7] to obtain SPI values in situ (Section 7.2). SPI is a quantitative parameter correlated to cartilage composition, structure and load bearing properties, and may

7 Pending approval. As of March 2011 the Arthro-BST device has not been approved for use in human surgery.

provide a more sensitive and complete assessment of cartilage compared to the blunt probe and possibly to other technologies under development for in situ cartilage assessment (Lyyra, et al., 1995; Niederauer, et al., 2004; Pan, et al., 2003; Saarakkala, et al., 2004).

The blunt probe provides tactile information to the surgeon, who can then distinguish between firm and softened cartilage, as well as observe surface changes such as fibrillation (**Figure 1.11**). Cartilage integrity is often rated using qualitative arthroscopic grades, such as the ICRS macroscopic score, which provide a standardized means of describing cartilage degeneration. The arthroscopic examination is considered a gold standard for clinical cartilage evaluation, although surgeons report difficulty distinguishing between low- and high-grade cartilage lesions, and acknowledge that more objective measures of cartilage evaluation could aid in discriminating among intermediate levels of degeneration (Spahn, et al., 2009). In addition, early osteoarthritic changes may not manifest as visible surface disruptions and cartilage softening at this preliminary stage may be too modest for blunt probe detection. Streaming potentials could provide a more sensitive method for detecting early degenerative changes as demonstrated during the experiments described in Article II. Localized impact injury averaging 28 MPa resulted in minimal cartilage surface disruptions, visualized by faint India ink staining with evidence of minor cracking at some sites, but nonetheless produced statistically significant changes in SPI. These surface changes could not be seen without the contrast provided by the black India ink and, as it is not possible to apply India ink in an arthroscopic setting, it is unlikely that these mild surface alterations would be detected during a standard arthroscopic evaluation. The impact stress level of 28 MPa is similar to the range of impact stresses shown to initiate cartilage degeneration in animal models (Haut, 1989; Repo & Finlay, 1977; Scott & Athanasiou, 2006), and early detection of these types of changes could help identify an opportunity for early therapeutic intervention.

In situ biomechanical measurements of cartilage stiffness have been correlated to independent assessments of cartilage structure and histological appearance (Bae, et al., 2003; Franz, et al., 2001; Henderson, et al., 2007; Lyyra, et al., 1999; Niederauer, et al., 2004). These devices can provide consistent information about cartilage stiffness intra-operatively when they

are correctly positioned, although the influence of cartilage thickness on indentation stiffness cannot be ignored for cartilage less than 2 mm (Lyyra, et al., 1995; Niederauer, et al., 2004). Thickness effects are minimal for cartilage greater than 2 mm, making clinical indentation measurements in the human knee feasible as cartilage here typically ranges from 2-4 mm. Additionally, the effect of thickness can be lessened by measuring stiffness at lesional or repair tissue sites and normalizing to measurements of adjacent normal cartilage. However, comparisons between biomechanical parameters, macroscopic scores, and histological measures indicate that stiffness measurements alone may be insufficient to distinguish low grade cartilage changes (Kleemann, et al., 2005) particularly because of the large range of mechanical properties possible for normal cartilage and the substantial overlap with properties of osteoarthritic cartilage (Brown, Crawford, & Oloyede, 2007). Decreases in cartilage stiffness, in a bovine explant model of cartilage degradation, corresponded to reduced Safranin-o staining and collagen organization; although the effect sizes appeared to be lower for stiffness measurements compared to histological assessments. Consequently, milder depletions in ECM components produced statistically significant differences in quantitative histological assessments but not in stiffness reduction (Lyyra, et al., 1999).

Streaming potentials were shown previously to be more sensitive than biomechanical testing at detecting cartilage changes due to degradation produced by enzymes or cytokines (Bonassar, et al., 1995; Bonassar, et al., 1997; Chen, et al., 1997; Frank, et al., 1987; Legare, et al., 2002). Similar findings were obtained in Articles I & II, where SPI detected minor changes occurring in cartilage due to freezing (Article I) and was more responsive to blunt impact (Article II) than biomechanical parameters obtained by fitting stress relaxation data, produced by unconfined compression tests of isolated disks, with the fibril-network-reinforced model (Section 1.1.4). Further, correlations between SPI and these biomechanical parameters, which correspond to intrinsic cartilage structure (Korhonen, et al., 2003), demonstrated that SPI measurements reflect the whole cartilage, while indentation stiffness primarily reflects superficial zone properties (Korhonen, et al., 2002). This increased sensitivity of the streaming potential method compared to mechanical tests could be advantageous for intra-operative detection of low-grade cartilage changes associated with early osteoarthritis.

Cartilage assessment using OCT or US technologies provide cross-sectional images of cartilage that have a resolution comparable to low-powered histology. OCT images, formed from backscattered infrared light, reveal certain optical characteristics that can distinguish healthy from degraded cartilage. This imaging modality is suited to identifying structural deviations, including subsurface tears (Pan, et al., 2003), but OCT characteristics do not directly reflect cartilage composition or structure. Streaming potentials exploit the relationship between ECM components and reflect cartilage structure and behaviour during load bearing, thereby linking SPI to both biochemical composition (Bonassar, et al., 1997; Frank, et al., 1987; Legare, et al., 2002) and biomechanical properties (Frank, et al., 1987; Garon, 2007; Legare, et al., 2002), which adds value to the arthroscopic assessment by providing relevant information about cartilage quality that cannot be obtained by the blunt probe or other technologies described here that are currently being explored for in situ cartilage assessment.

Quantitative US parameters calculated from cartilage surface reflections, correspond well with SZ degradation (Viren, et al., 2009), and measurements of surface roughness may be sensitive enough to distinguish between normal and low-grade cartilage changes that may not be visible arthroscopically (Kaleva, et al., 2011; Viren, et al., 2009). US appears to be more sensitive to changes related to the collagen network compared to proteoglycan content (Toyras, et al., 2002). Streaming potentials may have an advantage over US because they are sensitive to both collagen network disruption, by enzymatic depletion (Frank, et al., 1987) or blunt trauma (Article II), as well as proteoglycan loss (Frank, et al., 1987). Because the streaming potential method reflects the whole cartilage tissue during compression, it may be more likely to respond to cartilage changes occurring below the superficial zone, which are possible in early OA, compared to US.

The above comparison between the streaming potential method and other technologies for in situ cartilage assessment, including the blunt probe, mechanical measurements and imaging technologies, shows the strengths and weaknesses of these approaches. The substantial research efforts in this area emphasize the desire, of both clinicians and researchers, for more objective measures of cartilage quality in situ.

7.1.2 Polarized Light Microscopy

The qualitative PLM score for evaluating collagen network organization, described in Article III, provides a new histological score for assessing collagen architecture in unstained histological sections. It can enhance the evaluation of cartilage repair tissue quality in clinical trials, as direct histological assessment of repair cartilage biopsies is the predominant method for assessing the efficacy of cartilage repair procedures. Presently, histological scoring systems for assessing biopsies of repair cartilage rate a number of characteristics thought to contribute to the long term success of repair cartilage. However, these systems lack a comprehensive category where different levels of collagen organization are specifically evaluated. Such an assessment, which is now afforded by the PLM score, could be particularly informative as collagen network structure is heavily implicated in cartilage load bearing and is likely indicative of long term durability.

The PLM score was able to distinguish collagen organization in normal, degraded and repair human biopsy samples with excellent inter-reader reliability (Article III). PLM is sensitive to fibrillar collagen orientation however, it is important to recognize that in PLM orientation is inferred from the birefringence characteristics of the sample being observed. Conversely, SEM offers high resolution imaging thus providing a direct visualization of collagen fibres. Comparison studies, where collagen network structure was assessed using PLM and analogous SEM methods (Article IV), provided a validation of the PLM score, as excellent agreement between collagen orientations observed independently in PLM and SEM confirmed that birefringence characteristics are a consequence of true collagen fibre direction.

These studies (Articles III & IV) describe the development, testing and validation of the PLM score for evaluating collagen organization in histological sections of repair cartilage tissues. It is a valuable addition to the spectrum of histological scores presently available (Rutgers, et al., 2010) because it is the only one that offers a systematic assessment of collagen structure where different levels of organization are described. The PLM score was successfully used to assess

repair cartilage biopsies retrieved during a randomized controlled clinical trial[8], where the ability of microfracture augmented with the cartilage repair device, BST-CarGel (Shive, et al., 2006), was compared to microfracture alone for repairing focal cartilage defects. The PLM score provided a qualitative assessment of the functionally important collagen network that complemented ICRS I and ICRS II scoring, thereby providing a more complete picture of repair cartilage quality (Changoor, et al., 2010; Methot, et al., 2010).

7.2 Implementation of the Arthro-BST device in Laboratory and Clinical Settings

The Arthro-BST device (**Figure 1.16**) can be used to evaluate cartilage quality during in vitro or in vivo animal experiments, as well as in clinical settings. The device is optimized for use in arthroscopic procedures, where the dimensions of the sterile tip allow it to be inserted through standard arthroscopic portals. Cartilage is assessed non-destructively as measurements are made by lightly indenting the articular surface at compressive forces that are within a physiological range. Normal, healthy cartilage recovers from the indentation within minutes, allowing multiple, highly repeatable measurements to be performed (Article I). The resulting quantitative parameter, or SPI, reflects cartilage biomechanical properties, composition and structure (Garon, 2007) Article II). The Arthro-BST can be incorporated into a variety of experimental and clinical situations, adding value by providing a rapid means of quantitatively assessing cartilage, without inflicting permanent tissue damage.

The Arthro-BST is suitable for in vitro studies involving explants from large animals or cadavers. To make measurements on these samples, which may be whole joint surfaces or smaller osteochondral pieces, they must be submerged in a solution containing electrolytes, such as phosphate buffered saline or lactated Ringer's solution, in sufficient quantity to cover the reference electrode (**Figure 1.16**). Examples of applications for the Arthro-BST could include using the device to map normal cartilage electromechanical properties over joint surfaces,

8 Sponsored by Piramal Healthcare (Canada), Montreal, Quebec, Canada.

comparing cartilage properties before and after inducing damage or applying therapeutics, or distinguishing regions of degenerated cartilage and exploring the extent of degeneration in samples obtained from osteoarthritic joints. Studies where explants are maintained in culture conditions (Thibault, et al., 2002) may benefit from using the Arthro-BST to assess cartilage at multiple time points, as the non-destructive nature of the device allows for sequential monitoring of cartilage changes over time. The size of the tip that contacts the cartilage surface has a radius of 3.1 mm, and these dimensions are best suited to the curvature found in larger articular joints, including human knees, shoulders and hips, and equivalents in large animals. Similar joints in smaller animals, such as rabbits, would require a scaled-down version of the tip, with smaller overall dimensions and increased electrode density, to accommodate joint surface curvature and to permit electromechanical measurements at a comparable spatial resolution.

In vivo animal studies, such as animal models of osteoarthritis or other degenerative joint diseases, could benefit from cartilage assessment with the Arthro-BST. These types of models are useful for studying disease progression and testing the efficacy of potential therapeutic interventions. The Arthro-BST could provide information about cartilage composition and load bearing properties in situ, as well as assess the severity and extent of cartilage damage quantitatively. The device is designed for arthroscopic studies, which are possible in large animals such as the horse and to a more limited extent in sheep. However, the Arthro-BST could still be used in open surgical procedures with the construction of a containment chamber around the joint surface to hold enough saline to sufficiently cover the joint surface and sterile tip during electromechanical measurements. The non-destructive nature of the streaming potential method and the ability to perform second-look arthroscopies in animal studies provides an opportunity for sequential assessment of cartilage over time. An important consideration for these types of studies, where the articular surfaces are evaluated at different time points, is the need to identify reproducible landmarks for locating measurement sites.

In humans, arthroscopic procedures are used for pre-operative planning as well as for performing certain surgical procedures, including lavage and debridement (Moseley et al., 2002). Arthroscopies are most often performed in the knee, but are also widely used in the shoulder, hip,

elbow, ankle and wrist joints[9]. The dimensions of the Arthro-BST make it appropriate for larger joints such as the knee and shoulder, while a smaller tip with a greater electrode density would be required to assess cartilage in smaller joints such as the elbow and wrist.

It is common practice for surgeons to explore the articular surface with a blunt probe to qualitatively appreciate cartilage softening and investigate fibrillated or detached cartilage. The Arthro-BST could be used during these procedures[10] to acquire quantitative measurements of cartilage quality at multiple locations on the articular surfaces. This data could contribute to planning repair procedures for treating focal cartilage defects by providing an objective means for staging the cartilage lesion and thereby determining the quantity of damaged cartilage that should be resected. In addition, other regions, away from the main defect site, could be evaluated with the Arthro-BST to ascertain whether minor degradation is occurring, which may be difficult to distinguish qualitatively with a blunt probe. Regions exhibiting early degenerative changes are expected to be asymptomatic and are not candidates for surgical intervention, but they could eventually progress to osteoarthritic lesions. Identifying these regions may represent an opportunity for early therapeutic intervention to prevent or slow the progression of OA (Lotz, 2010).

Since SPI is correlated to biomechanical properties and cartilage thickness (Article II), prior knowledge of cartilage thickness may be required to correctly interpret SPI measurements in a clinical setting. Cartilage thickness varies over joint surfaces but exhibits similar patterns among individuals (Brama, Barneveld, Karssenberg, Van Kampen, & van Weeren, 2001; Changoor, et al., 2006; Frisbie, et al., 2006; Kurkijarvi, et al., 2008; Thambyah, Nather, & Goh, 2006), making it possible to develop a spatial map of expected cartilage thicknesses for human articular joints. The Arthro-BST would add value to arthroscopic procedures by providing information about cartilage quality that cannot be obtained by other devices currently available to the orthopaedic surgeon.

---

9 American Academy of Orthopaedic Surgeons (http://orthoinfo.aaos.org/topic.cfm?topic=A00109)

10 Pending approval. As of March 2011 the Arthro-BST device has not been approved for use in human surgery.

In summary, the Arthro-BST device provides a method for obtaining streaming potential measurements without destroying cartilage. At present, the Arthro-BST device would be best suited to in vivo studies where arthroscopic access to joint surfaces is possible, as well as in cartilage explant studies, where the joint surface can be submerged in a saline solution during electromechanical measurements. The Arthro-BST device can provide rapid, spatially-resolved, non-destructive evaluation of cartilage properties, where the computed quantitative parameter reflects cartilage composition and load-bearing properties.

7.3 Rationale for the Experimental Approach of Articles I & II

Several decisions regarding the experimental approach were made during the studies described in Articles I & II. These included selecting the species and age of the cartilage tissues used in the experiments, choosing sample sizes, as well as applying appropriate statistical methods.

7.3.1 Species and Age

The motivation for exploring the effects of refrigerated or frozen storage on cartilage (Article I) arose during the development of the protocol for cartilage electromechanical and biomechanical testing, which was later employed in Article II. The experiment was designed to simulate the storage conditions and time-frame, from acquiring fresh cartilage tissue to testing, that are typically observed in our laboratory.

Acquiring fresh cartilage tissue from large animals, such as cows or horses, is challenging. Bovine tissue can be obtained from local butchers or abattoirs that generally provide articular joints from younger, sexually immature animals. This means that they may not have developed the mature anisotropic structure of cartilage, which coincides with puberty (Hunziker, et al., 2007). These suppliers can estimate the time between sacrifice and when articular joints are provided for research, but cannot provide specific details about the animal's history. On the contrary, fresh equine articular joints can be obtained from veterinary schools, such as the

Ontario Veterinary College[11], where articular joints from horses of different ages are possible and the controlled environment means that the exact time of sacrifice and many aspects of the animal's history are recorded. This is a more desirable tissue source for research, but opportunities for obtaining fresh equine tissue, particularly for in vitro studies, are limited.

The relative availability of these tissue types informed the decision to use more readily available bovine cartilage wherever possible during protocol development, which included exploring the effects of cold storage on cartilage (Article I). The bovine stifle (knee) joint employed in Article I was obtained from a local butcher approximately 24 hours after the animal was sacrificed. This represented a typical delay between sacrifice and tissue reception. Equine articular joints can be collected immediately after sacrifice and refrigerated but must then be shipped, introducing a similar time delay. Obtaining cartilage tissue from large animals at the time of sacrifice may not always be practical.

The bovine stifle used in Article I was from a cow estimated to be approximately 6 months of age and histological sections viewed in polarized light (data not shown) revealed a laminar collagen network structure similar to that reported in immature animals (Julkunen, et al., 2009; Nissi, et al., 2006). The absolute electromechanical and biomechanical properties measured for immature bovine cartilage were different than mature equine cartilage (Articles I & II), however the relative effects of refrigerated and frozen storage on electromechanical and biomechanical properties were expected to be similar among these tissue types. These assessment methods, involving sequential electromechanical measurements on whole joint surfaces followed by biomechanical testing on isolated cartilage disks, require that the integrity of the extracellular matrix be preserved during storage, but not necessarily a population of healthy chondrocytes, as is desired in other applications such as fresh allograft implantation (Williams, et al., 2003). A review of the literature indicates that freezing and refrigeration have greater effects on chondrocytes than the extracellular matrix, which is comparatively inert (Allen, et al., 2005; Ball, et al., 2004; Williams, et al., 2003). Immature cartilage has a higher cell density (Nixon &

11 University of Guelph, Guelph ON, Canada

Fortier, 2001; Palmer, Wilson, Baum, & Levenston, 2009), which can contribute to the production of enzymes that degrade the extracellular matrix over time. This suggests that these storage protocols assessed in immature cartilage may produce less pronounced effects in mature cartilage.

In addition to differences between immature and mature cartilage, species-specific differences exist in cartilage biomechanical properties (Athanasiou 1991), and chondrocyte proliferation profiles (Akens & Hurtig, 2005). However, the general biochemical composition of articular cartilage is similar among species and for this type of comparative study (Article I), where the effects of storage on the extracellular matrix of cartilage was of interest, these components were expected to experience similar degradation due to storage, meaning that the choice of animal model was less critical for this particular investigation.

The subsequent experiments (Article II), where cartilage changes occurring immediately after local impact were investigated, were performed in equine cartilage. This was required because the species-specific characteristics of cartilage were expected to influence study outcomes, based on pilot studies performed in bovine and equine cartilage (bovine data not shown, (Changoor, Quenneville, et al., 2009). Future in vivo development of the described equine model system of early PTOA will directly rely on results obtained in vitro (Article II), further requiring that in vitro experiments be conducted in the same species. The findings of Article I were considered in these experiments and storage-related degradation was minimized by keeping tissue at 4°C in humid chambers as much as possible. Safranin-o staining was consistent among all samples with no pattern of diminished staining observed with respect to storage time.

In summary, fresh bovine cartilage was used to explore the effects of cold storage on the electromechanical and biomechanical properties of cartilage, where changes were appreciated by comparing properties measured prior to and after storage at various conditions. Using this information during the planning of subsequent experiments in mature equine cartilage (Article II) was deemed appropriate because the effects of storage on the extracellular matrix of cartilage were not expected to be drastically different in bovine versus equine cartilage, or immature

versus mature cartilage, given the inert nature of the extracellular matrix. Moreover, the effects of storage on immature tissue may be greater than in mature cartilage because of the higher density of chondrocytes, meaning that using these storage limits for mature tissue may provide a conservative estimate of storage time.

7.3.2 Sample Size

The experiments described in Articles I & II were conducted using either one stifle joint (Article I) or a pair of stifle joints from the same animal (Article II). A number of experimental sites on these joint surfaces were identified and assigned to the different treatment groups. Cartilage properties can vary among individuals (Eckstein, Winzheimer, Hohe, Englmeier, & Reiser, 2001) as well as over single joint surfaces (Brama, et al., 2001; Changoor, et al., 2006; Thambyah, et al., 2006). However, although absolute measurements may differ, common patterns in cartilage properties exist over joint surfaces among individuals (Brama, et al., 2001; Changoor, et al., 2006; Frisbie, et al., 2006; Kurkijarvi, et al., 2008; Thambyah, et al., 2006). By generating many independent samples from a single joint surface, cartilage with different properties could be assessed, but inter-individual variability was not.

This approach met the objectives of these studies (**Section 2.1**), while minimizing the number of animals required for the experiment[12]. Sample site locations were determined during pilot studies and selected so that each treatment group included independent cartilage samples from different regions of the joint surface, covering a range of cartilage properties. In these studies, the effects of storage conditions (Article I) or impact injury (Article II) were assessed by comparing cartilage electromechanical properties prior to and after treatment, or biomechanical and histological properties between treated and control groups.

While this experimental approach allows comparisons between treated and untreated cartilage to be appreciated, it is limited because cartilage from other individuals may have a different response to the absolute impact values used. The variation in response is not expected to

be large, as these impact levels created similar cartilage changes in pilot studies conducted on equine tissue from a separate horse. In addition, recent work has involved mapping electromechanical measurements at high spatial resolutions over equine stifle joints originating from different animals. Preliminary results demonstrate consistent SPI patterns with low variability among absolute values from different individual animals (unpublished data). However this limitation should still be considered when applying the impact levels used in Article II to future development of this model system of early PTOA.

The results from Articles I & II do not reflect inter-individual variability because cartilage tissues from single animals were used. Prior literature shows that cartilage properties vary over the joint surface in a comparable pattern among individuals, suggesting that it is reasonable to expect that the cartilage response to storage or impact would be similar in other similar individuals. The use of additional animals would provide further insight into inter-individual variability, however the data obtained in these studies adequately addressed the study hypotheses and minimized animal tissue use.

7.3.3 Statistical Approach

In these studies a number of independent samples, meaning that they were not influenced by neighbouring sites on the joint surfaces, were generated from either an individual cow stifle joint (Article I) or pair of horse stifle joints (Article II). For statistical analyses, sample size is not determined by the number of animals, but from the number of independent samples used.

The general statistical approach involved testing for normality, with the Shapiro-Wilk test, and subsequently applying appropriate parametric or non-parametric tests to compare measured parameters among groups. For the dataset in Article I, more than 90% of the groups were normally distributed, with $p>0.05$ for Shapiro-Wilk tests (data not shown). Groups without

---

12 Canadian Council on Animal Care, Animal Use Guidelines (http://www.ccac.ca/en_/standards/guidelines)

normal distributions included matrix modulus (Em) for both day 6 and day 12 of refrigerated storage, and permeability (k) from the control group in the freezing experiment. Since the majority of the data was normal, t-tests were used to compare among groups, and this data reported in the paper. These findings were confirmed, where comparisons involved the groups without normal distributions, using an equivalent non-parametric test, the Mann-Whitney U.

A similar approach was applied in Article II and a mixture of groups with and without normal distributions was observed. Because of this, parametric and equivalent non-parametric tests were performed and compared, with the most relevant statistics included in the paper. Since parametric tests are more sensitive than non–parametric tests, they were always reported and results from non-parametric tests included only when they contributed additional information. For example, results from the paired t-test and equivalent non-parametric Wilcoxon matched pairs test were both reported for electromechanical measurements because the Wilcoxon test identified additional statistical differences that contributed to data interpretation. However, for the correlations between electromechanical and biomechanical parameters, only the parametric Pearson's correlations were reported because they were similar to equivalent non-parametric Spearman rank order correlations.

An important aspect of analyzing these data involved determining whether or not the statistics reflected biologically important cartilage changes. For example, SPI measurements made after a single freeze-thaw cycle (Article I) tended to decrease to an average of 94% of day 1 SPI values. This change was detected as a statistical trend, $p=0.083$, obtained using a paired t-test, with an estimated power of 60%. Increasing the sample size to approximately 40 would produce statistical power of 80%, which could theoretically produce a statistically significant difference. However, from a biological perspective, this nominal change in SPI due to freezing reflects minor extracellular matrix degradation, which was not detectable by biomechanical or histological assessments. Freezing is therefore not expected to have a substantial influence in these types of in vitro experiments involving electromechanical and biomechanical tests. That is, the effect of freezing will be minor compared to other treatment effects (for example, those

produced by impact injury) even if additional samples are tested and a statistically significant difference is achieved.

Similarly, in the refrigeration experiment, statistically significant differences in biomechanical parameters were detected 12 days after storage at 4°C but not after 6 days. These groups had comparatively small sample sizes of 4 and powers ranging from approximately 50% to 99%, depending on the biomechanical parameter. Calculations indicated that achieving statistical power of 80% would require increasing the sample size to a range of six to ten. However, when considering the data set, it is apparent that the statistics support the biological changes observed in cartilage. Cartilage at 6 days was similar to day 1 controls in electromechanical, biomechanical and histological aspects, but exhibited drastic decreases in properties by 12 days. This implies that increasing sample size will not produce a different outcome, that is, the biologically important changes observed in day 12 analyses will persist.

In summary, considering the biological importance of observed cartilage changes, in addition to statistical analyses, is essential for proper data interpretation. The results of these experiments related to the cold storage of cartilage suggest that refrigerating fresh cartilage for up to 6 days produces changes with the least biological significance among the conditions tested, and that freezing produces smaller changes that are not expected to significantly influence in vitro experiments. In this case, instead of increasing sample sizes to meet statistical power criteria, research efforts would be better spent on exploring storage effects in other cartilage tissue types, for example, it would be beneficial to explore the effects of storage on cartilage obtained from osteoarthritic joints.

CONCLUSIONS & RECOMMENDATIONS

Streaming potentials and polarized light microscopy were appropriate cartilage evaluation methods capable of addressing the requirements of two specific assessment needs identified in the areas of cartilage degeneration and repair. First, streaming potentials were shown to be a promising method for evaluating the subtle cartilage changes expected during early degeneration in pre-clinical models of PTOA. In vitro tests in an impact injury model showed that streaming potentials decreased as a function of peak impact stress level and were more sensitive than biomechanical tests at detecting cartilage changes produced by impact loading. In addition, the consequences of refrigerated and frozen storage to biomechanical and electromechanical properties of cartilage were elucidated, providing pertinent recommendations for cartilage testing. Second, a new qualitative PLM score was developed and validated, providing a method for systematically evaluating collagen organization in repair cartilage, a critical feature for successful cartilage function and likely indicative of an enduring repair tissue. This new histological score can enhance the assessment of cartilage repair tissue quality as collagen architecture is not adequately evaluated by other scoring systems. Further studies of collagen network structure in PLM and SEM identified a number of differences related to tissue type, including variations in fibre diameter distributions and zonal proportions in degraded and repair cartilage compared to normal. Streaming potentials and polarized light microscopy provided appropriate evaluation methodologies for articular cartilage in degeneration and repair scenarios.

The studies contained in this thesis contributed several new relevant findings. Articles I and II were the first to report the sensitivity of the streaming potential method to cartilage changes produced by impact injury or cold storage conditions. The versatility of the streaming potential method was demonstrated and correlations with intrinsic cartilage properties established. Article III introduced a new qualitative PLM score that offers a systematic method for evaluating different levels of collagen organization in repair cartilage tissues. Finally, Article

IV provided the first ultrastructural evidence that collagen fibres in repair tissues could approach the stratified collagen network structure of adult hyaline articular cartilage.

Recommendations

This thesis contributed new data related to cartilage assessment methodologies and generates new questions that could be explored in future studies. Several ideas for potential experiments are described in the following paragraphs.

Additional experiments to elucidate the mechanisms of cartilage degeneration occurring during refrigerated or frozen storage would be beneficial. A limitation identified in Article I, was the possibility that the sequential electromechanical measurements, which required the joint surface to be submerged in physiological saline at room temperature during testing for one to three hours at a time, may have contributed to accelerating degradation, since proteoglycans can be lost to liquid media by diffusion. This effect would be more pronounced in the refrigeration group, where by day 12, the joint surface had undergone three sets of electromechanical measurements. The role of these testing conditions could be explored in future experiments that include separate day 6 and day 12 controls, and where saline samples, collected following electromechanical testing, could be assessed with the dimethylmethylene blue assay to quantify GAG loss to the media. The repeated indentations of the cartilage surface with the Arthro-BST device was not expected to cause direct physical damage as it has been shown that repeated indentation at physiological stress levels leads to softening only after approximately 24 hours (Kempson, et al., 1971).

Degradation during refrigerated storage could be further explored by comparing refrigerated cartilage to cartilage where controlled degradation is induced by enzymes, which target the extracellular matrix (Frank, et al., 1987), or cytokines, which elicit a broader degradative response from chondrocytes (Bonassar, et al., 1997; Legare, et al., 2002). Assessing additional time points, particularly between days 6 and 12, during which significant proteoglycan loss was observed, could provide more precise information about when and how this degradation occurs.

Freezing-induced degeneration could be further investigated in studies where the rate of freezing is monitored with instrumentation at different locations on the joint surface. The rate of freezing varies over larger joint surfaces, where cartilage at the centre experiences slowing cooling compared with cartilage at the edges (Szarko, Muldrew, & Bertram, 2010). Cartilage degeneration due to freezing was expected to result from two degradative mechanisms, specifically ice crystal formation, causing direct damage to the extracellular matrix (Muldrew, Hurtig, Novak, Schachar, & McGann, 1994; Muldrew et al., 2000; Szarko, et al., 2010), and enzymatic degradation following chondrocyte necrosis, since freezing typically results in extensive loss of chondrocyte viability (Brighton, et al., 1979; Muldrew, et al., 1994; Rodrigo, Thompson, & Travis, 1987; Yablon & Covall, 1978). Our findings (Article I) indicate that while minor degradative changes occurred, which were detected by electromechanical measurements, the degradation was not extensive enough to affect cartilage biomechanical properties, similar to other studies (Kiefer, et al., 1989; Szarko, et al., 2010). We selected a comparatively simple freezing process in which the entire joint surface was placed within a -20ºC freezer, where a slow cooling rate, on the order of 1ºC per second, was expected to prevail. Slower cooling, where intra- and extra-cellular water are more likely to remain equilibrated throughout the freezing process, is thought to reduce damage to the cells, including preventing the formation of ice within the cell itself, cell shrinkage, and cell membrane damage (Szarko, et al., 2010; Tomford, Fredericks, & Mankin, 1984).

Further development of the pre-clinical model system proposed for early PTOA (Article II) could be undertaken. This would involve testing the model in vivo, where localized impacts at similar stress levels would be delivered to the articular surfaces during an initial surgery and streaming potentials used to follow degradative changes at the impact site and surrounding cartilage sequentially over time. This is possible because of the non-destructive nature of the streaming potential method, which would permit cartilage assessment at an intermediate time point in the study during a second-look arthroscopy. This type of study would provide a characterization of the model where the time course of degeneration associated with different levels of impact stress could be established. Subsequent experiments could then focus on testing

the efficacy of pharmaceutical therapies or other interventions designed to moderate or halt the progression of PTOA.

The qualitative PLM score represents a first attempt at classifying levels of collagen organization in cartilage repair tissues. Future studies could look at improving the score by providing more detailed descriptions of normal cartilage in human and animal tissues, including features like zone proportions and a more precise definition of transitional zone appearance, which was observed to vary among species. Depending on the results of these types of studies a modified score could be proposed that provides a more discriminating assessment of collagen organization in repair tissues.

On a final note, a situation where both methodologies described in this thesis could be used together is in the context of a clinical trial to evaluate repair cartilage. Second look arthroscopies are typically performed where a biopsy of repair tissue is retrieved. The Arthro-BST device for arthroscopic assessment of streaming potentials could be used here, prior to isolating the biopsy, to obtain a measurement of repair cartilage function. Subsequent histological analysis of the biopsy to characterize repair cartilage quality would include the PLM score for collagen organization. The resulting data set would allow relationships between SPI, which is correlated to intrinsic cartilage properties, and histological appearance to be explored in repair cartilage tissues. The possibilities are endless!

REFERENCES

Aigner, T., Rose, J., Martin, J., & Buckwalter, J. (2004). Aging theories of primary osteoarthritis: from epidemiology to molecular biology. *Rejuvenation Res, 7*(2), 134-145.

Akens, M. K., & Hurtig, M. B. (2005). Influence of species and anatomical location on chondrocyte expansion. *BMC Musculoskelet Disord, 6*, 23.

Allen, R. T., Robertson, C. M., Pennock, A. T., Bugbee, W. D., Harwood, F. L., Wong, V. W., et al. (2005). Analysis of stored osteochondral allografts at the time of surgical implantation. *Am J Sports Med, 33*(10), 1479-1484.

Anderson, D. D., Brown, T. D., Yang, K. H., & Radin, E. L. (1990). A dynamic finite element analysis of impulsive loading of the extension-splinted rabbit knee. *J Biomech Eng, 112*(2), 119-128.

Archer, C. W., Redman, S., Khan, I., Bishop, J., & Richardson, K. (2006). Enhancing tissue integration in cartilage repair procedures. *J Anat, 209*(4), 481-493.

Armstrong, C. G., Lai, W. M., & Mow, V. C. (1984). An analysis of the unconfined compression of articular cartilage. *J Biomech Eng, 106*(2), 165-173.

Arokoski, J. P., Hyttinen, M. M., Lapvetelainen, T., Takacs, P., Kosztaczky, B., Modis, L., et al. (1996). Decreased birefringence of the superficial zone collagen network in the canine knee (stifle) articular cartilage after long distance running training, detected by quantitative polarised light microscopy. *Ann Rheum Dis, 55*(4), 253-264.

Aspden, R. M., Jeffrey, J. E., & Burgin, L. V. (2002). Impact loading of articular cartilage. *Osteoarthritis Cartilage, 10*(7), 588-589; author reply 590.

Ateshian, G. A. (2009). The role of interstitial fluid pressurization in articular cartilage lubrication. *J Biomech, 42*(9), 1163-1176.

Athanasiou, K. A., Rosenwasser, M. P., Buckwalter, J. A., Malinin, T. I., & Mow, V. C. (1991). Interspecies comparisons of in situ intrinsic mechanical properties of distal femoral cartilage. *J Orthop Res, 9*(3), 330-340.

Bae, W. C., Temple, M. M., Amiel, D., Coutts, R. D., Niederauer, G. G., & Sah, R. L. (2003). Indentation testing of human cartilage: sensitivity to articular surface degeneration. *Arthritis Rheum, 48*(12), 3382-3394.

Ball, S. T., Amiel, D., Williams, S. K., Tontz, W., Chen, A. C., Sah, R. L., et al. (2004). The effects of storage on fresh human osteochondral allografts. *Clin Orthop Relat Res*(418), 246-252.

Bank, R. A., Bayliss, M. T., Lafeber, F. P., Maroudas, A., & Tekoppele, J. M. (1998). Ageing and zonal variation in post-translational modification of collagen in normal human articular cartilage. The age-related increase in non-enzymatic glycation affects biomechanical properties of cartilage. *Biochem J, 330 (Pt 1)*, 345-351.

Bashir, A., Gray, M. L., Hartke, J., & Burstein, D. (1999). Nondestructive imaging of human cartilage glycosaminoglycan concentration by MRI. *Magn Reson Med, 41*(5), 857-865.

Bear, D. M., Williams, A., Chu, C. T., Coyle, C. H., & Chu, C. R. (2010). Optical coherence tomography grading correlates with MRI T2 mapping and extracellular matrix content. *J Orthop Res, 28*(4), 546-552.

Benninghoff, A. (1925). Form und Bau der Gelenkknorpel in ihren Beziehungen zur Funktion. *Zeitschrift fur Zellforschung, 2*, 783-862.

Bi, X., Li, G., Doty, S. B., & Camacho, N. P. (2005). A novel method for determination of collagen orientation in cartilage by Fourier transform infrared imaging spectroscopy (FT-IRIS). *Osteoarthritis Cartilage, 13*(12), 1050-1058.

Black, J., Shadle, C. A., Parsons, J. R., & Brighton, C. T. (1979). Articular cartilage preservation and storage. II. Mechanical indentation testing of viable, stored articular cartilage. *Arthritis Rheum, 22*(10), 1102-1108.

Bland, Y. S., & Ashhurst, D. E. (1996). Development and ageing of the articular cartilage of the rabbit knee joint: distribution of the fibrillar collagens. *Anat Embryol (Berl), 194*(6), 607-619.

Bolam, C. J., Hurtig, M. B., Cruz, A., & McEwen, B. J. (2006). Characterization of experimentally induced post-traumatic osteoarthritis in the medial femorotibial joint of horses. *Am J Vet Res, 67*(3), 433-447.

Bonassar, L. J., Jeffries, K. A., Paguio, C. G., & Grodzinsky, A. J. (1995). Cartilage degradation and associated changes in biochemical and electromechanical properties. *Acta Orthop Scand Suppl, 266*, 38-44.

Bonassar, L. J., Sandy, J. D., Lark, M. W., Plaas, A. H., Frank, E. H., & Grodzinsky, A. J. (1997). Inhibition of cartilage degradation and changes in physical properties induced by IL-1beta and retinoic acid using matrix metalloproteinase inhibitors. *Arch Biochem Biophys, 344*(2), 404-412.

Bora, F. W., Jr., & Miller, G. (1987). Joint physiology, cartilage metabolism, and the etiology of osteoarthritis. *Hand Clin, 3*(3), 325-336.

Borrelli, J., Jr., Zhu, Y., Burns, M., Sandell, L., & Silva, M. J. (2004). Cartilage tolerates single impact loads of as much as half the joint fracture threshold. *Clin Orthop Relat Res*(426), 266-273.

Bottcher, P., Zeissler, M., Maierl, J., Grevel, V., & Oechtering, G. (2009). Mapping of split-line pattern and cartilage thickness of selected donor and recipient sites for autologous osteochondral transplantation in the canine stifle joint. *Vet Surg, 38*(6), 696-704.

Brama, P. A., Barneveld, A., Karssenberg, D., Van Kampen, G. P., & van Weeren, P. R. (2001). The application of an indenter system to measure structural properties of articular

cartilage in the horse. Suitability of the instrument and correlation with biochemical data. *J Vet Med A Physiol Pathol Clin Med, 48*(4), 213-221.

Brazier, J. E., Harper, R., Jones, N. M., O'Cathain, A., Thomas, K. J., Usherwood, T., et al. (1992). Validating the SF-36 health survey questionnaire: new outcome measure for primary care. *BMJ, 305*(6846), 160-164.

Brighton, C. T., Shadle, C. A., Jimenez, S. A., Irwin, J. T., Lane, J. M., & Lipton, M. (1979). Articular cartilage preservation and storage. I. Application of tissue culture techniques to the storage of viable articular cartilage. *Arthritis Rheum, 22*(10), 1093-1101.

Brittberg, M., Lindahl, A., Nilsson, A., Ohlsson, C., Isaksson, O., & Peterson, L. (1994). Treatment of deep cartilage defects in the knee with autologous chondrocyte transplantation. *N Engl J Med, 331*(14), 889-895.

Brown, C. P., Crawford, R. W., & Oloyede, A. (2007). Indentation stiffness does not discriminate between normal and degraded articular cartilage. *Clin Biomech (Bristol, Avon), 22*(7), 843-848.

Buckwalter, J., Hunziker, E., Rosenberg, L., Coutts, R., Adams, M., & Eyre, D. (1988). Articular cartilage: composition and structure. In S. L.-Y. Woo & J. Buckwalter (Eds.), *Injury and repair of the musculoskeletal soft tissues* (pp. 405-425). Park Ridge: American Academy of Orthopaedic Surgeons.

Buckwalter, J. A., & Brown, T. D. (2004). Joint injury, repair, and remodeling: roles in post-traumatic osteoarthritis. *Clin Orthop Relat Res*(423), 7-16.

Bullough, P., & Goodfellow, J. (1968). The significance of the fine structure of articular cartilage. *J Bone Joint Surg Br, 50*(4), 852-857.

Buschmann, M. D., Soulhat, J., Shirazi-Adl, A., Jurvelin, J. S., & Hunziker, E. B. (1998). Confined compression of articular cartilage: linearity in ramp and sinusoidal tests and the importance of interdigitation and incomplete confinement. *J Biomech, 31*(2), 171-178.

Changoor, A., Fereydoonzad, L., Yaroshinsky, A., & Buschmann, M. D. (2010). Effects of refrigeration and freezing on the electromechanical and biomechanical properties of articular cartilage. *J Biomech Eng, 132*(6), 064502.

Changoor, A., Hurtig, M. B., Runciman, R. J., Quesnel, A. J., Dickey, J. P., & Lowerison, M. (2006). Mapping of donor and recipient site properties for osteochondral graft reconstruction of subchondral cystic lesions in the equine stifle joint. *Equine Vet J, 38*(4), 330-336.

Changoor, A., Nelea, M., Fereydoonzad, L., Rossomacha, E., Shive, M. S., & Buschmann, M. D. (2009). *Assessment of collagen orientation in repair cartilage by polarized light and scanning electon microscopies (Abstract).* Paper presented at the Transactions of the 55th Annual Meeting of the Orthopaedic Research Society, Las Vegas, Nevada.

Changoor, A., Nelea, M., Tran-Khanh, N., Méthot, S., Fereydoonzad, L., Rossomacha, E., et al. (2009). *Analysis of hyaline structure in human osteochondral biopsies by polarization light microscopy (Abstract).* Paper presented at the Transactions of the International Cartilage Repair Society, Miami, Florida.

Changoor, A., Nelea, M., Tran-Khanh, N., Methot, S., Restrepo, A., Stanish, W. D., et al. (2010). *BST-CarGel™ treatment shows trend of improved collagen architecture and stratified hyaline structure compared to microfracture in 13 month biopsies from an interim analysis of a randomized controlled clinical trial (Abstract).* Paper presented at the International Cartilage Repair Society Congress, Sitges, Spain.

Changoor, A., Quenneville, E., Garon, M., Cloutier, L., Hurtig, M., & Buschmann, M. D. (2007). *Streaming Potential-Based Arthroscopic Device Discerns Topographical Differences In Cartilage Covered And Uncovered By Meniscus In Ovine Stifle Joints (Abstract).* Paper presented at the Annual Meeting of the Orthopaedic Research Society, San Diego, California, USA.

Changoor, A., Quenneville, E., Garon, M., Hurtig, M. B., & Buschmann, M. D. (2009). *Streaming Potential-Based Arthroscopic Device Can Detect Changes Immediately*

Following Localized Impact in an Equine Impact Model of Osteoarthritis (Abstract). Paper presented at the World Congress on Osteoarthritis, Montreal, Quebec, Canada.

Changoor, A., Tran-Khanh, N., Methot, S., Garon, M., Hurtig, M. B., Shive, M. S., et al. (2011). A polarized light microscopy method for accurate and reliable grading of collagen organization in cartilage repair. *Osteoarthritis Cartilage, 19*(1), 126-135.

Charlebois, M., McKee, M. D., & Buschmann, M. D. (2004). Nonlinear tensile properties of bovine articular cartilage and their variation with age and depth. *J Biomech Eng, 126*(2), 129-137.

Charnley, J. (1960). The lubrication of animal joints in relation to surgical reconstruction by arthroplasty. *Ann Rheum Dis, 19*, 10-19.

Chatterjee, S., & Hadi, A. S. (2006). Simple Linear Regression *Regression Analysis by Example* (Fourth Edition ed., pp. 21-52). Hoboken, New Jersey: John Wiley & Sons, Inc.

Chen, A. C., Bae, W. C., Schinagl, R. M., & Sah, R. L. (2001). Depth- and strain-dependent mechanical and electromechanical properties of full-thickness bovine articular cartilage in confined compression. *J Biomech, 34*(1), 1-12.

Chen, A. C., Nguyen, T. T., & Sah, R. L. (1997). Streaming potentials during the confined compression creep test of normal and proteoglycan-depleted cartilage. *Ann Biomed Eng, 25*(2), 269-277.

Chen, M. H., & Broom, N. (1998). On the ultrastructure of softened cartilage: a possible model for structural transformation. *J Anat, 192 (Pt 3)*, 329-341.

Chrisman, O. D., Ladenbauer-Bellis, I. M., Panjabi, M., & Goeltz, S. (1981). 1981 Nicolas Andry Award. The relationship of mechanical trauma and the early biochemical reactions of osteoarthritic cartilage. *Clin Orthop Relat Res*(161), 275-284.

Chu, C. R., Izzo, N. J., Irrgang, J. J., Ferretti, M., & Studer, R. K. (2007). Clinical diagnosis of potentially treatable early articular cartilage degeneration using optical coherence tomography. *J Biomed Opt, 12*(5), 051703.

Chu, C. R., Williams, A., Tolliver, D., Kwoh, C. K., Bruno, S., 3rd, & Irrgang, J. J. (2010). Clinical optical coherence tomography of early articular cartilage degeneration in patients with degenerative meniscal tears. *Arthritis Rheum, 62*(5), 1412-1420.

Clark, J. M., & Simonian, P. T. (1997). Scanning electron microscopy of "fibrillated" and "malacic" human articular cartilage: technical considerations. *Microsc Res Tech, 37*(4), 299-313.

Clarke, I. C. (1971). Articular cartilage: a review and scanning electron microscope study. 1. The interterritorial fibrillar architecture. *J Bone Joint Surg Br, 53*(4), 732-750.

Cohen, B., Lai, W. M., Chorney, G. S., Dick, H. M., & Mow, V. C. (1992). Unconfined compression of transversely-isotropic biphasic tissues. *Transactions of the ASME*, 187-190.

Cohen, B., Lai, W. M., & Mow, V. C. (1998). A transversely isotropic biphasic model for unconfined compression of growth plate and chondroepiphysis. *J Biomech Eng, 120*(4), 491-496.

Crawford, D. C., Heveran, C. M., Cannon, W. D., Jr., Foo, L. F., & Potter, H. G. (2009). An autologous cartilage tissue implant NeoCart for treatment of grade III chondral injury to the distal femur: prospective clinical safety trial at 2 years. *Am J Sports Med, 37*(7), 1334-1343.

Dodge, G. R., & Poole, A. R. (1989). Immunohistochemical detection and immunochemical analysis of type II collagen degradation in human normal, rheumatoid, and osteoarthritic articular cartilages and in explants of bovine articular cartilage cultured with interleukin 1. *J Clin Invest, 83*(2), 647-661.

Donohue, J. M., Buss, D., Oegema, T. R., Jr., & Thompson, R. C., Jr. (1983). The effects of indirect blunt trauma on adult canine articular cartilage. *J Bone Joint Surg Am, 65*(7), 948-957.

Duda, G. N., Eilers, M., Loh, L., Hoffman, J. E., Kaab, M., & Schaser, K. (2001). Chondrocyte death precedes structural damage in blunt impact trauma. *Clin Orthop Relat Res*(393), 302-309.

Eckstein, F., Hudelmaier, M., & Putz, R. (2006). The effects of exercise on human articular cartilage. *J Anat, 208*(4), 491-512.

Eckstein, F., Winzheimer, M., Hohe, J., Englmeier, K. H., & Reiser, M. (2001). Interindividual variability and correlation among morphological parameters of knee joint cartilage plates: analysis with three-dimensional MR imaging. *Osteoarthritis Cartilage, 9*(2), 101-111.

Elder, B. D., & Athanasiou, K. A. (2008). Effects of confinement on the mechanical properties of self-assembled articular cartilage constructs in the direction orthogonal to the confinement surface. *J Orthop Res, 26*(2), 238-246.

Eliasziw, M., Young, S. L., Woodbury, M. G., & Fryday-Field, K. (1994). Statistical methodology for the concurrent assessment of interrater and intrarater reliability: using goniometric measurements as an example. *Phys Ther, 74*(8), 777-788.

Elmore, S. M., Sokoloff, L., Norris, G., & Carmeci, P. (1963). Nature of "imperfect" elasticity of articular cartilage. *Journal of Applied Physiology, 18*(2), 393-396.

Eyre, D. (2002). Collagen of articular cartilage. *Arthritis Res, 4*(1), 30-35.

Fortin, M., Soulhat, J., Shirazi-Adl, A., Hunziker, E. B., & Buschmann, M. D. (2000). Unconfined compression of articular cartilage: nonlinear behavior and comparison with a fibril-reinforced biphasic model. *J Biomech Eng, 122*(2), 189-195.

Frank, E. H., & Grodzinsky, A. J. (1987). Cartilage electromechanics--I. Electrokinetic transduction and the effects of electrolyte pH and ionic strength. *J Biomech, 20*(6), 615-627.

Frank, E. H., Grodzinsky, A. J., Koob, T. J., & Eyre, D. R. (1987). Streaming potentials: a sensitive index of enzymatic degradation in articular cartilage. *J Orthop Res, 5*(4), 497-508.

Franz, T., Hasler, E. M., Hagg, R., Weiler, C., Jakob, R. P., & Mainil-Varlet, P. (2001). In situ compressive stiffness, biochemical composition, and structural integrity of articular cartilage of the human knee joint. *Osteoarthritis Cartilage, 9*(6), 582-592.

Frisbie, D. D., Cross, M. W., & McIlwraith, C. W. (2006). A comparative study of articular cartilage thickness in the stifle of animal species used in human pre-clinical studies compared to articular cartilage thickness in the human knee. *Vet Comp Orthop Traumatol, 19*(3), 142-146.

Frisbie, D. D., Oxford, J. T., Southwood, L., Trotter, G. W., Rodkey, W. G., Steadman, J. R., et al. (2003). Early events in cartilage repair after subchondral bone microfracture. *Clin Orthop Relat Res*(407), 215-227.

Fukui, N., Purple, C. R., & Sandell, L. J. (2001). Cell biology of osteoarthritis: the chondrocyte's response to injury. *Curr Rheumatol Rep, 3*(6), 496-505.

Gardner, D. L., Salter, D. M., & Oates, K. (1997). Advances in the microscopy of osteoarthritis. *Microsc Res Tech, 37*(4), 245-270.

Garon, M. (2007). *Conception et Validation d'une sonde arthroscopique pour l'évaluation des propriétés électromécaniques fonctionelles du cartilage articulaire.* Doctoral Dissertation, Ecole Polytechnique de Montreal, Montreal.

Garon, M., Cloutier, L., Legare, A., Quenneville, E., Shive, M. S., & Buschmann, M. D. (2007). *Reliability and Correlation to Human Articular Cartilage Mechanical Properties of a*

Streaming Potential based Arthroscopic Instrument (Abstract). Paper presented at the Annual Meeting of the Orthopaedic Research Society, San Diego, California, USA.

Garon, M., Legare, A., Guardo, R., Savard, P., & Buschmann, M. D. (2002). Streaming potentials maps are spatially resolved indicators of amplitude, frequency and ionic strength dependant responses of articular cartilage to load. *J Biomech, 35*(2), 207-216.

Gillogly, S. D., Voight, M., & Blackburn, T. (1998). Treatment of articular cartilage defects of the knee with autologous chondrocyte implantation. *J Orthop Sports Phys Ther, 28*(4), 241-251.

Goldring, S. R., & Goldring, M. B. (2004). The role of cytokines in cartilage matrix degeneration in osteoarthritis. *Clin Orthop Relat Res*(427 Suppl), S27-36.

Gooding, C. R., Bartlett, W., Bentley, G., Skinner, J. A., Carrington, R., & Flanagan, A. (2006). A prospective, randomised study comparing two techniques of autologous chondrocyte implantation for osteochondral defects in the knee: Periosteum covered versus type I/III collagen covered. *Knee, 13*(3), 203-210.

Gudas, R., Kalesinskas, R. J., Kimtys, V., Stankevicius, E., Toliusis, V., Bernotavicius, G., et al. (2005). A prospective randomized clinical study of mosaic osteochondral autologous transplantation versus microfracture for the treatment of osteochondral defects in the knee joint in young athletes. *Arthroscopy, 21*(9), 1066-1075.

Guilak, F., Ratcliffe, A., Lane, N., Rosenwasser, M. P., & Mow, V. C. (1994). Mechanical and biochemical changes in the superficial zone of articular cartilage in canine experimental osteoarthritis. *J Orthop Res, 12*(4), 474-484.

Gyarmati, J., Foldes, I., Kern, M., & Kiss, I. (1987). Morphological studies on the articular cartilage of old rats. *Acta Morphol Hung, 35*(3-4), 111-124.

Harris, E. D., Jr., & McCroskery, P. A. (1974). The influence of temperature and fibril stability on degradation of cartilage collagen by rheumatoid synovial collagenase. *N Engl J Med, 290*(1), 1-6.

Haut, R. C. (1989). Contact pressures in the patellofemoral joint during impact loading on the human flexed knee. *J Orthop Res, 7*(2), 272-280.

Haut, R. C., Ide, T. M., & De Camp, C. E. (1995). Mechanical responses of the rabbit patello-femoral joint to blunt impact. *J Biomech Eng, 117*(4), 402-408.

Heckman, J. D. (2006). Are validated questionnaires valid? *J Bone Joint Surg Am, 88*(2), 446.

Hedlund, H., Mengarelli-Widholm, S., Reinholt, F. P., & Svensson, O. (1993). Stereologic studies on collagen in bovine articular cartilage. *APMIS, 101*(2), 133-140.

Henderson, I., Lavigne, P., Valenzuela, H., & Oakes, B. (2007). Autologous chondrocyte implantation: superior biologic properties of hyaline cartilage repairs. *Clin Orthop Relat Res, 455*, 253-261.

Hodge, W. A., Carlson, K. L., Fijan, R. S., Burgess, R. G., Riley, P. O., Harris, W. H., et al. (1989). Contact pressures from an instrumented hip endoprosthesis. *J Bone Joint Surg Am, 71*(9), 1378-1386.

Hoemann, C. D. (2004). Molecular and biochemical assays of cartilage components *Cartilage and Osteoarthritis Volume 2: Structure and In Vivo Analysis* (Vol. 2, pp. 127-156): Humana Press.

Hoemann, C. D., Hurtig, M., Rossomacha, E., Sun, J., Chevrier, A., Shive, M. S., et al. (2005). Chitosan-glycerol phosphate/blood implants improve hyaline cartilage repair in ovine microfracture defects. *J Bone Joint Surg Am, 87*(12), 2671-2686.

Hoemann, C. D., Tran-Khanh, N., Methot, S., Chen, G., Marchand, C., Lascau-Coman, V., et al. (2010). *Correlation of tissue histomorphometry with ICRS histology scores in biopsies obtained from a randomized controlled clinical trial comparing BST-CarGel™ versus microfracture (Abstract).* Paper presented at the International Cartilage Repair Society Congress, Sitges, Spain.

Hollander, A. P., Pidoux, I., Reiner, A., Rorabeck, C., Bourne, R., & Poole, A. R. (1995). Damage to type II collagen in aging and osteoarthritis starts at the articular surface, originates around chondrocytes, and extends into the cartilage with progressive degeneration. *J Clin Invest, 96*(6), 2859-2869.

Hughes, L. C., Archer, C. W., & ap Gwynn, I. (2005). The ultrastructure of mouse articular cartilage: collagen orientation and implications for tissue functionality. A polarised light and scanning electron microscope study and review. *Eur Cell Mater, 9*, 68-84.

Hunziker, E. B. (1992). Articular cartilage structure in humans and experimental animals. In K. E. Kuettner, R. Schleyerbach, J. G. Peyron & V. C. Hascall (Eds.), *Articular cartilage and osteoarthritis: workshop conference Hoechst Werk Kalle-Albert* (pp. 183-199). New York: Raven Press.

Hunziker, E. B. (2002). Articular cartilage repair: basic science and clinical progress. A review of the current status and prospects. *Osteoarthritis Cartilage, 10*(6), 432-463.

Hunziker, E. B. (2002). Articular cartilage repair: basic science and clinical progress. A review of the current status and prospects. *Osteoarthritis Cartilage, 10*(6), 432-463.

Hunziker, E. B. (2009). The elusive path to cartilage regeneration. *Adv Mater, 21*(32-33), 3419-3424.

Hunziker, E. B., Kapfinger, E., & Geiss, J. (2007). The structural architecture of adult mammalian articular cartilage evolves by a synchronized process of tissue resorption and neoformation during postnatal development. *Osteoarthritis Cartilage, 15*(4), 403-413.

Hunziker, E. B., Quinn, T. M., & Hauselmann, H. J. (2002). Quantitative structural organization of normal adult human articular cartilage. *Osteoarthritis Cartilage, 10*(7), 564-572.

Hwang, W. S., Li, B., Jin, L. H., Ngo, K., Schachar, N. S., & Hughes, G. N. (1992). Collagen fibril structure of normal, aging, and osteoarthritic cartilage. *J Pathol, 167*(4), 425-433.

Hwang, W. S., Ngo, K., & Saito, K. (1990). Silver staining of collagen fibrils in cartilage. *Histochem J, 22*(9), 487-490.

Hyttinen, M. M., Arokoski, J. P., Parkkinen, J. J., Lammi, M. J., Lapvetelainen, T., Mauranen, K., et al. (2001). Age matters: collagen birefringence of superficial articular cartilage is increased in young guinea-pigs but decreased in older animals after identical physiological type of joint loading. *Osteoarthritis Cartilage, 9*(8), 694-701.

Hyttinen, M. M., Holopainen, J., van Weeren, P. R., Firth, E. C., Helminen, H. J., & Brama, P. A. (2009). Changes in collagen fibril network organization and proteoglycan distribution in equine articular cartilage during maturation and growth. *J Anat, 215*(5), 584-591.

Isaac, D. I., Meyer, E. G., Kopke, K. S., & Haut, R. C. (2010). Chronic changes in the rabbit tibial plateau following blunt trauma to the tibiofemoral joint. *J Biomech, 43*(9), 1682-1688.

Jeffrey, J. E., Gregory, D. W., & Aspden, R. M. (1995). Matrix damage and chondrocyte viability following a single impact load on articular cartilage. *Arch Biochem Biophys, 322*(1), 87-96.

Julkunen, P. (2008). *Relationships between Structure, Composition and Function of Articular Cartilage.* Doctoral Dissertation, University of Kuopio, Kuopio.

Julkunen, P., Harjula, T., Iivarinen, J., Marjanen, J., Seppanen, K., Narhi, T., et al. (2009). Biomechanical, biochemical and structural correlations in immature and mature rabbit articular cartilage. *Osteoarthritis Cartilage, 17*(12), 1628-1638.

Jurvelin, J. S., Buschmann, M. D., & Hunziker, E. B. (1997). Optical and mechanical determination of Poisson's ratio of adult bovine humeral articular cartilage. *J Biomech, 30*(3), 235-241.

Kaab, M. J., Gwynn, I. A., & Notzli, H. P. (1998). Collagen fibre arrangement in the tibial plateau articular cartilage of man and other mammalian species. *J Anat, 193 (Pt 1)*, 23-34.

Kaleva, E., Viren, T., Saarakkala, S., Sahlman, J., Sirola, J., Puhakka, J., et al. (2011). *Ultrasound arthroscopy of articular cartilage in human knee joint in vivo: a potential diagnostic method?(Abstract).* Paper presented at the Annual Meeting of the Orthopaedic Research Society, Long Beach, California, USA.

Kandel, R. A., Grynpas, M., Pilliar, R., Lee, J., Wang, J., Waldman, S., et al. (2006). Repair of osteochondral defects with biphasic cartilage-calcium polyphosphate constructs in a sheep model. *Biomaterials, 27*(22), 4120-4131.

Kelly, T. A., Ng, K. W., Wang, C. C., Ateshian, G. A., & Hung, C. T. (2006). Spatial and temporal development of chondrocyte-seeded agarose constructs in free-swelling and dynamically loaded cultures. *J Biomech, 39*(8), 1489-1497.

Kempson, G. E., Spivey, C. J., Swanson, S. A., & Freeman, M. A. (1971). Patterns of cartilage stiffness on normal and degenerate human femoral heads. *J Biomech, 4*(6), 597-609.

Kennedy, E. A., Tordonado, D. S., & Duma, S. M. (2007). Effects of freezing on the mechanical properties of articular cartilage. *Biomed Sci Instrum, 43*, 342-347.

Kiefer, G. N., Sundby, K., McAllister, D., Shrive, N. G., Frank, C. B., Lam, T., et al. (1989). The effect of cryopreservation on the biomechanical behavior of bovine articular cartilage. *J Orthop Res, 7*(4), 494-501.

Kim, D. K., Ceckler, T. L., Hascall, V. C., Calabro, A., & Balaban, R. S. (1993). Analysis of water-macromolecule proton magnetization transfer in articular cartilage. *Magn Reson Med, 29*(2), 211-215.

Kiraly, K., Hyttinen, M. M., Lapvetelainen, T., Elo, M., Kiviranta, I., Dobai, J., et al. (1997). Specimen preparation and quantification of collagen birefringence in unstained sections of articular cartilage using image analysis and polarizing light microscopy. *Histochem J, 29*(4), 317-327.

Kish, G., Modis, L., & Hangody, L. (1999). Osteochondral mosaicplasty for the treatment of focal chondral and osteochondral lesions of the knee and talus in the athlete. Rationale, indications, techniques, and results. *Clin Sports Med, 18*(1), 45-66.

Kleemann, R. U., Krocker, D., Cedraro, A., Tuischer, J., & Duda, G. N. (2005). Altered cartilage mechanics and histology in knee osteoarthritis: relation to clinical assessment (ICRS Grade). *Osteoarthritis Cartilage, 13*(11), 958-963.

Knutsen, G., Drogset, J. O., Engebretsen, L., Grontvedt, T., Isaksen, V., Ludvigsen, T. C., et al. (2007). A randomized trial comparing autologous chondrocyte implantation with microfracture. Findings at five years. *J Bone Joint Surg Am, 89*(10), 2105-2112.

Knutsen, G., Engebretsen, L., Ludvigsen, T. C., Drogset, J. O., Grontvedt, T., Solheim, E., et al. (2004). Autologous chondrocyte implantation compared with microfracture in the knee. A randomized trial. *J Bone Joint Surg Am, 86-A*(3), 455-464.

Kon, E., Delcogliano, M., Filardo, G., Fini, M., Giavaresi, G., Francioli, S., et al. (2010). Orderly osteochondral regeneration in a sheep model using a novel nano-composite multilayered biomaterial. *J Orthop Res, 28*(1), 116-124.

Korhonen, R. K. (2003). *Experimental Analysis and Finite Element Modeling of Normal and Degraded Articular Cartilage.* Doctoral Dissertation, University of Kuopio, Kuopio.

Korhonen, R. K., Laasanen, M. S., Toyras, J., Lappalainen, R., Helminen, H. J., & Jurvelin, J. S. (2003). Fibril reinforced poroelastic model predicts specifically mechanical behavior of normal, proteoglycan depleted and collagen degraded articular cartilage. *J Biomech, 36*(9), 1373-1379.

Korhonen, R. K., Wong, M., Arokoski, J., Lindgren, R., Helminen, H. J., Hunziker, E. B., et al. (2002). Importance of the superficial tissue layer for the indentation stiffness of articular cartilage. *Med Eng Phys, 24*(2), 99-108.

Kovach, I. S., & Athanasiou, K. A. (1997). Small-angle HeNe laser light scatter and the compressive modulus of articular cartilage. *J Orthop Res, 15*(3), 437-441.

Kurkijarvi, J. E., Nissi, M. J., Rieppo, J., Toyras, J., Kiviranta, I., Nieminen, M. T., et al. (2008). The zonal architecture of human articular cartilage described by T2 relaxation time in the presence of Gd-DTPA2. *Magn Reson Imaging, 26*(5), 602-607.

Kurz, B., Lemke, A. K., Fay, J., Pufe, T., Grodzinsky, A. J., & Schunke, M. (2005). Pathomechanisms of cartilage destruction by mechanical injury. *Ann Anat, 187*(5-6), 473-485.

Laasanen, M. S., Toyras, J., Hirvonen, J., Saarakkala, S., Korhonen, R. K., Nieminen, M. T., et al. (2002). Novel mechano-acoustic technique and instrument for diagnosis of cartilage degeneration. *Physiol Meas, 23*(3), 491-503.

Langelier, E., & Buschmann, M. D. (2003). Increasing strain and strain rate strengthen transient stiffness but weaken the response to subsequent compression for articular cartilage in unconfined compression. *J Biomech, 36*(6), 853-859.

Langsjo, T. K., Vasara, A. I., Hyttinen, M. M., Lammi, M. J., Kaukinen, A., Helminen, H. J., et al. (2010). Quantitative Analysis of Collagen Network Structure and Fibril Dimensions in Cartilage Repair with Autologous Chondrocyte Transplantation. *Cells Tissues Organs, 192(6),351-60*.

Legare, A., Garon, M., Guardo, R., Savard, P., Poole, A. R., & Buschmann, M. D. (2002). Detection and analysis of cartilage degeneration by spatially resolved streaming potentials. *J Orthop Res, 20*(4), 819-826.

Levin, A., Burton-Wurster, N., Chen, C. T., & Lust, G. (2001). Intercellular signaling as a cause of cell death in cyclically impacted cartilage explants. *Osteoarthritis Cartilage, 9*(8), 702-711.

Li, L., Shirazi-Adl, A., & Buschmann, M. D. (2003). Investigation of mechanical behavior of articular cartilage by fibril reinforced poroelastic models. *Biorheology, 40*(1-3), 227-233.

Li, L. P., Buschmann, M. D., & Shirazi-Adl, A. (2003). Strain-rate dependent stiffness of articular cartilage in unconfined compression. *J Biomech Eng, 125*(2), 161-168.

Li, L. P., Korhonen, R. K., Iivarinen, J., Jurvelin, J. S., & Herzog, W. (2008). Fluid pressure driven fibril reinforcement in creep and relaxation tests of articular cartilage. *Med Eng Phys, 30*(2), 182-189.

Li, L. P., Soulhat, J., Buschmann, M. D., & Shirazi-Adl, A. (1999). Nonlinear analysis of cartilage in unconfined ramp compression using a fibril reinforced poroelastic model. *Clin Biomech (Bristol, Avon), 14*(9), 673-682.

Li, X., Martin, S., Pitris, C., Ghanta, R., Stamper, D. L., Harman, M., et al. (2005). High-resolution optical coherence tomographic imaging of osteoarthritic cartilage during open knee surgery. *Arthritis Res Ther, 7*(2), R318-323.

Li, Z., Yasuda, Y., Li, W., Bogyo, M., Katz, N., Gordon, R. E., et al. (2004). Regulation of collagenase activities of human cathepsins by glycosaminoglycans. *J Biol Chem, 279*(7), 5470-5479.

Lippiello, L., Hall, D., & Mankin, H. J. (1977). Collagen synthesis in normal and osteoarthritic human cartilage. *J Clin Invest, 59*(4), 593-600.

Liu, B., Harman, M., Giattina, S., Stamper, D. L., Demakis, C., Chilek, M., et al. (2006). Characterizing of tissue microstructure with single-detector polarization-sensitive optical coherence tomography. *Appl Opt, 45*(18), 4464-4479.

Loeser, R. F. (2006). Molecular mechanisms of cartilage destruction: mechanics, inflammatory mediators, and aging collide. *Arthritis Rheum, 54*(5), 1357-1360.

Lotz, M. K. (2010). New developments in osteoarthritis. Posttraumatic osteoarthritis: pathogenesis and pharmacological treatment options. *Arthritis Res Ther, 12*(3), 211.

Lotz, M. K., & Kraus, V. B. (2010). Correction: Posttraumatic osteoarthritis: pathogenesis and pharmacological treatment options. *Arthritis Res Ther, 12*(6), 408.

Lu, X. L., Miller, C., Chen, F. H., Guo, X. E., & Mow, V. C. (2007). The generalized triphasic correspondence principle for simultaneous determination of the mechanical properties and proteoglycan content of articular cartilage by indentation. *J Biomech, 40*(11), 2434-2441.

Lyyra, T., Arokoski, J. P., Oksala, N., Vihko, A., Hyttinen, M., Jurvelin, J. S., et al. (1999). Experimental validation of arthroscopic cartilage stiffness measurement using enzymatically degraded cartilage samples. *Phys Med Biol, 44*(2), 525-535.

Lyyra, T., Jurvelin, J., Pitkanen, P., Vaatainen, U., & Kiviranta, I. (1995). Indentation instrument for the measurement of cartilage stiffness under arthroscopic control. *Med Eng Phys, 17*(5), 395-399.

Madry, H., van Dijk, C. N., & Mueller-Gerbl, M. (2010). The basic science of the subchondral bone. *Knee Surg Sports Traumatol Arthrosc, 18*(4), 419-433.

Mainil-Varlet, P., Aigner, T., Brittberg, M., Bullough, P., Hollander, A., Hunziker, E., et al. (2003). Histological assessment of cartilage repair: a report by the Histology Endpoint Committee of the International Cartilage Repair Society (ICRS). *J Bone Joint Surg Am, 85-A Suppl 2*, 45-57.

Mainil-Varlet, P., Van Damme, B., Nesic, D., Knutsen, G., Kandel, R., & Roberts, S. (2010). A New Histology Scoring System for the Assessment of the Quality of Human Cartilage Repair: ICRS II. *Am J Sports Med, 38(5), 880-890.*

Mandelbaum, B., & Waddell, D. (2005). Etiology and pathophysiology of osteoarthritis. *Orthopedics, 28*(2 Suppl), s207-214.

Mankin, H. J. (1982). The response of articular cartilage to mechanical injury. *J Bone Joint Surg Am, 64*(3), 460-466.

Maroudas, A. (1967a). *Fixed charge density in articular cartilage (Abstract).* Paper presented at the 7th International Conference on Medical and Biological Engineering, Stockholm, Sweeden.

Maroudas, A. (1967b). *Fixed Charge Density in Articular Cartilage (Abstract).* Paper presented at the 7th International Conference on Medical and Biological Engineering, Stockholm, Sweden.

Maroudas, A. (1968). Physicochemical properties of cartilage in the light of ion exchange theory. *Biophys J, 8*(5), 575-595.

Maroudas, A., Muir, H., & Wingham, J. (1969). The correlation of fixed negative charge with glycosaminoglycan content of human articular cartilage. *Biochim Biophys Acta, 177*(3), 492-500.

Marx, R. G., Stump, T. J., Jones, E. C., Wickiewicz, T. L., & Warren, R. F. (2001). Development and evaluation of an activity rating scale for disorders of the knee. *Am J Sports Med, 29*(2), 213-218.

Matthews, L. S., Sonstegard, D. A., & Henke, J. A. (1977). Load bearing characteristics of the patello-femoral joint. *Acta Orthop Scand, 48*(5), 511-516.

Maurice, D. M. (1957). The structure and transparency of the cornea. *J Physiol, 136*(2), 263-286.

McGraw, K. O., & Wong, S. P. (1996a). Forming inferences about some intraclass correlation coefficients. *Psychological Methods, 1*(1), 30-46.

McGraw, K. O., & Wong, S. P. (1996b). Forming inferences about some intraclass correlations coefficients (vol 1, pg 30, 1996). *Psychological Methods, 1*(4), 390-390.

Meachim, G. (1972). Light microscopy of Indian ink preparations of fibrillated cartilage. *Ann Rheum Dis, 31*(6), 457-464.

Meachim, G., Denham, D., Emery, I. H., & Wilkinson, P. H. (1974). Collagen alignments and artificial splits at the surface of human articular cartilage. *J Anat, 118*(Pt 1), 101-118.

Méthot, S., Hoemann, C., Rossomacha, E., Garon, M., Shive, M. S., Tremblay, J., et al. (2009). *ICRS I and ICRS II scoring of human osteochondral biopsies: Reader variability and*

sensitivity to staining method (Abstract). Paper presented at the Transactions of the International Cartilage Repair Society, Miami, Florida.

Methot, S., Hoemann, C., Rossomacha, E., Restrepo, A., Stanish, W. D., MacDonald, P., et al. (2010). *ICRS histology scores of biopsies from an interim analysis of a randomized controlled clinical trial show significant improvement in tissue quality at 13 months for BST-CarGel™ versus microfracture (Abstract).* Paper presented at the International Cartilage Repair Society Congress, Sitges, Spain.

Minns, R. J., & Steven, F. S. (1977). The collagen fibril organization in human articular cartilage. *J Anat, 123*(Pt 2), 437-457.

Mithoefer, K., McAdams, T., Williams, R. J., Kreuz, P. C., & Mandelbaum, B. R. (2009). Clinical efficacy of the microfracture technique for articular cartilage repair in the knee: an evidence-based systematic analysis. *Am J Sports Med, 37*(10), 2053-2063.

Mlynarik, V., Szomolanyi, P., Toffanin, R., Vittur, F., & Trattnig, S. (2004). Transverse relaxation mechanisms in articular cartilage. *J Magn Reson, 169*(2), 300-307.

Modis, L. (1991). Physical backgrounds of polarization microscopy. In L. Modis (Ed.), *Organization of the extracellular matrix: a polarization microscopic approach* (pp. 9-30). Boca Raton: CRC Press.

Moger, C. J., Arkill, K. P., Barrett, R., Bleuet, P., Ellis, R. E., Green, E. M., et al. (2009). Cartilage collagen matrix reorientation and displacement in response to surface loading. *J Biomech Eng, 131*(3), 031008.

Morel, V., Berutto, C., & Quinn, T. M. (2006). Effects of damage in the articular surface on the cartilage response to injurious compression in vitro. *J Biomech, 39*(5), 924-930.

Moriya, T., Wada, Y., Watanabe, A., Sasho, T., Nakagawa, K., Mainil-Varlet, P., et al. (2007). Evaluation of reparative cartilage after autologous chondrocyte implantation for osteochondritis dissecans: histology, biochemistry, and MR imaging. *J Orthop Sci, 12*(3), 265-273.

Moseley, J. B., O'Malley, K., Petersen, N. J., Menke, T. J., Brody, B. A., Kuykendall, D. H., et al. (2002). A controlled trial of arthroscopic surgery for osteoarthritis of the knee. *N Engl J Med, 347*(2), 81-88.

Mosher, T. J., & Dardzinski, B. J. (2004). Cartilage MRI T2 relaxation time mapping: overview and applications. *Semin Musculoskelet Radiol, 8*(4), 355-368.

Mow, V. C., Gibbs, M. C., Lai, W. M., Zhu, W. B., & Athanasiou, K. A. (1989). Biphasic indentation of articular cartilage--II. A numerical algorithm and an experimental study. *J Biomech, 22*(8-9), 853-861.

Mow, V. C., & Lai, W. M. (1979). Mechanics of Animal Joints. *Annual Review of Fluid Mechanics, 11*(1), 247-288.

Mow, V. C., Kuei, S. C., Lai, W. M., & Armstrong, C. G. (1980). Biphasic creep and stress relaxation of articular cartilage in compression? Theory and experiments. *J Biomech Eng, 102*(1), 73-84.

Muldrew, K., Hurtig, M., Novak, K., Schachar, N., & McGann, L. E. (1994). Localization of freezing injury in articular cartilage. *Cryobiology, 31*(1), 31-38.

Muldrew, K., Novak, K., Yang, H., Zernicke, R., Schachar, N. S., & McGann, L. E. (2000). Cryobiology of articular cartilage: ice morphology and recovery of chondrocytes. *Cryobiology, 40*(2), 102-109.

Neame, P. J. (1993). Extracellular Matrix of Cartilge: Proteoglycans. In J. F. Woessner & D. S. Howell (Eds.), *Joint cartilage degeneration: basic and clinical aspects* (pp. 109-138). New York: Marcel Dekker, Inc.

Nelea, M., Changoor, A., Méthot, S., Garon, M., Shive, M. S., Tremblay, J., et al. (2009). *Collagen ultrastructure in human osteochondral biopsies (Abstract).* Paper presented at the Transactions of the International Cartilage Repair Society, Miami, Florida.

Nelson, F., Dahlberg, L., Laverty, S., Reiner, A., Pidoux, I., Ionescu, M., et al. (1998). Evidence for altered synthesis of type II collagen in patients with osteoarthritis. *J Clin Invest, 102*(12), 2115-2125.

Newberry, W. N., Mackenzie, C. D., & Haut, R. C. (1998). Blunt impact causes changes in bone and cartilage in a regularly exercised animal model. *J Orthop Res, 16*(3), 348-354.

Niederauer, G. G., Niederauer, G. M., Cullen, L. C., Jr., Athanasiou, K. A., Thomas, J. B., & Niederauer, M. Q. (2004). Correlation of cartilage stiffness to thickness and level of degeneration using a handheld indentation probe. *Ann Biomed Eng, 32*(3), 352-359.

Nissi, M. J., Rieppo, J., Toyras, J., Laasanen, M. S., Kiviranta, I., Jurvelin, J. S., et al. (2006). T(2) relaxation time mapping reveals age- and species-related diversity of collagen network architecture in articular cartilage. *Osteoarthritis Cartilage, 14*(12), 1265-1271.

Nixon, A. J., & Fortier, L. A. (2001). *New Horizons in articular cartilage repair.* Paper presented at the Proceedings of the 47th Annual Convention of the American Association of Equine Practitioners, San Diego, CA, USA.

O'Hara, B. P., Urban, J. P., & Maroudas, A. (1990). Influence of cyclic loading on the nutrition of articular cartilage. *Ann Rheum Dis, 49*(7), 536-539.

Ortmann, R. (1975). Use of polarized light for quantitative determination of the adjustment of the tangential fibres in articular cartilage. *Anat Embryol (Berl), 148*(2), 109-120.

Pacifici, M., Koyama, E., Shibukawa, Y., Wu, C., Tamamura, Y., Enomoto-Iwamoto, M., et al. (2006). Cellular and molecular mechanisms of synovial joint and articular cartilage formation. *Ann N Y Acad Sci, 1068*, 74-86.

Palmer, A. W., Wilson, C. G., Baum, E. J., & Levenston, M. E. (2009). Composition-function relationships during IL-1-induced cartilage degradation and recovery. *Osteoarthritis Cartilage, 17*(8), 1029-1039.

Pan, Y., Li, Z., Xie, T., & Chu, C. R. (2003). Hand-held arthroscopic optical coherence tomography for in vivo high-resolution imaging of articular cartilage. *J Biomed Opt, 8*(4), 648-654.

Panula, H. E., Hyttinen, M. M., Arokoski, J. P., Langsjo, T. K., Pelttari, A., Kiviranta, I., et al. (1998). Articular cartilage superficial zone collagen birefringence reduced and cartilage thickness increased before surface fibrillation in experimental osteoarthritis. *Ann Rheum Dis, 57*(4), 237-245.

Park, S., Krishnan, R., Nicoll, S. B., & Ateshian, G. A. (2003). Cartilage interstitial fluid load support in unconfined compression. *J Biomech, 36*(12), 1785-1796.

Parsons, J. R., & Black, J. (1977). The viscoelastic shear behavior of normal rabbit articular cartilage. *J Biomech, 10*(1), 21-29.

Patwari, P., Fay, J., Cook, M. N., Badger, A. M., Kerin, A. J., Lark, M. W., et al. (2001). In vitro models for investigation of the effects of acute mechanical injury on cartilage. *Clin Orthop Relat Res*(391 Suppl), S61-71.

Pennock, A. T., Robertson, C. M., Wagner, F., Harwood, F. L., Bugbee, W. D., & Amiel, D. (2006). Does subchondral bone affect the fate of osteochondral allografts during storage? *Am J Sports Med, 34*(4), 586-591.

Poole, C. A. (1993). The stucture and function of articular cartilage matrices. In J. F. Woessner & D. S. Howell (Eds.), *Joint cartilage degeneration: basic and clinical aspects* (pp. 1-35). New York: Marcel Dekker, Inc.

Poole, C. A. (1997). Articular cartilage chondrons: form, function and failure. *J Anat, 191 (Pt 1)*, 1-13.

Quinn, T. M., Allen, R. G., Schalet, B. J., Perumbuli, P., & Hunziker, E. B. (2001). Matrix and cell injury due to sub-impact loading of adult bovine articular cartilage explants: effects of strain rate and peak stress. *J Orthop Res, 19*(2), 242-249.

Redler, I. (1974). A scanning electron microscopic study of human normal and osteoarthritic articular cartilage. *Clin Orthop Relat Res*(103), 262-268.

Repo, R. U., & Finlay, J. B. (1977). Survival of articular cartilage after controlled impact. *J Bone Joint Surg Am, 59*(8), 1068-1076.

Responte, D. J., Natoli, R. M., & Athanasiou, K. A. (2007). Collagens of articular cartilage: structure, function, and importance in tissue engineering. *Crit Rev Biomed Eng, 35*(5), 363-411.

Richardson, J. B., Caterson, B., Evans, E. H., Ashton, B. A., & Roberts, S. (1999). Repair of human articular cartilage after implantation of autologous chondrocytes. *J Bone Joint Surg Br, 81*(6), 1064-1068.

Rieppo, J., Hallikainen, J., Jurvelin, J. S., Kiviranta, I., Helminen, H. J., & Hyttinen, M. M. (2008). Practical considerations in the use of polarized light microscopy in the analysis of the collagen network in articular cartilage. *Microsc Res Tech, 71*(4), 279-287.

Rieppo, J., Hyttinen, M. M., Halmesmaki, E., Ruotsalainen, H., Vasara, A., Kiviranta, I., et al. (2009). Changes in spatial collagen content and collagen network architecture in porcine articular cartilage during growth and maturation. *Osteoarthritis Cartilage, 17*(4), 448-455.

Rieppo, J., Toyras, J., Nieminen, M. T., Kovanen, V., Hyttinen, M. M., Korhonen, R. K., et al. (2003). Structure-function relationships in enzymatically modified articular cartilage. *Cells Tissues Organs, 175*(3), 121-132.

Riesle, J., Hollander, A. P., Langer, R., Freed, L. E., & Vunjak-Novakovic, G. (1998). Collagen in tissue-engineered cartilage: types, structure, and crosslinks. *J Cell Biochem, 71*(3), 313-327.

Roberts, S., Darby, A. J., Menage, J., Evans, E. H., & Richardson, J. B. (2001). A histological assessment of ACI-treated patients as an outcome of cartilage repair (Abstract). *Int J Exp Path, 82*, A18-19.

Roberts, S., McCall, I. W., Darby, A. J., Menage, J., Evans, H., Harrison, P. E., et al. (2003). Autologous chondrocyte implantation for cartilage repair: monitoring its success by magnetic resonance imaging and histology. *Arthritis Res Ther, 5*(1), R60-73.

Roberts, S., Menage, J., Sandell, L. J., Evans, E. H., & Richardson, J. B. (2009). Immunohistochemical study of collagen types I and II and procollagen IIA in human cartilage repair tissue following autologous chondrocyte implantation. *Knee, 16*(5), 398-404.

Rodrigo, J. J., Thompson, E., & Travis, C. (1987). Deep-freezing versus 4 degrees preservation of avascular osteocartilaginous shell allografts in rats. *Clin Orthop Relat Res*(218), 268-275.

Roos, E. M., & Lohmander, L. S. (2003). The Knee injury and Osteoarthritis Outcome Score (KOOS): from joint injury to osteoarthritis. *Health Qual Life Outcomes, 1*, 64.

Rosenberg, L. (1975). Structure of cartilage proteoglycans. In P. M. C. Burleigh & A. R. Poole (Eds.), *Dynamics of Connective Tissue Macromolecules* (pp. 105-124). North Holland.

Rutgers, M., van Pelt, M. J., Dhert, W. J., Creemers, L. B., & Saris, D. B. (2010). Evaluation of histological scoring systems for tissue-engineered, repaired and osteoarthritic cartilage. *Osteoarthritis Cartilage, 18*(1), 12-23.

Saarakkala, S., Korhonen, R. K., Laasanen, M. S., Toyras, J., Rieppo, J., & Jurvelin, J. S. (2004). Mechano-acoustic determination of Young's modulus of articular cartilage. *Biorheology, 41*(3-4), 167-179.

Sandell, L. J., & Aigner, T. (2001). Articular cartilage and changes in arthritis. An introduction: cell biology of osteoarthritis. *Arthritis Res, 3*(2), 107-113.

Saris, D. B., Vanlauwe, J., Victor, J., Haspl, M., Bohnsack, M., Fortems, Y., et al. (2008). Characterized chondrocyte implantation results in better structural repair when treating symptomatic cartilage defects of the knee in a randomized controlled trial versus microfracture. *Am J Sports Med, 36*(2), 235-246.

Schachar, N. S., Cucheran, D. J., McGann, L. E., Novak, K. A., & Frank, C. B. (1994). Metabolic activity of bovine articular cartilage during refrigerated storage. *J Orthop Res, 12*(1), 15-20.

Schenk, R. K., Eggli, P. S., & Hunziker, E. B. (1986). Articular Cartilage Morphology. In K. Kuettner, R. Schleyerbach & V. C. Hascall (Eds.), *Articular Cartilage Biochemistry* (pp. 3-22). New York: Raven Press.

Scott, C. C., & Athanasiou, K. A. (2006). Mechanical impact and articular cartilage. *Crit Rev Biomed Eng, 34*(5), 347-378.

Selmi, T. A., Verdonk, P., Chambat, P., Dubrana, F., Potel, J. F., Barnouin, L., et al. (2008). Autologous chondrocyte implantation in a novel alginate-agarose hydrogel: outcome at two years. *J Bone Joint Surg Br, 90*(5), 597-604.

Sernert, N., Kartus, J., Kohler, K., Stener, S., Larsson, J., Eriksson, B. I., et al. (1999). Analysis of subjective, objective and functional examination tests after anterior cruciate ligament reconstruction. A follow-up of 527 patients. *Knee Surg Sports Traumatol Arthrosc, 7*(3), 160-165.

Shive, M. S., Hoemann, C. D., Restrepo, A., Hurtig, M. B., Duval, N., Ranger, P., et al. (2006). BST-CarGel: In situ chondroinduction for cartilage repair. *Operative Techniques in Orthopaedics, 16*, 271-278.

Shrout, P. E., & Fleiss, J. L. (1979). Intraclass correlations: uses in assessing rater reliability. *Psychol Bull, 86*(2), 420-428.

Silver, F. H., Bradica, G., & Tria, A. (2001). Relationship among biomechanical, biochemical, and cellular changes associated with osteoarthritis. *Crit Rev Biomed Eng, 29*(4), 373-391.

Soulhat, J., Buschmann, M. D., & Shirazi-Adl, A. (1999). A fibril-network-reinforced biphasic model of cartilage in unconfined compression. *J Biomech Eng, 121*(3), 340-347.

Spahn, G., Klinger, H. M., & Hofmann, G. O. (2009). How valid is the arthroscopic diagnosis of cartilage lesions? Results of an opinion survey among highly experienced arthroscopic surgeons. *Arch Orthop Trauma Surg, 129*(8), 1117-1121.

Speer, D. P., & Dahners, L. (1979). The collagenous architecture of articular cartilage. Correlation of scanning electron microscopy and polarized light microscopy observations. *Clin Orthop Relat Res*(139), 267-275.

Stanish, W. D., Restrepo, A., MacDonald, P., Mohtadi, N., Marks, P., Malo, M., et al. (2010). *A randomized, multicenter clinical trial comparing BST-CarGel™ to microfracture in repair of focal articular cartilage lesions on the femoral condyle: interim results from 41 patients (Abstract).* Paper presented at the International Cartilage Repair Society Congress, Sitges, Spain.

Sun, D. D., Guo, X. E., Likhitpanichkul, M., Lai, W. M., & Mow, V. C. (2004). The influence of the fixed negative charges on mechanical and electrical behaviors of articular cartilage under unconfined compression. *J Biomech Eng, 126*(1), 6-16.

Swann, A. C. (1988). *The Effect of Mechanical Stress on the Stiffness of Articular Cartilage and its Role in the Aetiology of Osteoarthrosis.* Doctoral Dissertation, University of Leeds, Leeds.

Szarko, M., Muldrew, K., & Bertram, J. E. (2010). Freeze-thaw treatment effects on the dynamic mechanical properties of articular cartilage. *BMC Musculoskelet Disord, 11*, 231.

Tegner, Y., & Lysholm, J. (1985). Rating systems in the evaluation of knee ligament injuries. *Clin Orthop Relat Res*(198), 43-49.

Temple-Wong, M. M., Bae, W. C., Chen, M. Q., Bugbee, W. D., Amiel, D., Coutts, R. D., et al. (2009). Biomechanical, structural, and biochemical indices of degenerative and

osteoarthritic deterioration of adult human articular cartilage of the femoral condyle. *Osteoarthritis Cartilage, 17(11), 1469-1476*.

Thambyah, A., Nather, A., & Goh, J. (2006). Mechanical properties of articular cartilage covered by the meniscus. *Osteoarthritis Cartilage, 14*(6), 580-588.

Thibault, M., Poole, A. R., & Buschmann, M. D. (2002). Cyclic compression of cartilage/bone explants in vitro leads to physical weakening, mechanical breakdown of collagen and release of matrix fragments. *J Orthop Res, 20*(6), 1265-1273.

Thomas, V. J., Jimenez, S. A., Brighton, C. T., & Brown, N. (1984). Sequential changes in the mechanical properties of viable articular cartilage stored in vitro. *J Orthop Res, 2*(1), 55-60.

Thompson, R. C., Jr., Oegema, T. R., Jr., Lewis, J. L., & Wallace, L. (1991). Osteoarthrotic changes after acute transarticular load. An animal model. *J Bone Joint Surg Am, 73*(7), 990-1001.

Tomford, W. W., Fredericks, G. R., & Mankin, H. J. (1984). Studies on cryopreservation of articular cartilage chondrocytes. *J Bone Joint Surg Am, 66*(2), 253-259.

Torzilli, P. A., Grigiene, R., Borrelli, J., Jr., & Helfet, D. L. (1999). Effect of impact load on articular cartilage: cell metabolism and viability, and matrix water content. *J Biomech Eng, 121*(5), 433-441.

Toyras, J., Korhonen, R. K., Voutilainen, T., Jurvelin, J. S., & Lappalainen, R. (2005). Improvement of arthroscopic cartilage stiffness probe using amorphous diamond coating. *J Biomed Mater Res B Appl Biomater, 73*(1), 15-22.

Toyras, J., Nieminen, H. J., Laasanen, M. S., Nieminen, M. T., Korhonen, R. K., Rieppo, J., et al. (2002). Ultrasonic characterization of articular cartilage. *Biorheology, 39*(1-2), 161-169.

Trattnig, S., Domayer, S., Welsch, G. W., Mosher, T., & Eckstein, F. (2009). MR imaging of cartilage and its repair in the knee--a review. *Eur Radiol, 19*(7), 1582-1594.

Treppo, S., Koepp, H., Quan, E. C., Cole, A. A., Kuettner, K. E., & Grodzinsky, A. J. (2000). Comparison of biomechanical and biochemical properties of cartilage from human knee and ankle pairs. *J Orthop Res, 18*(5), 739-748.

Ugryumova, N., Attenburrow, D. P., Winlove, C. P., & Matcher, S. J. (2005). The collagen structure of equine articular cartilage, characterized using polarization-sensitive optical coherence tomography. *Journal of Physics D: Applied Physics, 38*, 2612-2619.

Ugryumova, N., Jacobs, J., Bonesi, M., & Matcher, S. J. (2009). Novel optical imaging technique to determine the 3-D orientation of collagen fibers in cartilage: variable-incidence angle polarization-sensitive optical coherence tomography. *Osteoarthritis Cartilage, 17*(1), 33-42.

Vaatainen, U., Kiviranta, I., Jaroma, H., Arokosi, J., Tammi, M., & Kovanen, V. (1998). Collagen crosslinks in chondromalacia of the patella. *Int J Sports Med, 19*(2), 144-148.

van Turnhout, M. C., Schipper, H., Engel, B., Buist, W., Kranenbarg, S., & van Leeuwen, J. L. (2010). Postnatal development of collagen structure in ovine articular cartilage. *BMC Dev Biol, 10*, 62.

Vasara, A. I., Hyttinen, M. M., Pulliainen, O., Lammi, M. J., Jurvelin, J. S., Peterson, L., et al. (2006). Immature porcine knee cartilage lesions show good healing with or without autologous chondrocyte transplantation. *Osteoarthritis Cartilage, 14*(10), 1066-1074.

Vidal Bde, C., & Vilarta, R. (1988). Articular cartilage: collagen II-proteoglycans interactions. Availability of reactive groups. Variation in birefringence and differences as compared to collagen I. *Acta Histochem, 83*(2), 189-205.

Viren, T., Saarakkala, S., Kaleva, E., Nieminen, H. J., Jurvelin, J. S., & Toyras, J. (2009). Minimally invasive ultrasound method for intra-articular diagnostics of cartilage degeneration. *Ultrasound Med Biol, 35*(9), 1546-1554.

Viren, T., Saarakkala, S., Tiitu, V., Puhakka, J., Kiviranta, I., Jurvelin, J. S., et al. (2011). *Ultrasound evaluation of the mechanical injury of bovine knee articular cartilage under*

arthroscopic control (Abstract). Paper presented at the Annual Meeting of the Orthopaedic Research Society, Long Beach, California, USA.

Vrahas, M. S., Smith, G. A., Rosler, D. M., & Baratta, R. V. (1997). Method to impact in vivo rabbit femoral cartilage with blows of quantifiable stress. *J Orthop Res, 15*(2), 314-317.

Wang, F., Ying, Z., Duan, X., Tan, H., Yang, B., Guo, L., et al. (2009). Histomorphometric analysis of adult articular calcified cartilage zone. *J Struct Biol, 168*(3), 359-365.

Ware, J. E., Jr., & Sherbourne, C. D. (1992). The MOS 36-item short-form health survey (SF-36). I. Conceptual framework and item selection. *Med Care, 30*(6), 473-483.

Weaver, B. T., & Haut, R. C. (2005). Enforced exercise after blunt trauma significantly affects biomechanical and histological changes in rabbit retro-patellar cartilage. *J Biomech, 38*(5), 1177-1183.

Weiss, C., Rosenberg, L., & Helfet, A. J. (1968). An ultrastructural study of normal young adult human articular cartilage. *J Bone Joint Surg Am, 50*(4), 663-674.

White, L. M., Sussman, M. S., Hurtig, M., Probyn, L., Tomlinson, G., & Kandel, R. (2006). Cartilage T2 assessment: differentiation of normal hyaline cartilage and reparative tissue after arthroscopic cartilage repair in equine subjects. *Radiology, 241*(2), 407-414.

Willett, T. L., Whiteside, R., Wild, P. M., Wyss, U. P., & Anastassiades, T. (2005). Artefacts in the mechanical characterization of porcine articular cartilage due to freezing. *Proc Inst Mech Eng [H], 219*(1), 23-29.

Williams, J. M., Uebelhart, D., Thonar, E. J., Kocsis, K., & Modis, L. (1996). Alteration and recovery of the spatial orientation of the collagen network of articular cartilage in adolescent rabbits following intra-articular chymopapain injection. *Connect Tissue Res, 34*(2), 105-117.

Williams, J. M., Virdi, A. S., Pylawka, T. K., Edwards, R. B., 3rd, Markel, M. D., & Cole, B. J. (2005). Prolonged-fresh preservation of intact whole canine femoral condyles for the potential use as osteochondral allografts. *J Orthop Res, 23*(4), 831-837.

Williams, S. K., Amiel, D., Ball, S. T., Allen, R. T., Wong, V. W., Chen, A. C., et al. (2003). Prolonged storage effects on the articular cartilage of fresh human osteochondral allografts. *J Bone Joint Surg Am, 85-A*(11), 2111-2120.

Wright, R. W. (2009). Knee injury outcomes measures. *J Am Acad Orthop Surg, 17*(1), 31-39.

Xia, Y., Moody, J. B., Alhadlaq, H., & Hu, J. (2003). Imaging the physical and morphological properties of a multi-zone young articular cartilage at microscopic resolution. *J Magn Reson Imaging, 17*(3), 365-374.

Xie, T., Guo, S., Zhang, J., Chen, Z., & Peavy, G. M. (2006a). Determination of characteristics of degenerative joint disease using optical coherence tomography and polarization sensitive optical coherence tomography. *Lasers Surg Med, 38*(9), 852-865.

Xie, T., Guo, S., Zhang, J., Chen, Z., & Peavy, G. M. (2006b). Use of polarization-sensitive optical coherence tomography to determine the directional polarization sensitivity of articular cartilage and meniscus. *J Biomed Opt, 11*(6), 064001.

Xie, T., Xia, Y., Guo, S., Hoover, P., Chen, Z., & Peavy, G. M. (2008). Topographical variations in the polarization sensitivity of articular cartilage as determined by polarization-sensitive optical coherence tomography and polarized light microscopy. *J Biomed Opt, 13*(5), 054034.

Yablon, I. G., & Covall, D. (1978). The preservation of articular cartilage. *Am J Med Technol, 44*(8), 799-802.

Yao, J. Q., Laurent, M. P., Johnson, T. S., R., B. C., & D., C. R. (2003). The influences of lubricant and material on polymer/CoCr sliding friction. *Wear, 255*, 780-784.

Yarker, Y. E., Aspden, R. M., & Hukins, D. W. (1983). Birefringence of articular cartilage and the distribution on collagen fibril orientations. *Connect Tissue Res, 11*(2-3), 207-213.

Zarins, B. (2005). Are validated questionnaires valid? *J Bone Joint Surg Am, 87*(8), 1671-1672.

Zhang, H., Vrahas, M. S., Baratta, R. V., & Rosler, D. M. (1999). Damage to rabbit femoral articular cartilage following direct impacts of uniform stresses: an in vitro study. *Clin Biomech (Bristol, Avon), 14*(8), 543-548.

Zhou, W., Apkarian, R. P., Wang, Z. L., & Joy, D. (2006). Fundamentals of Scanning Electron Microscopy. In W. Zhou & Z. L. Wang (Eds.), *Scanning Microscopy for Nanotechnology: Techniques and Applications* (pp. 1-40). New York: Springer.

APPENDIX 1 – ETHICS APPROVAL CERTIFICATES

The following are copies of the ethics certificates confirming that the equine and human tissue samples, described in Articles II, III & IV, were used under institution-approved protocols. Included are two certificates from École Polytechnique de Montréal covering the use of human osteochondral biopsies, as well as a certificate from the Ontario Veterinary College at the University of Guelph for the equine tissue samples. These protocols were renewed on an annual basis and were valid for the duration of the studies described in this thesis.

ÉCOLE
POLYTECHNIQUE
MONTRÉAL

Comité d'éthique de la recherche avec des sujets humains

Adresse civique
Campus de
l'Université de Montréal
2900, boul. Édouard-Montpetit
École Polytechnique
2500, chemin de Polytechnique
Montréal (Québec) H3T 1J4

Adresse postale
C.P. 6079, succursale Centre-ville
Montréal (Québec) H3C 3A7

Téléphone : (514) 340-4852
Télécopieur : (514) 340-4811

École affiliée à
l'Université de Montréal

Membres du comité :

Mme Ginette Denicourt, IRSST
M. Daniel Imbeau, MAQI
M. Bernard Lapierre, MAQI
Dr. André Prud'homme, Fac. Méd. Dent.
Pierre Savard, IGB, président

CERTIFICAT D'ACCEPTATION D'UN PROJET DE RECHERCHE PAR LE COMITÉ D'ÉTHIQUE DE LA RECHERCHE AVEC DES SUJETS HUMAINS DE L'ÉCOLE POLYTECHNIQUE

Montréal, le 7 juin 2005

M. Michael BUSCHMANN
Département de génie chimique
École Polytechnique de Montréal

N/Réf : Dossier CÉR-04/05-08

Cher M BUSCHMANN,

J'ai le plaisir de vous informer que le *Comité d'éthique de la recherche avec des sujets humains de l'École Polytechnique* (CÉRSHÉP) a approuvé, lors de sa réunion du 7 juin 2005, votre projet de recherche intitulé :

> « *Analyse des propriétés physicochimiques, biochimiques et histologiques d'articulations humaines.* »

Il est entendu que le présent certificat est valable pour le projet tel que soumis au CÉRSHÉP. Le CÉRSHÉP devra être informé de toute modification qui pourrait être apportée ultérieurement au protocole expérimental, de même que de tout problème imprévu pouvant avoir une incidence sur la santé, le bien-être et la sécurité des personnes impliquées dans le projet de recherche (sujets, professionnels de recherche ou chercheurs).

Nous vous prions également de nous faire parvenir un bref rapport annuel ainsi qu'un avis à la fin de vos travaux.

Je vous souhaite bonne chance dans vos travaux de recherche,

Bernard Lapierre
Éthicien conseil
Comité d'éthique de la recherche avec des sujets humains

C.C. : M. Jean Choquette

ÉCOLE
POLYTECHNIQUE
MONTRÉAL

Comité d'éthique de la recherche avec des sujets humains

Adresse civique :
Campus de l'Université de Montréal
2900, boul. Édouard-Montpetit
École Polytechnique
2500, chemin de Polytechnique
H3T 1J4

Adresse postale :
C.P. 6079, succursale Centre-ville
Montréal (Québec) Canada
H3C 3A7

Téléphone : (514)340-4990
Télécopieur : (514)340-4992

École affiliée à l'Université de Montréal

CERTIFICAT D'ACCEPTATION D'UN PROJET DE RECHERCHE PAR LE COMITÉ D'ÉTHIQUE DE LA RECHERCHE AVEC DES SUJETS HUMAINS DE L'ÉCOLE POLYTECHNIQUE

Montréal, le 25 septembre 2008

M. Jun Sun
Mme Caroline Hoemann
Département de Génie chimique
École Polytechnique de Montréal

N/Réf : Dossier CÉR-08/09-02

Madame, Monsieur,

J'ai le plaisir de vous informer que les membres du Comité d'éthique de la recherche ont procédé à l'évaluation en comité restreint de votre projet intitulé « *Biochemical and histological assays of osteoarthritic cartilage* ».

Les membres du Comité ont recommandé l'approbation finale de ce projet sur la base de la documentation soumise à la DRI en date du 23 septembre.

Veuillez noter que le présent certificat est valable pour le projet tel que soumis au Comité d'éthique de la recherche avec des sujets humains. La secrétaire du Comité d'éthique de la recherche avec des sujets humains devra immédiatement être informée de toute modification qui pourrait être apportée ultérieurement au protocole expérimental, de même que de tout problème imprévu pouvant avoir une incidence sur la santé et la sécurité des personnes impliquées dans le projet de recherche (sujets, professionnels de recherche ou chercheurs).

Nous vous prions également de nous faire parvenir un bref **rapport annuel** ainsi qu'un avis à la fin de vos travaux.

Je vous souhaite bonne chance dans vos travaux de recherche,

Bernard Lapierre
Président
Comité d'éthique de la recherche avec des sujets humains

c.c. : Pierre Savard, Génie électrique
Céline Roehrig, DRI
Gilles Savard, DRI

UNIVERSITY OF GUELPH

ANIMAL CARE COMMITTEE

November 24, 2010

Dear Dr. M. Hurtig:

Your Renewal/Amendment for the Animal Utilization Protocol number **10R014** entitled **"A research program for preclinical studies of osteoarthritis and cartilage repair using sheep and horse models"** has been approved by the University of Guelph Animal Care Committee (ACC) **with the proviso and comment outlined below**.

APPROVAL DATE: November 9, 2010

ADDITIONAL ANIMAL USE APPROVED:	**Species**	**Number Authorized**
	None	

PROVISO:

1. That all members of the research team be given copies of the **approved** renewal/amendment and this letter, so that any changes and stipulations are understood.

COMMENT:

1. Changes have been made or information added to section 9. Please review the document and inform the Animal Care Committee immediately, if any inaccuracies are present.

If you have any queries or comments, please contact me.

Anna Bolinder

Dr. Anna Bolinder, Interim Director
Animal Care Services

PLEASE SIGN AND DATE BELOW, INDICATING THAT THIS PROVISO MEETS WITH YOUR APPROVAL AND WILL BE IMPLEMENTED. RETURN ONE COPY TO ANIMAL CARE SERVICES, THE OTHER IS FOR YOUR FILES. THANK YOU.

Signature of Researcher Dec 1, 2010 **Date**

cc Facility AUP Contact – H. Bailey, APS; E. Smith, CS; M. Fowler, CAF; J. McFarlane, Ponsonby Sheep; D. Vandenberg, Arkell Equine
Department Chair – C. Kerr, Clinical Studies
Other – J. Beehler, Clincial Studies

AB/sl